Gas Separation by Poly(Ether Block Amide) Membranes

by

Li Liu

A thesis
presented to the University of Waterloo
in fulfillment of the
thesis requirement for the degree of
Doctor of Philosophy
in
Chemical Engineering

Waterloo, Ontario, Canada, 2008

I hereby declare that I am the sole author of this thesis. This is the true copy of the thesis, including any required final revisions, as accepted by my examiners.

I understand that my thesis may be made electronically available to the public.

Abstract

This study deals with poly(ether block amide) (PEBA) (type 2533) membranes for gas separation. A new method was developed to prepare flat thin film PEBA membranes by spontaneous spreading of a solution of the block copolymer on water surface. The membrane formation is featured with simultaneous solvent evaporation and solvent exchange with the support liquid, i.e. water. The formation of a uniform and defect-free membrane was affected by the solvent system, polymer concentration in the casting solution and temperature.

Propylene separation from nitrogen, which is relevant to the recovery of propylene from the de-gassing off-gas during polypropylene manufacturing, was carried out using flat PEBA composite membranes formed by laminating the aforementioned PEBA on a microporous substrate. The propylene permeance was affected by the presence of nitrogen, and vice versa, due to interactions between the permeating components. Semi-empirical correlations were developed to relate the permeance of a component in the mixture to the pressures and compositions of the gas on both sides of the membrane, and the separation performance at different operating conditions was analyzed in terms of product purity, recovery and productivity on the basis of a cross flow model.

To further understand gas permeation behavior and transport mechanism in the membranes, sorption, diffusion, and permeation of three olefins (i.e., C_2H_4, C_3H_6, and C_4H_8) in dense PEBA membranes were investigated. The relative contribution of solubility and diffusivity to the preferential permeability of olefins over nitrogen was elucidated. It was revealed that the favorable olefin/nitrogen permselectivity was primarily attributed to the solubility selectivity, whereas the diffusivity selectivity may affect the permselectivity negatively or positively, depending on the operating temperature and pressure. At a given temperature, the pressure dependence of solubility and permeability could be described empirically by an exponential function. The limiting

solubility at infinite dilution was correlated with the reduced temperature of the permeant.

The separation of volatile organic compounds (VOCs), which are more condensable than olefin gases, from nitrogen stream by the thin film PEBA composite membranes for potential use in gasoline or other organic vapour emission control was also studied. The membranes exhibited good separation performance for both binary VOC/N_2 and multi-component VOCs/N_2 gas mixtures. The permeance of N_2 in the VOC/N_2 mixtures was shown to be higher than pure N_2 permeance due to membrane swelling induced by the VOCs dissolved in the membrane. The effects of feed VOC concentration, temperature, stage cut, and permeate pressure on the separation performance were investigated.

Additionally, hollow fiber PEBA/polysulfone composite membranes were prepared by the dip coating technique. The effects of parameters involved in the procedure of polysulfone hollow fiber spinning and PEBA layer deposition on the permselectivity of the resulting composite membranes were investigated. Lab scale PEBA hollow fiber membrane modules were assembled and tested for CO_2/N_2 separation with various flow configurations using a simulated flue gas (15.3% carbon dioxide, balance N_2) as the feed. The shell side feed with counter-current flow was shown to perform better than other configurations over a wide range of stage cuts in terms of product purity, recovery and productivity.

Acknowledgements

I wish to carry my sincere appreciation to my supervisors, Professor X. Feng and Professor A. Chakma for giving me such a great opportunity to study in the University of Waterloo. Their diligent guidance, advice, encouragement and generous support throughout the course of this study and in the preparation of the thesis are invaluable.

I would like to thank all the members of the Membrane Research Lab in the Department of Chemical Engineering, University of Waterloo, for their help and friendship in the past several years during my study.

The financial support by the Natural Sciences and Engineering Research Council (NSERC) of Canada is gratefully acknowledged. The Ontario Graduate Scholarship (OGS), Ontario Graduate Scholarship of Science and Technology (OGSST), President's Graduate Scholarship (PGS), the University of Waterloo Graduate Scholarship, the Faculty of Engineering Graduate Scholarship, and the Institute of Polymer Research Scholarship for Academic Excellence in Polymer Science/Engineering awarded to me during the course of my doctoral programme are appreciated.

Last but not least, my appreciation also goes to my husband and my parents for their encouragement, love and support.

Table of Contents

Table of Contents ..... **vi**

List of Tables ..... **x**

List of Figures ..... **xi**

Nomenclature ..... **xvi**

CHAPTER 1

Introduction **1**

1.1 Background 1

1.2 Scope of the thesis 4

CHAPTER 2

Literature Review **7**

2.1 Characteristics of membrane gas separation 8

2.2 Gas transport in membranes 10

2.2.1 Mechanism of gas permeation 10

2.2.2 Gas transport in glassy and rubbery polymers 14

2.2.3 Determination of solubility and diffusivity coefficients 17

2.2.4 Gas transport in composite membranes 21

2.3 Membrane formation 25

2.4 Processes and applications 28

2.4.1 Non-condensable gas separation 29

2.4.2 Condensable gas and vapor separation 30

2.5 Poly(ether block amide) membranes 33

CHAPTER 3

A Novel Method of Preparing Ultrathin Poly(ether block amide) Membranes **40**

3.1 Introduction 40

3.2 Experimental 41

3.2.1 Materials 41
3.2.2 Membrane preparation 41
3.2.3 Solvent-nonsolvent exchange during membrane formation on water surface 43
3.2.4 Gas permeation test 44
3.3 Results and discussion 44
3.3.1 Membrane formation 44
3.3.2 Gas permselectivity 51
3.4 Summary 57

CHAPTER 4

Propylene Separation from Nitrogen by Poly(ether Block Amide) Composite Membranes 58

4.1 Introduction 58
4.2 Experimental 59
4.2.1 Membrane preparation 59
4.2.2 Gas permeation test 60
4.3 Results and discussion 62
4.3.1 Pure gas permeability and ideal selectivity 62
4.3.2 Pure gas permeation through PEBA/PSf composite membranes 64
4.3.3 Propylene/nitrogen gas mixture permeation 67
4.3.4 Process simulation for propylene separation from nitrogen 74
4.4 Summary 80

CHAPTER 5

Sorption, Diffusion, and Permeation of Light Olefins in Poly(Ether Block Amide) Membranes 81

5.1 Introduction 81
5.2 Experimental 82
5.2.1 Membrane preparation and permeation test 82
5.2.2 Equilibrium sorption 82
5.2.3 Time-lag technique 84

5.3 Results and discussion 84
5.3.1 Permeation 84
5.3.2 Equilibrium sorption 91
5.3.3 Diffusion 100
5.3.4 Membrane Selectivity 104
5.4 Summary 106

CHAPTER 6

Separation of VOCs from N_2 Using Poly(Ether Block Amide) Composite Membranes 108

6.1 Introduction 108
6.2 Experimental 110
6.2.1 Materials 110
6.2.2 Membrane preparation and VOCs/N_2 separation 110
6.3 Results and discussion 112
6.3.1 Separation of binary VOC/N_2 gas mixtures 112
6.3.2 Effect of temperature 122
6.3.3 Effect of stage cut and process simulation 124
6.3.4 Effect of permeate pressure 131
6.3.5 Separation of multi-component VOCs from nitrogen 132
6.4 Summary 135

CHAPTER 7

Preparation of Hollow Fiber Poly(Ether Block Amide)/Polysulfone Composite Membranes 136

7.1 Introduction 136
7.2 Experimental 137
7.2.1 Materials 137
7.2.2 Membrane preparation 137
7.2.3 Gas permeation 139
7.3 Results and discussion 140

7.3.1 Gas permeation through dense flat membranes 140
7.3.2 PEBA/PSf hollow fiber composite membranes 145
7.4 Summary 155

CHAPTER 8

CO_2/N_2 Separation by Poly(Ether Block Amide) Thin Film Hollow Fiber Composite membranes 156

8.1 Introduction 156
8.2 Experimental 157
8.2.1 Membrane preparation 157
8.3 Results and discussion 160
8.3.1 Comparison of flow configurations 160
8.3.2 Effect of operating pressure 166
8.3.3 Effect of operating temperature 171
8.3.4 Bore side feed vs shell side feed 174
8.4 Summary 178

CHAPTER 9

General Conclusions, Original Contributions and Recommendations 179

9.1 General conclusions and contributions 179
9.2 Recommendations 181

APPENDIX

Estimation of Experimetal Errors 183

Bibliography 185

The Published Papers Resulting from Thesis Research 196

List of Tables

Table 2.1 Membranes and membrane modules for various gas separation applications 28
Table 2.2 Chemical component and physical properties of some grades of PEBA 34
Table 2.3 PEBA for membrane separation..... 38
Table 3.1 Physical properties of solvent at 25 ^{o}C 46
Table 3.2 Swelling of PEBA 2533 in solvents..... 48
Table 3.3 Permeability measured with multilayered PEBA membranes 54
Table 4.1 Parameters (D_o/ϕ) and ($\omega\phi$) obtained by non-linear regression 72
Table 5.1 Some physical properties of gases 87
Table 5.2 Parameters characterizing pressure dependence of permeability and solubility 88
Table 5.3 Polymer/penetrant interaction parameters..... 99
Table 5.4 Olefins/nitrogen selectivity 105
Table 6.1 Physical properties of VOC components 116
Table 6.2 Parameters (D_0/ϕ) and ($\omega\phi$) obtained by non-linear regression 117
Table 6.3 The effect of the permeate pressure on the separation of hexane/nitrogen mixture 132
Table 6.4 Separation of mixed VOC components from nitrogen 133
Table 7.1 Activation energy for permeation 145
Table 7.2 Hollow fiber spinning conditions..... 146
Table 7.3 The gas permeation performance of CO_2/N_2 through PEBA/PSf composite membranes 147

List of Figures

Figure 1.1 Construction of the thesis illustrated in terms of chapters and content relevance. 6

Figure 2.1 Crucial issues controlling successful membrane based gas separation. 9

Figure 2.2 Mechanisms of gas permeation through porous and nonporous membranes 10

Figure 2.3 Schematic diagram of the solution-diffusion mechanism. 11

Figure 2.4 Typical sorption isotherms for polymeric media. 15

Figure 2.5 Time-lag measurement of gas permeation. 18

Figure 2.6 Composite membranes for gas separation. 22

Figure 2.7 Hybrid compression-condensation-membrane design for propylene recovery from resin degassing vent gas in polyolefin plant 32

Figure 3.1 Schematic diagram of solution spreading on water surface..... 42

Figure 3.2 Solvent-nonsolvent exchange rate at different spreading temperature of polymer solutions. Water temperature: 25^{o}C. 50

Figure 3.3 Scanning electron micrographs of membrane surface. The membranes were prepared at a spreading temperature of 80 ^{o}C. 52

Figure 3.4 Scanning electron micrograph of the cross-section of a multiplayered PEBA 2533 membrane supported by a porous polysulfone substrate. 53

Figure 3.5 Effect of the feed pressure on gas permeance and selectivity through a multilayered PEBA membranes supported by polysulfone substrate. Test temperature: 23 ^{o}C. 56

Figure 4.1 Schematic diagram of the experimental set-up for gas permeation test. 61

Figure 4.2 Permeation performance of pure propylene and nitrogen through PEBA 2533 dense membrane. Test temperature: 25^{o}C. 63

Figure 4.3 Permeance of propylene for pure gas permeation through PEBA/PSf composite membranes..... 65

Figure 4.4 Permeance of nitrogen vs. reciprocal of operation temperature for pure gas permeation through PEBA/PSf composite membranes. Feed pressure: 170-584 kPa. 66
Figure 4.5 Permeance ratio of C_3H_6/N_2 for pure gas permeation through the PEBA/PSf composite membrane. 67
Figure 4.6 Effect of propylene feed concentration on the permeate concentration of gas mixture permeation. Feed pressure: 791 kPa. 68
Figure 4.7 Effect of feed concentration on the permeance of propylene in gas mixture permeation. Feed pressure: 791 kPa. 69
Figure 4.8 Effect of feed concentration on the permeance of nitrogen in gas mixture permeation. Feed pressure: 791 kPa. 70
Figure 4.9 Effect of feed concentration on the selectivity of propylene/nitrogen in gas mixture permeation. Feed pressure: 791 kPa. 71
Figure 4.10 Comparison of propylene permeance for pure and gas mixture permeation. Total feed pressure in gas mixture permeation: 791 kPa. 73
Figure 4.11 Effect of temperature on the permeance of propylene and nitrogen in gas mixture permeation. Feed pressure: 791 kPa..... 75
Figure 4.12 (a) Schematic diagram of membrane process for propylene/nitrogen separation. (b) A differential unit of the membrane for gas separation based on cross flow model. 76
Figure 4.13 Product recovery vs. product purity determined on the basis of cross flow model. Total feed pressure: 1480 kPa. 78
Figure 4.14 Productivity vs. product purity determined on the basis of cross flow model. Total feed pressure: 1480 kPa. 79
Figure 5.1 Schematic diagram of gas sorption set-up. 83
Figure 5.2 Permeability of olefin in PEBA 2533 as a function of transmembrane pressure difference. 86
Figure 5.3 Temperature dependence of gas permeability at $\Delta p = 0$ 90
Figure 5.4 Permeability of paraffins (ethane and propane) and olefins (ethylene and propylene) in PEBA 2533 membranes at 25^{o}C. 91
Figure 5.5 Sorption isotherms of olefins in PEBA 2533 membranes 92

Figure 5.6 Solubility of olefin in PEBA 2533 membranes at different temperatures and pressures 94
Figure 5.7 Sorption isotherms of paraffin and olefin in PEBA 2533 membranes at 30 ^{o}C..... 95
Figure 5.8 Infinite dilute solubility as a functions of boiling point T_b or critical temperature T_c..... 95
Figure 5.9 Infinite dilute solubility as a function of reduced temperature (T/T_c).. 96
Figure 5.10 Local diffusivity of olefins as a function of sorbate concentration in the membrane..... 102
Figure 5.11 Average diffusivity of olefins as a function of feed pressure. 103
Figure 5.12 Temperature dependence of average diffusivity at p=0..... 104
Figure 6.1 Schematic diagram of experimental setup for VOC/N_2 separation. 111
Figure 6.2 Permeation flux of VOC as a function of feed VOC concentration. 113
Figure 6.3 VOC permeance vs. feed VOC concentration... 114
Figure 6.4 Permeance of nitrogen vs. feed VOC concentration..... 119
Figure 6.5 Membrane selectivity for VOC/N_2 vs feed VOC concentration..... 120
Figure 6.6 Permeate VOC concentration vs. feed VOC concentration..... 121
Figure 6.7 Permeate Effects of temperature on the separation of binary VOC/N_2 mixtures..... 123
Figure 6.8 a) Schematic diagram of VOC/N_2 separation with cross flow configuration. (b) A differential unit of the membrane for gas separation based on the cross model..... 125
Figure 6.9 Concentration of n-hexane in residue and the percentage hexane removal as a function of stage cut. Feed hexane concentration 12.6 mol%. 126
Figure 6.10 Permeate n-hexane concentration as a function of stage cut. Feed hexane concentration 12.6 mol%..... 127
Figure 6.11 VOC concentration in residue as a function of stage cut. Feed mixtures: nitrogen with 70% saturated VOC vapors. 128
Figure 6.12 Percent VOC removal as a function of stage cut. Feed mixtures: nitrogen with 70% saturated VOC vapors. 129

Figure 6.13 Permeate VOC concentration as a function of stage cut. Feed mixtures: nitrogen with 70% saturated VOC vapors. 130
Figure 6.14 A schematic illustrating the VOC separation process without using cold traps. 131
Figure 6.15 Enrichment factors for VOCs in the separation of multi-component VOCs from nitrogen. 134
Figure 7.1 Schematic diagram of hollow fiber spinning system. 138
Figure 7.2 PEBA/PSf hollow fiber composite membrane 139
Figure 7.3 Schematic diagram of hollow fiber module 139
Figure 7.4 Permeability of carbon dioxide and nitrogen through the dense PEBA membrane as a function of feed pressure at different temperatures. 141
Figure 7.5 Temperature dependence of CO_2/N_2 permselectivity through the dense PEBA membrane. 144
Figure 7.6 Effect of PEBA concentration in coating solution on the performance of PEBA/PSf hollow fiber composite membranes (PEBA coating once, coating temperature 50°C, permeation test at 446 kPa, 25°C)..... 149
Figure 7.7 Effect of PEBA coating temperature on the performance of PEBA/PSf hollow fiber composite membranes (PEBA concentration in coating solution, 3 wt%, PEBA coating once, permeation test at 446 kPa, 25°C). 151
Figure 7.8 Permeance of carbon dioxide and nitrogen through PEBA/PSf hollow fiber composite membrane at various pressures and temperatures. 153
Figure 7.9 Effect of temperature on the permeance and selectivity of carbon dioxide and nitrogen through the PEBA/PSf hollow fiber composite membrane .. 154
Figure 8.1 Schematic diagram of the experimental set-up for CO_2/N_2 separation by a hollow fiber membrane module. 158
Figure 8.2 Configurations of membrane modules 159
Figure 8.3 Concentration of CO_2 in permeate as a function of stage cut at a feed pressure of 790 kPa and 23°C 162
Figure 8.4 Concentration of N_2 in residue as a function of stage cut. 163
Figure 8.5 Productivity and recovery of CO_2 as a function of CO_2 concentration in permeate. 164

Figure 8.6 Productivity and recovery of N_2 as a function of N_2 concentration in residue.. 165
Figure 8.7 Effects of feed pressure on CO_2 concentration and recovery in permeate for counter-current flow at 23^oC.. 167
Figure 8.8 Effects of feed pressure on N_2 concentration and recovery in residue for counter-current flow.. 168
Figure 8.9 Comparison of pure gas and gas mixture permeating through the hollow fiber membranes at 23^oC..... 170
Figure 8.10 Permeance and permeance ratio of pure gases as a function of operating temperature. Feed pressure, 790 kPa. 171
Figure 8.11 CO_2 concentration in permeate and N_2 concentration in residue at different temperatures. Feed pressure 790 kPa. 172
Figure 8.12 Effects of temperature on CO_2 recovery and productivity. Feed pressure 790 kPa. 173
Figure 8.13 Effects of temperature on N_2 recovery and productivity. Feed pressure 790 kPa. 174
Figure 8.14 CO_2 concentration in permeate as a function of stage cut with bore side and shell side feed. Temperature 23^oC, feed pressure 790 kPa..... 175
Figure 8.15 Permeate productivity and CO_2 recovery as a function of CO_2 concentration by bore feed and shell side feed. Temperature 23^oC, feed pressure 790 kPa. 176
Figure 8.16 Pure gas permeance and permeance ratio for shell side feed and bore side feed. Temperature 23^oC..... 177

Nomenclature

A	Membrane area for permeation, cm^2
C	Molar concentration of penetrant in polymer, mol/cm^3
D	Diffusivity coefficient, cm^2/s
F	Gas flow rate in feed side, $cm^3(STP)/s$
J	Gas permeance, $cm^3(STP)/cm^2.s.cmHg$
J^0	Gas permeation flux, $cm^3(STP)/cm^2.s$
l	membrane thickness, cm
P	Permeability coefficient, $cm^3(STP).cm/cm^2.s.cmHg$
p	Gas pressure, cmHg
p^0	Saturated vapor pressure, cmHg
Δp	Pressure difference across membrane, cmHg
Q	Gas permeation rate, $cm^3(STP)/s$
Q_t	amount of penetrant per unit membrane area, $cm^3(STP)/cm^2$
q	Quantity of gas sorbed in membrane, $cm^3(STP)$
R	Gas constant, J/mol.K
S	Solubility coefficient, $cm^3(STP)/cm^3$ polym..cmHg
T	Temperature, K
t	permeation/sorption time, s
T_c	Critical temperature, K
T_r	Dimensionless reduced temperature
V	Volume, cm^3
$\overline{V}$	Partial molar volume of penetrant, cm^3/mol
x	Dimensionless gas mole fraction in feed side
y	Dimensionless gas mole fraction in permeate side
Z	Thickness along cross section of membrane, cm

Greek letters

α	Dimensionless permeability/permeance ratio or selectivity
χ	Dimensionless Flory-Huggins interaction parameter
Φ	Dimensionless volume fraction of dissolved gas in amorphous phase
Φ_a	Dimensionless volume fraction of amorphous phase in polymer
ϕ	Constant, cm^3/mol
θ	Time lag, s
ω	Dimensionless equilibrium partition coefficient

CHAPTER 1
Introduction

1.1 Background

A membrane can be defined as a selective barrier between two phases, the 'selective' being inherent to a membrane or a membrane process (Mulder, 1996). In recent years, membrane-based technology has found use in industrial processes (Koros, 2004). It is widely applied in purification, concentration and fractionation of fluid mixtures with evident advantages of energy saving, compactness, ease of operation and maintenance, continuous operation, and environmental friendliness. Membranes have found applications in areas that were previously dominated by more traditional processes, such as distillation, absorption, adsorption, and extraction and filtration. Even if in many cases membranes could not completely replace these technologies, hybrid systems combining membranes with one of the traditional techniques are accepted as attractive options (Spillman, 1989).

Gas separation by selective permeation through polymer membranes is one of the fastest growing branches in membrane technology. In membrane gas separation, non-porous membranes are normally used. The gas mixture to be separated (feed) is placed in contact with one side of a membrane at a high pressure and permeates through the membrane to a low-pressure side (permeate). The components that permeate more rapidly become enriched on the permeate side, while the slower components are concentrated in the retentate (residue). The driving force for the mass transfer is the pressure difference across the membrane, which may derive from compression of feed gas to a high pressure; and/or evacuation of the permeant at the downstream side. For most gas separation processes, including H_2 recovery, N_2 enrichment, and CO_2 removal, a high feed pressure is used at the feed side, because the feed streams are normally already at a relatively high

pressure or require only moderate compression for the separation. In vapor/gas separation processes, such as organic vapors removal or gas dehydration, vacuum or purge gas is commonly applied in the permeate side to maintain the permeate vapor pressure lower than the saturated vapor pressure of the penetrants.

Though extensive research and development have been carried out in the past two decades, membrane based gas separation is still in a far less advanced state compared with other more mature membrane processes such as dialysis, reverse osmosis, microfiltration, and ultrafiltration. The development of new membranes and membrane processes are required to improve the process efficiency for industrial applications.

In 1980, Permea (now a division of Air Products) launched Prism® membranes for hydrogen recovery from ammonia synthesis purge gas streams, the first large commercial application of gas separation membranes. Since then, membrane-based gas separation has grown into a $150 million/year business and it is likely to maintain a substantial growth rate in the near future (Baker, 2002). However, more than 90% of the business involves the separation of non-condensable gases, including the separation of hydrogen from nitrogen, argon, or methane, nitrogen separation from air, and carbon dioxide separation from methane (CO_2 often behaves an intermediate between condensable and non-condensable gases). Due to the concerns with fossil fuel depletion and increasingly stringent environmental regulations, a large potential market lies in separating mixtures containing condensable gases. Recovery of light hydrocarbons and volatile organic compounds (VOCs) from various industrial gases or natural gas streams, olefin/paraffin separation, and CO_2 separation from flue gases relevant to green house gas emission control, are all potential applications.

Although several hundred new polymeric membrane materials have been reported so far, only a few, including polysulfone (PSf), cellulose acetate, polyimide, poly(phenylene oxide) and silicone rubber, have been used to make 90% of the commercial gas separation membranes (Baker 2002). Silicone rubber is thus far the only rubbery material for commercial membranes applied in the separation of condensable gases or vapors from non-condensable gases. Membranes with improved permeability, selectivity, and stability are required for the future applications.

Poly(ether block amide) (PEBA) is a family of copolymers, consisting of polyamide hard segments and polyether soft segments in the polymer chains. Because of their bi-phasic micro structure, the copolymers offer many properties that are not readily available in either constituent polymer. It was found that the PEBA polymers in general exhibit substantially high permselectivity for polar (or quadrupolar)/nonpolar gas pairs (e.g. CO_2/N_2, SO_2/N_2 or CO_2/H_2). PEBA membranes have been investigated for the enrichment of ester aroma compounds from dilute solutions and phenol removal from phenolic resin wastewater, and they have shown good performance for the liquid separation.

Membrane separation is a rate controlled process, and the industrial success of membrane gas separation is to a large extent attributed to the engineering approach of reducing the effective thickness of the membrane and increasing the packing density of the membrane module so as to optimize the product throughput. In most of previous studies on the PEBA membranes, relatively thick (20 ~ 500 μm) homogeneous membranes prepared by melt extrusion or solvent casting technique were used. From an application point of view, thin membranes in the form of asymmetric and/or composite membranes are desired to reduce the membrane resistance to permeation. Compared with flat membranes, hollow fiber membranes have the advantages of self-supporting and large membrane area per unit module volume, a feature favourable for practical applications. However, till now no systematic study has been reported in the literature on the development of hollow fiber PEBA membranes.

Generally rubbery polymers are selected for condensable vapor/gas separation because of the high solubility of the condensable components in the membrane. PEBA (type 2533) comprises of 80 wt% poly(tetramethylene oxide) as the rubbery domains. The good chemical resistance and high thermal and mechanical stabilities make it a promising membrane material for condensable gas separation, for which unfortunately very little work can be found in the literature.

Moreover, the understanding of the permeation of condensable gases is still incomplete. Because of the significant plasticization, swelling of the membranes and coupling effects of permeants in mixed gas permeation, permeation behavior of condensable gases in the rubbery membranes is often different from that of permanent

gases (e.g., H_2, N_2 and O_2). Due to much faster permeation rates of condensable gases than permanent gases, the mass transport resistance in the substrate and the concentration polarization along membrane surface become more significant when a composite membrane is used. Therefore, the transport mechanism and permeation behavior of condensable gases in the membranes were investigated in this research in an attempt to explore new potential applications of PEBA membranes for gas separations.

The objectives of this research have been derived in light of the aforementioned discussions and are presented below.

1. To investigate the transport behavior of condensable gases and vapors in PEBA membranes by studying their solubilities and diffusivities.
2. To develop ultrathin PEBA membranes and hollow fiber composite membranes to achieve a high permeation flux, which is important for practical application.
3. To explore new applications of PEBA membranes in the gas separation field based on the membranes developed in this study, mainly on condensable gas or vapor separation, including the recovery of olefins and other light hydrocarbons from N_2, VOCs separations, and CO_2 removal from flue gas.

1.2 Scope of the thesis

In order to have an overview of the research in the thesis, the thesis structure is briefly illustrated in Figure 1.1. Chapter 1 presents background and the objectives of this study. Chapter 2 contains an overview of membrane based gas separation concerning gas transport in membranes, membrane formation, processes and applications. The recent studies on PEBA membranes are also included in this chapter.

A new method of preparing ultrathin PEBA membranes by spontaneous spreading of a solution of the block copolymer on water surface is carried out in Chapter 3. It is demonstrated that the solvent-nonsolvent exchange is primarily responsible for membrane formation.

Chapter 4 studies propylene separation from nitrogen using composite membranes containing a thin film PEBA layer prepared in Chapter 3. Both pure gas permeation and gas mixtures separation were conducted. Semi-empirical correlations of the membrane permeance were developed to analyze the separation performance at different operating

conditions based on a cross flow model. To further understand the mass transfer in the membranes, sorption, diffusion and permeation of three olefins (i.e., C_2H_4, C_3H_6 and C_4H_8) at different temperatures and pressures were investigated in Chapter 5. This study elucidated the relative contribution of solubility and diffusivity to the preferential permeability of olefins over nitrogen. Moreover, the solubility and the permeability were described empirically.

Chapter 6 deals with the separation of the volatile organic vapors from nitrogen by the PEBA thin film membranes. The permeances of both VOCs and nitrogen were studied in either binary VOC/N_2 or multi component VOCs/N_2 gas mixtures at different operating conditions.

Thin film PEBA hollow fiber composite membranes were developed in Chapter 7. The CO_2/N_2 separation with various flow configurations on lab-scale hollow fiber membrane modules was studied in Chapter 8 for potential use in CO_2 capture from flue gas for greenhouse gas emission control.

Finally, the general conclusions drawn from the study, along with the major contribution to research and recommendations for future work, are summarized in Chapter 9.

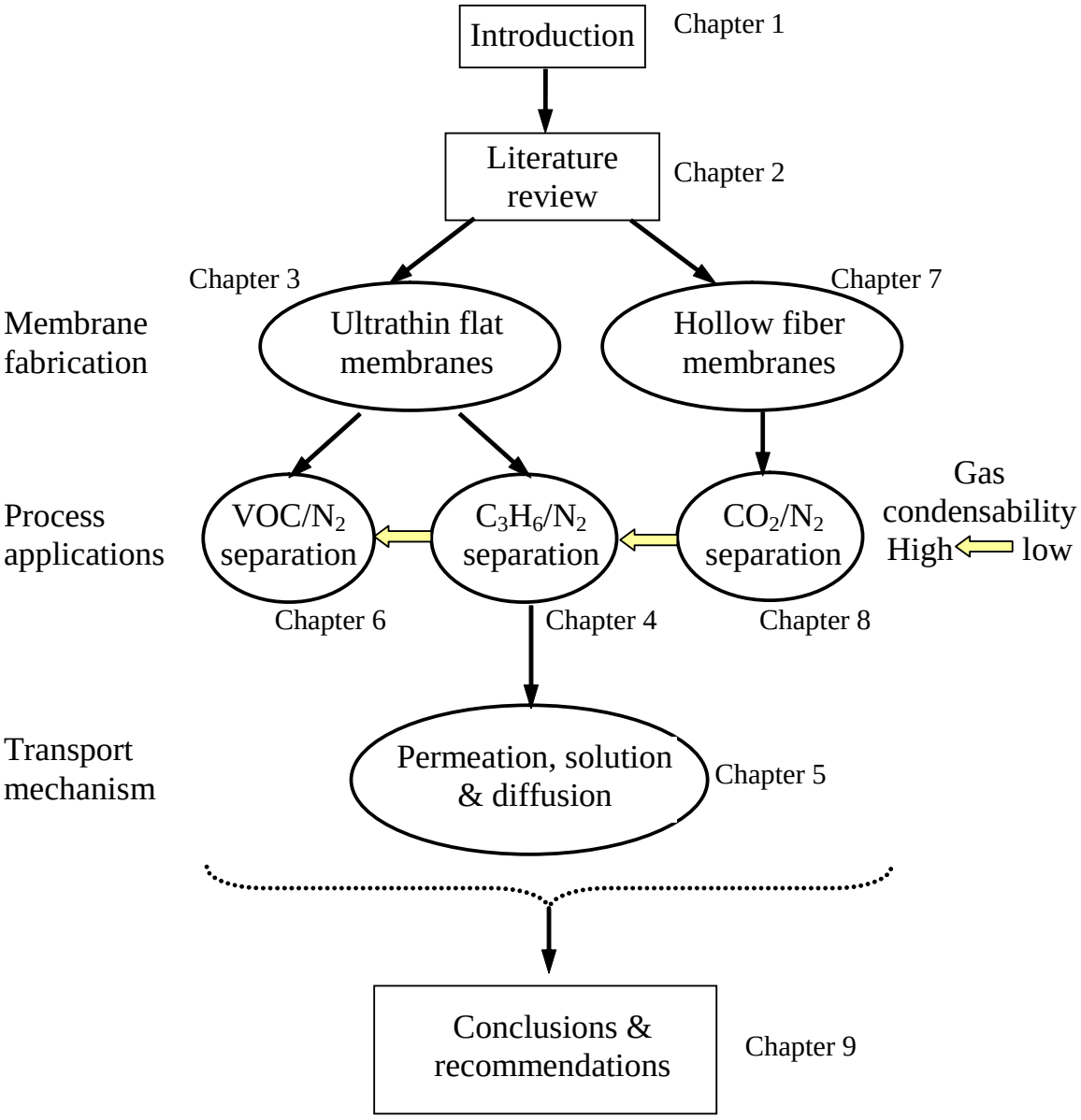

Figure 1.1 Thesis structure illustrated in terms of chapters and content relevance.

CHAPTER 2
Literature Review

Gas separation has become a major industrial application of membrane technology only in the past 20 years or so, but the study of gas separation by membrane has a long history. Graham was the first to demonstrate the potential of membrane gas separation by showing that air can be enriched in O_2 through a natural rubber film in 1866. However, the gas separation membranes in the early days did not lead to commercial applications, primarily due to the low permeation flux obtained with relatively thick polymer films. A significant breakthrough in this area was the formation of a high flux asymmetric membrane made of cellulose acetate for reverse osmosis by Loeb and Sourirajan (1963) in the 1960s. Unfortunately, when the membrane was dried for gas separation, pinholes developed on the membrane surface. Then Henis and Tripodi (1980) developed a defect-free composite membrane based on the "resistance model" concept using asymmetric polysulfone membrane with surface defects being sealed by silicone rubber. This is a milestone in the development of membrane-based gas separation technology. Based on this approach, Monsanto developed the first commercial hollow fiber membrane for hydrogen separation. Since then, the separation of gas mixtures of industrial interest by membranes has become economically competitive.

Extensive work has been done in the literature that relates to the development of membranes and membrane processes for gas separation. Several books have been published on membrane science and technology. The process principles, membrane materials, membrane formation, membrane modules, process design and applications for various major membrane processes are presented in the books of Ho and Sirkar (1992), Mulder (1996), Baker (2004) and Matsuura (1994). The book edited by Paul and Yampol'skii (1994) devotes entirely to gas separation membranes. Kesting (1985) discussed the preparation of polymeric membranes by the phase inversion technique. In the past decade, a few review papers were also published addressing the development,

perspective, and strategies of membrane gas separation (Baker, 2002; Koros, 2000; Stern, 1994; Koros, 1993). This chapter is attempted to give a review of the current literature concerning polymeric membrane gas separation and to address some issues that need to be solved; more specific literature reviews will be presented in the relevant chapters.

2.1 Characteristics of membrane gas separation

Comparing to other well-developed gas separation processes, such as cryogenic distillation, pressure swing adsorption and liquid absorption, membrane gas separation has the following features:

- Membrane gas separation does not involve phase change.
- Membrane gas separation is efficient for bulk separation. The driving force for gas permeation is the partial pressure difference across the membrane. Generally, it is no significantly economical to obtain products with very high purities due to the quite low driving force available under this condition.
- The membranes are modular in design and easy to scale up. They can be used in either a large or small processing capacity without significant economy of scale. At small to medium scales, membrane is generally more competitive than the traditional separation technologies.
- Membranes can be easily integrated with other separation techniques so that the hybrid processes will be more effective than by using either technique alone.
- Membrane gas separation is environmentally friendly. It does not require additional mass agent for separation and thus does not generate secondary waste (e.g., vapor, solvents and solid particles).
- Membranes are compact and light, easy to operate and maintain.

Prasad et al. (1994) made a systematic comparison of membranes with other more established separation processes for air separation and hydrogen recovery, the two areas where gas separation membranes have made the most impact, in terms of power consumption, capital cost, product purity and recovery. Though it is difficult to define an exact scale boundary for different competitive technologies, it was found that membranes are most suitable at small or moderate capacities for higher purities and at larger capacities for lower purities.

In the development of membranes and membrane processes, three key considerations must be addressed: membrane productivity, membrane selectivity and membrane stability. Membrane productivity is concerned with the permeation rate, determined by the intrinsic permeability of the polymer, the effective membrane thickness, and the membrane packing density, (i.e., the amount of membrane area per unit module volume). High permeation flux can be achieved by using asymmetric or thin film composite membranes with thin permselective layers, and using hollow fibers for a large membrane area. The membrane selectivity depends on not only the intrinsic selectivity of the polymer and the integrity of the selective layer but also the process conditions, which affect the significance of the concentration polarization and transport resistance of the support layer. Membrane stability is the ability to maintain membrane permeability and selectivity for a long period of time. For the applications of condensable gas separation, membranes with good chemical resistance, and thermal and mechanical stabilities are required.

Therefore, a successful membrane gas separation process is determined by several factors, including membrane material, membrane formation and structure, membrane module as well as fluid management, as indicated in Figure 2.1. It has been used to depict the crucial issues dealing with a pervaporation process (Feng, 1994), but it is also applicable to gas separation.

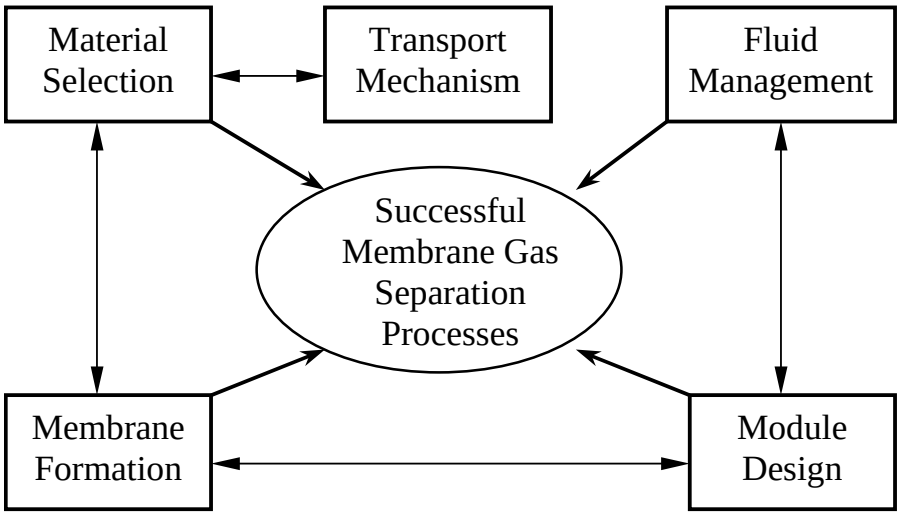

Figure 2.1 Crucial issues controlling successful membrane based gas separation.

2.2 Gas transport in membranes

2.2.1 Mechanism of gas permeation

The mechanism of gas transport in membranes depends on whether the membrane is porous or nonporous. Normally nonporous polymeric membranes are used as selective gas permeation barriers while porous membranes are used as substrates for mechanical support. Figure 2.2 illustrates the mechanisms of gas permeation. Gas permeation in dense nonporous membranes can be described by the solution-diffusion mechanism, while in porous membrane the gas transport follows viscous flow (convective flow), Knudsen flow, molecular sieving or a combination of them (Baker 2004; Ho & Sirkar, 1992; Mulder, 1996; Koros, 1993), depending on the relative size of the permeant molecules and the pores of the membrane.

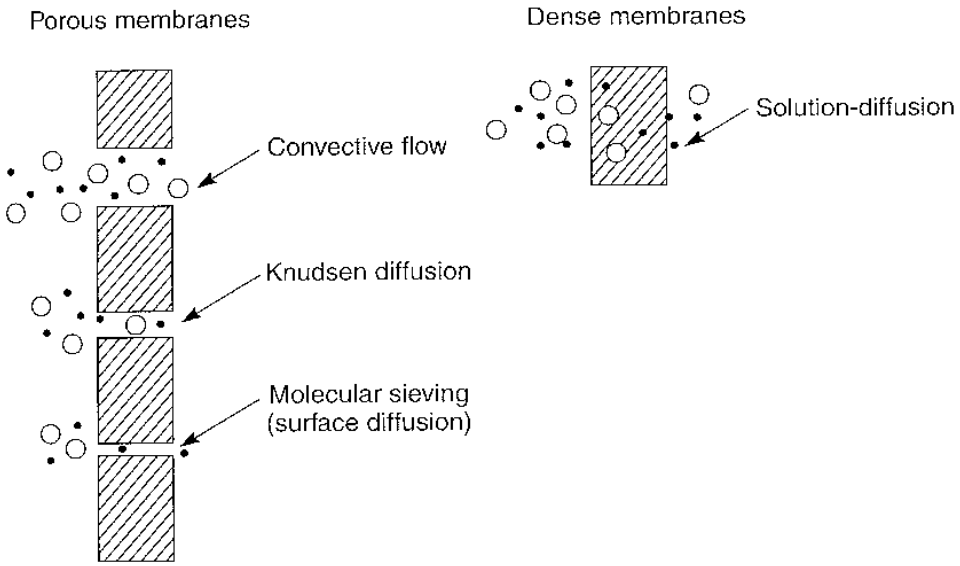

Figure 2.2 Mechanisms of gas permeation through porous and nonporous membranes (Koros, 1993).

2.2.1.1 Solution-diffusion model

The solution-diffusion mechanism is accepted widely by the majority of researchers for gas transport in nonporous membranes (Wijmans and Baker, 1995).

According to this mechanism, gas permeation through a membrane includes three consecutive steps (shown in Figure 2.3): (1) Gas dissolves into the membrane at high pressure side; (2) Penetrant gas molecules diffuse through the membrane under the concentration difference across the membrane; (3) Gas molecules desorb at the low pressure side of the membrane. Gas permeation is controlled by the diffusion of the penetrant gas molecules in the membrane matrix, while sorption/desorption equilibria are assumed to be established at the two interfaces between the gas and the membrane. A gas mixture is separated because of the differences in the solubility and mobility of the gas components in the membrane matrix.

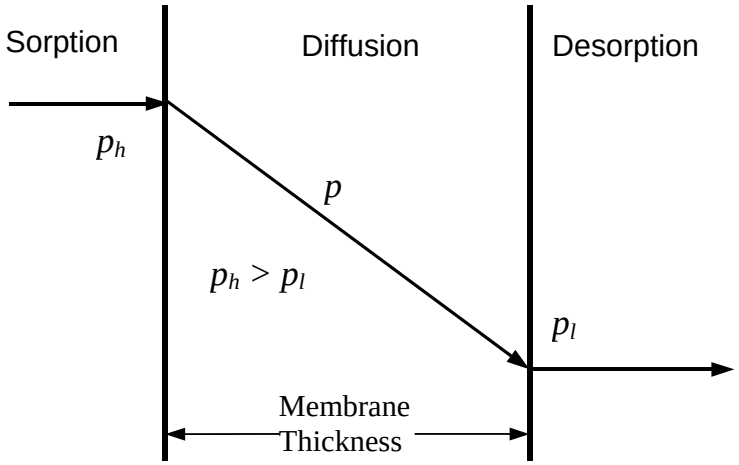

Figure 2.3 Schematic diagram of the solution-diffusion mechanism.

Gas diffusion through a nonporous homogenous membrane at steady state can be described by the Fick's first law (Crank and Park, 1968; Crank, 1975). For one-dimensional diffusion, the permeation flux through the membrane can be written as

$$J^0 = -D(c)\frac{dc}{dZ} \tag{2.1}$$

where J^0 is the permeation flux, c the concentration of the permeating species dissolved in the membrane, and $D(c)$ diffusion coefficient. For permanent gases (e.g., O_2, N_2, and H_2), D can normally be regarded as a constant that is independent of concentration. When condensable gases or vapors permeate through the membrane, D is usually concentration dependent due to the plasticization or swelling of the polymer by the permeant. The

concentration dependence of diffusion coefficient can be expressed by an exponential or a linear expression (Greenlaw et al., 1977; Raucher and Sefcik, 1983).

The equilibrium concentration c is related to the gas pressure, p, by

$$c = S(c) \cdot p \tag{2.2}$$

where $S(c)$ is a solubility coefficient.

When the concentration of the penetrant in the polymer is very low, Eq. (2.2) can be represented by the Henry's law and S becomes a constant. When D is also a constant, substituting Eq. (2.2) into Eq. (2.1) and integrating, yield

$$J^0 = DS\frac{(p_h - p_l)}{l} = (\frac{P}{l})\Delta p = J \cdot \Delta p \tag{2.3}$$

where P ($P=DS$) is the permeability, p_h and p_l are the pressures of upstream and downstream, respectively, l is the effective membrane thickness, and J the permeance for gas permeation.

The permeability (or permeance) ratio of two gas species (i and j) is often defined as the ideal selectivity (or ideal separation factor) α, shown in Eq. (2.4).

$$\alpha_{i/j} = \frac{P_i}{P_j} = \frac{J_i}{J_j} = \frac{D_i}{D_j} \cdot \frac{S_i}{S_j} \tag{2.4}$$

where the ratios D_i/D_j and S_i/S_j represent, respectively, the "diffusivity (or mobility) selectivity", reflecting the difference in the molecular sizes of the two permeants, and the "solubility selectivity", reflecting the relative condensabilities of the two gases. These ratios represent the contributions of the sorption and diffusion steps to the overall selectivity due to the differences in the diffusivities and solubilities of the two gases in the membrane.

2.2.1.2 Pore flow model

If the membrane pores are much larger than the mean free path of the gas molecules, e.g., from 0.1 to 10 μm, viscous flow takes place. The permeation rate is inversely proportional to the gas viscosity and directly proportional to the average pressure across the pores. Almost no separation can be achieved by viscous flow.

When the pore size is similar or smaller than the mean free path of the gas molecules (typically less than 0.1 μm), Knudsen diffusion governs the gas flow, and the

gas transport rate is inversely proportional to the square root of its molecular weight. Though Knudsen diffusion can offer a little selectivity, depending on the relative molecular weight of the gases, there is essentially no commercial application in polymeric membranes because they are economically unattractive. The only large-scale application of Knudsen diffusion was the separation of uranium isotopes, as a part of the Manhattan Project. The ideal separation factor for $U^{235}F_6$ over $U^{238}F_6$ is only 1.0064 and thousands of membrane stages were used.

If the membrane pores are extremely small, on the order of 0.5 to 2 nm, gases are separated by molecular sieving. This type of separation is currently applied only to limited gas separations using ceramic, glass, zeolite or other inorganic membranes.

Under certain special cases, gas permeation may also occur based on surface diffusion or capillary condensation. When strongly adsorbed gases or vapors diffuse through pores, the penetrants could adsorb on the wall of the membrane pores. The multilayer of adsorbates so formed is driven by the spreading pressure to move to the low-pressure side resulting in a surface flow (Gilliland, 1958). When the amount of adsorbates in the pores is large enough, capillary condensation will occur. If the surface diffusion and capillary condensation mechanisms allow the readily condensable components to effectively exclude the noncondensable components from the porous network, a high selectivity could be achieved. Six different modes of surface diffusion and capillary condensation are described by Lee and Hwang (1986) depending on the pressure distribution and the film thickness of the adsorbed layer. These phenomena were well discussed for ceramic or glass inorganic membranes (Lee and Hwang, 1986; Uhlhorn et al., 1992; Bhandarkar et al., 1992; Qiu and Hwang, 1991), and they also can be applied to polymeric membranes. Porous asymmetric poly(ether amide) (Feng et al.,1993; Deng et al., 1995, 1998) and aromatic polyimide membranes (Feng et al., 1991) exhibited quite high selectivities to the separation of organic vapors or water vapor from air or nitrogen streams, which were attributed to the effects of surface diffusion and capillary condensation. Poly(1-trimethylsilyl-1-propane), a glassy polymer with an ultra large free volumn, was also suspected to have capillary condensation when organic vapors transport through the polymer matrix due to the large space between the polymer chains (Pinnau and Toy, 1996). Furthermore, when composite membranes are used for

vapor/gas separation, the surface diffusion and capillary condensation may occur in the pores of the support membranes, where considerably high concentrations of condensable components, caused by the preferential permeation of vapors through the skin layer, could lead to either enhanced gas permeation or extra resistance for mass transfer. This issue has rarely been addressed in the literature.

2.2.2 Gas transport in glassy and rubbery polymers

A rubbery polymer is an amorphous polymeric material above its glass transition temperature T_g under the conditions of use (Billmeyer, 1971). In this case, the polymer chains are soft and highly mobile. The sorption of low molecular weight penetrants in rubbery materials is typically described by the Henry's law, and the sorption isotherms are linear (Figure 2.4 (a)). In the presence of high-activity gases or vapors, positive deviations from the simple Henry's law sorption are observed. The sorption isotherms are typically convex to the pressure axis (Merkel et al., 2000; Singh et al., 1998; Lin et al., 2004; Bondar et al., 1999; Rezac et al, 1997) (Figure 2.4 (b)). In the case of weak polymer-penetrant interactions, the Flory-Huggins expression (Flory, 1969; Fleming and Koros, 1986) can be used to describe the penetrant solubility (Eq. 2.5). Its modified form, the Flory-Rehner expression (Flory, 1950) (Eq. 2.6), is frequently used for crosslinked rubbery polymer.

$$\ln(p/p^0) = \ln\Phi + (1-\Phi) + \chi(1-\Phi)^2 \qquad (2.5)$$

$$\ln(p/p^0) = \ln\Phi + (1-\Phi) + \chi(1-\Phi)^2 + V_1(\frac{\upsilon_e}{V_0})[(1-\Phi)^{1/3} - (\frac{1-\Phi}{2})] \qquad (2.6)$$

where p/p^0 is the relative pressure of the penetrant, Φ the volume fraction of dissolved penetrant in the polymer, which can be determined from the equilibrium penetrant concentration in the polymer, and χ the Flory-Huggins interaction parameter, reflecting the interactions between the polymer and the penetrant molecules. Yamiya et al. (1996) estimated the χ values for 23 gases in five rubbery polymers from either the literature data on Henry's law coefficient and the partial molar volume or those on sorptive dilation for each polymer/gas system. In Eq. (2.6), V_1 is the molar volume of the penetrant, and υ_e/V_0 is the effective number of crosslinks per unit volume of penetrant-free polymer (expressed in moles/volume).

If the polymer is below its glass transition temperature, the polymer chains are essentially fixed and do not rotate. The polymer is tough and rigid, and thus is called the glassy polymer. The most popular phenomenological description of gas transport in glassy polymers is the "dual-mode" model (Paul and Koros, 1976; Koros and Chern, 1987). Gas sorption in glassy polymers is governed by both the Henry's law dissolution and Langmuir adsorption. The latter occurs in an excess "unrelaxed" volume or "microvoids" caused by the extraordinarily long relaxation time for segmental motions when the material is quenched below the glass transition temperature T_g. The overall sorption is the sum of the Henry's law sorption and Langmuir adsorption, and the permeation flux J^0 is given in terms of the two contributions:

$$J^0 = -D_D \frac{dc_D}{dZ} - D_H \frac{dc_H}{dZ} \tag{2.7}$$

where D_D and D_H refer to the mobility of the sorbed components based on Henry's law sorption and Langmuir adsorption, respectively. The sorption isotherms are typically concave to the pressure axes (Figure 2.4 (c)) due to the gradually "saturated" Langmuir sorption sites when the pressure increases (Bondar and Freeman, 1999a, b; Marchese et al., 2003).

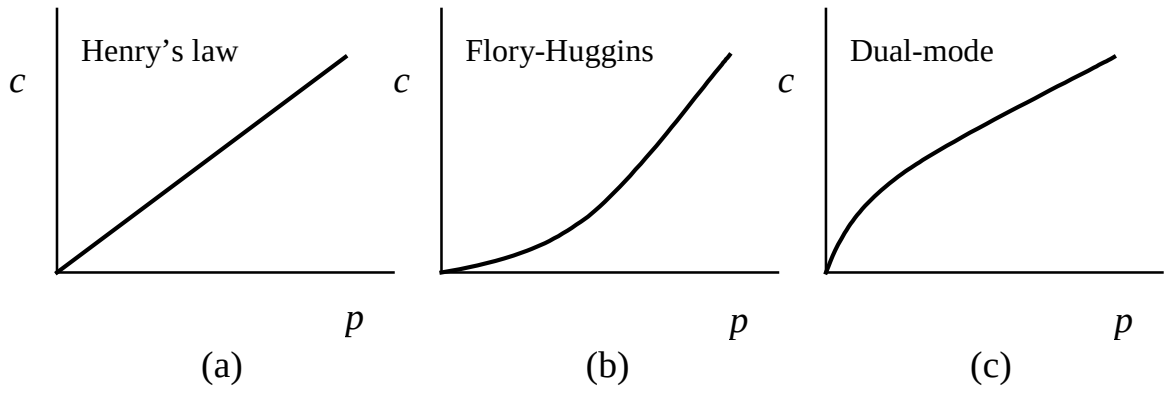

Figure 2.4 Typical sorption isotherms for polymeric media.

Due to the more restricted segmental motions, glassy polymers offer enhanced "mobility selectivity" or "size sieving" as compared with rubbery polymers (Stannett et

al., 1979; Koros and Chern, 1987). They are able to discriminate effectively a small difference in the molecular size of common gases, and thus they are commonly used as the selective layer of membranes for the separation of various gases (e.g., H_2/N_2, O_2/N_2, He/N_2, CO_2/N_2 and CO_2/CH_4). On the contrary, rubbery polymers generally have very low mobility selectivities for gas molecules due to their large free volume in the polymer matrix, but their permeability can be 10-100 times higher than glassy polymers (Baker et al., 1998).

In some relatively new applications, such as the removal of C_{3+} hydrocarbons and water vapor from natural gas for dew point and heat-value control, the recovery of light olefins from nitrogen in polyolefin manufacturing, and the separation of valuable or toxic organic vapors from air (or nitrogen) streams, membranes that are more permeable to the larger, more condensable components in the gas mixtures are generally required for an efficient operation. These organic components are usually the minor components in the feed streams. When membranes preferentially permeable to vapors are used, the membrane area required is relatively small because less feed stream needs to permeate through the membrane to remove the bulk of the vapor. Generally, rubbery polymers are chosen for this type of applications. Rubbery polymers, such as polydimethylsiloxane, are more permeable to large condensable molecules than to smaller, less condensable ones because the large condensable gases tend to have a higher solubility. Poly(1-trimethylsilyl-1-propyne), a special glassy polymer, also has similar permeation properties, primarily because of its ultra high free volume. Its network of nanoscale channels permits rapid surface diffusion of the organic vapor components along the channel walls but the channels are small enough to partially block the permeation of nitrogen or air (Pinnau, 1996). The gas separation using solubility-selective polymers was reviewed by Freeman and Pinnau (1997).

Gas permeation properties through polymer membranes generally have a trade-off: polymers that are more permeable tend to be less selective and vice versa. Robeson (1991) investigated the permselectivity of binary gas mixtures of He, H_2, O_2, N_2, CH_4 and CO_2 in various rubbery and glassy polymers and showed an “upper bound” in the membrane selectivity and permeability. The trade-off indicates possible limits of the separation performance of current generation of polymer membranes (Stern, 1994).

However, solubility-selective membranes for condensable gas separation may be an exception. When the favourable solubility selectivity overcomes the diffusivity selectivity, the membrane will yield a higher permeability for the larger, more condensable components because of the high solubility. Therefore, for these separations a well-designed material will be needed to achieve both a high permeability and selectivity. However, currently not many polymers can be used for these applications, and silicone rubber is essentially the only commercial rubbery membrane that has been used for vapor separations.

2.2.3 Determination of solubility and diffusivity coefficients

Diffusivity coefficient

For an ideal system where both the gas diffusivity and permeability coefficients are constant, the diffusivity coefficient is commonly determined by the gas permeation method, i.e., the time-lag method, which has been described extensively by Barrer (1939). From the Fick's second law, the amount of penetrant per unit membrane area (Q_t) passing through a membrane is given by the following equation if (i) the membrane is free of the penetrant molecules at the start of the permeation, (ii) the feed gas pressure (p_h) is kept constant, and (iii) the feed pressure is much larger than the permeate pressure.

$$\frac{Q_t}{l \cdot c_h} = \frac{Dt}{l^2} - \frac{1}{6} - \frac{2}{\pi^2}\sum_{n=1}^{\infty}\frac{(-1)^n}{n^2}\exp\left[\frac{-Dn^2\pi^2 t}{l^2}\right] \tag{2.8}$$

where c_h is the concentration in the membrane on the feed side. During the initial stage of permeation, Q_t increases as t increases, but not linearly (Figure 2.5). However, when $t \to \infty$, a steady state is approached and the Q_t vs. t plot becomes linear:

$$Q_t = \frac{Dc_h}{l}\left(t - \frac{l^2}{6D}\right) = \frac{DS}{l}p_h\left(t - \frac{l^2}{6D}\right) = \frac{P}{l}p_h\left(t - \frac{l^2}{6D}\right) \tag{2.9}$$

By extrapolating the steady state permeation curve, the intercept (θ) on the t-axis can be obtained, which is referred to as the time lag:

$$\theta = \frac{l^2}{6D} \tag{2.10}$$

Therefore, the gas permeability (P) and diffusivity coefficient (D) can be obtained from the slope ($\frac{P}{l} p_h$) and the intercept (θ) of the steady state permeation curve, and the gas solubility coefficient (S) can thus be determined from the relation $P=DS$.

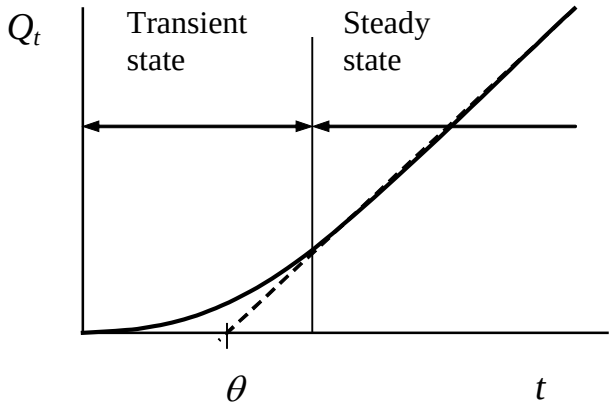

Figure 2.5 Time-lag measurement of gas permeation.

The diffusivity coefficient can also be determined from gas sorption kinetics (Crank and Park, 1967). When D is constant, two methods may be used, the short time and the long time methods. At short times (early stage of sorption), the plot of (M_t/M_∞) (normalized mass uptake, i.e., the ratio of sorption amount at time t over equilibrium sorption amount) vs. $(t/l^2)^{1/2}$ is a straight line, and the diffusion coefficient can be estimated from the slope $[4(D/\pi)^{1/2}]$ of the sorption uptake curve. When D is a function of concentration, the value so obtained is the apparent diffusivity coefficient. The short time method can be applied up to 50% (M_t/M_∞) with negligible deviations from the exact solution of the Fick's second law. For moderate and large times, the diffusivity coefficient can be obtained from the half time of sorption, the time that adsorption achieves the half amount of the maximum adsorption amount

$$D = \frac{0.04919}{(t/l^2)_{1/2}} \tag{2.11}$$

Normally the diffusivity coefficients obtained using the two methods are very close to each other (Rezac and John, 1998).

Using the data of gas permeability at different pressures and the sorption isotherms, the concentration dependence of the diffusivity coefficient may also be determined. For systems with concentration dependent solubility and diffusivity coefficients, the gas permeability coefficient P is the product of the average diffusivity coefficient $\overline{D}$ and solubility coefficient $\overline{S}$:

$$P = \overline{D} \times \overline{S} \tag{2.12}$$

where $\overline{D}$ is a mean diffusivity coefficient defined as:

$$\overline{D} = \frac{1}{c_h - c_l} \int_{c_l}^{c_h} D(c)dc \tag{2.13}$$

and $\overline{S}$ is a function defined by the relation:

$$\overline{S} = \frac{(c_h - c_l)}{(p_h - p_l)} \tag{2.14}$$

The subscripts *h* & *l* represent upstream and downstream of the membrane, respectively.

Therefore, the local effective diffusivity coefficient D could be derived using Eq. (2.15) when $c_l = 0$ (which is the case when high vacuum is applied at the downstream side of the membrane) (Koros et al., 1977; Koros and Chern, 1987).

$$D(c)\Big|_{p_h} = (P + p_h \cdot \frac{dP}{dp}) / \frac{dC}{dp}\Big|_{p_h} \tag{2.15}$$

This method has been used to estimate the diffusivity coefficients of gases and vapors permeating through polymeric membranes (Lin and Freeman, 2004; Singh et al., 1997; Merkel, 1999; Stern et al, 1987, Stannett et al., 1982).

A continuous-flow dynamic permeation technique has also been developed to measure the permeability coefficient and the concentration dependence of diffusivity coefficient, based on transient permeation (Waston and Payne, 1990; Waston and Baron, 1995; Kim, et al., 2001; Kim and Lee, 2001; Yeom et al., 2000, 2002). Unlike the integral technique of the "time-lag" method, the continuous-flow technique withdraws the permeate continuously, and the transient permeation flux is measured precisely. The diffusivity coefficient can be determined by either the half-time of the transient permeation stage or the maximum slope of the transient state in the plot of permeance vs. time. Additionally, this technique can be applied to the permeation of gas mixtures.

Barrer and Brook (1953) have used a “successively smaller intervals” method to determine the concentration dependence of the diffusivity coefficient based on the short time sorption by a series of sorption experiments. It is rarely used due to the substantially large amount of experimental work required and the complicated processes involved.

Solubility coefficient

Gas solubility in membranes can be determined by equilibrium sorption based on Eq. (2.2). There are two principal techniques to measure the equilibrium sorption uptake: gravimetric sorption and barometric (pressure-delay) techniques. Generally, gravimetric technique is suitable for the sorption of organic vapor and water vapor, which have relatively high sorption capacity and low saturated pressures (less than atmosphere). (Suwandi and Stern, 1973; Stannett et al., 1982; Cen et al., 2002; Enneking et al., 1996; Singh et al., 1997; Rezec et al., 1997). For gases with a low sorption capacity or when the sorption experiments need to be carried out at a relatively high pressure, the pressure-delay technique (also called the barometric technique) is often used (Shah et al., 1986; Lin and Freeman, 2004; Bondar, et al., 1999a; Bondar et al., 1999b; Michaels and Bixler, 1961; Merkel et al., 1999; Marchese et al., 2003). The system consists of two chambers with known volumes, a sample chamber and a reference chamber. The penetrant from the reference chamber is introduced into the sample chamber, and the pressure gradually decreases due to the sorption and then becomes constant when the sorption reaches equilibrium. By measuring the pressures at the start of sorption and at sorption equilibrium, the sorption capacity can be determined.

Both of the two techniques are affected by experimental errors caused by system leaking and wall adsorption as well as the accuracy of mass, pressure and volume measurements, especially when the sorption capacity is small. For permanent gases with a quite small sorption capacity, even barometric technique is hard to measure accurately. Recently, Bo et al. (2002) developed a “vapor phase calibration” method that used headspace to determine the solubility of gases and vapors. The solubility coefficient is calculated as a dimensionless partition coefficient determined by the equilibrium concentration of a compound in the membrane phase and in the gas phase. Though this technique is quite simple to determine the gas solubility in membranes, the reproducibility is poor for gases with low sorption capacities, and it is difficult to operate

at high pressures. In addition, the competitive adsorption of the penetrant with air in the membrane is not taken into account.

2.2.4 Gas transport in composite membranes

Asymmetric or composite membranes are used in most industrial gas separation processes in order to maximize the permeation flux by using a thin selective membrane layer. These membranes generally have a thin dense layer for selective permeation, supported on a porous substrate to retain the mechanical strength of the membranes. The selective layer and the substrate can be formed separately from different materials. Alternatively, they can also be formed simultaneously from the same polymer material so that the skin layer will be an integral part of the membrane. An extra layer from a highly permeable polymer, generally silicone rubber, is sometimes applied on the surface of the asymmetric or composite membranes to 'seal' the defects (Henis and Tripodi, 1980, 1981; Kesting et al., 1989, 1990), to protect membranes, or as a 'gutter' layer between the skin layer and the support layer of the composite membranes (Cabasso et al., 1986; Chung et al., 1999; Shieh et al., 1999, 2000). Two types of composite membranes are widely used, the "resistance model" composite membranes and thin-film composite membranes, as shown in Figure 2.6.

The concept of "resistance model" composite membrane was first presented by Henis and Tripodi (1980, 1981) and successfully used in hydrogen recovery from ammonia synthesis purge gas. The membrane consists of an asymmetric substrate (Loeb-Sourirajan phase inversion membrane) and a silicon-coating layer. The skin layer of the substrate is responsible for the separation while the porous substrate layer offers mechanical support. The coating layer is used to seal the defects on the surface of the asymmetric membranes. The mass transport through the membrane could be described in analogue to an electric circuit. Different electric circuit arrangements have been used to describe this type of membrane. All the models neglect the transport resistance of the porous support layer. In Henis and Tripodi's model, gas first permeates through the coating layer, and then splits into two parts: one through the polymer matrix and the other through the pores on the skin layer of the substrate. This means there is no resistance for

the "cross flow" at the interface between the coating layer and the substrate. This is true when the surface porosity of the asymmetric membrane is large enough. Considering the small surface porosity and the thin skin layer of the substrate, which are more realistic for the membranes used in industrial applications, an alternative parallel resistance model was addressed by Feng et al. (1989, 2002). One-dimensional mass transfer through the membrane was assumed in the model. In a study of laminate composite membranes, Fouda et al. (1991) noted that Henis and Tripodi's model was invalid, and a resistance model in analogue to the Wheatstone bridge was proposed. The resistance of the "cross flow" R_x was considered. Interestingly, the two aforementioned models are the special cases of the Wheatston bridge model. When R_x is zero, i.e., neglecting the resistance of the cross flow, the Wheatston bridge model is the same as the Henis and Tripodi's model, and when R_x is infinite, the model is in agreement with the parallel model.

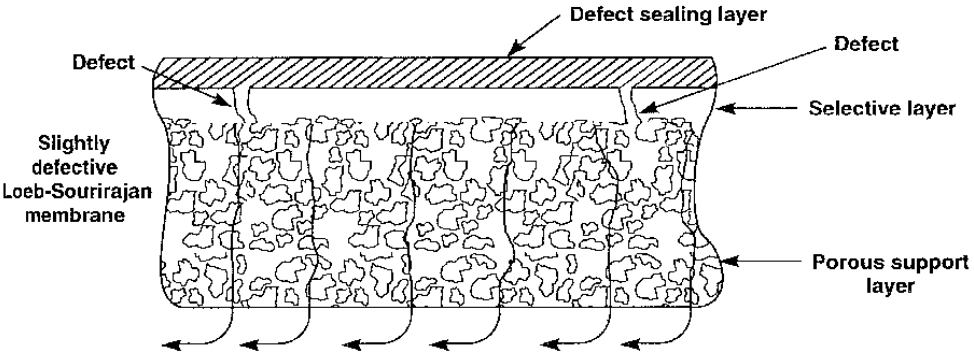

(a) "Resistance model" composite membrane

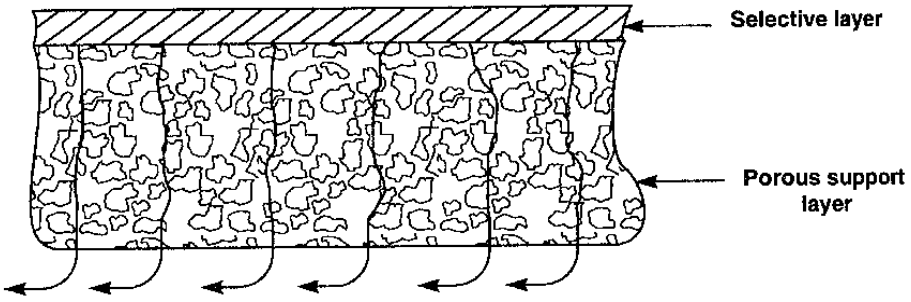

(b) Thin-film composite membrane

Figure 2.6 Composite membranes for gas separation (Baker, 2004).

Another type of composite membranes is the thin-film composite membrane. In this type of membranes, a thin dense selective film is coated on a porous support membrane, and the coating layer is made of materials that are different from the support layer. Additional layers of very permeable polymers such as silicone rubber may also be applied to protect the selective layer or to seal any defects. In general, it is difficult to form a defect-free selective layer as thin as that of the Loeb-Sourirajan asymmetric membrane. A potential drawback of the thin-film composite membranes is that they cannot withstand a high pressure difference as compared with the "resistance model" composite membranes due to the relatively large pore size and porosity of the support membranes as well as different degrees of swelling between the selective layer and the substrate caused by the sorption of the penetrant, especially when organic compounds are present. However, it is the most effective way to prepare thin-film composite membranes from rubbery polymers because of their low mechanical strength and the difficulty to form asymmetric structure from rubbery polymers. The relatively low mechanical strength can be improved by the use of the substrate support that can be formed from glassy polymers. In recent years, with the development of many high performance polymers, thin-film composite membranes have attracted attention because: (1) Only a limited number of materials can form high performance asymmetric membranes by the phase inversion technique; (2) Thin-film composite membranes are relatively easier to prepare than the Loeb-Sourirajian type of membranes; (3) The newly developed membrane materials are normally more expensive, which can cost $10-20/g or more (Baker, 2002). The Loeb-Sourirajian type of membranes need 40-60 g polymers per m^2 of membrane formed, while the thin-film composite membranes only use less than 1g per m^2 of membrane produced; (4) Except for a few special gas separation processes (e.g., hydrogen separation from ammonia synthesis purge gas and acid gas removal from nature gas) where the operating pressure is considerably high, a relatively low pressure (normally less than 2 MPa) is generally needed in most other applications. Therefore, the mechanical strength of the membrane is not very critical, and the membrane permeability and selectivity are thus the most important considerations.

For an ideal case of permeation through asymmetric or composite membranes, the mass transport resistance is dominated by the defect-free selective layer, and the

resistance of the support layer or other auxiliary layers can be neglected. In this case, the selectivity and permeance are determined mainly by the intrinsic property of the selective layer. This is true when the permeance of the penetrant is not too high. However, when the permeance of the penetrant through the membrane selective layer is very high, the resistance of the support layer cannot be neglected. This is the case for the permeation of fast permanent gases (H_2 or He) through membranes with ultra thin selective layer (less than 100 nm) or for the permeation of organic vapors or water vapor where the membrane is much more permeable than permanent gases. The influence of the support layer resistance becomes more significant when the average pressure across the membrane is low, especially when vacuum is applied to the permeate side. As mentioned before, gas permeation through a porous membrane consists of viscous flow and Knudsen flow. When the operating pressure decreases, (1) gas transport tends to change from viscous flow to Knudsen flow because of the increased mean free path of the gas molecules, leading to a lower flow rate; (2) the flow rate of viscous flow decreases because it is proportional to the average pressure across the pores. Therefore, the transport resistance of the support layer become larger as the operating pressure decreases. It is most unfavourable for organic vapor separation processes because an atmospheric pressure at the feed side and a vacuum at the permeate side are generally used.

Gales et al. (2002) investigated VOCs (acetone, ethyl acetate and ethanol) removal from air using three poly(dimethylsiloxane) (PDMS)/poly(etherimide) composite membranes manufactured by GKSS with different thicknesses of PDMS layers. The permeabilities of the VOCs decrease with a decrease in the thickness of the PDMS layers, while the permeabilities of N_2 and O_2 are almost the same for the three membranes. This indicates that the sub-layer has a non-negligible mass transfer resistance to VOCs permeation.

Clausi et al. (1999) characterized the substrate resistance by investigating fast/slow gas permeation (e.g. He/N_2) in defect-free composite membranes. A constant transmembrane pressure differential was applied while the average pressure within the membrane varied. If the permeance increases with system pressure at low pressures but eventually level off, it indicates that the resistance of the substrate is significant. The

substrate resistance gradually diminishes at high pressure because gas transport in the substrate transits to viscous flow.

Liu et al. (2001) presented water vapor permeation through a PDMS/PSf resistance model composite membrane. A high vacuum was applied at the permeate side. It was found that the mass transport resistance is mainly on the porous substrate instead of the skin layer of the asymmetric membrane. The effect of membrane structure on the resistance distribution for water permeation in the membrane was also investigated. This information has been used to tailor make membranes for enhanced dehumidification of gases by altering the membrane morphology and structure.

Beuscher et al. (1997, 1999) described the resistance of a VOC (trichloroethylene) permeation through the support layer of a thin-film composite membrane by a mathematic model, with both a sweep gas and vacuum modes of operation to withdraw permeate. The VOC permeation was again found to be dominated by the resistance of the support layer, while the coating layer permeability did not affect the overall membrane performance significantly. The supporting membrane described in the model has a porous skin layer and a more open substructure. It was found that more than a half of the resistance toward permeation was attributed by the thin porous skin layer.

Huang and Feng (1993) used a resistance model approach to analyze the selectivity of asymmetric membranes for pervaporation, and showed that the selectivity is influenced not only by the relative resistance of the skin layer and the substrate but also by the relative resistance of the polymer matrix and the pores in the substrate. Therefore, the development of high flux membranes should be directed at not only producing a thin skin layer but also reducing the substrate resistance.

2.3 Membrane formation

Dense homogenous membranes are frequently used in laboratory research to characterize the intrinsic permeation properties. They are normally prepared by the solvent casting or melt extrusion techniques. For the solvent casting technique, the polymer solution with a certain viscosity is cast on a flat plate followed by solvent evaporation at a given temperature. For polymers such as polyethylene, polypropylene and polyamide that are difficult to dissolve in solvents, the membranes can be produced

by the melt extrusion technique. The membranes are formed by compressing the polymers between two heated plates at a temperature just below the melt point of the polymers.

Most of the membranes for gas separations are asymmetric or composites membranes. These membranes have a very thin selective layer, formed by solvent casting or dipcoating, supported on a porous substrate so as to achieve a high permeation flux.

Asymmetric membranes

Asymmetric membranes are layered structures in which the porosity, pore size or the membrane composition changes gradually from one side to the other side of the membrane. The membranes are normally prepared by the phase inversion process, in which a polymer solution is separated into two phases: a solid, polymer-poor phase that forms the matrix of the membrane, and a liquid, polymer-poor phase that forms the pore of the membrane. The phase inversion technique has been described by Kesting (1985). Precipitation of polymers from a solution to form asymmetric membranes can be achieved in several ways: immersion precipitation, water vapor phase precipitation, thermal gelation and solvent evaporation. Immersion precipitation is the most common technique to prepare asymmetric membranes, which was first developed by Loeb and Sourirajan in the 1960s. The cast polymer membrane is immersed into a nonsolvent (generally water or an aqueous solution) and the polymer precipitates as a result of solvent and nonsolvent exchange. A relatively dense layer forms on the surface of the membrane due to the fast polymer participation. Depending on the component and content of the polymer solution and the casting conditions, the membrane can be formed for various applications. Gas separation membranes consist of a dense surface layer on the top of a microporous substrate, while ultrafiltration membranes have a fine microporous membrane surface with more open porous structure.

Composite membranes

Composite membranes are formed primarily for two reasons: to seal the defects on the surface of asymmetric membrane (“resistance model” composite membrane), or to form a dense selective layer on the top of a porous substrate (thin-film composite

membrane). Several methods have been developed to prepare composite membranes: solution coating, interfacial polymerization, thin-film lamination and plasma polymerization.

Solution coating is the simplest method suitable for most polymers. Almost all the "resistance model" composite membranes and most thin-film composite membranes are prepared by this method. The membrane formation is similar to the aforementioned solvent casting technique for the preparation of homogenous membranes, except that more dilute polymer solutions are used. The polymer solution can be cast onto an asymmetric porous substrate, and the substrate membrane can also be directly dipped into the polymer solution followed by an appropriate drying process, thereby forming a thin coating layer on the surface of the substrate. For the 'resistance model' composites membranes, vacuum is often used to force the coating polymer to enter the surface pores of the substrate to seal (or 'plug') defects. For thin-film composite membranes, the penetration of the coating solution into the pores of the support membrane may lower the performance of the composite membranes. It will not only result in extra resistance of the substrate to gas permeation but may also lead to defects on the coating layer due to the failed bridging of the coating layer on the pores of the substrate. A defect-free coating layer depends on the properties of the coating solution (e.g. viscosity), coating conditions (e.g. temperature, and coating time), affinity between the coating solution and the substrate, and the state of the substrate (e.g. pre-wetting, surface pore size and pore size distribution). During membrane preparation, there is normally a trade-off between the membrane thickness and surface integrity.

Interfacial polymerization, plasma polymerization and thin-film lamination can also be used to prepare thin-film composites membrane without or with little solution penetration, but these methods are not suitable for all polymers. The composite membrane prepared by lamination approach is suitable for transport studies since the thickness of the lamination layer can be determined easily. This type of membranes was first developed by Ward et al. (1976, 1981) of General Electric. A dilute polymer solution (such as silicone rubber) with a volatile water-insoluble solvent is spread over the surface of a water-filled trough. After solvent evaporation, membranes as thin as 0.1-0.2 μm were obtained. The membranes were used for oxygen/nitrogen separation in the 1970s. Similar

methods were developed to prepare ultrathin membranes from polymer blends of silicone/polycarbonate copolymer with polymethylpentene (Kimura et al., 1979) and with poly(phenylene oxide) (Ward et al., 1983).

2.4 Processes and applications

Membrane gas separation involves in both non-condensable gas separation and condensable gas and vapor separation. Non-condensable gases (or permanent gas) are those gases with a critical temperature lower than the room temperature, and they do not condense even when a very high pressure is applied at room temperature (e.g. H_2, N_2, O_2 and He). In contrast, condensable gases are the gases or vapors that could be condensed at the room temperature. Most membrane processes for non-condensable gas separation (such as hydrogen separation and air separation) have been well established, while processes for condensable gas separation, including CO_2 separation, organic vapor separation and gas dehydration, are being developed or to be developed. Table 2.1 summarizes the membranes and membrane modules for a few gas separation applications. The main gas separation processes and applications have been reviewed by Baker (2002, 2004), Koros and Fleming (1993), and Paul and Yampol'skii (1994).

Table 2.1 Membranes and membrane modules for various gas separation applications (Baker, 2004)

Application	Typical membrane material	Selectivity (α)	Permeance (GPU*)	Module design commonly used
O_2/N_2	Polyimide	6-7	1-2	Hollow fiber
H_2/N_2	Polysulfone	100	10-20	Hollow fiber
CO_2/CH_4	Cellulose acetate	15-20	2-5	Spiral or hollow fiber
VOC/N_2	Silicone rubber	10-30	100	Spiral
H_2O/Air	Polyimide	>200	5	Capillary — bore side feed

* 1 GPU = 10^{-6} cm^3 (STP)/cm^2.s.cmHg, or 3.35×10^{-10} mol/m^2.s.Pa in SI unit.

2.4.1 Non-condensable gas separation

Hydrogen separation

Hydrogen separation from N_2 in ammonia synthesis purge gas streams is the first large-scale commercial application of membrane gas separation. Hydrogen is a small, non-condensable gas, which is highly permeable compared with other gases in glassy polymers. Polysulfone and cellulose acetate are the membrane materials used for hydrogen separation in the early days, and now a variety of membrane materials are being used, including polyimides (Ube, Praxair), polyaramide (Medal) or brominted polysulfone (Permea) (Baker, 2004).

Recently, large scale applications of hydrogen recovery have been extended to waste gases (refinery fuel gas stream, PSA vent gas and hydrocracker/hydrotreater off-gas) in refinery plants because of the increase in hydrogen demand in refineries with ever increasingly stringent environmental regulations and heavier crude feed stocks. The problems that affect this application are the membrane reliability, caused by fouling, plasticization and condensation of hydrocarbon vapors on the membrane surface. These problems may be resolved by either developing more robust membranes or using better pre-treatment techniques to reduce the dew point of the hydrocarbon in the feed gas streams to be treated by membranes.

Oxygen/nitrogen separation

The production of nitrogen from air is by far the largest membrane gas separation process. The current membranes have O_2/N_2 selectivities up to 8, and can generate a 99% nitrogen product at an overall nitrogen recovery of 50% at an operating pressure of 0.8 – 1.0 MPa.

It is much more difficult to produce high-purity oxygen from air than high-purity nitrogen because of the low concentration of oxygen in feed than nitrogen and the oxygen product is in the permeate side of the membrane. The maximum possible oxygen concentration is only 68% by a one-step membrane process with an O_2/N_2 selectivity of 8. To be competitive with current cryogenic technology, membranes with both a high selectivity and a high flux are required. Facilitated transport membranes are one of approaches to improve the membrane permselectivity. In these membranes, an oxygen-

complexing carrier compound acts as a “shuttle” to selectively transport oxygen across the membrane (Figoli, 2001). However, the stability of the carrier is still an issue for large scale applications.

2.4.2 Condensable gas and vapor separation

Carbon dioxide separation

Both glassy polymers and rubbery polymers can be used for CO_2 separation, taking advantage of their mobility selectivity and solubility selectivity, respectively. In practice, glassy polymer membranes are usually used for the separation of CO_2 from natural gas. In spite of the simple flow configuration and low maintenance, only small-scale membrane systems can compete with traditional amine absorption systems mainly because of the limited selectivity and flux of current membranes. Membrane swelling caused by carbon dioxide and hydrocarbons will significantly lower the membrane selectivity. Currently, cellulose acetate membranes only have a selectivity of 12-15 for CO_2/N_2 under the normal operating conditions. These membranes are now slowly replaced by the more selective polyimide and polyamide membranes whose selectivities are in the range of 20-25.

Another application of increasing interest is the separation of CO_2 from flue gases. The emission of carbon dioxide from combustion flue gas is a major contributor to global warming, and the capture/separation of carbon dioxide from flue gas is an important step for greenhouse gas emission control. Membrane process is very efficient for bulk separation where a very high purity is not required, which makes membrane process particularly attractive for flue gas separation. Membrane gas separation is a pressure driven process, where a pressure difference across the membrane should be maintained to provide the driving force necessary for permeation. For this process, a critical issue is the energy used to power the compressors or vacuum pumps for the separation. The quantity of flue gas to be treated is very large with relatively low source pressure. Increasing the operating pressure will increase the membrane productivity, but this is at the expenses of increased compression costs. Considering the cost of gas compression, membranes with a high permeance and reasonable selectivity are needed in order to make the separation process economical.

Vapor/gas separation

In the separation of vapor/gas mixtures, in principle, either rubbery polymers (such as silicone rubber, which can selectively permeate the more condensable vapor) or glassy polymer (which can permeate the smaller gas preferentially) can be used. In most industrial applications, vapor permeable rubbery membranes are used because of their both high permeation flux and selectivity. To achieve a target product concentration and recovery, either multi-stage membrane systems or hybrid systems combining vapor permeation with condensation or sorption are often used.

Figure 2.7 shows a hybrid design of membrane separation combined with condensation for propylene recovery from resin degassing vent gas in polypropylene plant. In this design, the compressed feed gas enters a condenser, where a portion of the propylene is removed as a condensed liquid. The remaining uncondensed gas is admitted to the membrane systems. A high concentration nitrogen stream (>98% nitrogen) is obtained in the residue stream, which can be reused in the resin degassing. The hydrocarbon enriched permeate gas is recycled to the system for enhanced recovery. The separation efficiency depends on the membrane selectivity, the temperature of the condenser as well as the pressure. From an energy consumption point of view, it is not suitable to operate the condenser at a very low temperature or the compressor at a vey high pressure. Therefore, the membrane selectivity is a key factor determining the efficiency of the system. Currently, the only commercial membrane for this application is silicone rubber, which only has a vapor/gas selectivity in the range of 10-30, as shown in Table 2.1. The membranes with higher selectivities are required in order to achieve a better process efficiency. Even if a highly selective membrane has a lower permeability than silicon rubber, the cost of increased membrane area requirement can be offset by the decreased sizes of the compressor and the condenser. Additionally, one advantage of the hybrid membrane/condenser system is that the low temperature of the feed streams from the condenser favors the membrane selectivity because the solubility selectivity generally increases with a decrease in the temperature.

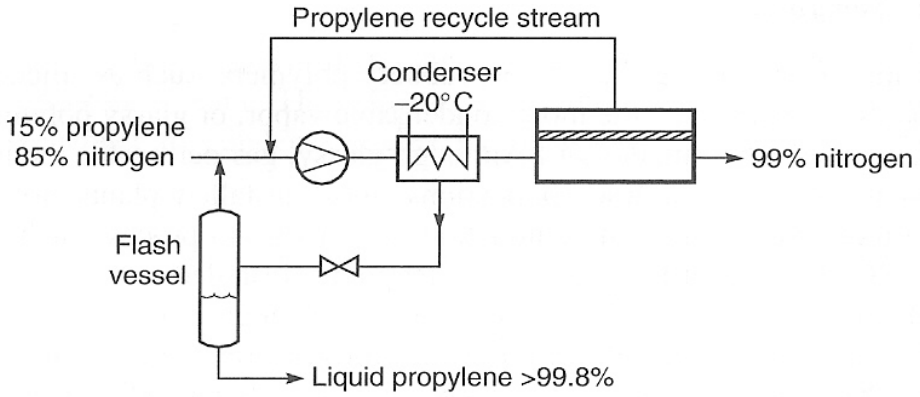

Figure 2.7 Hybrid compression-condensation-membrane design for propylene recovery from resin degassing vent gas in polyolefin plant (Baker, 2004).

Paraffin/oleffin separation

Membrane is a promising technology for the separation of light olefin from their associated paraffins because the currently used low temperature distillation is capital- and energy-intensive due to the similar volatilities of the components in the mixtures. Some work has been done using the traditional solution-diffusion membranes, such as polyimide (Staudt-Bickel, 2000; Krol, 2001). The selectivities are, however, low because of membrane plasticization, and there is a substantial loss in the selectivity under the plant operating conditions. Facilitated transport membranes have received much attention as a potential technology for olefin/paraffin separation. They are based on selective and reversible reaction of unsaturated hydrocarbons with certain metal ions by π-complexation. The metal ions act as a carrier for the olefin transport, thereby facilitating the permeation of olefin through the membrane. Membranes made from polymer electrolytes of poly(ethylene oxide) and $AgBF_4$ have shown a very high permeability and selectivity for olefin/paraffin separation (Pinnau, et al., 1997, 2001). However, this type of membranes suffers from problems associated with the membrane stability (Park et al., 2003; Liu et al., 2004). Further efforts are needed to improve the membrane stability before they can be used for commercial applications.

2.5 Poly(ether block amide) membranes

Poly(ether block amide) (PEBA), a thermoplastic elastomer comprising of hard polyamide and soft polyether, is produced by a molten state polycondensation reaction from a dicarboxylic polyamide and a polyether diol. The copolymer consists of a linear chain of polyamide segments interspaced with polyether segments, having the following general chemical formula:

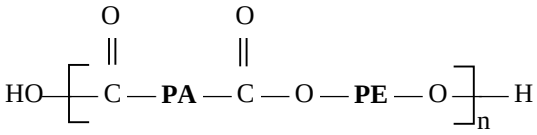

where PA and PE represent the polyamide and polyether segments, respectively. In the segmented block copolymer, there are two microphase-separated domains: the polyamide crystalline domains provide mechanical strength, and the polyether amorphous domains offer high permeability due to the high chain mobility of the ether linkage (Joseph, 1986; Elf Atochem).

The specific properties of a PEBA polymer are affected by the chemical nature and the relative content of the polyamide and polyether segments. Different grades of PEBA polymers are commercially available, and they generally have excellent mechanical strength and good chemical resistance. Table 2.2 shows the properties of some grades of PEBA copolymers. Several types of polyamide can be used to synthesize the PEBA, including nylon 6, nylon 66, nylon 11, nylon 6/11, nylon 12 and nylon 6/12, while the available polyethers include poly(ethylene glycol), poly(propylene glycol) and poly(tetramethylene ether glycol). The properties of each segment affect the overall properties of the PEBA copolymers. The type and the molecular weight of a polyamide affect its melting point T_m and its chemical resistance of the copolymer, while the type of polyether influences the glass transition temperature T_g of the copolymer. Interestingly, the copolymers retain a high T_m of polyamide, in the range of 120 ^oC to 210 ^oC, and a low T_g of polyether (-60^oC to -70^oC). The relative amount of polyamide and polyether determines the hardness and flexibility of the copolymer (Joseph, 1986). Table 2.2 shows the chemical components and the physical properties of a few PEBA copolymers.

Because of the micro-biphasic structure, PEBA copolymers offer many properties that are not readily available in either constituent polymer. PEBA not only has favourable

membrane-forming properties but also good chemical resistance to acid, basic and organic solvents and high thermal and mechanical stability. There have been some studies on gas permeation and pervaporation with membranes made from certain grades of PEBA copolymers.

Table 2.2 Chemical component and physical properties of some grades of PEBA (Kim et al., 2001; Bondar et al., 2000; Rezac, et al., 1997, 1998).

Grade	PA[a]	PE[b]	PE content (wt%)	Density (g/m^3)	T_g (^oC)	T_m (^oC)
2533	PA12	PTMO	80, 78.4	1.01	-77, -76	126, 137
3533	PA12	PTMO	70, 72.9	1.01	-72	155, 142
4033	PA12	PTMO	47, 44	1.01	-78	180, 159
5533	PA12	PTMO	37.8	N/A	-65	160
6333	PA12	PTMO	24.2	N/A	-60	170
1074	PA12	PEO	45	1.09	-55	156
4011	PA6	PEO	43	1.14	-53	201
1657	PA6	PEO	60	1.14	N/A	204

a. PA12 and PA6 represent polyamide (nylon) 12 or polyamide 6, respectively.
b. PTMO is poly(tetramethylene oxide) and PEO is poly(ethylene oxide).

Kim et al. (2001) investigated the effect of the chemical composition of PEBA copolymers on the permeation behavior of polar and nonpolar gas pairs such as CO_2/N_2 and SO_2/N_2. For small and nonpolar gases, the permeability was shown to decrease with an increase in the size of the gas permeant. For polar gases, however, a high permeability was observed because of their strong affinity to the polyether block in the PEBA copolymer.

Bondar et al. (2000) studied the permeation properties of H_2, N_2 and CO_2 through a series of PEBA copolymers and also observed extremely high selectivities for polar (or quadrupolar)/nonpolar gas pairs with a high CO_2 permeability. In the copolymers with higher concentration of polar groups, the selectivities of CO_2 /N_2 and CO_2/H_2 are higher.

The high selectivity derives from the large solubility selectivity in favor of CO_2. Furthermore, the permeability increases with an increase in the amount of polyether. Gas permeability is higher in polymers with less polar constituents, PTMO and PA12, than in those containing the more polar PEO and PA6 units. Bondar et al. (1999) also investigated gas sorption in a series of PEBA copolymers. The sorption isotherms for less soluble gases (He, H_2, N_2, O_2 and CH_4) are linear while they are convex to the pressure for more soluble gases (CO_2, C_3H_8, and n-C_4H_{10}). The high solubility selectivity of CO_2/N_2 and CO_2/H_2 is also observed. When the amount of polyether in the copolymer increases, the solubility of CO_2 increases. The gas solubility is higher in polymers with less polar constituents (PTMEO and PA12) than the polymer with more polar PEO and PA6 units. The selective sorption is consistent with the selective permeation, which indicates that sorption dominates the gas permeation in the PEBA membranes.

Liu et al. (2006) reported on the separation and recover gasoline vapors from nitrogen by membranes for emission control. Hollow fiber composite membranes comprising of a thin PEBA skin layer supported on a microporous poly(vinylidene fluoride) substrate were used. It was found that the membranes are effective for the recovery of gasoline vapor, but the composition profile of the recoverd gasoline was different from the gasoline in the feed gas.

Chen et al. (2004) studied the permeation of several gases through PEBA 2533 membranes. The membranes showed a high permeability to light hydrocarbons. Experiments with propane and propylene permeation showed a strong plasticization effect on PEBA copolymer matrix.

Rezac et al. (1997, 1998) studied sorption and diffusion of water and methanol vapors in series of PEBA membranes to study the possibility of separating hazardous air pollutant methanol from wet air streams, and PEBA 2533 was found to be most promising due to its high solubility and diffusivity. One unique property of PEBA 2533 polymer related to permeation is its rather high fractional free volume, which was determined to be 0.172 (Rezac et al., 1998). Moreover, a good linear relation between the logarithm of the diffusion coefficient and the inverse of the fractional free volume of several grades of PEBA copolymers was observed.

Besides gas separation, about two-third of the research work reported on PEBA membranes are related to pervaporation for the enrichment or removal of organic compounds (e.g. esters, phenols and other pollutants from dilute aqueous solutions) because of the organophilic properties of the copolymers. PEBA membranes exhibit excellent permselectivity for the separation of aroma compounds (Sampranpiboon et al., 2000; Baudot et al., 1999).

Table 2.3 summarizes the research work on PEBA membranes, including gas permeation, pervaporation, and sorption/diffusion of gases and vapors. It can be seen that most of work uses relatively thick PEBA homogenous membranes prepared by either solvent casting or melt extrusion technique. Considering that membrane permeation is a rate-controlled process, from an application point of view, composite membranes with thin selective layer are favourable for gas permeation. Besides, all of the studies use flat sheet membranes, and no work has been done on hollow fiber membranes that offer high processing capacity per module volume, which is desired feature for practical applications. Furthermore, as shown in Table 2.3, most work focuses on polar/nonpolar gas separations (i.e., CO_2/N_2, CO_2/H_2 and SO_2/N_2), but little work is done on the separation of condensable light hydrocarbons or VOCs, although PEBA is found to have good permselectivity (Chen, 2004). Additionally, almost all the studies reported in the literature are concerned with pure gas permeation, and pure gas permeability is used to characterize the membrane performance. However, it is known that the interactions between the permeant and the polymer matrix and the membrane plasticization by the penetrants affect the permeability and selectivity of the membrane for gas mixture permeation. The pure gas permeability cannot be taken for granted in evaluating the membrane performance for gas separations especially when the gas mixtures to be separated contain polar components, light hydrocarbons and other volatile organic compounds.

In light of the above, this study addresses the development of PEBA thin film composite membranes and hollow fiber membranes, and their applications for the separation of gas mixtures containing CO_2, light hydrocarbons and other condensable organic vapors. PEBA 2533 is chosen for the proposed research because: (i) It has a considerably large volume offered by the large amount polyether segments in the

copolymer, which favors the permeation of the condensable gases and vapors; (ii) It has the best membrane formation properties among all the PEBA copolymers presently available.

Table 2.3 PEBA for membrane separation

Subject	Grade of PEBA	Membrane formation*	Membrane thickness (μm)	Reference
Gas separation: VOCs/N_2	2533	dip coating	N/A	Y. Liu et al. (2006)
Gas permeation: C_3H_6, C_3H_8, C_2H_4, C_2H_6, CO_2, and N_2	2533	solvent cast	20	Chen et al. (2004)
Gas permeation: H_2, CO_2, N_2 and He	2533, 3533, 4033, 1074, 4011	solvent cast	50-200	Barbi et al. (2003)
Gas permeation: CO_2, SO_2, N_2, O_2, He and H_2	2533, 3533, 4033, 1657	solvent cast	N/A	Kim, et al. (2001)
Gas permeation and separation: H_2, CO_2, CO and H_2S/H_2	2533, 3533	melt extruded	340-390	Wilks & Rezac (2001)
Gas permeation: CO_2, H_2 and N_2	2533, 4033, 1074, 4011	solvent cast / melt extruded	25-36	Bondar et al. (2000)
Vapor sorption and diffusion: methanol, water	2533, 3533, 5533, 6333	melt extruded	125-470	Rezac et al. (1997, 1998)
Gas sorption: H_2, N_2, O_2, CO_2, CH_4, C_2H_6, C_3H_8, and n-C_4H_{10}	2533, 4033, 5533, 1074, 4011	solvent cast	100	Bondar et al. (1999)
Gas separation: C_2H_4/C_2H_6	2533, 4011-$AgClO_4$	dip coating	2-3	Muller et al. (2002)
Gas permeation: CO_2, O_2, N_2 and He	1657-silica	solvent cast	N/A	Kim & Lee (2001)
Pervaporation: phenol/H_2O	4033	N/A	80	Kujawski et al. (2004)
Pervaporation: MTBE, BuAc, MeAc/ H_2O	4033	solvent cast	N/A	Kujawski et al. (2003)
Pervaporation: ethyl propionate/H_2O	3533	N/A	85	Favre (2003)
Pervaporation: TCE, ethylbenzene and MTBE/H_2O	N/A	N/A	N/A	Urkiagas et al. (2002)

Table 2.3 Continued

Pervaporation: ethylbutanoate/H_2O	3533/4033	solvent cast (dense/composite)	10-25	Jiraratananon et al. (2002)
Pervaporation: ethybutyrate, isopropanol /H_2O	3533	solvent cast	100±10	Sampranpiboon et al. (2000)
Pervaporation: aromatic compounds/ H_2O	40	N/A	70	Baudot et al. (1999)
Pervaporation: ester/H_2O	N/A	solvent cast	100	Djebbar et al. (1998)
Pervaporation: phenol/H_2O	N/A	N/A	N/A	Kondo & Sato (1994)
Pervaporation: phenol/H_2O	N/A	N/A	100	Boddeker et al. (1992)
Pervaporation: phenol/H_2O	5533	hot melt coat	45-180	Matsumoto et al. (1992)
Pervaporation: toluene, TCE and methylene chloride/H_2O	N/A	N/A	N/A	Ji et al. (1994 a, b)
Vapor permeation & sorption: benzene, hexane, cyclohexane	4033	N/A	100±20	Friess et al., (2004)
Vapor sorption of for pervaporation: water, alcohol, alkanes, aromatics, chlorinated hydrocarbons and ethers	N/A	solvent cast / melt extruded	25-30	Cen et al. (2002)
Sorption isotherms for pervaporation: aromatic compound/H_2O	4033	N/A	N/A	Groß & Heintz (1999)
Vapor/liquid sorption for pervaporation: benzene, cyclohexane, cyclohexane	N/A	N/A	N/A	Ennecking et al. (1996)
Diffusion coefficient for dialysis: aromatic compounds	4033/4033PE	solvent cast / N/A	100±20	Groß & Heintz (2000)

* All the membranes are homogenous dense flat membranes unless specified otherwise.

CHAPTER 3
A Novel Method of Preparing Ultrathin Poly(ether block amide) Membranes

3.1 Introduction

As presented in Chapter 2, PEBA membranes have exhibited good permselectivity and hold promise for certain applications in gas separations. However, in most of the previous studies, relatively thick (20 – 470 μm) (see Table 2.3) homogeneous membranes prepared by the melt extrusion or solvent casting technique were used. For practical applications, thin membranes in the form of asymmetric and/or composite membranes are desired to reduce the membrane resistance and achieve a high permeation flux. PEBA 2533, a rubbery polymer, is difficult to form an integrally asymmetric membrane with sufficient mechanical strength by the phase inversion technique. The use of composite membranes, where a thin selective skin layer is supported mechanically on a microporous substrate that is prepared separately and often from glassy polymers, is an alternative approach. As mentioned in Chapter 2, the composite membrane can be formed by dip coating, interfacial polymerization, plasma polymerization or thin film lamination. Blume and Pinnau (1990) disclosed a method of preparing composite PEBA membranes by coating the PEBA solution on a porous substrate followed by evaporation of the solvent to dry the membrane.

In this chapter, a new method of preparing thin PEBA 2533 membranes is developed on the basis of surface thermodynamics. The copolymer solution is spread on the surface of water using a solvent that has sufficient solubility in water. The membrane formation is caused by simultaneous solvent evaporation and solvent exchange with the support liquid (i.e., water). The various parameters involved in the procedure of

membrane formation (including the selection of suitable solvents, and the concentration and temperature of the polymer solution) were investigated. The solvent–nonsolvent exchange during membrane formation was investigated in order to provide an insight into the mechanism of the membrane formation. The membranes were tested for gas permeation, and it was shown that the membranes were defect-free and could be used for gas separations.

3.2 Experimental

3.2.1 Materials

Poly(ether block amide) 2533, comprising 80 wt% of poly(tetramethylene oxide) and 20 wt% of poly[imino(1-oxododecamethylene)] (nylon 12), was supplied by Atofina Inc. (now Arkema Inc.) in the form of elliptic pellets. Isopropanol (from EM Science), *n*-butanol (from Fisher Scientific), 1,1,2-trichloroethane and *N*, *N*-dimethyl acetamide (both from BDH Chemicals) were used as the solvent for preparing PEBA solutions. They were all of reagent grade and used as received. The ultrathin PEBA membranes were supported by microporous substrate membranes, which were prepared from Udel P-1700 polysulfone (Amoco Performance Products, OH) by the phase inversion technique using *N*-methyl-2-pyrrolidone and polyvinylpyrrolidone (average molecular weight 40,000) as the solvent and additive, respectively. The latter two chemicals were obtained from Aldrich Chemical. All gases used in the permeation experiments were of research grade (99.8–99.999% pure), and they were acquired from Praxair Specialty Gases and Equipment.

The materials mentioned above were also used in other parts of the thesis work, unless specified otherwise.

3.2.2 Membrane preparation

A predetermined amount of PEBA 2533 was dissolved in a solvent or a mixture of solvents to form a polymer solution. The polymer solution was stirred vigorously at 80 °C for over 4 days until a homogeneous solution was formed. It was allowed to stand without disturbance for at least 24 h to remove gas bubbles. The solution was then kept at given constant temperatures at which the membrane would be cast.

To prepare PEBA membranes by spreading the polymer solution on water surface, one or two drops (weighing about 0.01– 0.03 g) of the polymer solution was gently dripped by a capillary pipette onto the surface of deionized water in a dust free environment, as shown schematically in Figure 3.1. The tip of the pipette was held sufficiently close (a few mm) to the water surface so as to minimize the disturbance that would be caused to water surface by the dripping of the polymer solution. When a solvent with suitable surface energy was used, the polymer solution would spread quickly and spontaneously on the water surface, during which process the solvent exchanged with the nonsolvent water, resulting in the formation of a very thin PEBA membrane floating on the water surface. The PEBA membrane on water surface was picked up carefully by lowering an O-ring made of a Teflon sheet onto the PEBA membrane until the edge of the membrane adhered to the O-ring, and then lifting the O-ring that held the membrane. To insure an accurate measurement of the membrane thickness, 5 – 10 layers were laminated to determine the average thickness of an individual membrane layer.

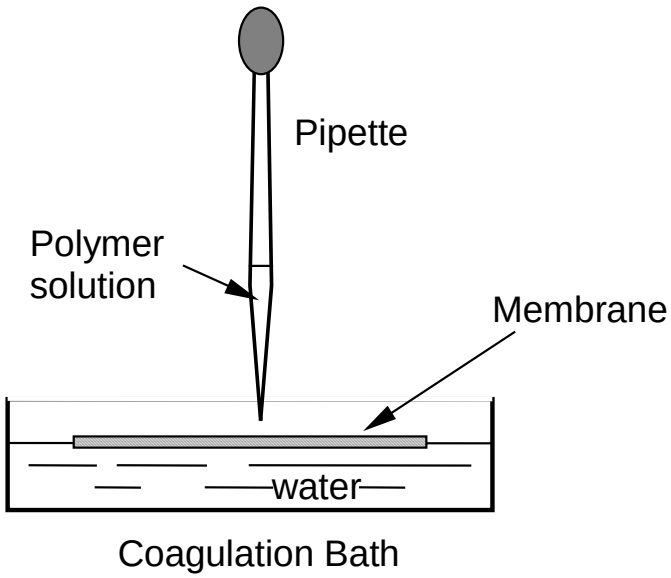

Figure 3.1 Schematic diagram of solution spreading on water surface

As the PEBA membrane so formed was very thin, it was decided to support the PEBA membrane externally during the permeation test by a microporous substrate membrane, which was prepared by the conventional "wet" phase inversion technique. A

homogeneous solution containing 15 wt% polysulfone and 5 wt% poly(vinyl pyrrolidone) in *N*-methyl-2-pyrrolidone was cast onto a nonwoven fabric, followed by immersion into deionized water. The resulting polysulfone membrane was then air-dried (thickness ~140 μm, excluding the thickness of the nonwoven fabric). Laminated PEBA 2533/polysulfone membranes were dried at 70 °C overnight prior to gas permeation tests.

It would be of interest to compare the permselectivity of the thin membrane with that of a thick dense membrane. Hence dense films of PEBA 2533 were also prepared by the solvent evaporation technique using 5wt% PEBA polymer solution (mixture of isopropanol/n-butanol in 3:1 weight ratio as the solvent). Basically, the polymer solution was cast onto a clean glass plate, followed by complete evaporation of the solvent at 70 °C in an oven for 1 day. Then the membrane was peel off from the glass plate, followed by complete drying at 50^{o}C under vacuum for 2 days to remove any residual solvent. The thickness of the resulting membrane was determined to be about 50 μm.

3.2.3 Solvent-nonsolvent exchange during membrane formation on water surface

In screening suitable solvents for membrane formation, a mixture of isopropanol and *n*-butanol was found to be the most appropriate solvent for making PEBA membranes. The rate of solvent (i.e. isopropanol and *n*-butanol) diffusing into water during membrane formation was investigated by measuring the concentration of the solvent in the water bath at different periods of time. After the polymer solution was spread on the surface of water for a given period of time, the membrane formed on the water surface was removed, and the water bath stirred to make it homogeneous. The total concentration of solvent in the water bath was then analyzed by a Shimadzu TOC 500 total organic carbon analyzer. This process was repeated numerous times to determine the quantity of the solvent diffusing into water at various spreading times during the course of membrane formation. Throughout the solvent exchange experiments, the area of water surface and the amount of water used remained the same, and the quantity of the polymer solution, though difficult to control precisely, was kept relatively constant.

3.2.4 Gas permeation test

The permeance of the composite membranes and the thick dense membranes for pure gas permeation was measured with carbon dioxide, oxygen and nitrogen using the conventional constant pressure/variable volume technique. The feed gas at a specific pressure was admitted to the membrane cell to contact with the PEBA layer of the membrane, and the permeate stream exited the permeation cell at atmospheric pressure. The permeation rate was determined volumetrically using a bubble flowmeter. The effective area for permeation was 13.85 cm^2.

3.3 Results and discussion

3.3.1 Membrane formation

3.3.1.1 Factors affecting membrane formation

When a slightly soluble liquid A is placed on the surface of a liquid B, there exist two possibilities as to what may happen: to form a lens or spreading. The criterion of spreading is determined by the spreading coefficient $S_{A/B}$ of A on B, which gives the free energy for the spread of a film of liquid A over liquid B, expressed by eqn. (3.1).

$$S_{A/B} = \gamma_B - \gamma_A - \gamma_{AB} \tag{3.1}$$

where γ_A and γ_B are the surface tension of liquid A and B, respectively, and γ_{AB} is the interfacial tension between A and B. If spreading is accompanied by a decrease in free energy, $S_{A/B}$ is positive, i.e., spreading is spontaneous. This typically happens when liquid A with a lower surface free energy is placed on liquid B with a relatively higher surface free energy (Adamson and Gast, 1997).

It is thus expected that if liquid A is a polymer solution comprising water-miscible solvent and water-insoluble polymer, it will spread when placed on the surface of water. During this process the two liquid phases are in contact to form an interfacial layer, and there will be mutual diffusion between water and the solvent in the polymer solution. Because of the limited solubility of the polymer in water, the polymer will precipitate to form a thin layer of polymer membrane floating on the water surface if the density of the polymer is not much higher than that of water. This is the basis of preparing thin PEBA membranes in the present study.

Obviously, as one anticipates, the membrane formation will be affected by numerous parameters, including the viscosity of the polymer solution, the solubility of the polymer in the solvent, the surface thermodynamic properties (e.g., surface tensions) of the solvent, the miscibility between the solvent and nonsolvent (i.e., water), and the densities of the spreading solution and water. For a given membrane casting system, some of the parameters are determined primarily by the compositions and temperatures of the polymer solution and the liquid on which the polymer solution spreads. These are the membrane preparation parameters that can be adjusted and controlled during membrane formation. Water was used as the trough liquid in this study because (i) it has a high surface tension (required to achieve solution spreading), (ii) it is a nonsolvent to the polymer (for polymer coagulation and precipitation), and (iii) it has a fairly good mutual solubility with certain solvents that can dissolve the polymer (for efficient exchange with nonsolvent to induce polymer precipitation).

Four common solvents (listed in Table 3.1) were chosen for preparing PEBA solutions in the screening experiments. They can dissolve the PEBA 2533 polymer at elevated temperatures (2 – 10 °C below their boiling points). Their physical properties relevant to membrane formation are summarized in Table 3.1. Although 1,1,2-trichloroethane was reported to be a stronger solvent for PEBA 2533 than other alcohol solvents (Kim et al., 2001; Blume and Pinnau, 1990), it was found that the PEBA 2533 solution with 1,1,2-trichloroethane as the solvent could hardly spread on water surface. This can be explained as follows. Thermodynamically, for a liquid (A) to spread spontaneously on another (B), not only should the surface tension of B be greater than that of A, but the surface tension difference should also be large enough to overcome the interfacial tension between the two liquids based on eqn. (3.1). In addition, if the two liquids have poor mutual solubility, they will soon become mutually saturated when they are in contact, and thus the rate of solvent–nonsolvent exchange is restricted, which tends to retract the spreading of the liquid. The surface tension of water at 25 °C is 71.98 mN/m. Comparing the solvents listed in Table 3.1, one can thus see that 1,1,2-trichloroethane has the least favorable surface tension and solubility properties. As a matter of fact, it was observed that when a drop of the PEBA in 1,1,2-trichloroethane

solution was placed on water, it neither spread nor floated on the water surface; instead, it settled down due to its higher density than water.

N, *N*-Dimethyl acetamide is a very common solvent used in membrane synthesis. Its surface tension is similar to that of 1,1,2-trichloroethane. In spite of the good mutual miscibility between water and *N*, *N*-dimethyl acetamide and the preferred lower density of *N*, *N*-dimethyl acetamide than water, the spreadability of the PEBA solution using *N*, *N*-dimethyl acetamide as solvent was very poor, presumably due to the insufficient difference in surface tension between water and *N*, *N*-dimethyl acetamide. These results suggest that the solutions of PEBA dissolved in other possible solvents (such as tetrachloroethane, *N*, *N*-dimethylformamide, and *N*-methyl-2-pyrrolidone) having similar surface tensions (32.9–36.4 mN/m at 25 °C) are not likely to be suitable for membrane formation by the solution spreading technique either.

Table 3.1 Physical properties of solvents at 25 ^{o}C

Solvent	Isopropanol	n-Butanol	1,1,2-Trichloroethane	N,N-Dimethyl acetamide
Boiling point[a], ^{o}C	82.3	117.3	113.8	165
Density [a], g/cm^3	0.781	0.810	1.440	0.937
Viscosity [a], cP	1.945	2.544	0.793	1.956
Solubility [b], wt%				
In water	∞	7.7	0.10	∞
Water in	∞	20.1	0.035	∞
Surface tension [a], mN/m	20.93	24.93	34.02	33.15[c]

[a] Lide (2002), [b] Kroschwitz and Howe-Grant (1998), [c] Dean (1999).

Compared with *N*, *N*-dimethyl acetamide and 1,1,2-trichloroethane, the surface tensions of isopropanol and *n*-butanol are relatively low (see Table 3.1). In the solvent screening study, it was found that PEBA solutions prepared using either pure isopropanol or pure *n*-butanol as solvent would spread on water. However, the resulting thin layer of PEBA membranes exhibited a discontinuous phase, and no integral structure was formed.

The reasons are the following. Isopropanol is a relatively weak solvent, and thus the polymer chains are not well stretched or extended in the polymer solution. Further, isopropanol is miscible with water. As the polymer solution spreads on water, there is a quick solvent–nonsolvent exchange between isopropanol and water, and the polymer chains aggregate and then precipitate during the phase inversion process, resulting in the formation of membranes with open net-like structures. On the other hand, *n*-butanol is a stronger solvent, but the mutual solubility between *n*-butanol and water is poorer. As such, *n*-butanol cannot diffuse into water immediately when the polymer solution is in contact with water, resulting in partial precipitation of the polymer during the course of spreading. It was observed that the polymer solution spread very rapidly. Because of the slow phase inversion and fast spreading processes, the membrane so obtained consisted of essentially discrete polymer phases scattered on the surface of water, which lacked the integrity required for separation membranes.

Considering the trade-offs between the solvent strength and water solubility of isopropanol and *n*-butanol, it was anticipated that balanced solvent characteristics could be obtained by using a mixture of the two solvents. This was found to indeed be the case. A solvent blend comprising of isopropanol and *n*-butanol in 3:1 weight ratio was shown to be appropriate for making defect-free PEBA membranes by the solution spreading technique. As expected, the solvent strength of the solvent blend was found to be between those of pure isopropanol and *n*-butanol, as shown by the swelling data presented in Table 3.2. At 25 °C, PEBA 2533 does not dissolve in the solvent, and the swelling degree (that is, solvent uptake per unit mass of the polymer) can be used to represent the relative solubility of the polymer in the solvents. The conventional procedure for swelling experiments, which can be found elsewhere (Blume and Pinnau, 1990; Huang and Feng, 1992), was used in the solubility study.

The concentration of the polymer in the spreading polymer solution is also important to the membrane formation process. While a relatively high concentration of the polymer solution was difficult to achieve due to the poor solubility of the polymer in the solvent, membranes with integral structures could not be formed when the polymer concentration was too low. In the latter case, the membrane tended to have an open net-like structure that is not effective for separation applications. One may expect that a very

high polymer concentration, if it is obtainable, will not be suitable for membrane formation either, because the high viscosity will restrict the spreading of the polymer solution. It was found that the polymer concentration in the range of 6–8 wt% was appropriate for making defect-free PEBA membranes with the isopropanol/ *n*-butanol (3:1 weight ratio) solvent system.

Table 3.2 Swelling of PEBA 2533 in solvents after 36 h

Solvents	Swelling degree in solvents (%)*
Isopropanol	198
Blend of isopropanol and n-butanol (3:1 weight ratio)	249
n-Butanol	757

* Swelling degree = [Solvent uptake (g) / Weight of dry PEBA polymer (g)]× 100

The temperature of the spreading polymer solution is another factor that influences membrane formation. Generally, both surface tension and viscosity decrease with an increase in temperature. The polymer solution temperature is preferably kept higher than the water temperature. At a given temperature of water, as the temperature of the spreading solution increases, the difference in the surface tension between the spreading solution and the trough liquid increases. This, together with the reduced viscosity of the polymer solution, will result in a better spreading of the polymer solution. It should be pointed out, however, that as the polymer solution spreads, its temperature quickly drops to the water temperature, which will speed up the precipitation of the polymer to form a thin film. A temperature range of 60 – 80 °C for the spreading solution used in the present study was found to be satisfactory. It is worth noting that at temperatures below 40 °C, the polymer solution can hardly spread because the polymer tends to form a gel as soon as it contacts water.

3.3.1.2 Solvent-nonsolvent exchange during membrane formation

Solvent–nonsolvent exchange is an essential step for polymer coagulation and precipitation during membrane formation. In order to understand the membrane formation mechanism, the rate of mutual exchange between the solvent (i.e., the mixture of isopropanol and *n*-butanol) in the polymer spreading solution and the coagulant (i.e., water) in the trough was investigated. The concentration of alcohols in the coagulation bath as a function of time at given temperatures of the polymer solutions was measured. Figure 3.2 shows the ratio of the measured concentration (C) to the limiting concentration (C_∞) that would be obtained if the solvents isopropanol and *n*-butanol in the membrane were completely dissolved in water. The concentration ratio (C/C_∞) represents the fraction of the solvent coming to the water bath as a result of solvent–nonsolvent exchange. In spite of the relative scatter of the experimental data, it is clearly shown that solvent diffusion into water occurred almost instantly as the polymer solution spread on water. The solvent–nonsolvent exchange was very rapid during the early stage of the membrane formation and then gradually slowed down. This is consistent with physical reasoning. The solvent–nonsolvent exchange occurs at the interface between the polymer solution film and the water surface, which leads to the formation of a gelled polymer layer. The gelled polymer layer acts as a barrier to the diffusion of solvent from the interior of polymer solution film to the water bath. The thickness of the gel layer increases as the solvent–nonsolvent exchange proceeds, and consequently the exchange rate gradually decreases. Similar results have been observed during the formation of asymmetric membranes by the traditional phase inversion technique based on solvent–nonsolvent exchange (Huang and Feng, 1995).

It can be seen from Figure 3.2 that the solvent–nonsolvent exchange is almost complete within 10–20 s, depending on the temperature of the polymer solution. This is in agreement with the visual observation that the polymer solution spread on water surface very rapidly and then spreading stopped quickly after a short period of time, and the membrane formation was complete almost as soon as the polymer solution stopped spreading. It should be noted that not all solvents entered the water phase during membrane formation. A portion of the solvents would have evaporated from the top surface of the spread polymer solution film into the air. This is shown by the C/C_∞ data in

Figure 3.2 that are less than 1 after solvent–nonsolvent exchange is complete. As one anticipates, the higher the polymer solution temperature, the greater the degree of solvent evaporation is. The partial evaporation of solvent during solution spreading, which tends to increase the local concentration of polymer, also contributes to the gelation and precipitation of the membrane. At a polymer solution temperature of 60 – 80 °C, which was found to be a proper temperature range for defect-free membrane preparation, approximately over 70% of the solvent was dissolved into water due to solvent–nonsolvent exchange, and the remaining portion was evaporated from the top surface of the cast polymer solution film. As such, it is mainly due to solvent–nonsolvent exchange that results in the coagulation of the polymer and the formation of the membrane.

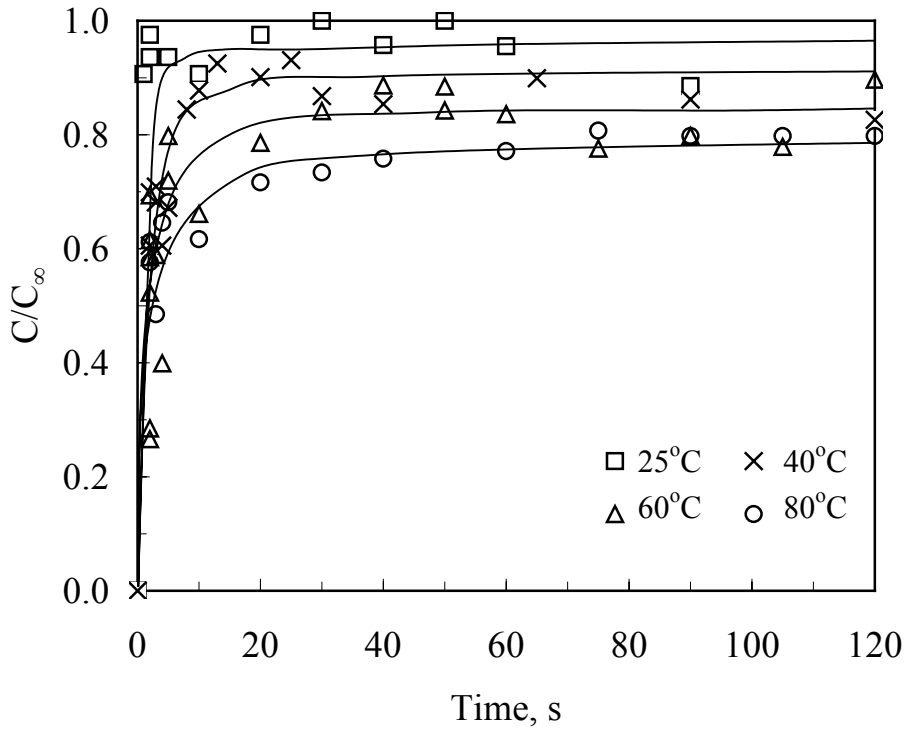

Figure 3.2 Solvent-nonsolvent exchange rate at different spreading temperature of polymer solutions. Water temperature, 25°C.

Unlike the traditional "dry–wet" phase inversion process for preparing asymmetric membranes where partial evaporation of solvent and solvent–nonsolvent exchange occur sequentially, the solution spreading process developed here involves simultaneous solvent evaporation and solvent–nonsolvent exchange. The elastic PEBA 2533 membranes prepared by the solution spreading technique were found to be transparent, with a dense and homogeneous structure. Figure 3.3 shows the typical scanning electron micrographs of the surfaces of a PEBA 2533 membrane prepared at a spreading solution temperature of 80 °C. No defects were observed on both surfaces, though the membrane surface facing water side exhibited some tiny ripples, which are believed to be caused by the disturbance of water surface when the polymer solution was placed on water and the rapid solvent–nonsolvent exchange at the membrane/water interface during the spreading of the polymer solution. Similar surface characteristics were also found for membranes prepared at other spreading temperatures.

It should be pointed out that the membrane preparation method developed here is different from those disclosed in patents for making silicone/polycarbonate copolymer membranes in several aspects. According to Ward et al. (1976, 1983) and Kimura et al. (1979), the solvent used for the casting system should be preferably immiscible with water, and the spread polymer solution desolvates to form a thin film after the solvent has evaporated. In the present study the solvent needs to have sufficient mutual solubility with water, and the mechanism of membrane formation involves solution spreading, solvent–nonsolvent exchange, and partial evaporation of the solvent. The membrane is formed primarily by polymer precipitation caused by solvent–nonsolvent exchange, and the solvent evaporation is just an accompanying step naturally occurring due to its volatility.

3.3.2 Gas permselectivity

Since the PEBA membranes were very thin (as thin as 0.3 μm), to ensure an adequate transmembrane burst pressure during gas permeation test, 3 – 5 layers of relatively thick membranes were laminated on a porous polysulfone substrate membrane. The cross-sectional structure of the resulting composite membrane is illustrated in Figure 3.4. The permeance of the polysulfone substrate, which was measured to be in the range

of 2000 – 2300 GPU for the permeation of carbon dioxide, nitrogen and oxygen at a transmembrane pressure differential of 70 – 700 kPa, is more than two orders of magnitude higher than the permeance of the polysulfone-supported PEBA membranes. Obviously, the resistance of the polysulfone substrate to the gas permeation is negligible in comparison with that of the PEBA membranes.

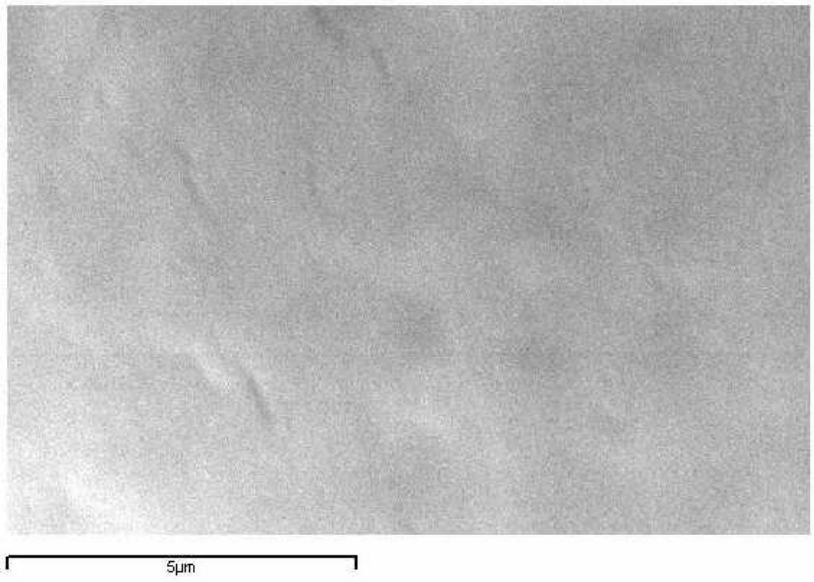

(a) Air side

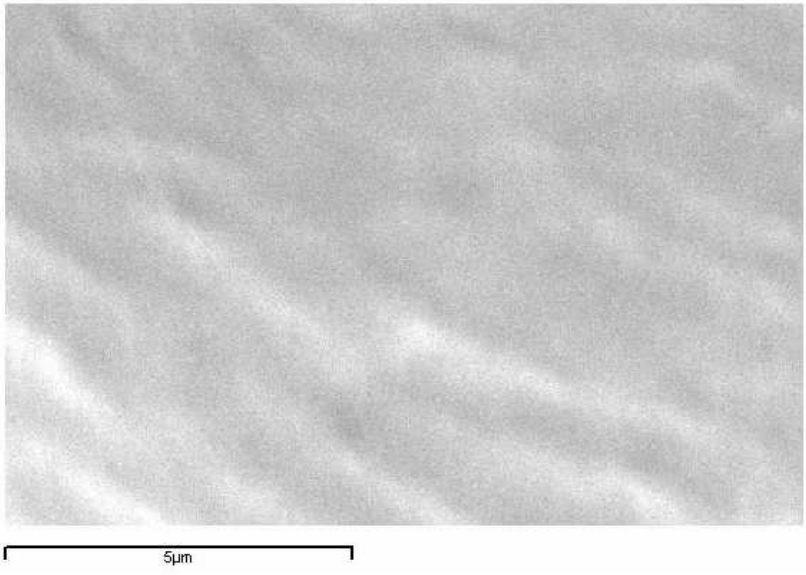

(b) Water side

Figure 3.3 Scanning electron micrographs of membrane surface. The membranes were prepared at a spreading temperature of 80 ^{o}C.

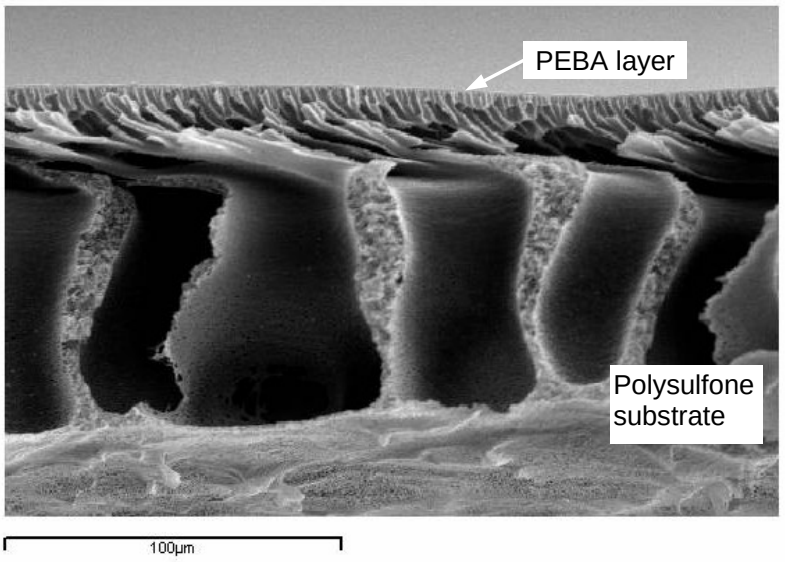

Figure 3.4 Scanning electron micrograph of the cross-section of a multiplayered PEBA 2533 membrane supported by a porous polysulfone substrate.

The typical permeation properties of gases through the composite membranes were presented in Table 3.3. It should be noted that for the ultrathin membranes showed in Table 3.3, the thickness of a single PEBA layer might not be the same, depending on the operating conditions. For comparison, the "intrinsic" permselectivity of PEBA 2533 determined using a dense film (thickness ~50 μm) is also shown in the table. The composite membranes are 4 – 14 times more permeable than the dense membrane, and the selectivities of the composite membranes are close to or slightly higher than that of the dense membrane, verifying that the membranes so prepared are almost defect-free. The data in Table 3.3 show that the membranes are effective for CO_2/N_2 and O_2/N_2 separations. At a temperature of 25 °C and a feed pressure of 345 kPa, the polysulfone-supported multilayered PEBA membranes exhibited a permeance of 20 – 70 GPU to carbon dioxide permeation with a carbon dioxide/nitrogen selectivity of 34 – 44. It is estimated that when a single layer of the thin PEBA membrane is used, the permeance would be 3 – 5 times greater with the selectivity remaining the same. Using the gas permeance data of the thick dense film and the multilayered PEBA membranes, the thickness of a single membrane layer can be estimated to be approximately 0.7 and 3.5 μm for the five-layered and three-layered PEBA membrane laminates, respectively, which are in agreement with direct measurements with a stack of 5 – 10 layers.

Table 3.3 Permeability measured with multilayered PEBA membranes

No. of PEBA membrane layers	Permeance, GPU			Selectivity	
	CO_2	O_2	N_2	CO_2/N_2	O_2/N_2
3	21.8	3.19	0.563	38.7	5.7
3	26.1	2.81	0.592	44.1	4.7
3	21.5	–	0.600	35.8	–
3	27.4	–	0.798	34.3	–
5	70.9	5.83	1.98	35.8	2.9
Dense film	5.08	0.467	0.155	32.7	3.1

Testing temperature: 25^{o}C, gas pressure: 345 kPa.

It should be pointed out that although membranes as thin as 0.3 μm had been prepared, the supported membrane laminates with 3 – 5 layers PEBA membranes could not tolerate the transmembrane pressures used in the experiment, mainly due to the relatively large pore size and rough surface of the polysulfone substrates. Substrates with finer pores and smoother surfaces would be needed to prevent the burst of the ultrathin membranes under pressure.

It can be calculated from the experimental data that the permeance of a single layer 0.7 μm thick membrane is 350 and 29 GPU for carbon dioxide and oxygen, respectively. While the permeance depends on the thickness of the membrane, the permeance ratio is characteristic of the membrane selectivity. The difference in the selectivity between the thin surface spreading membrane and the thick solvent casting membrane may be attributed to the microstructural change of the polymer caused by the spreading process. It has been reported that for the spreading of polydimethylsiloxane-containing block copolymers, the area of the spread block polymer film depends on the spreadability of the organic block (Gaines, 1975) and if it is spreadable, it contributes, but nonadditively, to the surface area of the spread copolymer film. This means that the spreading of a copolymer solution affects the micro-homogeneity of the spread copolymer film. PEBA 2533 is a block copolymer comprising of approximately 20 wt% hydrophilic polyamide segments and 80 wt% hydrophobic polyether segments. Considering the nature of the two blocks in PEBA, their spreadabilities on water surface are likely to be different. To verify whether the micro-homogeneity of PEBA 2533 was

altered by the spreading process, the hydrophilic–hydrophobic properties of the PEBA polymer was studied by measuring the contact angle of water on the membrane surface. The contact angles of water on both surfaces of the thin surface spread membranes were found to be 67°, whereas the contact angle of water on the surface of the solution cast dense membrane was 79°, indicating that the micro-homogeneity of PEBA 2533 was indeed affected by the membrane preparation process based on solution spreading on water surface.

Figure 3.5 illustrates the effect of feed pressure on the gas permeation performance of a multilayered composite membrane at 23 ^{o}C. In the feed pressure range from 140 to 690 kPa, the permeance of nitrogen and oxygen decreased very slightly with an increase in the gas pressure. However, the permeation of carbon dioxide is influenced by the feed gas pressure more significantly. For example, the permeance of carbon dioxide increased by about 15% when the feed pressure increased in the testing range, and consequently the permeance ratio of carbon dioxide to nitrogen also increased.

The effect of pressure on the gas permeability can be explained in terms of three competing effects: membrane compaction, plasticization, and dual mode sorption. The hardness of PEBA 2533 is low due to its low polyamide content (20 wt%). As such, an increase in pressure will cause membrane compaction, which tends to decrease the membrane permeability. On the other hand, there are two modes of sorption of gases in the membrane; one is the sorption in the polyether segment that follows the Henry´s law, and the other is the combined Henry sorption and Langmuir sorption in the glassy polyamide segment. The dual mode sorption in glassy polymers has been investigated extensively by Koros and Chern (1987). When the gas pressure increases, the gas uptake in the membrane increases, but the increase is less than proportional because of the Langmuir sorption where the active sorption “sites” are gradually saturated, thereby reducing the gas solubility and thus the permeability through the membrane. In addition, the penetrant tends to plasticize or swell polymers, resulting in an increase in mobility and thus permeability. It has been reported that the solubility of carbon dioxide in PEBA 2533 is 14 – 29 times greater than that of nitrogen and oxygen (Bondar et al., 1999), and therefore carbon dioxide will plasticize or swell the membrane much more significantly. When the plasticization effect is dominant, increasing gas pressure will lead to an

increase in the membrane permeability. The strong plasticization effect of carbon dioxide in polymers is well recognized (Koros and Chern, 1987; Koros, 1980; Petropoulos, 1994).

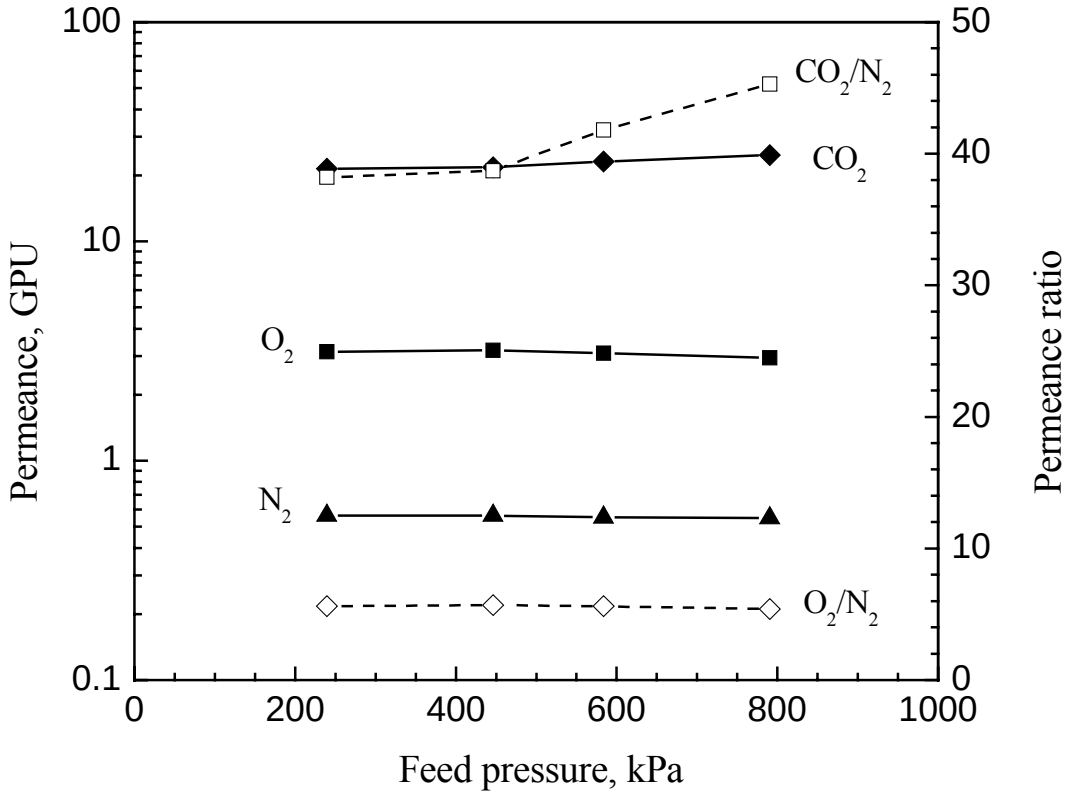

Figure 3.5 Effect of the feed pressure on gas permeance (solid lines) and selectivity (dotted lines) through a multilayered PEBA membranes supported by polysulfone substrate. Test temperature, 23 ^{o}C.

It may be pointed out that the experimental data of Bondar et al. (2000) on a melt-extruded PEBA 2533 film showed similar trend for the effect of pressure on membrane permeability. It should be mentioned that for the permeation of CO_2/N_2 gas mixtures, the plasticization of the membrane by CO_2 will enhance the permeation of both CO_2 and N_2, and the membrane selectivity is expected to decrease as the feed pressure increases.

3.4 Summary

A new method of preparing thin PEBA 2533 membranes was developed. It is characterized by spontaneous spreading of the copolymer solution on water surface. The casting solution used comprises the copolymer dissolved in a solvent blend of isopropanol/ *n*-butanol (weight ratio 3:1). The casting solution is deposited on water surface, and as it spreads solvent exchange with water occurs which induces polymer precipitation, thereby forming a thin membrane floating on water surface. The spreading process is accompanied by evaporation of solvent due to its volatility, but the solvent – nonsolvent exchange is primarily responsible for polymer desolvation during membrane formation. The formation of a uniform and defect-free membrane is found to be determined by the solvent system, polymer concentration in the casting solution and temperature. Substantially defect-free membranes as thin as 0.3 μm are prepared, and they exhibit a good permselectivity for carbon dioxide/nitrogen and oxygen/nitrogen permeations for pure gas tests. At 25 °C and a feed pressure of 345 kPa, the 0.7 μm thick membrane showed a carbon dioxide permeance of 350 GPU and a CO_2/N_2 permeance ratio of 35.

CHAPTER 4

Propylene Separation from Nitrogen by Poly(Ether Block Amide) Composite Membranes

4.1 Introduction

During polyolefin manufacturing, the raw polymer product from the polymerization process contains certain amounts of un-reacted monomers and process solvents, which must be removed before the polymer is further processed for ultimate applications. Nitrogen is often used to "strip off" the hydrocarbon compounds by passing the raw polymer to a degassing bin, and the vent gas from the degassing bin generally contains 10-20% valuable hydrocarbons. The vent stream is normally flared or used as a low grade fuel if there is no suitable method to recover the hydrocarbons, and this represents a significant loss of the olefin monomers. In a typical resin degassing operation, there are approximately 250-500 kg/hr of monomers and 500-1,000 kg/hr of nitrogen that could be recovered for reuse. Membrane process is a promising technology to recover olefins (e.g. ethylene and propylene) from the resin degassing vent gas. It has been shown that membrane systems are especially competitive with carbon adsorption and condensation, and the payback time can be as short as 12 months (Baker and Jacobs, 1996).

To separate hydrocarbon or other organic vapors from nitrogen or air, membranes preferentially permeable to the large but more condensable organic components are required. Generally, membranes made from rubbery polymers are appropriate for this type of applications. Rubbery polymers exhibit not only a high solubility-selectivity, they also tend to have a high permeability that can be 2-3 orders of magnitude higher than glassy polymers. The high permselectivity means small membrane area required (Baker, 1996). Currently, poly(dimethyl siloxane) is the primary polymer used to make

membranes for organic compound separation, including the recovery of gasoline vapor and other volatile organic compounds from nitrogen or air. It possesses high permselectivity to large, condensable organic vapors due to their high solubility in the polymer. Although most gas separations using nonporous polymeric membranes are based on the solution-diffusion mechanism, other transport mechanisms for organic vapor separation have also been exploited by taking advantage of the condensability characteristics of the organic vapors. For example, poly(1-trimethylsilyl-1-propane) is a glassy polymer with a super high free volume. Its network of nano-scale channels allow for rapid surface diffusion of the organic vapor components along the channel walls, but the channels are small enough to partially block the permeation of nitrogen or air, resulting in a good selectivity (Pinnau, 1996). The preferential permeation of organic vapors on the basis of surface flow and capillary condensation has also been investigated by Feng et al. in an attempt to develop aromatic polyimide and polyetherimide membranes for the separation of various volatile organic compounds from air (Feng 1991, 1993).

This chapter deals with propylene/nitrogen separation by PEBA 2533 membranes. Despite the advantageous characteristics of PEBA copolymers as a promising rubbery membrane material, very little work has been done in the literature to separate light olefins (such as propylene) from polyolefin vent gas. Thin film composite PEBA/polysulfone membranes were prepared by laminating a thin layer of PEBA onto a porous polysulfone (PSf) substrate. The effects of operating pressure and temperature on the membrane permeability and selectivity for the permeation of both pure gases and their mixtures were investigated. Based on the experimental data so obtained, the process performance for the separation of propylene from nitrogen using the composite membranes was evaluated on the basis of a simple mathematical model derived.

4.2 Experimental

4.2.1 Membrane preparation

The general procedures for membrane fabrication have been described in Chapter 3. Basically, a predetermined amount of PEBA 2533 was dissolved in a mixture solvent (isopropanol and n-butanol, mass ratio 3:1) at 80°C to form a homogenous solution

containing 7 wt% of the polymer. After standing without disturbance for at least one day to remove gas bubbles, the polymer solution was kept at 60 °C. One or two drops (ca 0.01-0.03 g) of the solution were dripped gently on the surface of deionized water, and the polymer solution spread quickly and spontaneously, during which process the solvent exchanged with nonsolvent water, forming a very thin PEBA film floating on water surface. The thin films were laminated on a porous polysulfone substrate as a mechanical support, thereby forming a thin film composite membrane. The polysulfone substrate, having a thickness of about 140 μm, was prepared by the phase inversion technique; detailed information on the formation and the structure of the substrate membrane can be found in Chapter 3.

In order to determine the intrinsic selectivity of the PEBA 2533 polymer for propylene/nitrogen separation, PEBA 2533 homogenous membranes were prepared by solution casting followed by solvent evaporation using the same PEBA solution. The thickness of the dense PEBA membranes was about 55 μm.

4.2.2 Gas permeation test

Figure 4.1 is a schematic setup for propylene/nitrogen separation by the membranes. The effective membrane area for permeation was 13.85 cm^2. The feed gas at a pre-set composition was obtained by a dynamic gas blending system comprised of two mass flow controllers and the gas composition was determined using a Varian CP-3800 gas chromatograph equipped with a thermal conductivity detector. The residue flow was controlled such that the stage cut, defined as the ratio of permeate flow rate to the feed flow rate, was always below 0.05. At such a low stage cut, the variation in the feed gas composition from the inlet to the outlet was negligibly small, and this was confirmed by direct measurements of the gas compositions using the gas chromatograph. As such, the membrane unit functioned as a "differential" permeator which allows one to determine the membrane permselectivity at a given feed composition. While the feed gas entered the permeator at different pressures, the permeate stream was withdrawn at atmospheric pressure. The permeate flow rate was measured by a bubble flow meter and its composition was analyzed using the gas chromatograph. The permeance of gas component *i* through the membranes was calculated by

$$J_i = \frac{Q \cdot y_i}{A \Delta P_i} \tag{4.1}$$

where J_i is the permeance, which can be expressed customarily in the gas permeation unit GPU (1GPU = 10^{-6} cm^3(STP)/(cm^2.s.cmHg), or 3.35×10^{-10} mol/(m^2.s.Pa) in SI unit), Q the total gas flow rate in permeate, y_i the mole fraction of component i in the permeate, A the effective membrane area for permeation, and ΔP_i the partial pressure difference of component i across the membrane. $\Delta P_i = P_h x_i - P_l y_i$, where P_h and P_l are the gas pressure in the feed and permeate, respectively, and x_i is the mole fraction of component i on the feed side. The membrane selectivity α for the gas mixture permeation can be characterized by the permeance ratio of the two components

$$\alpha = J_1 / J_2 \tag{4.2}$$

where subscripts 1 and 2 represent propylene and nitrogen, respectively.

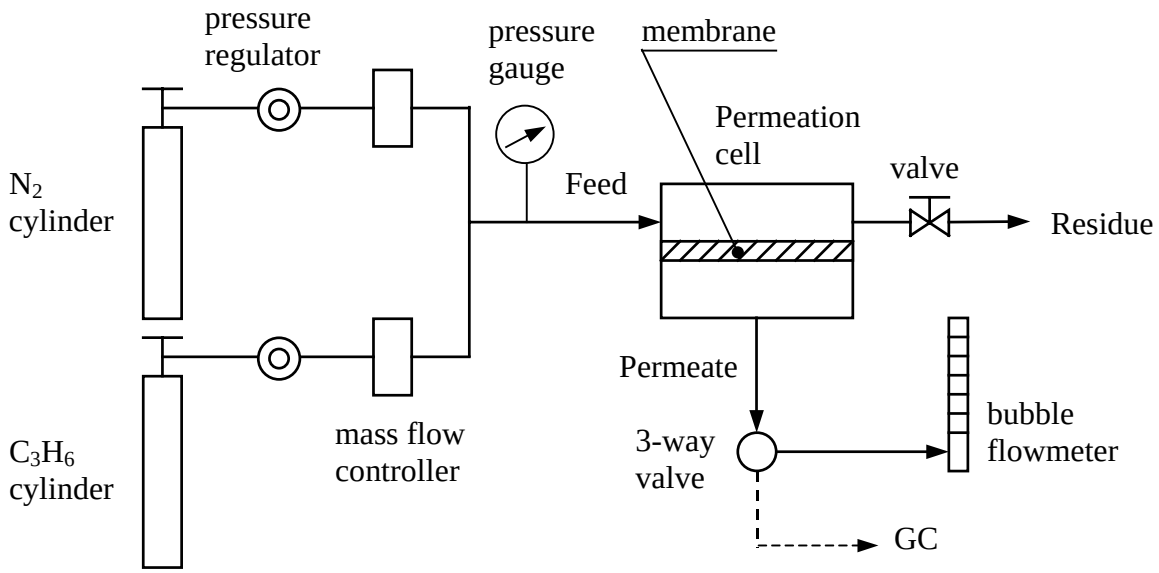

Figure 4.1 Schematic diagram of the experimental set-up for gas permeation test.

By switching off one of the mass flow controllers, the experimental setup was also used for the permeation tests of pure propylene and nitrogen. The gas permeance is simply the permeation flux normalized by the transmembrane pressure. For a homogeneous membrane, the membrane permeability, customarily expressed in unit

Barrer (1 Barrer = 10^{-10} cm^3(STP).cm/(cm^2.s.cmHg), or 3.35×10^{-16} mol.m/(m^2.s.Pa) in SI unit), is equal to the permeance multiplied by the membrane thickness *L*. The pure gas permeability (or permeance ratio) is referred to as the ideal selectivity of the membrane. The experimental error for pure gas permeance measurements was estimated to be within 5%, and the experimental error in permeance measurements of individual components, which involved composition analysis, was about 8-10%.

4.3 Results and discussion

4.3.1 Pure gas permeability and ideal selectivity

To evaluate the intrinsic permeability and the ideal selectivity of the PEBA copolymer, the permeability of pure propylene and nitrogen through a dense PEBA membrane was determined. Figure 4.2 shows the permeability to propylene and nitrogen as well as the membrane selectivity in terms of permeability ratio. At 25°C, there was little change in nitrogen permeability in the pressure range (170 to 722 kPa) tested, whereas the permeability of propylene was varied from ca. 300 to 1,000 Barrer, resulting in a propylene/nitrogen permeability ratio of 40-150. Thus PEBA 2533 membranes have a good permselectivity for propylene-nitrogen separation.

Based on Rezec's study (Rezec, 1997), the glass transition temperatures of the polyether and the polyamide blocks in PEBA 2533 are -76^{o}C and 65-75 ^{o}C, respectively. At the experimental temperatures, the copolymer may contain both a rubbery polyether phase and a glassy polyamide phase. However, the polymer is still shows the properties of rubbery polymers due to the high content of polyether segments (about 80 wt%) and the high free volume (17.2%) of the polymer (Rezec 1998). In our research, we also found that the membranes showed a typical behavior of rubbery polymers. The solubility of condensable propylene is much higher than nitrogen, and propylene permeates through the membrane preferentially due to the high solubility-selectivity, in spite of the larger molecular size of propylene (and thus a relatively lower diffusivity) than nitrogen. Further, the increase in propylene permeability with an increase in propylene pressure can be attributed to the increased solubility and diffusivity. The high sorption uptake of propylene in the membrane tends to swell the polymer matrix, resulting in an increased

solubility and diffusivity of propylene in the polymer. As such, the permeability of propylene increases. This will be verified by studies on the sorption and diffusion of propylene in the polymer in next chapter. The results shown in Figure 4.2 are in agreement with the results from sorption studies of Bondar et al. (Bondar, 1999), who found that the isotherms of hydrocarbon molecules (e.g., propane and butane) in PEBA 2533 were convex to the pressure axis while the isotherms of permanent gases (e.g. N_2, H_2 and O_2) were linear.

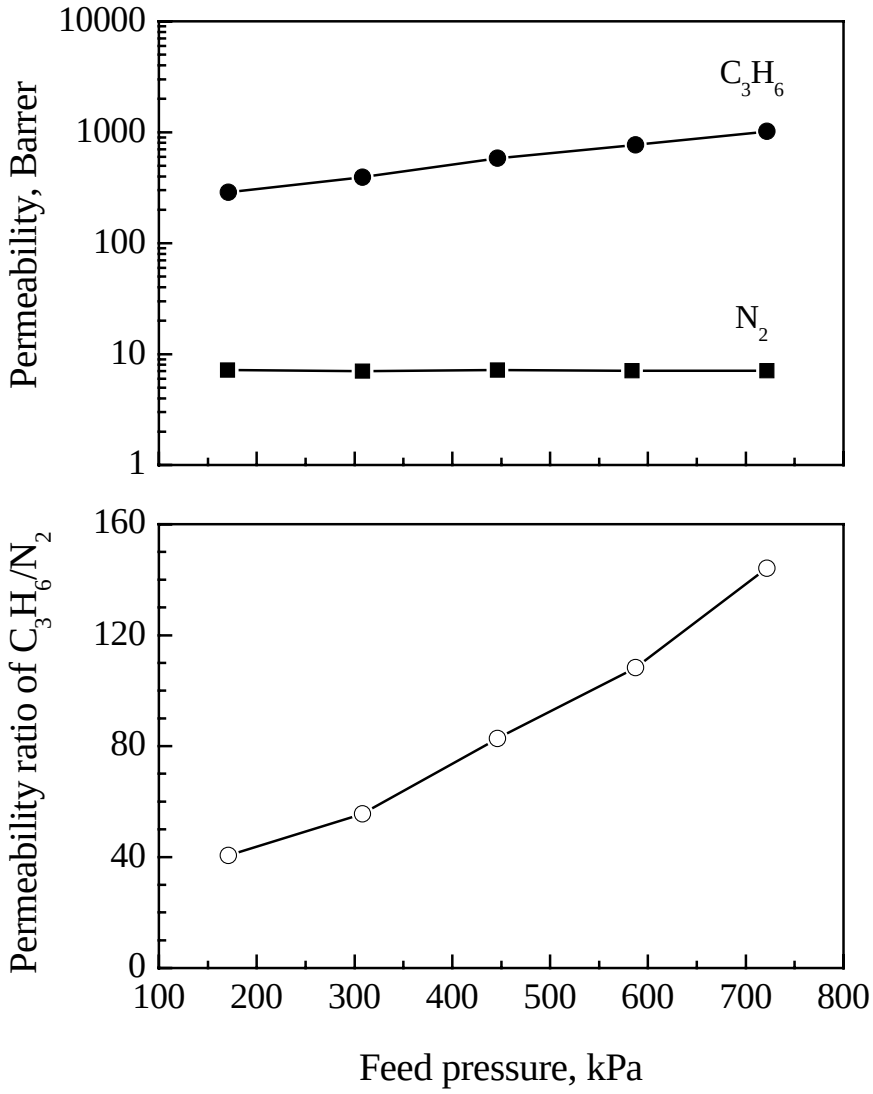

Figure 4.2 Permselectivity of PEBA 2533 dense membrane to pure propylene and nitrogen. Temperature: 25^{o}C.

4.3.2 Pure gas permeation through PEBA/PSf composite membranes

As membrane gas separation is a rate-controlled process, a higher permeation rate can be achieved by using a thinner membrane. In this work, PEBA/PSf composite membranes were fabricated by laminating a thin skin layer of PEBA 2533 on microporous PSf substrates. The permeance of propylene and nitrogen and their permeance ratio as functions of temperature at different feed pressures are shown in Figures 4.3 – 4.5. At room temperature, the propylene/nitrogen permeance ratio was ranged from 50 to 150 in the feed pressure range of 170-584 kPa, which is consistent with the results observed with the dense homogeneous membrane. This demonstrates that the composite membranes are defect free. The permeance of nitrogen through the substrate membrane was measured to be 2×10^4 GPU, which is several orders of magnitude higher than the nitrogen permeance through the composite membrane (see Figure 4.4). This indicates that the mass transfer resistance of the porous support is negligible as compared to the skin layer. From the permeance data of nitrogen in the composite membrane (Figure 4.4) and the intrinsic permeability through the dense membrane (Figure 4.2), the thickness of the PEBA skin layer of the composite membrane can be estimated to be 3 - 4 μm.

From Figure 4.3 it can be seen that the temperature dependency of the propylene permeance through the PEBA membrane does not show a monotonic trend, and obviously the effect of temperature on propylene permeance does not follow an Arrhenius type of relation, which is generally valid for the permeation of permanent gases. At a low feed pressure, the permeance of propylene increases with an increase in temperature, but the opposite is true when the pressure is sufficiently high. This can be explained from the opposing effects of temperature on the solubility and diffusivity. The permeation of propylene is determined by both the solution and the diffusion aspects. Generally, sorption is exothermic; as temperature increases, the solubility decreases, whereas the diffusivity increases. In addition, the significance of the temperature effect on solubility and diffusivity is influenced by the pressure, which also affects the sorption uptake of the permeant in the membrane. At a high pressure, the sorption uptake is high and the polymer chains are thus flexible, and therefore the diffusivity is high; increasing temperature is expected to cause a more significant reduction in the solubility than the

further increase in the diffusivity, leading to a decrease in the permeance. Similarly, at a low pressure and/or a high temperature, the sorption uptake is limited, and an increase in temperature is likely to increase the diffusivity more significantly than the decrease in the solubility, resulting in an increased permeance. This is consistent with the common observations that sorption is more dominating than diffusion on membrane permselectivity at low temperatures, and that solubility-selective membranes often become more permselective at lower temperatures. Apparently, at certain point when the reduction in solubility due to an increase in temperature is just compensated by the increased diffusivity, the permeance will reach a minimum, as shown by the "deflection" point in Figure 4.3. At a pressure of 446 kPa, a minimum propylene permeance occurred at approximately 20°C, and the temperature corresponding to the minimum permeance tends to shift to a higher value when the feed pressure increases.

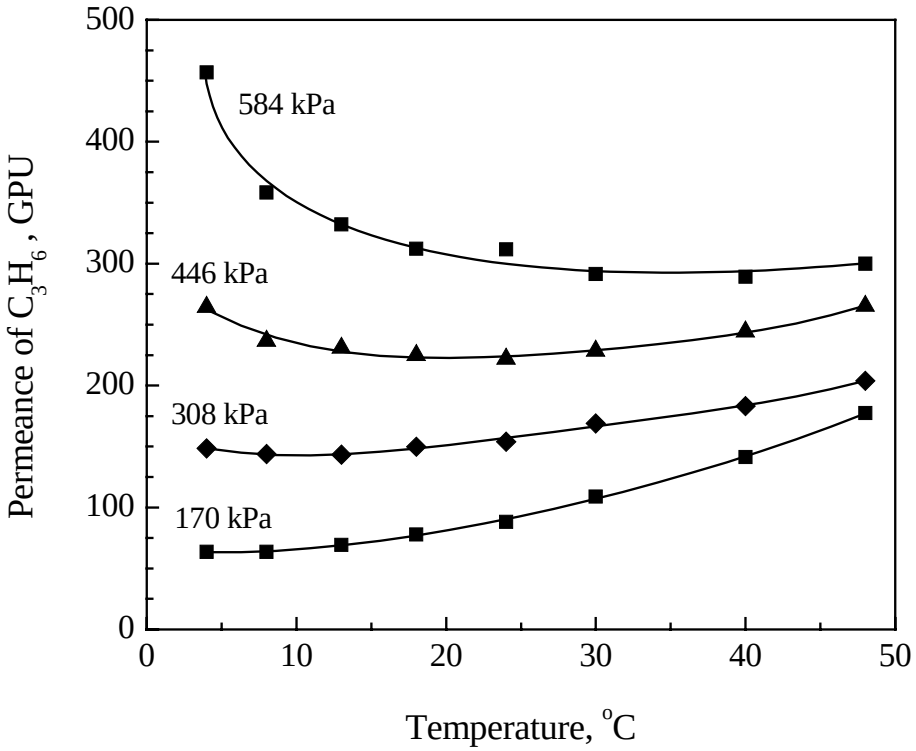

Figure 4.3 Permeance of pure propylene gas through PEBA/PSf composite membranes.

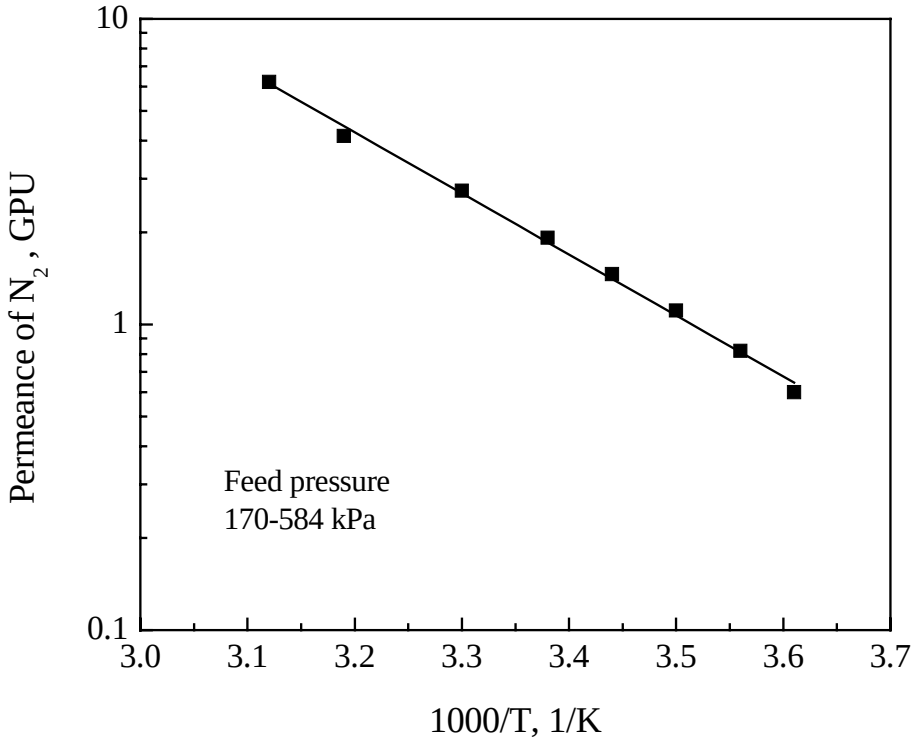

Figure 4.4 Permeance of nitrogen vs. reciprocal of operating temperature for pure nitrogen through PEBA/PSf composite membranes.

At a given temperature, increasing the feed propylene pressure clearly increases its permeance, and the pressure dependency of propylene permeance is more significant at lower temperatures. For example, at 50°C, an increase in the feed pressure from 170 to 584 kPa resulted in a 80% increase in propylene permeance (from 180 to 300 GPU), while at 4°C the propylene permeance changed by more than **7** times (from 60 to 460 GPU). Therefore, a low temperature and a high feed pressure are favorable to the permeation of propylene.

Figure 4.4 shows the permeance of nitrogen as a function of operating temperature. The permeance of nitrogen was found to be independent of the feed pressure, which is consistent with the results from nitrogen permeation through dense homogeneous PEBA 2533 films. Like the permeation of permanent gases through polymeric membranes, the temperature dependence of nitrogen permeability can be

represented by an Arrhenius type of relation. Because of the significantly low permeance of nitrogen at low operating temperatures, the pure propylene and nitrogen permeance ratio increases with a decrease in the temperature, as shown in Figure 4.5. The increase in propylene/nitrogen permeance ratio becomes more significant at higher feed pressures.

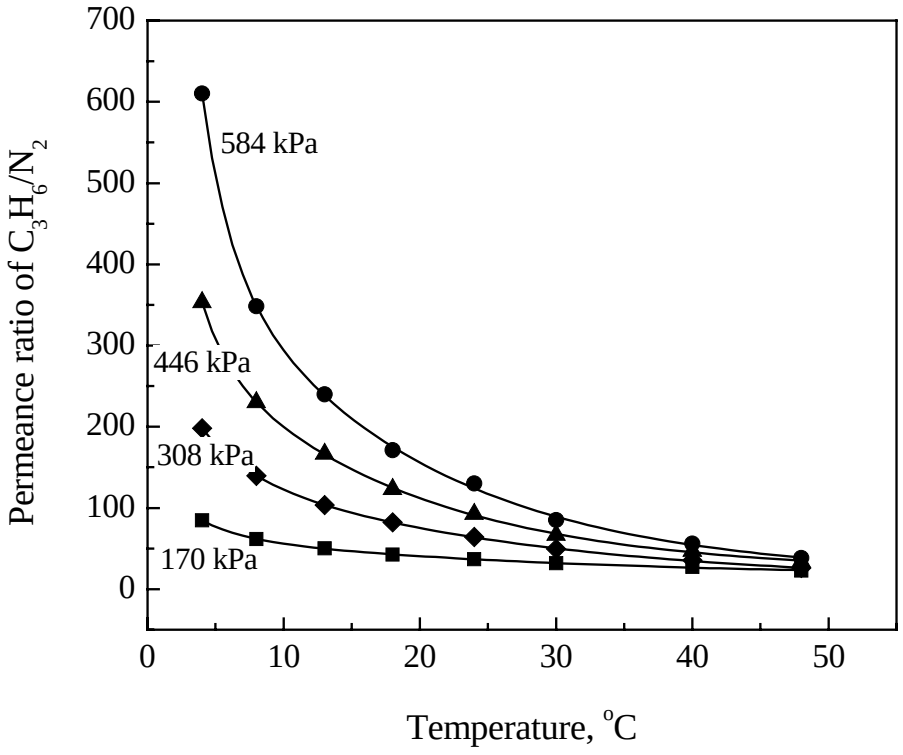

Figure 4.5 C_3H_6/N_2 permeance ratio for pure gas permeation through the PEBA/PSf composite membrane.

4.3.3 Propylene/nitrogen gas mixture permeation

It is generally known that the actual permselectivity of a membrane for gas mixture permeation may be different from the ideal permselectivity based on pure gas permeation. The separation of propylene/nitrogen gas mixtures by the PEBA/PSf composite membrane was investigated. For convenience of characterizing the membrane performance, a small stage cut (less than 0.05) was used in all the experiments so that the

concentration of the gas on the feed side can be considered as a constant along the membrane surface.

At a feed pressure of 791 kPa, the permeate concentration as a function of the feed propylene concentration is shown Figure 4.6, which demonstrates that the PEBA/PSf composite membrane has a good selectivity for propylene/nitrogen separation. At 25°C, when the feed concentration is 6-30 mol% propylene, the permeate contains 40 to 90 mol% of propylene. The increase in the permeate propylene concentration becomes less significant when the feed propylene increases. This is due to the fact that propylene is more permeable than nitrogen and a high concentration of propylene in the permeate will reduce the driving force for propylene permeation through the membrane, which affects the permeate concentration negatively. In addition, Figure 4.6 also shows that lowering the operating temperature tends to increase the concentration of propylene in the permeate, and the influence of temperature is not very significant especially at relatively high feed propylene concentrations.

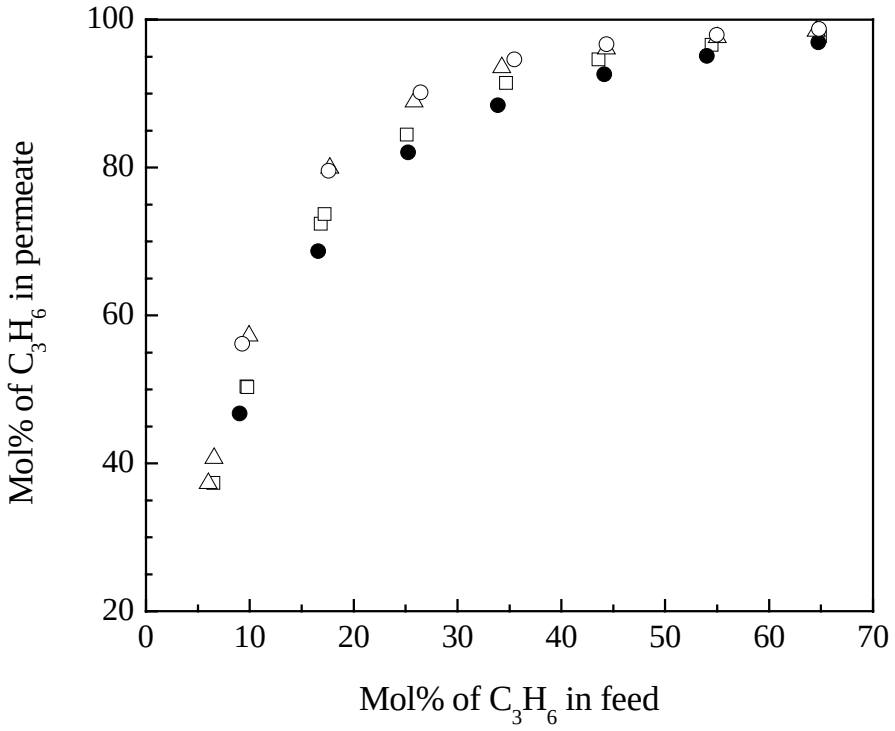

Figure 4.6 Effect of propylene feed concentration on the permeate concentration (● 50°C, □ 25 °C, Δ 15 °C, ○ 3 °C). Feed pressure: 791 kPa.

The permeance of propylene and nitrogen for gas mixture permeation under different feed concentrations and temperatures are presented in Figures 4.7 and 4.8. When the feed propylene concentration increases, the permeance of both propylene and nitrogen increases, whereas as shown in Figure 4.9, there is no significant change in the propylene/nitrogen permeance ratio, which characterizes the actual selectivity of the membrane for propylene/nitrogen separation. This means that for the permeation of gas mixtures, the membrane swelling caused by propylene increases the permeance of both permeating species to a similar extent. The data in the figures also show that an increase in the temperature leads to an increase in the permeance of both propylene and nitrogen and a decrease in the selectivity.

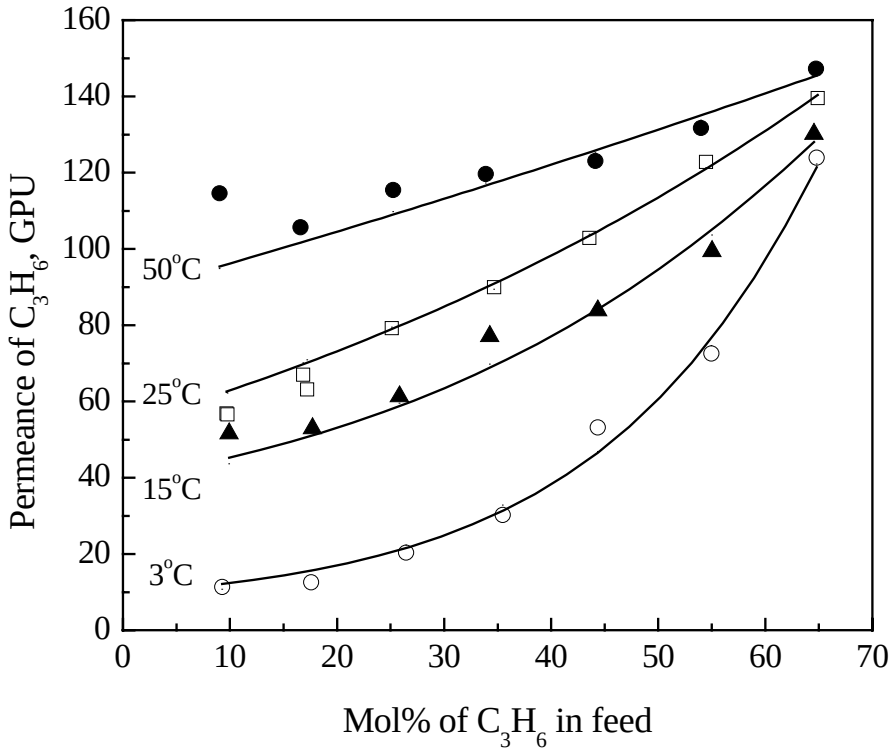

Figure 4.7 Effect of feed concentration on the permeance of propylene in gas mixture permeation. Feed pressure: 791 kPa. The symbols represent experimental data, and the solid lines are calculated results based on the semi-empirical equation of permeance.

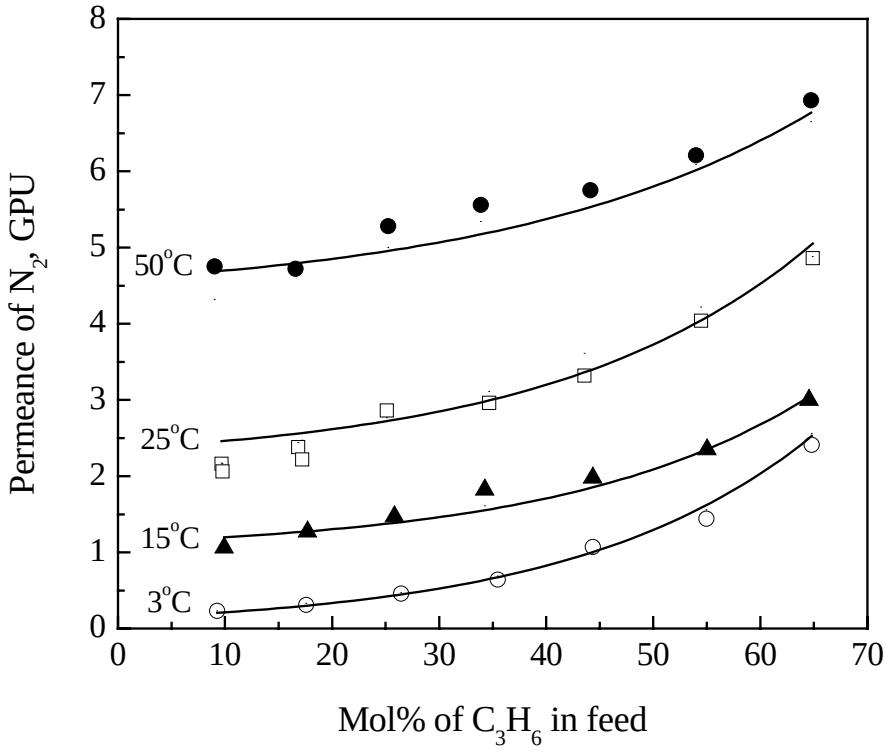

Figure 4.8 Effect of feed concentration on the permeance of nitrogen in gas mixture permeation. Feed pressure: 791 kPa. The symbols represent experimental data, and the solid lines are calculated results based on the semi-empirical equation of permeance.

Based on the experimental results of gas mixture permeation, a semi-empirical relation was attempted to correlate propylene permeance with operating conditions. At steady state of gas permeation, the permeation flux J^0 of propylene can be described by the Fick's law,

$$J^0 = -D\frac{dC}{dl} \tag{4.3}$$

where D is the diffusivity coefficient of propylene and C is the concentration of propylene in the membrane. Assume the concentration dependency of diffusivity can be expressed by an exponential form

$$D = D_0 \exp(\phi \cdot C) \tag{4.4}$$

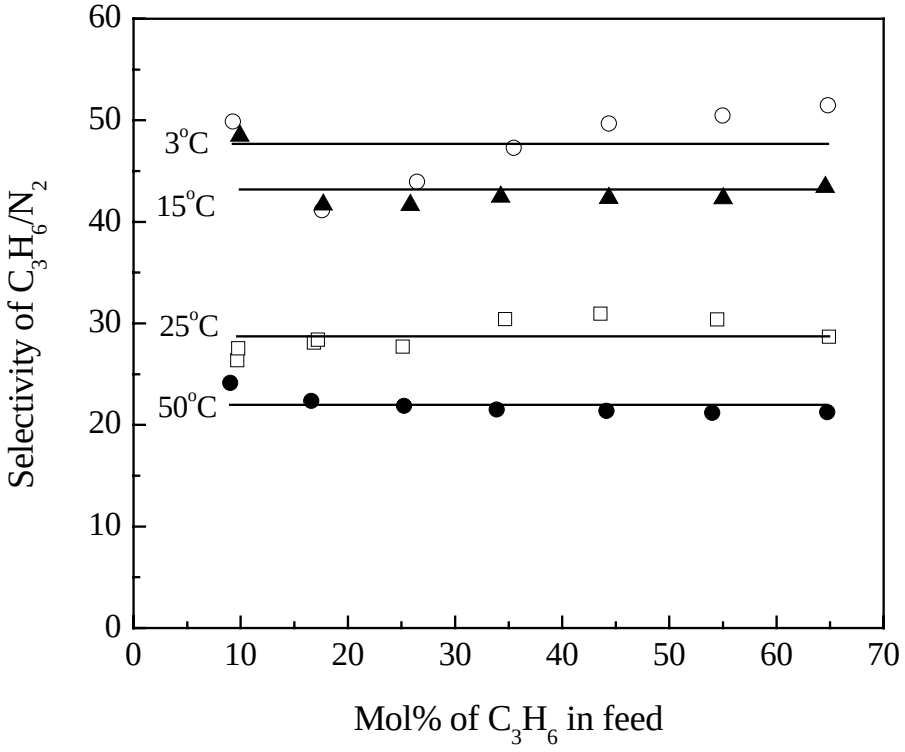

Figure 4.9 Effect of feed concentration on the selectivity of propylene/nitrogen in gas mixture permeation. Feed pressure: 791 kPa.

where D_0 and ϕ are constants. The permeation flux of propylene can thus be obtained by integrating Eq. (4.3)

$$J^0 = \frac{D_0}{\phi \cdot L}[\exp(\phi \cdot C_h) - \exp(\phi \cdot C_l)] \tag{4.5}$$

where L is the membrane thickness, and C_h and C_l are propylene concentrations in the membrane on the high pressure and the low pressures sides, respectively. Suppose thermodynamic equilibria are established at both membrane interfaces, then $C_h = \omega P_h x$ and $C_l = \omega P_l y$, where ω is the equilibrium partition coefficient, which is assumed to be independent of concentration. This is considered to be adequate because of the generally low permeant concentration in polymers. Thus Eq. (4.5) can be re-written as

$$J^0 = \frac{D_0}{\phi \cdot L}[\exp(\phi \cdot \omega \cdot P_h \cdot x) - \exp(\phi \cdot \omega \cdot P_l \cdot y)] \tag{4.6}$$

From the permeation experiments the three parameters D_o, ϕ and ω cannot be determined individually, but the quantities (D_o/ϕ) and ($\omega\phi$) can be obtained by a non-linear regression of the propylene flux at different feed concentrations and operating pressures. The results so obtained are presented in Table 4.1; the correlation coefficients were found to be higher than 0.998. Similar treatment has been widely used in the study of mass transfer in pervaporation processes (Feng, 1997; Huang, 1991). Note that a similar equation could also be obtained to describe the permeation flux of nitrogen; however, for convenience, the nitrogen permeation flux can be represented by

$$J^{0}{}' = J^{0}\left(\frac{1-y}{y}\right) = \frac{D_0}{\phi \cdot L}\left(\frac{1-y}{y}\right)[\exp(\phi \cdot \omega \cdot P_h \cdot x) - \exp(\phi \cdot \omega \cdot P_l \cdot y)] \tag{4.7}$$

As such, the permeance of propylene and nitrogen can thus be written as

$$J = \frac{q}{P_h x - P_l y} = \frac{D_0/\phi}{(P_h x - P_l y)\cdot L}\left[\exp(\phi\omega \cdot P_h x) - \exp(\phi\omega \cdot P_l y)\right] \tag{4.8}$$

$$J' = \frac{q'}{P_h(1-x) - P_l(1-y)} = \frac{(D_0/\phi)(1-y)}{[P_h(1-x) - P_l(1-y)]yL}\left[\exp(\phi\omega \cdot P_h x) - \exp(\phi\omega \cdot P_l y)\right] \tag{4.9}$$

Eqs. (4.8) and (4.9) are the basic semi-empirical correlations that relate the permeance with the pressures and compositions of the gases on both sides of the membrane. To verify the applicability of the correlations, the permeance was calculated using the parameters shown in Table 4.1, and the calculated results are also shown in Figures 4.7 and 4.8 (the solid lines). The agreement with the experimental data justifies the use of the correlations for analysis of membrane permeance to individual components in the mixture gas permeation. The semi-empirical correlations will be used for simulation calculations and parametric studies later.

Table 4.1 Parameters (D_o/ϕ) and ($\omega\phi$) obtained by non-linear regression

Temperature (^oC)	D_o/ϕ [cm^3(STP)/cm.s]	$\omega\phi$ (kPa^{-1})
3	6.4×10^{-6}	1.1×10^{-2}
15	3.4×10^{-5}	5.3×10^{-3}
25	5.1×10^{-5}	4.1×10^{-3}
50	8.6×10^{-5}	2.2×10^{-3}

For gas mixture permeation, in addition to permeant-membrane interactions, there also exist interactions between the different permeating species. Figure 4.10 shows the permeance of propylene at different partial pressures in the feed gas mixture in comparison with the permeance of pure propylene. Since the overall permeate pressure was atmospheric, the data presented for gas mixture permeation here are only those with permeate propylene concentrations of over 90% so that the partial pressures of propylene in the permeate are all similar and close to permeate pressure of pure propylene.

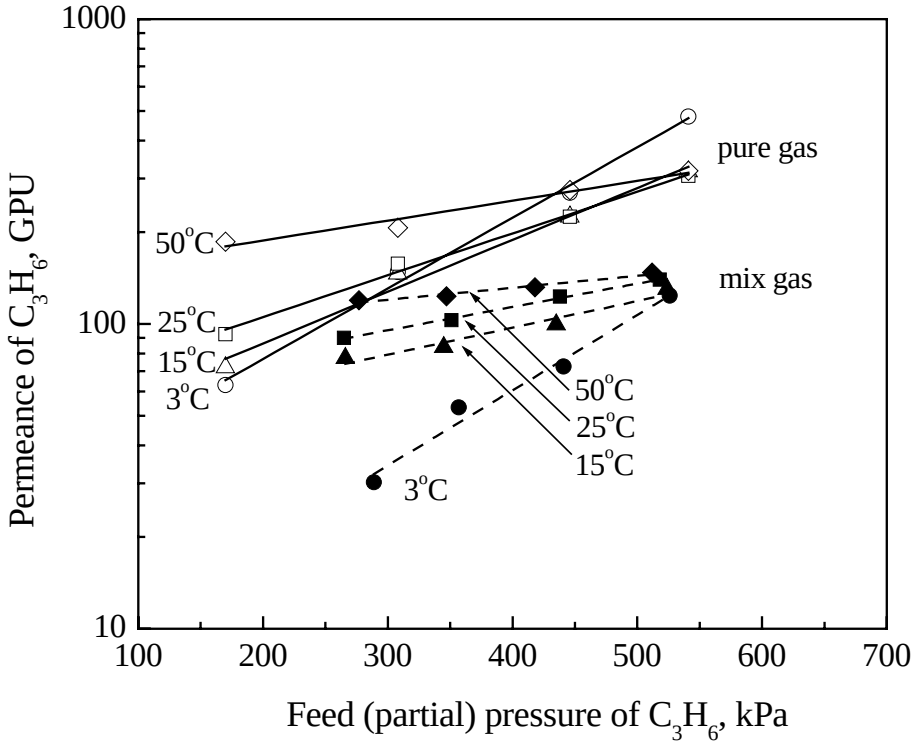

Figure 4.10 Comparison of propylene permeance for pure and gas mixture permeation. Total feed pressure in gas mixture permeation: 791 kPa.

It is clearly shown that the permeance of propylene in a gas mixture is lower than the permeance of pure propylene, indicating that the membrane permeability to propylene is lowered by the presence of nitrogen in the gas mixture. For pure propylene permeation, the membrane permeability is determined by the interactions between propylene molecules and the membrane material. Compared to propylene, nitrogen is a slow gas.

When nitrogen is present, the permeation is complicated by competitive sorption and coupling transport between the two permeating components, which results in a reduced permeability to propylene. On the other hand, no such an analysis can be made for nitrogen because of the significant difference between the permeate nitrogen partial pressures and the permeate pressure in pure nitrogen permeation; however, the data in Figure 4.8 shows that the permeation of nitrogen was enhanced by the presence of propylene. Consequently, the membrane selectivity for propylene/nitrogen mixture permeation will be lower than the membrane selectivity based on pure gas permeation, which is indeed the case as clearly shown by the data in Figures 4.5 and 4.9.

Figure 4.11 illustrates the effect of temperature on the permeance of propylene and nitrogen in gas mixture permeation. While the permeance of propylene shows a concave increase to the temperature, the permeance of nitrogen exhibits a slightly convex change with the temperature. The corresponding propylene/nitrogen permeance ratio decreases with an increase in temperature and the gas composition does not appear to affect the temperature dependence significantly.

4.3.4 Process simulation for propylene separation from nitrogen

As mentioned before, in the gas mixture separation experiments, the stage cut had been kept very low (less than 0.05) so as to retain a relatively constant concentration on the feed side of the membrane. For practical applications, the stage cut is not limited to a low value and a considerably high stage cut should be used in order to achieve a recovery as high as possible under a given permeate propylene concentration required. The potential separation performance of the membrane process was evaluated on the basis of a simple cross flow model, which provides a conservative estimate on the separation. The cross flow model was used in consideration that the membrane is comprised of an active PEBA layer on a microporous substrate that help prevent back diffusion from of the bulk permeate. Figure 4.12 illustrates the gas separation by the membrane using a cross flow configuration, where the pressure variations along both feed and permeate sides are assumed to be negligible. The following relations can be formulated based on permeation and mass balance equations for a differential unit of the membrane area:

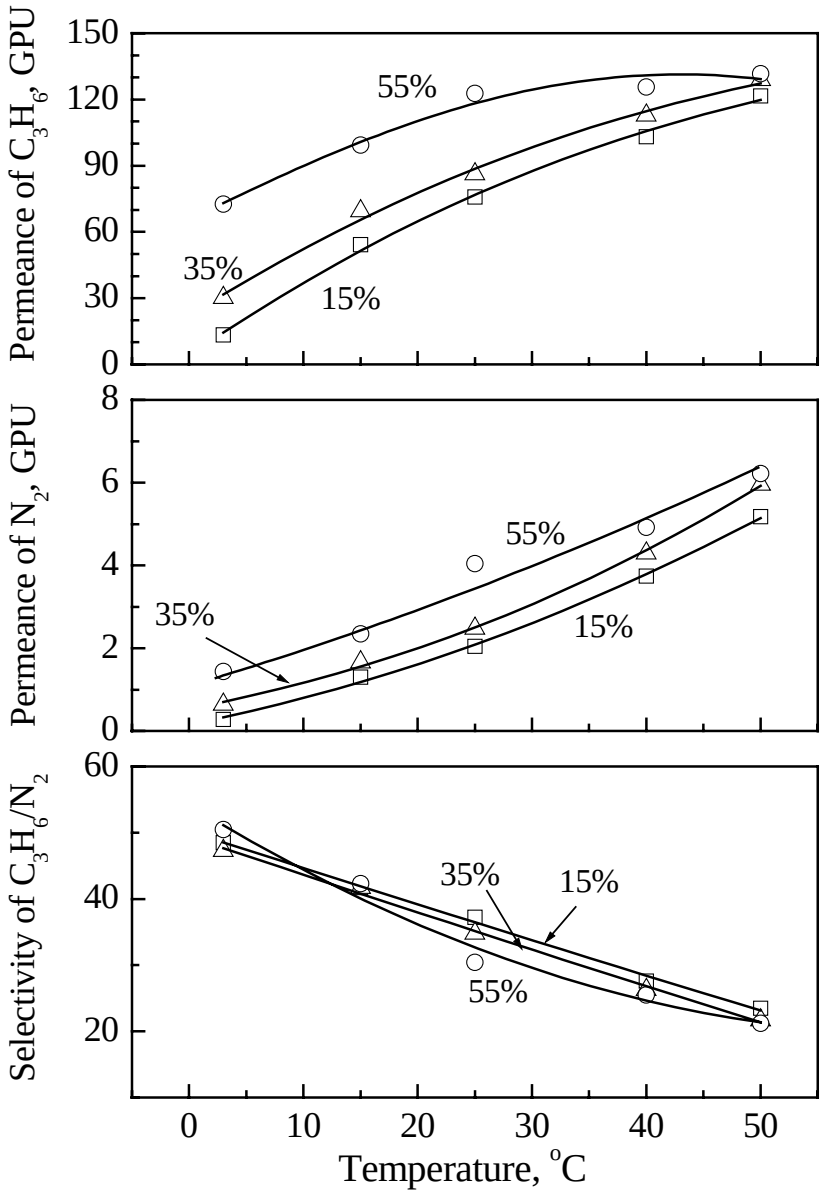

Figure 4.11 Effect of temperature on the permeance of propylene and nitrogen in gas mixture permeation. Feed pressure: 791 kPa.

$$-ydF = J(P_h x - P_l y)\cdot dA \tag{4.10}$$

$$-(1-y)dF = J'\cdot[(P_h(1-x) - P_l(1-y)]\cdot dA \tag{4.11}$$

$$d(F\cdot x) = ydF \tag{4.12}$$

where F is the gas flow rate on the feed side and A is the membrane area. Using the aforementioned semi-empirical correlations [Eqs. (4.8) and (4.9)], when the operating pressure (P_h and P_l), temperature, feed flow rate (F_0) and feed concentration (x_o) are given, the flow rates and concentrations of the residue and permeate streams can be obtained by solving Eqs. (4.10) - (4.12) with the boundary conditions $F = F_0$ and $x = x_o$ at $A = 0$. The calculations were performed for the following cases: Feed propylene concentration 15 and 30 mol%, and temperature 3 and 25°C.

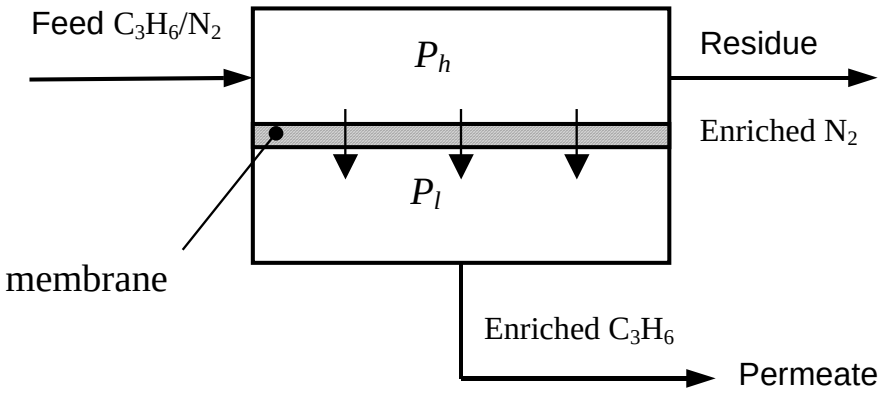

(a)

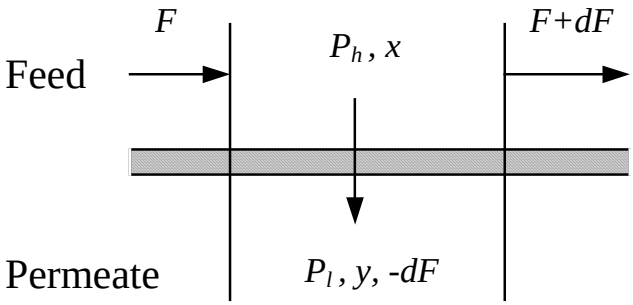

(b)

Figure 4.12 (a) Schematic diagram of membrane process for propylene/nitrogen separation. (b) A differential unit of the membrane for gas separation based on cross flow model.

In general, three issues need to be addressed in assessing the performance of a membrane permeator: product purity, recovery and productivity. The propylene enriched in the permeate is the product, and the product recovery is defined as the fractional amount of propylene in the feed that has been recovered in the permeate stream. At a given stage cut, the permeate and residue concentrations do not depend on the membrane area, and the membrane area affects only the feed processing capacity proportionally. Thus the productivity is defined here as the amount of product in terms of equivalent pure propylene generated per unit time per unit membrane area.

Figure 4.13 shows the recovery of propylene as a function of propylene concentration in the permeate product. The recovery of propylene decreases with an increase in the product purity, and the reduction in the recovery appears to be more profound at higher product purities. This clearly shows a trade-off relationship between the product recovery and purity; either a high recovery or a high purity can be obtained by the "single pass" membrane process, but not both. For a given feed concentration, the separation performance can be improved by using a lower operating temperature to increase the membrane permselectivity. As expected, the higher the concentration of propylene in the feed is, the higher the product purity is obtained while retaining the same recovery. A permeate propylene purity of 88 mol% can be achieved with 80% recovery at an operating temperature of 3^{o}C when the feed contains 30 mol% propylene. However, at a relatively low feed propylene concentration (i.e., 15%), it is difficult to get a product purity over 85 mol% even at a low recovery. Further, unless the stage cut is very large, which corresponds to a low product purity, the propylene concentration in the residue is still quite significant. In this case, multiple-stage membrane systems or hybrid processes combining membrane with other traditional separation technologies (e.g., condensation) can be employed to enhance the separation.

The membrane productivity for propylene separation as a function of product purity is shown in Figure 4.14. As shown above, a high product purity is obtained at the expense of a low recovery, and as such propylene will not be significantly depleted on the feed side. Therefore, the productivity will be increased when the product purity is increased because of the large driving force across the membranes available for propylene permeation. The calculated results show that the PEBA/PSf composite

membrane has a good performance for propylene separation from nitrogen, which is relevant to the recovery of propylene from the degassing off-gas in polypropylene production.

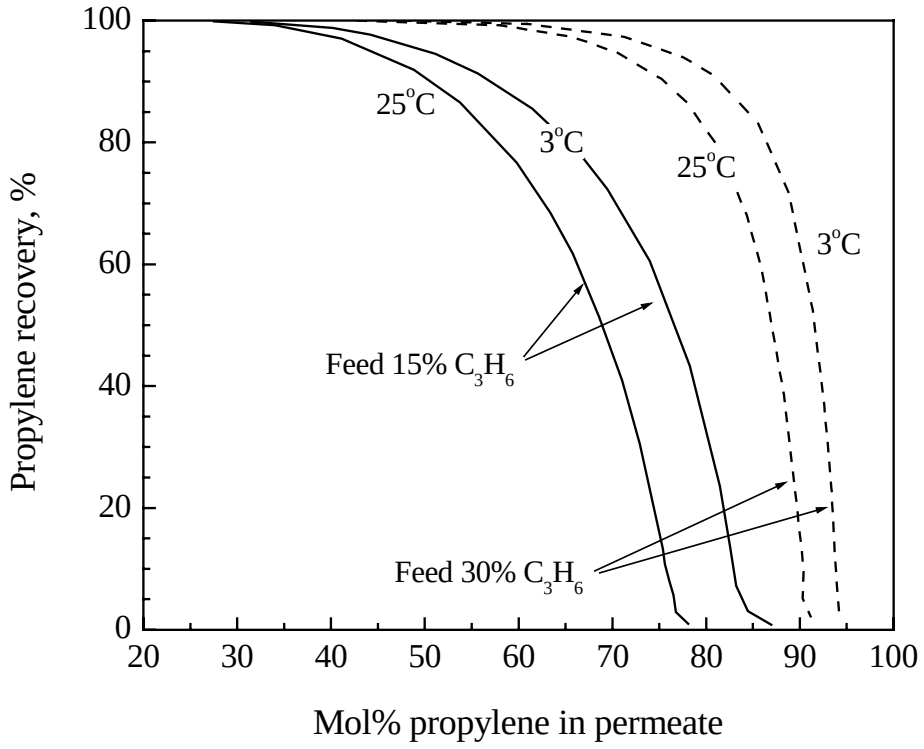

Figure 4.13 Product recovery vs. product purity determined on the basis of cross flow model. Total feed pressure: 1,480 kPa.

It is interesting to notice from Figure 4.14 that under the same operating conditions, the feed propylene concentration has no significant influence on the propylene productivity for a given product purity. Although lowering the operating temperature from ambient to a lower temperature (e.g., 3°C) leads to a reduction in the productivity, which means more membrane area would be needed to fulfill the processing capacity requirement, the resulting product purity and/or recovery will be better. The overall separation performance of the membrane should be considered in terms of all the three parameters (i.e., productivity, product purity and recovery) to determine the optimal

operating temperature. In hybrid condensation/membrane processes, the process gas from the condenser is already at a sub-ambient temperature, and thus in this case membrane separation at a low temperature is likely more preferable than operation at the ambient temperature.

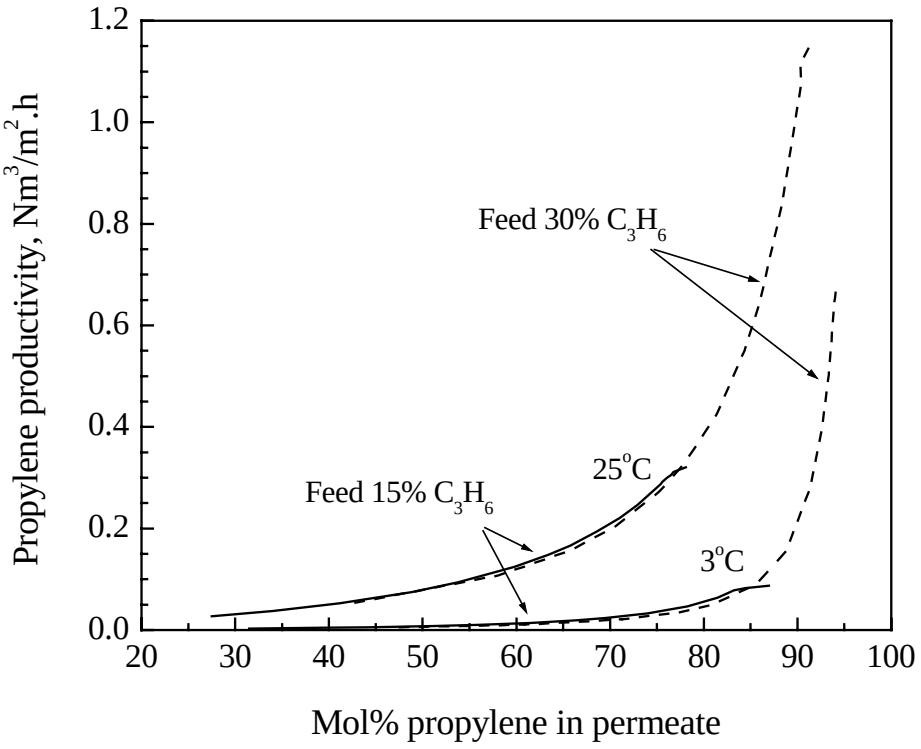

Figure 4.14 Productivity vs. product purity determined on the basis of cross flow model. Total feed pressure: 1480 kPa.

As mentioned earlier, the above analysis is for flat membranes based on a simple cross flow configuration, which is generally less efficient than a counter current configuration. The results so obtained represent a conservative estimate of the membrane performance for propylene/nitrogen separation. It is expected that should a counter current configuration be used in practical applications, the separation performance would be better.

4.4 Summary

Poly(ether block amide)/polysulfone thin film composite membranes exhibited a good permselectivity for the separation of propylene from nitrogen. Studies with pure gas permeation showed that the permeance of propylene increased with an increase in the feed pressure, while the permeance of nitrogen was independent of the pressure. Unlike the permeation of nitrogen for which the effect of temperature on the permeance followed an Arrhenius type of relation, the propylene permeance did not change with temperature monotonously. Whether propylene permeance increases or decreases with temperature depends on the pressure.

Binary propylene/nitrogen gas mixture separation was determined on the basis of a differential permeator with low stage cuts (< 0.05). It was found that the presence of propylene affected the permeance of nitrogen, and vice versa, due to interactions between the permeating species. Compared to pure gas permeation, both the permeance of propylene and the propylene/nitrogen selectivity were lower for the separation of the gas mixtures. Semi-empirical correlations were developed to relate membrane permeance with the pressures and compositions on both sides of the membrane, and the performance of the composite membrane for propylene/nitrogen mixture separation at different operating conditions (e.g. temperature, pressure and composition) was analyzed parametrically in terms of product purity, recovery and productivity. It was shown that the poly(ether block amide)/polysulfone composite membranes were promising for the separation of propylene from nitrogen, which is relevant to monomer recovery from the degassing off gas during polypropylene manufacturing.

CHAPTER 5

Sorption, Diffusion, and Permeation of Light Olefins in Poly(Ether Block Amide) Membranes

5.1 Introduction

Gas permeability is determined by its solubility and diffusivity, and the studies of gas sorption and diffusion will help understand gas permeation behavior and transport mechanism in the membrane. Preliminary studies of propylene permeation through the membranes show that the pressure and temperature dependencies of propylene permeance are different from those of permanent gases, presumably due to the competitive effects of sorption and diffusion. This will be further studied by looking into the sorption and diffusion behavior directly.

This work attempts to study of the sorption, diffusion and permeation behavior of three light olefins, i.e., ethylene, propylene, and 1-butylene, in homogenous PEBA 2533 membranes. The solubility and permeability were determined experimentally, and the diffusivity was evaluated using the permeability and solubility data. The effects of pressure and temperature on the sorption, diffusion and permeation were investigated. Since the solubility is governed by the membrane-penetrant interactions whereas the diffusivity is determined by both the molecular size of the penetrant and the membrane-penetrant interactions, an attempt was made to decouple the effects of membrane swelling on solubility and selectivity in order to differentiate the contribution of solubility and diffusivity to the preferential permeability of the membrane to olefins. It was revealed that the favorable olefin/nitrogen permselectivity is derived primarily from the solubility selectivity, whereas the diffusivity selectivity may affect the permselectivity negatively, depending upon temperature and pressure.

5.2 Experimental

5.2.1 Membrane preparation and permeation test

Dense PEBA membranes were used in this chapter for permeation and sorption experiments. The general procedures for membrane fabrication have been described in Chapter 3. Membranes used for permeation tests had a thickness of 55 μm, and relatively thick (ca. 140 μm) membranes were used for the sorptiom test. The permeability of pure gases through the membranes was determined by the constant pressure/variable volume technique as described in Chapter3.

5.2.2 Equilibrium sorption

The sorption isotherms were determined by the pressure decay technique. A schematic diagram of the experimental set-up is shown in Figure 5.1. The sorption system consists of two stainless steel chambers: a sample chamber and a reference chamber. Three stainless steel ball valves were used to control the gas flow. The various components of the apparatus were connected by stainless steel tubings (1/8 and 1/16 inch) using Swagelok compression fittings. The membrane sample was placed into the sample chamber, which is subjected to evacuation under vacuum for degassing. The system pressure was monitored by a precision pressure gauge (accuracy ±0.25% full scale). The apparatus was kept at isothermal conditions using a thermal bath. The void volumes of the sample chamber and the reference chamber (including associated connecting tubings) were 1.94 cm^3 (V_S) and 4.55 cm^3 (V_R), respectively.

To determine the sorption isotherms, the following steps were followed:

(1) The system was evacuated by opening Valves 2 and 3 (while keeping Valve 1 closed) for 3 h to remove gases present in the system including the gas sorbed in the sample.

(2) The sample chamber was isolated from the system by closing Valves 2 and 3.

(3) The gas was gradually admitted to the reference chamber by slowly opening Valve 1 until a desired pressure (p_1) was reached in the reference chamber, and Valve 1 was then closed.

(4) The pressurized gas in the reference chamber was allowed to enter the sample

chamber to contact the membrane sample by slowly opening Valve 2. An equilibrium sorption was considered to have been achieved after a constant pressure (p_2) was reached. The quantity (mol) of the gas sorbed in the membrane can be evaluated from $q_0 = [(p_1–p_2)V_R - p_2(V_S–V_m)]/RT$, where V_m is the volume of the membrane sample, and R and T are gas constant and temperature, respectively.

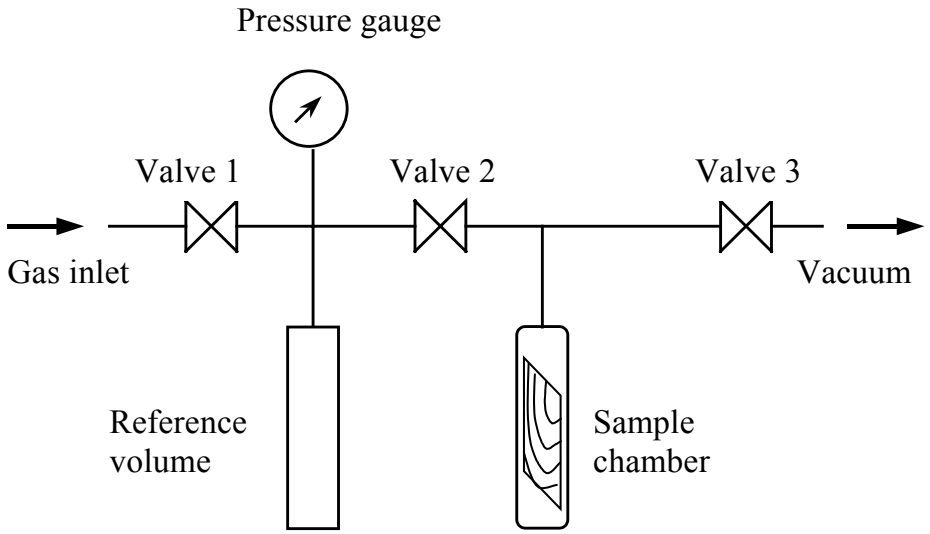

Figure 5.1 Schematic diagram of gas sorption setup.

(5) Close Valve 2, and repeat step (3) to increase the reference chamber pressure to p. Then, repeat step (4) to achieve a new sorption equilibrium at pressure p_e. The incremental sorption uptake (in mol) can thus be given by $\Delta q = [(p–p_e)V_R - (p_e – p_2)(V_S–V_m)]/RT$. Therefore, the overall quantity of the gas sorbed in the membrane at an equilibrium pressure of p_e is $q = q_0 + \Delta q = [(p_1 – p_2 + p)V_R - p_e(V_R + V_S – V_m)]/RT$. This step can be repeated so that the sorption uptakes at different pressures p_e can be obtained.

Note that assumptions were made in the proceeding procedure that the gas obeys ideal gas behavior and that the volume of the membrane sample remains constant. Although gases sorbed in the membrane may cause membrane swelling, because the membrane

sample (V_m) occupies only about 5% of the volume of the reference and sample chambers (V_R + V_S), a slight variation in the sample volume due to membrane swelling imposes little effect on the gas phase volume in the test system, which was used to determine the sorption uptake. In gas sorption studies, the sorption uptake is often expressed in the unit of cm^3(STP) gas per cm^3 polymer, thus the sorption uptake can be re-written as

$$q = [(p_1 - p_2 + p)V_R - p_e(V_R + V_S - V_m)]\frac{T_0}{T\,p_0 V_m} \quad (5.1)$$

where the T_0 and p_0 are the standard temperature and pressure, respectively, and the volumes are in the unit of cm^3.

5.2.3 Time-lag technique

The gas sorption apparatus described above is not capable of accurately measuring the solubilities of nitrogen and methane in the membranes because of their low sorption uptakes. As such, the solubility was determined indirectly from the diffusivity and permeability coefficients, which are essentially concentration independent, obtained from the time-lag measurement of transient permeation using a Toyoseiki gas permeation apparatus on the basis of constant volume/variable pressure technique. The diffusivity was calculated from the time lag θ by

$$D = l^2/(6\theta) \quad (5.2)$$

The principle of the time lag method can be found in Koros and Chern (Koros et al., 1987). The steady state permeability can also be measured in the time lag measurement. As a first approximation, the permeability is equal to the solubility multiply the diffusivity, and thus the solubility can be evaluated from the ratio of permeability and diffusivity, i.e.,

$$S = P/D \quad (5.3)$$

5.3 Results and discussion

5.3.1 Permeation

In order to avoid the possible effect of membrane plasticization/swelling by hydrocarbons on the permeation of nitrogen, the permeability of nitrogen was determined first. It was found that in the temperature range of 20-50 °C, the permeability of nitrogen

in the PEBA 2533 membranes ranges from 3.8 to 15.0 Barrer and is almost independent of the feed pressure. The temperature dependence of permeability will be further discussed later. The permeability of the three olefins, (i.e., C_2H_4, C_3H_6 and C_4H_8) in the membranes as a function of pressure difference across the membrane Δp at a temperature of 20, 30, 40, and 50 °C is shown in Figure 5.2. Clearly, at given feed and permeate pressures, the permeability of olefins increases with an increase in the carbon number of the olefins, and they are much higher than the permeability of nitrogen at the same operating temperature. The gas permeability in the membrane is in the order of C_4H_8 > C_3H_6 > C_2H_4 >> N_2, the same order of decreasing solubilities of the penetrants, which will be studied in more details later. The gas permeability in nonporous polymeric membranes depends on both the thermodynamic parameter (solubility) and the kinetic parameter (diffusivity). In general, the solubility is often correlated to the condensability; a more condensable gas tends to have a greater solubility. On the other hand, the diffusivity is governed by the molecular size of the penetrant and the membrane-penetrant interaction. Table 5.1 shows some physical quantities of the penetrant gases investigated; these quantities can be used to characterize their condensability and molecular sizes. The order in the condensability of the various penetrant gases, as represented by the boiling point T_b or critical temperature T_c, is opposite to that in the molecular size, indicating that the solubility and the diffusivity of the penetrants studied here will also follow an opposite order. Judging from the fact that the permeability of different gases in PEBA 2533 follows the same order as their solubility, the gas permeability appears to be mainly dominated by the solubility of the penetrants, whereas the difference in their diffusivity is not substantial enough for the membrane to differentiate the permeation of gases based solely on their molecular sizes. This is typical of gas permeation in rubbery polymers. As shown later, these qualitative observations and predictions can be verified by evaluating the solubility and diffusivity quantitatively.

The data in Figure 5.2 show that the pressure dependence of the hydrocarbon permeability can be expressed empirically by: $P = P_{(\Delta p=0)} \exp(m \cdot \Delta p)$, where the pre-exponential factor $P_{(\Delta p=0)}$ represents the gas permeability when the transmembrane pressure difference Δp approaches zero, and parameter m characterizes the significance of the pressure dependence of permeability. The correlation coefficient was found to be

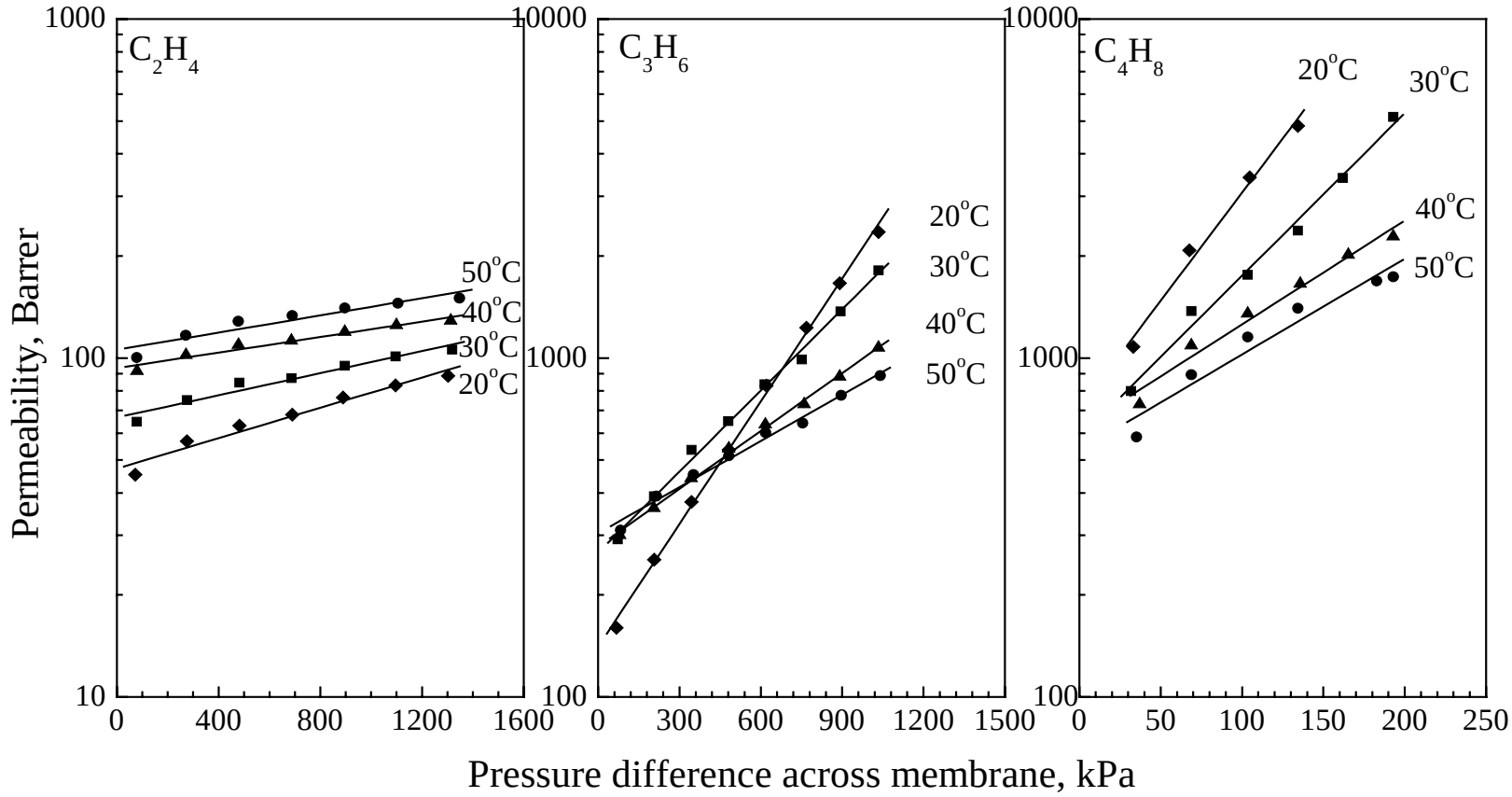

Figure 5.2 Permeability of olefin in PEBA 2533 as a function of transmembrane pressure difference.

greater than $R^2 = 0.995$, and the values of $P_{(\Delta p=0)}$ and m at different temperatures are presented in Table 5.2. The olefin permeability increases with an increase in pressure, presumably due to membrane plasticization of the glassy polyamide segments and swelling of the rubbery polyether segments. An increase in the sorption uptake of a penetrant in the polymer tends to enlarge the space between the polymer chains, making diffusion through the membrane easier. Among the three olefins, the m value of n-butylene is the highest, suggesting that the effect of pressure on its permeability is the most significant, whereas the pressure dependence of ethylene permeability is the least significant. Moreover, the m value of a given penetrant increases with a decrease in the operating temperature, and thus the pressure dependence of permeability becomes more significant at relatively lower temperatures. This is also consistent with the general observation that sorption is an exothermic process and a high sorption uptake is favored at low temperatures.

Table 5.1 Some physical properties of gases (Ride, 2004; Breck, 1976; Semenova, 2004)

	Condensability		Size of molecule		
	T_b (K)	T_c (K)	V_c (cm^3/mol)	σ_{LJ} (nm)	σ_{kt} (nm)
N_2	77.4	126.2	90.0	0.368	0.364
C_2H_4	169.4	282.3	131.0	0.423	0.390
C_2H_6	184.5	305.3	145.5	0.442	-
C_3H_6	225.5	364.9	181.0	0.468	0.450
C_3H_8	231.0	369.8	200.0	0.506	0.430
C_4H_8	266.9	419.6	240.0	0.528	0.560

σ_{LJ} is the molecular collision diameter calculated from the Lennard-Jones potential;

σ_{kt} is the molecular kinetic diameter determined using zeolite;

V_c is the critical molar volume.

Table 5.2 Parameters characterizing pressure dependence of permeability and solubility

	C_2H_4				C_3H_6				C_4H_8			
	$P_{(\Delta p=0)}$[a]	m $\times10^3$	$S_{(p=0)}$[b] $\times10^2$	n $\times10^3$	$P_{(\Delta p=0)}$[a]	m $\times10^3$	$S_{(p=0)}$[b] $\times10^2$	n $\times10^3$	$P_{(\Delta p=0)}$[a]	m $\times10^3$	$S_{(p=0)}$[b] $\times10^2$	n $\times10^3$
20°C	47	3.55	0.96	1.17	141	19.2	3.29	4.43	708	101.2	12.4	13.8
30°C	67	2.59	0.95	0	267	12.7	3.23	2.19	580	76.0	9.68	6.40
40°C	93	1.81	0.86	0	278	9.02	2.87	0.99	620	48.7	7.80	2.76
50°C	105	2.01	0.83	0	304	7.21	2.65	0	534	44.9	5.83	1.46

a. $P_{(\Delta p=0)}$ in Barrer

b. $S_{(p=0)}$ in cm^3(STP)/(cm^3 polym..kPa)

It may be pointed out that since temperature influences both solubility and diffusivity, the permeability of the olefins as a function of temperature shows different trends. As temperature increases, the permeability of high-solubility n-butylene decreases, whereas the permeability of low-solubility ethylene increases. For the permeation of propylene, whose solubility is the moderate, an increase in temperature may increase or decrease its permeability, depending on the operating pressure. This further demonstrates that the sorption aspect plays a more dominating role in the permeation of olefins with bigger molecular sizes.

The temperature dependence of the pre-exponential factor $P_{(\Delta p=0)}$ follows an Arrhenius type of relation, as shown in Figure 5.3. The apparent "activation energy" for permeation was calculated to be 35.7, 21.8, 18.8, and -6.15 kJ/mol for N_2, C_2H_4, C_3H_6 and C_4H_8, respectively. The activation energy for permeation is the sum of sorption heat and activation energy for diffusion. Generally, the former is negative because of the exothermic nature, and the latter is positive due to the energy barrier to overcome. The negative value of apparent activation energy for C_4H_8 permeation can be attributed to the stronger temperature dependency of the solubility than that of the diffusivity, which will be shown later. When the heat of sorption outweighs the activation energy of diffusion, a negative temperature dependence of permeability will occur; this is more likely to occur for more condensable penetrant such as C_4H_8 whose solubility in the membrane is considerably high.

Over the range of pressures and temperatures investigated, the pure gas permeability ratios of C_2H_4/N_2, C_3H_6/N_2, and C_4H_8/N_2 are 6-23, 20-165 and 39-1270, respectively. These data show that PEBA 2533 is a potential material that can be used for the separation of olefins from nitrogen streams, although the actual separation factor for a gas mixture may be lower due to coupling transport of the components, as shown in the last chapter.

It is of interest to see how an olefin permeates through the membrane differently from its respective paraffin as olefin/paraffin separation is another important separation in the petrochemical industry. Figure 5.4 shows the permeabilities of propylene, propane, ethylene and ethane at 25°C. It can be seen that in the PEBA 2533 membrane, olefins tend to exhibit a higher permeability than their respective paraffins in spite that the

paraffins are slightly more condensable than the olefins as expected on the basis of their boiling points and critical temperatures (see Table 5.1). Similar trend can be found for the permeation of olefin and paraffin through poly(ethylene oxide) membranes (Lin and Freeman, 2004). One reason could be that there is an interaction between the polar ether linkage in PEBA 2533 and unsaturated double bonds of olefins, which favors the solubility of olefin in the membrane. This hypothesis is supported by the sorption data discussed below. In addition, it can be seen from Table 5.1 that the molecular size of an olefin is smaller than its paraffin, and the faster diffusivity of olefin also contributes to its higher permeability. However, unlike propylene and propane whose permeabilities differ by a factor of about 2, ethylene permeability is only about 10% higher than the ethane permeability.

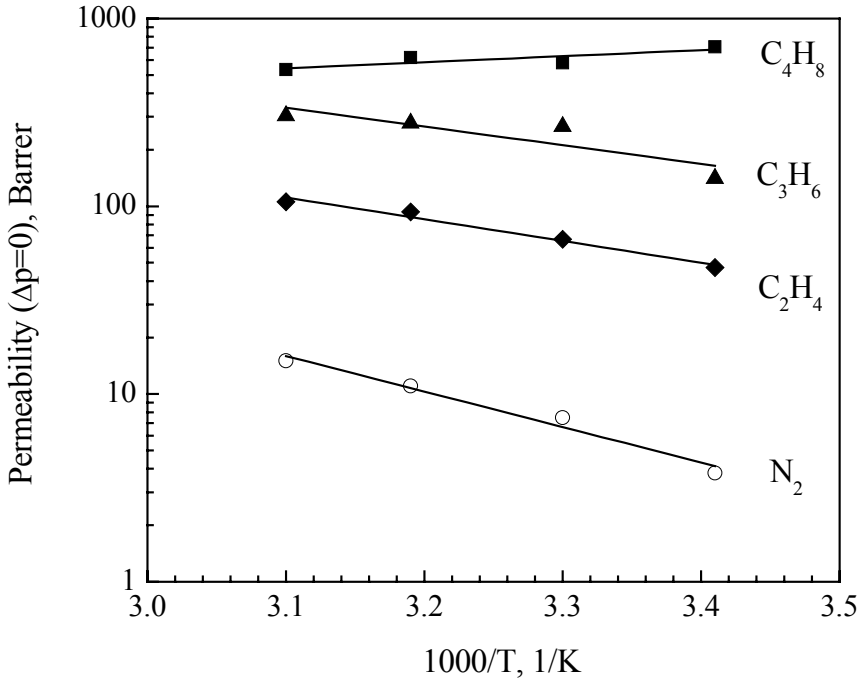

Figure 5.3 Temperature dependence of gas permeability at $\Delta p = 0$

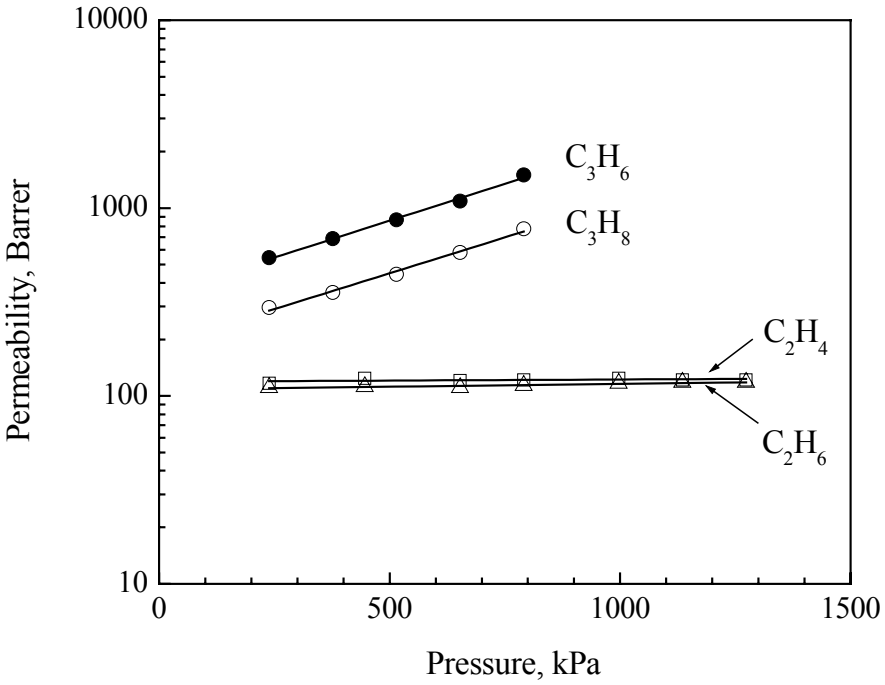

Figure 5.4 Permeability of paraffins (ethane and propane) and olefins (ethylene and propylene) in PEBA 2533 membranes at 25°C.

5.3.2 Equilibrium sorption

Figure 5.5 shows the sorption isotherms of the olefins in PEBA 2533 at different temperatures. The sorption isotherms are either linear or convex with respect to the gas phase pressure. At relatively low sorption uptakes, the sorption isotherms are almost linear, and can be approximated by the Henry's law. In this case, the pressure has little effect on the solubility. On the other hand, when the sorption uptake is high, the sorption isotherms show a positive deviation from Henry's law, and the gas solubility increases with an increase in the pressure. The positive deviation becomes more significant for the sorption of stronger sorbent olefins. This is in agreement with the common observations for the sorption of hydrocarbons or other organic vapors in rubbery polymers (Merkel et al., 2000). Bondar et al., who measured the solubilities of several gases in a series of

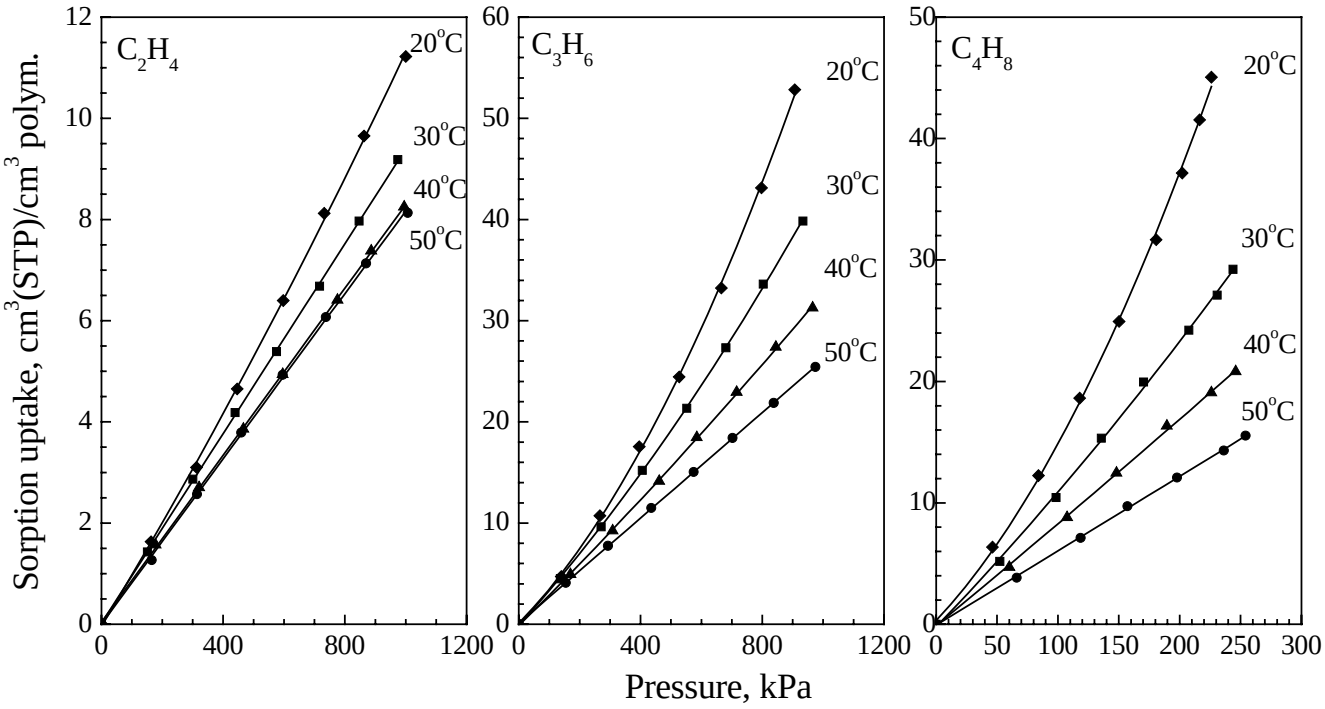

Figure 5.5 Sorption isotherms of olefins in PEBA 2533 membranes

PEBA copolymers, also found convex sorption isotherms for more condensable gases (e.g. butane, propane, ethane and CO_2) and linear isotherms for permanent gases (e.g. H_2, N_2, O_2 and CH_4) (Bondar et al., 1999).

From the sorption isotherms, the solubility coefficient can be evaluated by normalizing the sorption uptake by the gas phase pressure, that is, $S = q/p_e$. Figure 5.6 shows the solubility of the three olefins at different temperatures and pressures. The solubility decreases as the temperature increases. At a given temperature and pressure, the penetrant solubility is in the order of $C_4H_8 > C_3H_6 > C_2H_4$, the same order as their condensability. When the temperature is sufficiently high, the pressure has little effect on the solubility, but the solubility becomes increasingly pressure-dependent as the temperature is lowered. The pressure dependence of the solubility for the olefins can also be represented empirically by an exponential expression $S = S_{(p=0)} \exp(n \cdot p)$, with a correction coefficient R^2=0.995, where $S_{(p=0)}$ represents the limiting solubility at infinite dilution, and parameter n characterizes the significance of pressure on the solubility. The values of $S_{(p=0)}$ and n are also presented in Table 5.2. In general, the both values of $S_{(p=0)}$ and n are higher for more condensable gases and they tend to be lower at lower temperatures. For ethylene, which is the least sorptive olefin, the n value is close to zero at relatively high temperatures, and the ethylene pressure has little impact on its solubility.

As a comparison, the sorption isotherms of ethane and propane were also determined, and they were found to follow similar trends as the olefins, as shown in Figure 5.7 where the sorption uptakes of the olefins and paraffins at 30 °C are illustrated. Interestingly, the logarithmic solubility at infinite dilution $S_{(p=0)}$ for all the gases measured at 30 °C can be correlated linearly with their boiling points or critical temperatures. This is shown in Figure 5.8, where the sorption data of CO_2, a condensable non-hydrocarbon gas, is also included. It appears that the higher the boiling point or critical temperature, the higher the solubility.

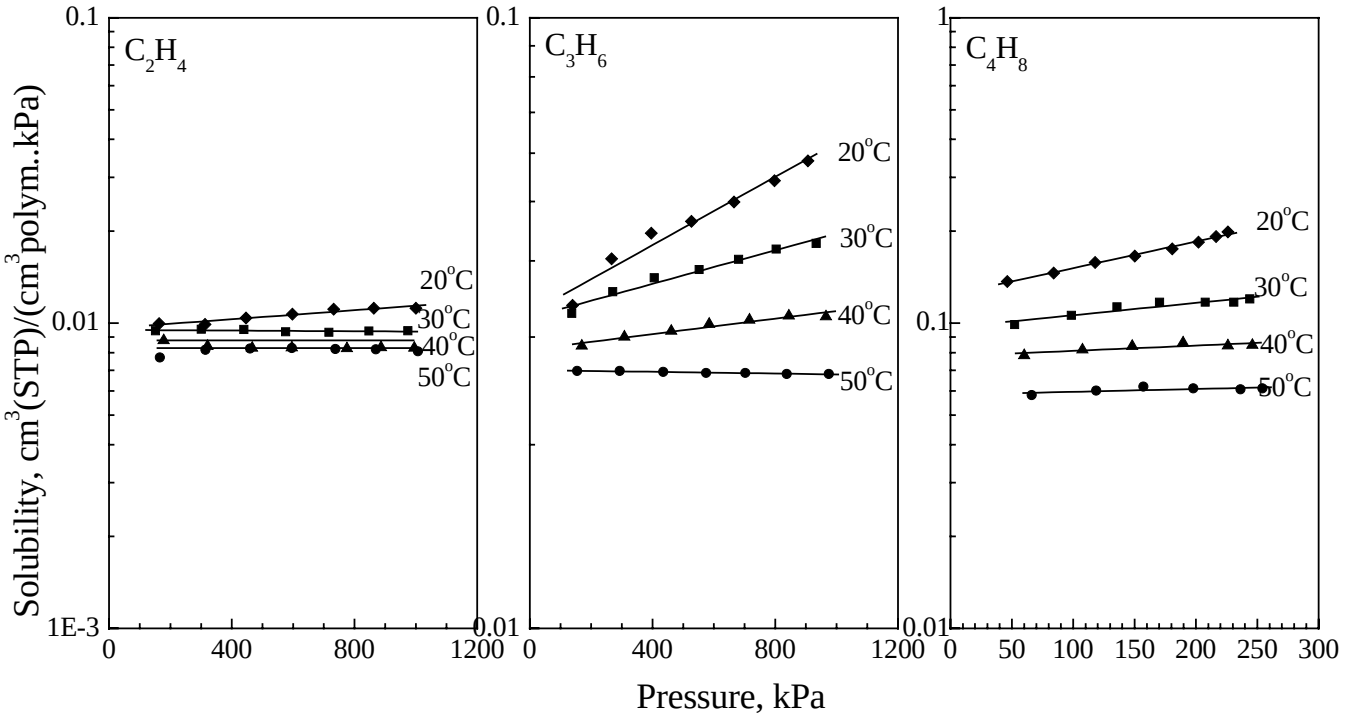

Figure 5.6 Solubility of olefin in PEBA 2533 membranes at different temperatures and pressures

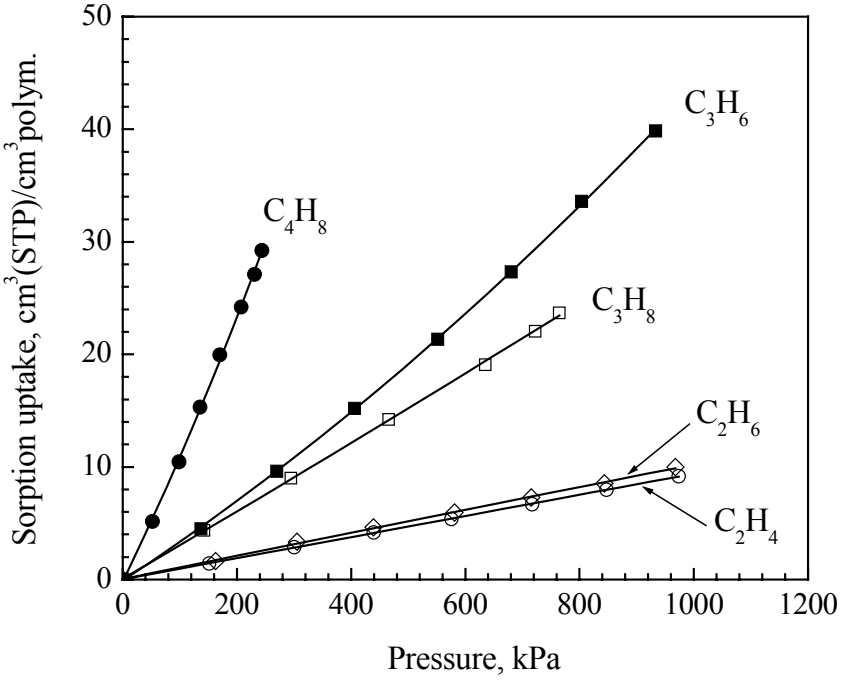

Figure 5.7 Sorption isotherms of paraffin and olefin in PEBA 2533 membranes at 30 ^{o}C.

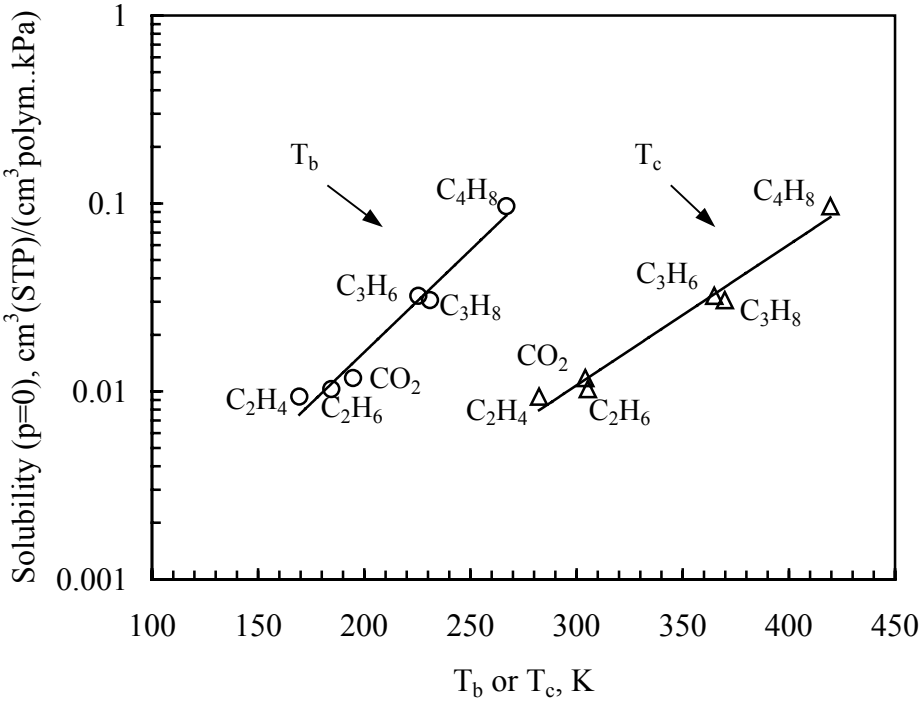

Figure 5.8 Infinite dilute solubility vs. boiling point T_b or critical temperature T_c.

In consideration of the linear relation between the solubility at infinite dilution for a given temperature and the critical point shown in Figure 5.8, it would be of great interest to obtain a general expression, at least empirically, that could take into account the effect of temperature on the solubility. Therefore, a correlation between the solubility at infinite dilution with the reduced temperature T_r (= T/T_c) was attempted. It was found that an empirical equation of the type $\log S_{(p=0)} = a + \frac{b}{T_r^2}$ was adequate to describe the relation quantitatively, as shown in Figure 5.9, where the solubility of non-condensable gases N_2 and CH_4 at various temperatures determined by the time-lag technique is also included. In addition, for the sake of comparison, the data for gases (including He, H_2, N_2, O_2, CH_4, CO_2, C_2H_6, C_3H_8 and n-C_4H_{10}) measured at 35 °C available in the literature (Bondar et al., 1999) are also shown in the figure.

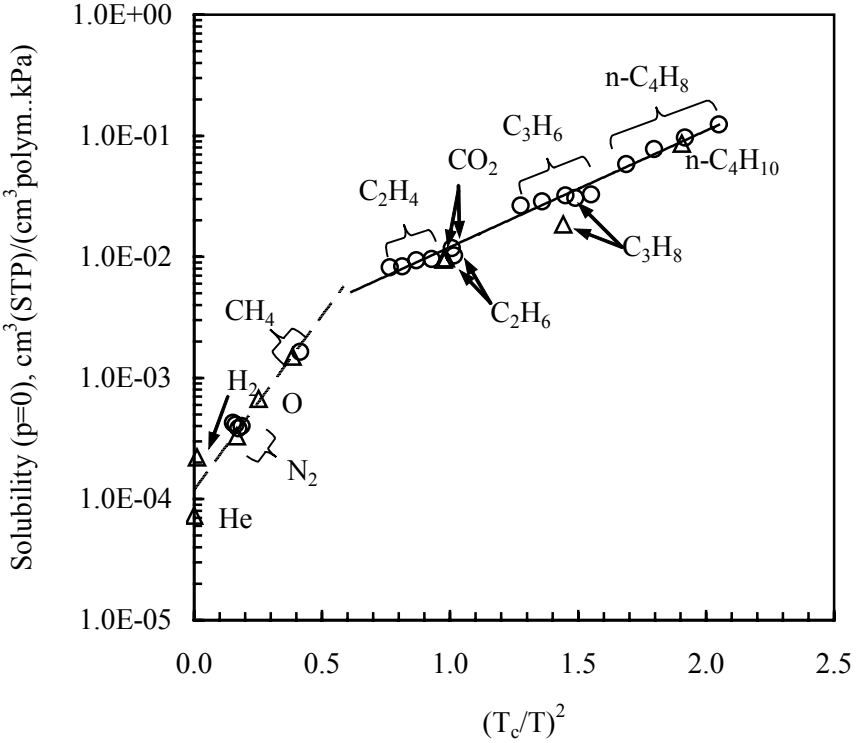

Figure 5.9 Infinite dilute solubility as a function of reduced temperature (T/T_c). (O) This work; (Δ) taken from Bondar et al. (1999).

It appears that for condensable gases, such as CO_2, C_2H_4, C_2H_6, C_3H_6, C_3H_8, C_4H_8 and n-C_4H_{10}, the data can be fitted to the empirical equation very well with values of parameters a = -2.89 and b = 0.96 (the solubility $S_{(p=0)}$ is in the unit of cm^3(STP)/(cm^3 polym. kPa)). The quantitative empirical relation seems to also hold for permanent gases (He, H_2, N_2, O_2, and CH_4), although deviations exist for H_2 and He, the two gases with very low critical temperatures. This is not surprising because the solubility is related to the cohesive properties of the solute gases. Gases with very weak cohesive forces between their own molecules will not be acted upon strongly by the polymer. In spite of the lesser extent of certainty due to the limited solubility data for only a few permanent gases available, the numerical values of the two empirical parameters for the permanent gases were evaluated to be a = -3.92 and b = 2.88.

It is interesting to notice that similar correlations can also be found for gas sorption in polyethylene and polydimethylsiloxane (Stern et al., 1969; Suwandi and Stern, 1973). It has been reported that the solubility data of twenty eight different substances in polyethylene, having $S_{(p=0)}$ values varying over five orders of magnitude and with critical temperatures in a wide range from 5.2 to 619.6 K, can be fitted into a single equation. That the parameters in the empirical correlations for PEBA 2533 membranes are different for condensable and permanent gases may be partly attributed to the micro-biphasic structure of PEBA 2533, which is a copolymer comprised of a rubbery polyether domain and a glassy polyamide domain. The observed overall sorption results from the joint contribution of sorption in each phase. It is well known that permanent gases and condensable gases behave differently in amorphous rubbery polymers and crystalline glassy polymers. For instance, glassy polymers often exhibit dual mode-like sorption for condensable gases, whereas dual mode of sorption is generally insignificant for permanent gases resulting in a linear isotherm. PEBA 2533 is comprised of a large portion of rubbery polyether phase (80 wt%). The sorption data in PEBA 2533 demonstrate that the membrane exhibits largely sorption features typical of rubbery polymers, but with some special characteristics due to the presence of glassy segments in the block copolymers.

The sorption of condensable hydrocarbons in rubbery polymers could be described by the Flory-Huggins equation:

$$\ln \frac{p}{p^0} = \ln \Phi + (1-\Phi) + \chi(1-\Phi)^2 \tag{5.4}$$

where p and p^0 are the gas phase pressure and the saturated vapor pressure of the penetrant, respectively, χ is the Flory-Huggins interaction parameter, and Φ is the volume fraction of dissolved gas in the amorphous phase of the polymer, which can be expressed by:

$$\Phi = \frac{C\overline{V}}{\Phi_a + C\overline{V}} \tag{5.5}$$

where $\overline{V}$ is the partial molar volume of penetrant, C is the molar concentration of the penetrant sorbed in the polymer, andΦ_a is the volume fraction of amorphous phase in the polymer. For PEBA 2533 the value of Φ_a can be considered to be 0.97 because the copolymer contains 3 vol% of the crystalline phase (Kim et al., 2001). The interaction parameter χ provides a measure of the interactions between the polymer segments and the penetrant molecules. Higher values of χ mean less favorable polymer/penetrant interactions with respect to sorption (Reid, et al., 1987). Following the approach of Kamiya et al. (1997), who found that the partial molar volume of an organic gas in rubbery polymers is a linear function of its van der Waals volume, the interaction parameter χ was determined from the sorption data using Equations (5.4) and (5.5). Table 5.3 shows the calculated χ values at various temperatures for the olefins and paraffins investigated along with their partial molar volumes used in the calculation.

The data in Table 5.3 show that the polymer-penetrant interaction parameters for olefins tend to be smaller than for their respective paraffins, and for both olefins and paraffins bigger molecules tend to have weaker interactions. In addition, the interaction parameter appears to decrease with an increase in temperature. Kamiya et al. (1997) investigated the effects of temperature on the interaction parameters of a series of hydrocarbons in such rubbery polymers as 1,2-polybutadiene, poly(ethylene-co-vinyl acetate), and similar trends have been observed.

The interaction parameter can be used to help understand the gas sorption behavior. Generally, gas solubility in a polymer depends on both the condensability of the penetrant and the polymer-penetrant interactions. The two factors jointly determine the overall solubility of the penetrant in the polymer. Let us look at again the data in

Figure 5.7, which shows the sorption isotherms of olefins (i.e., ethylene, propylene and butylenes) and paraffins (i.e., ethane and propane). As shown in Table 5.1, propylene and propane have similar condensabilities; the higher solubility of propylene than propane could be attributed to the stronger interaction between propylene and the polymer. On the other hand, ethylene is less condensable than ethane (which is reflected by their boiling and critical temperatures), but ethylene has a stronger interaction with the polymer. As a result, the solubility of ethane is only slightly higher than ethylene due to the opposite effects of condensability and interaction. For the three olefins considered, the effect of condensability appears to be more dominant than the interaction. The solubility increases with an increase in the carbon number or condensability in spite that the interaction becomes weaker. For a given penetrant, it becomes less condensable at a higher temperature although the penetrant-polymer interaction is more favorable to sorption. Considering the negative effect of temperature on the solubility observed above, it is further demonstrated that the gas solubility is affected by the condensability more significantly than the penetrant-polymer interaction. All these results illustrate the importance of penetrant condensability on the solubility in polymers, at least for a given homologous series of light hydrocarbons.

Table 5.3 Polymer/penetrant interaction parameters

	$\overline{V}$ [a]	χ			
	10^{-6} m^3/mol	20°C	30°C	40°C	50°C
C_2H_4	57	0.912	0.882	0.838	0.699
C_2H_6	61	-	1.19	-	-
C_3H_6	73	1.22	1.09	1.02	0.965
C_3H_8	80	-	1.41	-	-
C_4H_8	90	1.18	1.16	1.10	1.09

[a] Ref. (Suwandi and Stern, 1973).

5.3.3 Diffusion

Gas transport through a nonporous polymer membrane is commonly described by the solution-diffusion mechanism. As a first approximation, the permeability coefficient P can be correlated to the diffusivity and solubility of the penetrant in the membrane (Stern, 1994; Crank and Park, 1968):

$$P = \overline{D} \times \overline{S} \tag{5.6}$$

where $\overline{D}$ is a concentration-averaged diffusivity defined by

$$\overline{D} = \frac{1}{C_h - C_l} \int_{c_l}^{c_h} D_{eff}(c) dC \tag{5.7}$$

and $\overline{S}$ is an average solubility given by

$$\overline{S} = \frac{C_h - C_l}{p_h - p_l} \tag{5.8}$$

In the above equations, D_{eff} is the local effective diffusivity characterizing the mobility of the penetrant at a given concentration (C) in the membrane, p is the gas phase pressure of the penetrant, and subscripts h and l represent the upstream and the downstream sides of the membrane, respectively. Substitution of Equations (5.7) and (5.8) into Equation (5.6) and differentiation yield the following relation,

$$D(c)_{eff}\Big|_{C_h} = \left(P + \Delta p \frac{dP}{d\Delta p}\right)_{p_h} \left(\frac{dp}{dC}\right)_{p_h} \tag{5.9}$$

which has been widely used to evaluate the effective diffusivity from experimental data of steady state permeability and sorption isotherms (see, for example, Merkel et al., 2000; Koros et al., 1976; Stern et al., 1987; Singh et al., 1998). As shown before, for the systems studied here, the permeability P and solubility S (= C/p) can be represented by an exponential function of Δp and p, respectively, and Equation (5.9) can be simplified as

$$D(c)_{eff} = \frac{P_{(\Delta p=0)}}{S_{(p=0)}} \frac{(1 + m\Delta p)\exp(m\Delta p)}{(1 + np)\exp(np)} \tag{5.10}$$

The corresponding sorbate concentration in the membrane is $C = S_{(p=0)}\, p \exp(n\, p)$. Figure 5.10 shows the calculated local diffusivity of olefins as a function of the sorbate concentration C. It can be seen that the diffusivity increases with an increase in the sorbate concentration in the membrane. This is understandable because the membrane swelling/plasticization induced by the sorbed penetrant molecules increases the space between the polymer chains, making it easier for the penetrant to the move in the polymer matrix. This is consistent with previous reasoning that a higher permeability can be achieved at a higher feed pressure because of the enhanced diffusivity through the membrane. Lin et al. (2004) also reported that the diffusivities of several hydrocarbons increase at higher concentrations in poly(ethylene oxide) membranes due to membrane swelling and plasticization. Similar observations can be found for CO_2 permeation in a series of PEBA copolymers (Bondar et al., 2000) and C_2H_6 and C_3H_8 permeation in poly(dimethyl siloxane) (Merkel et al., 2000). This is, however, not always the case. It has been reported that (Singh et al., 1998) the diffusivity of acetone in poly(dimethyl siloxane) membranes decreases with an increase in acetone concentration presumably due to clustering of acetone molecules under hydrogen bonding interactions. In this work, as mentioned above, the concentration dependence of olefin diffusivity exhibits the general behavior of membrane swelling and plasticization instead of clustering of penetrant molecules.

Figure 5.11 shows the average diffusivity calculated as a function of the feed pressure at zero permeate pressure. Similar to the pressure dependencies of the permeability and the solubility shown in Figures 5.2 and 5.6, the average diffusivity can also be fitted to an exponential relation with the feed pressure. For the three olefins studied, the significance of the pressure dependence of diffusivity follows the same order as their solubility. At a given temperature and pressure, the magnitude of the diffusivity is in the order of $C_2H_4 < C_3H_6 < C_4H_8$. The diffusivity of 1-butylene, which is the most strongly adsorptive gas, increases drastically as the pressure increases. In general, the temperature dependence of diffusivity tends to be intensified at lower temperatures. Thus the diffusivity appears to be affected by the membrane swelling more significantly than the molecular size of the penetrants.

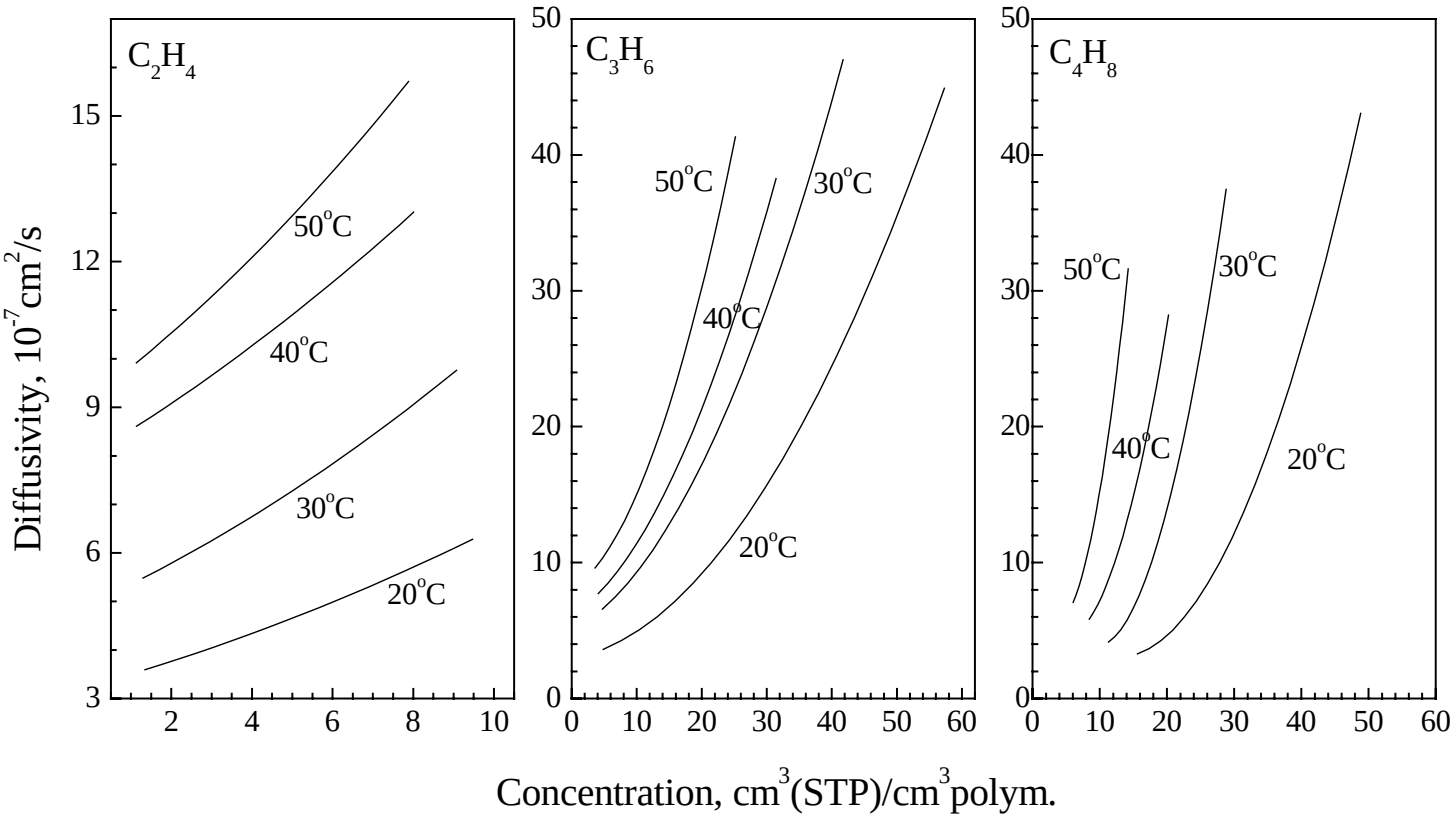

Figure 5.10 Local diffusivity of olefins as a function of sorbate concentration in the membrane.

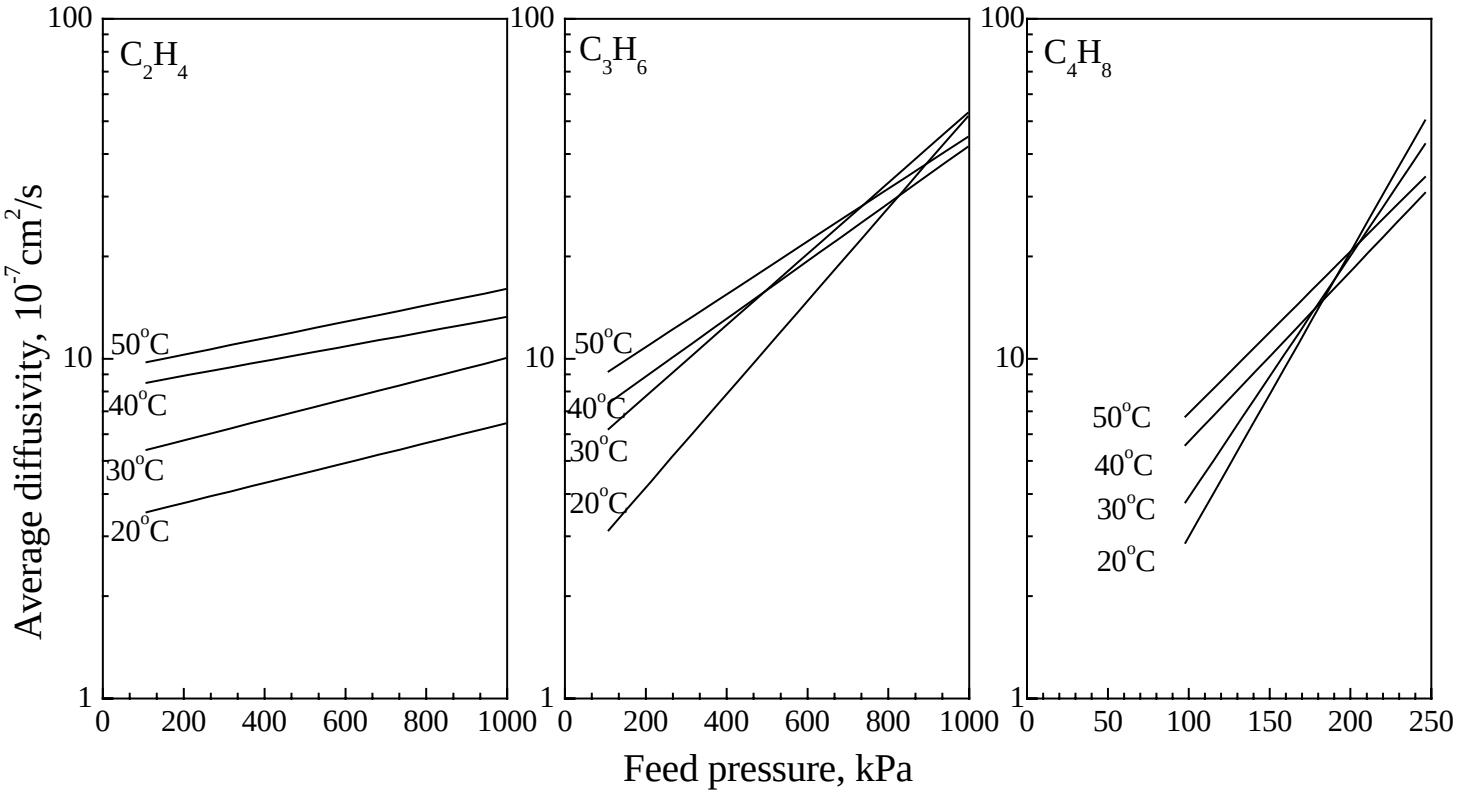

Figure 5.11 Average diffusivity of olefins as a function of feed pressure.

When the pressure approaches zero, the membrane swelling due to penetrant uptake is minimized. As such, the hypothetical diffusivity at zero pressure ($\overline{D}_{(p=0)}$) would correlate with the molecular size of penetrant directly. This is indeed the case as shown in Figure 5.12, which indicates that in the absence of membrane swelling, smaller molecules have a higher diffusivity. As expected, the effect of temperature on $\overline{D}_{(p=0)}$ follows the Arrhenius relation. The corresponding activation energy for diffusion was determined to be 28.8, 30.9 and 46.6 kJ/mol for C_2H_4, C_3H_6 and C_4H_8, respectively.

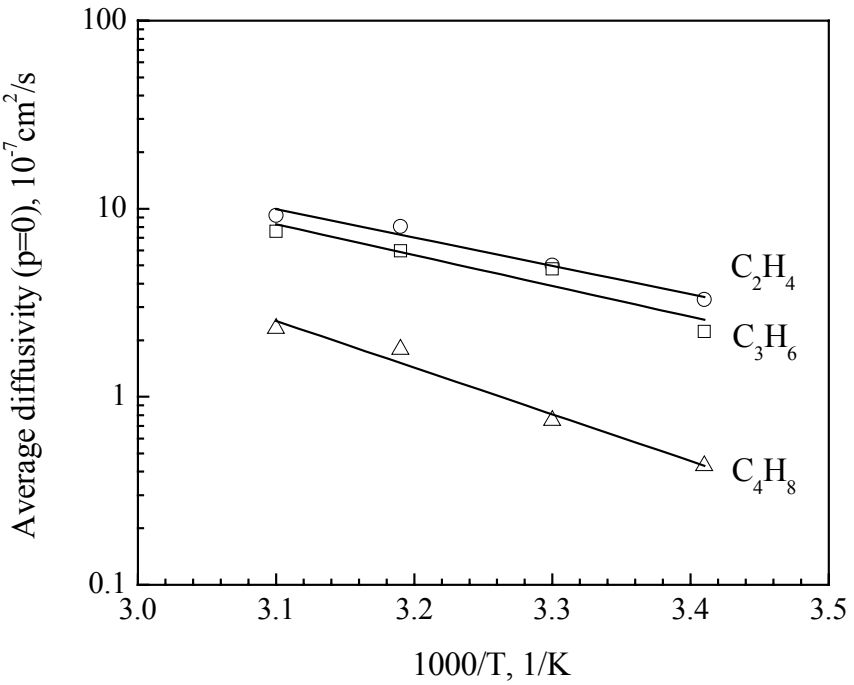

Figure 5.12 Temperature dependence of average diffusivity at p=0.

5.3.4 Membrane Selectivity

The overall permselectivity (i.e., permeability ratio) of the PEBA membrane can be attributed to two aspects: the solubility selectivity (i.e., solubility ratio) and the

diffusivity selectivity (i.e., diffusivity ratio). The permeability selectivity, solubility selectivity and diffusivity selectivity of the PEBA membranes to olefin/nitrogen are evaluated, as shown in Table 5.4. It is clear that for the three olefins considered, the permeability selectivity is consistent with the solubility selectivity, that is, both increase with a decrease in the operating temperature and an increase in the olefin condensability. In fact, the diffusivity selectivity is quite low, and it is mainly the solubility selectivity that gives rise to the considerably high olefin/nitrogen permselectivity.

Table 5.4 Olefins/nitrogen selectivity

	Solubility selectivity			Diffusivity [a] selectivity			Permeability selectivity		
	C_2H_4 [b]	C_3H_6 [b]	C_4H_8 [c]	C_2H_4 [b]	C_3H_6 [b]	C_4H_8 [c]	C_2H_4 [b]	C_3H_6 [b]	C_4H_8 [c]
20°C	27.6	124.1	465	0.54	2.05	2.46	14.9	254	1145
30°C	24.5	104.7	305	0.51	1.63	1.44	12.6	170	440
40°C	20.2	77.1	207	0.50	1.02	0.86	10.1	78.8	178
50°C	19.2	61.2	143	0.43	0.83	0.71	8.21	51.1	102

[a] Based on local diffusivity. [b] Evaluated at 689 kPa. [c] Evaluated at 207 kPa.

Recently, Lin et al. (2006a, 2006b) have synthesized highly branched poly(ethylene oxide) gel membranes for CO_2/H_2 and CO_2/CH_4 separations where the high permselectivity was also found to derive from the high solubility selectivity. In addition, the membrane selectivity was shown to be enhanced by using a lower temperature. These results are consistent with the current study where the PEBA copolymer used contains 80 wt% of poly(tetramethylene oxide) as the soft rubbery segments. Lin and Freeman (2005) reviewed the strategies of incorporating ethylene oxide units into polymers for developing CO_2 separation membranes with high selectivity as a result of solubility selectivity.

As mentioned earlier, the mobility of a penetrant is affected by both its molecular size and the degree of membrane swelling caused by the penetrant sorbed in the membrane. As shown by the data in Table 5.4, the ethylene/nitrogen diffusivity selectivity is less than 1 at the temperatures studies because of the larger ethylene

molecules than nitrogen. The membrane does not favor the diffusion of ethylene because the limited sorption uptake in the membrane is not sufficient to swell the membrane significantly. On the other hand, for propylene and butylene, which swell the membrane more significantly, the diffusivity selectivity relative to nitrogen is greater than 1 at low temperatures. As the temperature increases, the membrane swelling is less significant and the effect of molecular size of the penetrant becomes increasingly important, rendering the diffusivity selectivity (<1) less favorable to olefin. In this case, the solubility selectivity needs to compensate for the less favorable diffusivity selectivity in order to achieve the desired permeability selectivity (i.e., preferential permeability of olefin over nitrogen). Obviously, a low temperature is preferred so that both the solubility selectivity and diffusivity selectivity will contribute positively to the preferential permeation of olefin over nitrogen.

It should be pointed out that this study deals with the behavior of pure gases in the membranes. For gas mixtures, the solubility and diffusivity (and thus the permeability) of an individual component may be different from the pure gas data obtained here, and care should be exercised in using the pure gas data explaining mixed gas permeation. This has been shown in the last chapter on propylene separation from nitrogen using a PEBA composite membrane.

5.4 Summary

The sorption, diffusion and permeation of three olefins (i.e., C_2H_4, C_3H_6 and C_4H_8) in PEBA 2533 membranes were investigated at different operating temperatures to elucidate the relative contribution of solubility and diffusivity to the preferential permeability of the membrane to olefins. It was revealed that the favorable olefin/nitrogen permselectivity is primarily due to the solubility selectivity, whereas the diffusivity selectivity may affect the permselectivity negatively when the operating temperature was considerably low. The olefin permeability follows the order of $C_4H_8 > C_3H_6 > C_2H_4$, which is the same order as their solubilities in the membrane. With an increase in pressure and/or a decrease in temperature, the sorption uptake of the olefin penetrant in the membrane increases progressively, and the solubility and diffusivity (and hence the permeability) become increasingly dependent of the operating pressure. For

considerably sorptive olefins such as propylene and butylenes, the olefin sorption uptake in the membrane was found to have a more profound impact on its diffusivity than the molecular size. At a given temperature, the pressure dependence of solubility and permeability could be described by an exponential function empirically. The limiting solubility at infinite dilution was correlated with the reduced temperature of the penetrant, and the hypothetical diffusivity at zero pressure was related to temperature by the Arrhenius equation.

CHAPTER 6

Separation of VOCs from N_2 Using Poly(Ether Block Amide) Composite Membranes

6.1 Introduction

There are many gas streams from manufacturing processes in the chemical, petrochemical and pharmaceutical industries (e.g., solvent storage, loading and unloading, and painting operations) that contain a large amount of volatile organic compounds (VOCs). In addition to the economic loss due to the commodity value of these organic solvents, the emission of the VOCs into atmosphere also represents environmental, health and safety problems. In order to capture these pollutants and reuse the VOC substances, separation processes are needed to recover the VOCs and mitigate their emissions into air. Technologies currently available for VOC treatment include carbon adsorption, condensation and incineration. However, these processes have so far been found not to be always satisfactory in terms of separation performance and energy consumption. In recent years, membrane technology has attracted attention as a promising alternative. The utilization of membranes to remove or recover organic vapors from waste gas streams has the potential advantages of low operating cost, simple and compact equipment, and easy operation requiring no regeneration steps (Qiu and Hwang, 1991). Membrane processes are considered to be a strong contender to other competing processes when the VOC concentration is not too low, especially for vent streams containing 1 mol% VOC or more (Paul and Yampol'skii, 1994).

For membranes used in organic vapor separation from air or nitrogen streams, silicone rubber is generally regarded as one of the most attractive membrane materials due to its high permeability and good selectivity to organic vapor permeation. However, for the actual separation of VOC/N_2 or VOC/air mixtures, the membrane selectivity is

often much lower than the ideal selectivity based on pure gas permeability because the VOCs sorbed in the membrane tend to swell the membrane, making it easier for N_2 or air in the mixture to permeate as well. It has been reported that the selectivities for VOCs/N_2 separation with silicone rubber membranes are only 15-60 for such organic compounds as acetone and octane (Park and Lee, 2002). Membrane based vapor/gas separation is a pressure driven process. Since the membrane selectivity affect separation efficiency directly, membranes with high VOC permselectivities are thus desired.

In this work, membranes were prepared from poly(ether block amide) (PEBA) (type 2533), as an alternative to silicone rubber, for VOC separation from nitrogen. The block copolymer has a biphase-separated microstructure: the soft polyether amorphous domains offer a high permeability due to the high chain mobility of the ether linkage and the hard polyamide crystalline domains provide mechanical strength (Joesph and Flesher, 1986). Therefore, the copolymer combines the advantages of rubbery and glassy polymers, and it is expected that the membrane will be preferentially permeable to organic vapors due to the rubbery polyether segments while excessive swelling of the membrane by the sorbed VOCs will be refrained by the hard glassy polyamide domains, thereby maintaining a good permselectivity. Previous work on the sorption, diffusion and permeation of light hydrocarbons ($C_2 - C_4$) showed that the good permeability of PEBA to these condensable hydrocarbons is mainly due to their favorable solubilities in the polymer and the high fractional free volume of the polymer. Liu et al. (2006) reported that hollow fiber membranes comprising of a PEBA skin layer supported on a microporous poly(vinylidene fluoride) substrate are effective for recovering gasoline vapors from nitrogen for hydrocarbon emission control. As representative VOCs, n-pentane, n-hexane, cyclohexane, n-heptane, methanol, ethanol, n-propanol, n-butanol, acetone, dimethyl carbonate (DMC) and methyl *tert*-butyl ether (MTBE) were chosen in the present study. Most of them are the main compounds of gasoline (e.g., the paraffins) or gasoline additives (e.g., methanol, ethanol, DMC and MTBE). For comparison purposes, some other organic compounds (e.g., n-propanol, n-butanol and acetone) were also studied.

Integrally asymmetric membranes with a thin selective skin layer and a microporous substrate are hard to fabricate from such rubbery polymers as silicone

rubber and PEBA. Instead, thin film composite membranes having a selective rubbery coating layer supported on a porous substrate prepared from a glassy polymer are generally used. The porous substrate acts only as a mechanical support and is supposed to have little or no resistance to mass transport. Dip coating technique is most widely used to prepare thin film composite membranes. However, during the coating process, some coating solution often 'leaks' into the pores of the substrate, resulting in an increase in the mass transfer resistance of the substrate, especially for the gases and vapors with relatively high permeance. This will not only lower the overall permeance of the membrane but also affect the membrane selectivity. In the present work, to address this issue, a thin PEBA skin layer was formed by spreading a PEBA solution on water surface, as presented in Chapter 3, and then laminated onto a porous polysulfone substrate so as to form a composite membrane. This way, the pore plugging in the substrate is prevented, rendering the substrate resistance lower than what would be encountered in a composite membrane prepared by the traditional dip coating technique.

6.2 Experimental

6.2.1 Materials

The gases and chemicals for membrane formation and permeation test are the same as used in previous Chapters. Microporous PSf membranes from Pall Corporation were used as the substrates. All other organic solvents used to generate VOCs were from Aldrich.

6.2.2 Membrane preparation and VOCs/N_2 separation

The general procedures for membrane fabrication have been described in Chapter 3. Fig. 6.1 shows the experimental set-up for VOCs/N_2 separation. The VOC/N_2 gas mixture was generated by bubbling nitrogen at a given pressure through a solvent tank. The VOC concentration in the feed stream was controlled by adjusting the gas bubbling pressure in the solvent tank. The gas mixture was then admitted to the membrane cell at atmospheric pressure. The effective membrane area for permeation was 13.85 cm^2. During the experiments, vacuum (< 1 kPa abs.) was applied to the permeate side. The

VOCs permeated through the membrane were collected in a cold trap and then weighed using a digital balance to determine the VOC permeation rate. The gas flow rate of the feed stream was measured by a bubble flow meter. A gas chromatography (HP 5890) equipped with a packed column (Porapak Q) and a thermal conductivity detector was used to determine the compositions of the feed and the permeate streams. An air-actuated six-port sampling/switching valve was mounted in the GC for gas sampling, and because of the low pressure of permeate stream, a relatively large sampling loop was used when determining the permeate concentration on-line.

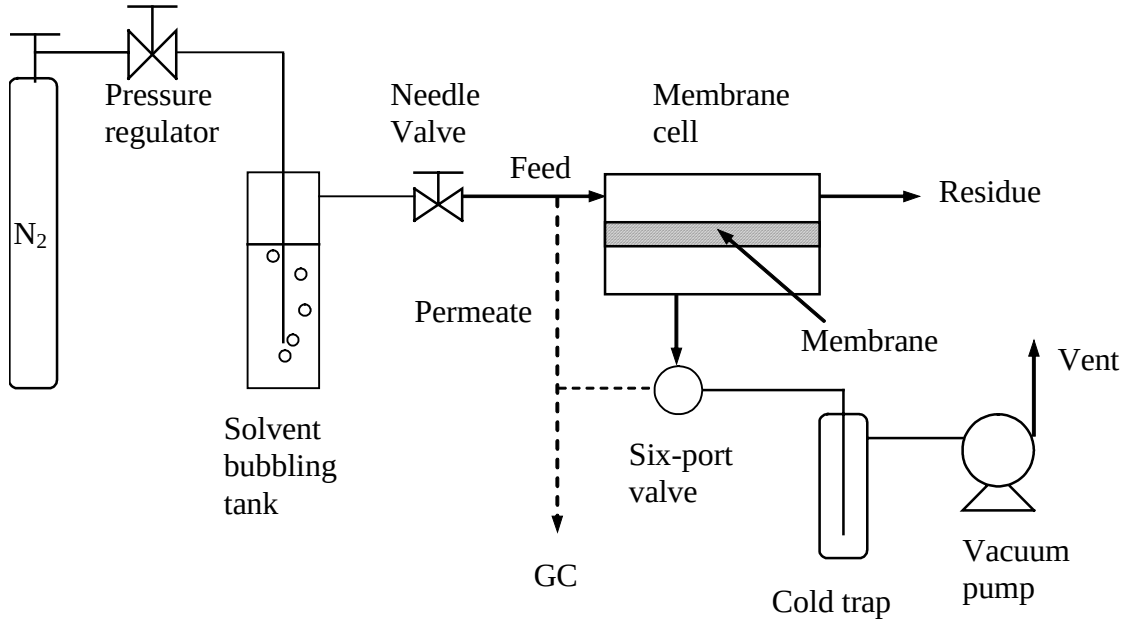

Figure 6.1 Schematic diagram of experimental setup for VOC/N_2 separation.

The overall gas permeation rate is determined from the VOC permeation rate Q_{VOC} and the VOC concentration y_{VOC} in the permeate

$$Q = \frac{Q_{VOC}}{y_{VOC}} \tag{6.1}$$

The calculation of the membrane permeance and selectivity are the same as those shown in the Chapter 4.

6.3 Results and discussion

6.3.1 Separation of binary VOC/N_2 gas mixtures

A relatively low stage cut (less than 0.05) was used in the experiments to maintain an almost constant concentration of VOCs along the membrane surface at the feed side so that the membrane performance at a given feed concentration can be evaluated. Moreover, because of the high permeability and selectivity to VOCs, a potential concern is that concentration polarization might take place in the boundary layer adjacent to the membrane surface, which reduces both the permeation rate of VOCs and the selectivities. This has been discussed by Yeom et al. (2002a; 2002c) for VOC/N_2 gas mixtures permeation through poly(dimethyl siloxane) membrane. To abate this effect, a high feed flow rate (as high as 400 sccm) was used in the present work. A further increase in the feed flow rate did not change the membrane permselectivity, indicating that the effect of concentration polarization was insignificant under the experimental conditions studied.

The permeation of binary VOC/N_2 mixtures was studied at different feed VOC concentrations. In the following studies, the binary gas permeation was carried out at 25°C using a membrane with a PEBA layer of 5.2 μm unless specified otherwise. Fig. 6.2 shows the permeation flux of VOCs as a function of the feed VOC concentrations for the separation of different VOCs from their binary VOC/N_2 mixtures. At a given feed concentration, the permeance of the four paraffin compounds tested follows the order of n-heptane > cyclohexane > n-hexane > n-pentane. For other VOCs, the magnitude of the permeance is n-butanol > n-propanol > DMC > ethanol > methanol > acetone > MTBE. In general, the permeation flux of the VOCs increases significantly with an increase in the feed VOC concentration, and all the curves are convex to the feed concentration. This means that the increase in the permeation flux is not only due to the increased driving force for VOC permeation, but rather the permeabilities of VOCs were enhanced at higher feed VOC concentrations. This is shown in Fig. 6.3 where the concentration dependency of the VOC permeance is illustrated. Clearly, the VOC permeance increases with an increase in the VOC content (i.e., partial pressure) in the feed. Generally speaking, the gas permeability through a membrane is determined by both the solubility and the diffusivity. The condensable VOC components have high sorption uptakes in

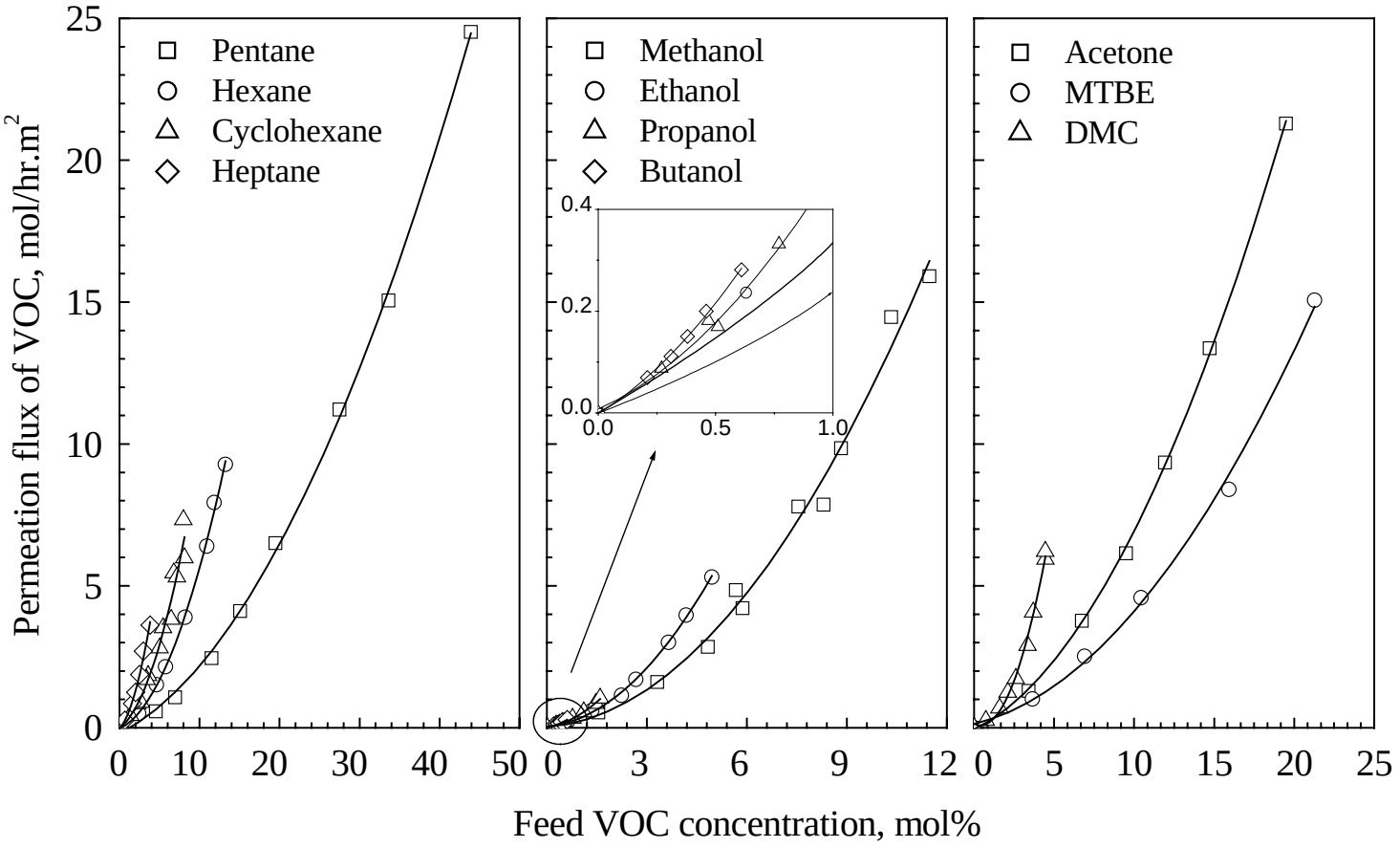

Figure 6.2 Permeation flux of VOC as a function of feed VOC concentration.

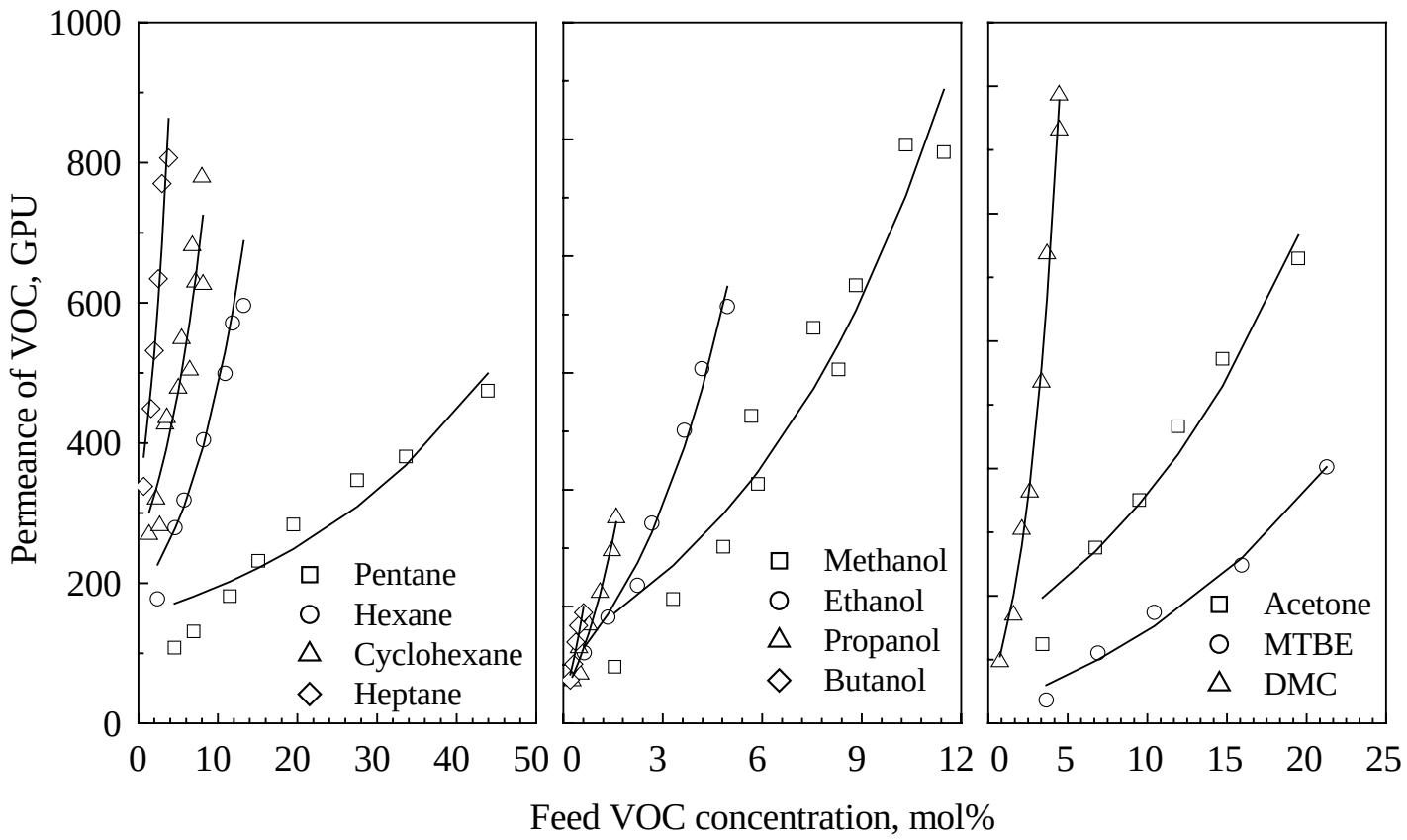

Figure 6.3 VOC permeance vs. feed VOC concentration. Symbols represent experimental data and solid lines represent calculated data based on a semi-empirical equation of permeance.

organophilic polymers (e.g., PEBA 2533) and tend to swell or plasticize the membranes. The enlarged gaps between polymer chains in the membrane due to membrane swelling not only favor the diffusion of the penetrant but also allow for a high solubility to these species. Thus, the effect of membrane swelling is more significant at higher VOC concentrations. As a result, an increase in the feed VOC concentration will increase the VOC permeability of the membrane progressively. Similar behavior can also be found for the permeation condensable gases and vapors through other rubbery polymers (Yeom et al., 2002b; Singh et al., 1998).

In order to get an insight into the permeation of VOCs through the membrane, let us look at the two groups of paraffin and alcohol VOCs evaluated. For both groups of VOC penetrants, the VOC permeance was shown to increase with an increase in the molecular size of the penetrant, that is, the membrane is more permeable to larger VOC compound. In general, a more condensable component tends to have a higher sorption amount in the membrane. The condensabilities of the VOCs can be related to their boiling points, as shown in Table 6.1. On the other hand, for a given membrane, the diffusivity is affected primarily by the size and/or shape of the penetrant. Normally, the contribution of the solubility aspect dominates over the diffusivity aspect for gas permeation through polymers with large free volumes and low crosslinking densities. PEBA 2533, composed of 80% soft polyether segments, offers a high fractional free volume of 0.172 (Rezac and John, 1998). Therefore, that larger VOCs are more permeable through the PEBA membrane is mainly due to their higher condensabilities, in spite of their bigger molecular sizes. As mentioned earlier, the magnitude of the membrane permeability follows the order of n-heptane > cyclohexane > n-hexane > n-pentane for the paraffins and n-butanol > n-propanol > ethanol > methanol for the alcohols, which are in the same order as their condensabilities but opposite to the order of their molecular sizes. These results confirm that it is the VOC solubility that predominates its permeability through the membrane. In addition, it is shown that at a given feed concentration, the alcohol VOC compounds tend to have a higher permeance and VOC/N_2 selectivity than the paraffin compounds, presumably due to the stronger affinity of the polar alcohol molecules to the polyether segments in PEBA 2533. The fact that PEBA 2533 can be dissolved in propanol and butanol at evaluated temperatures

demonstrates the high affinity between these solvents and the polymer.

Table 6.1 Physical properties of VOC components[a]

	Molecular weight	Boiling point (^oC)	Vapor pressure (kPa)
n-Pentane	72.2	36.0	68.32
n-Hexane	86.18	68.7	20.17
Cyclohexane	84.16	80.7	13.01
n-Heptane	100.2	98.4	6.09
Methanol	32.0	64.6	16.94
Ethanol	46.7	78.3	7.86
n-Propanol	60.1	97.2	2.73
n-Butanol	74.1	117.7	0.82
Acetone	58.1	56.05	30.59
Dimethyl carbonate	90.1	90.3	7.40
Methyl *tert*-butyl ether	88.2	55.2	32.66

a. CRC Press, *CRC Hand Book of Chemistry and Physics*, 83rd ed., (2002-2003).

Similar to the treatment in our previous work on propylene/N_2 separation, based on the experimental results of VOC/N_2 separation, a semi-empirical correlation was attempted to relate the VOC permeance and the operating conditions. For steady state permeation, the permeation flux J^0 of a VOC can be described by the Fick's law

$$J^0 = -D\frac{dC}{dl} \tag{6.2}$$

where D and C are the diffusivity coefficient and concentration of the VOC in the membrane, respectively. Assuming the diffusivity is exponentially dependent on concentration

$$D = D_0 \exp(\phi.C) \tag{6.3}$$

where D_0 and ϕ are parameters measuring the concentration dependence of diffusivity, integrating Eqn. (6.2) gives

$$J^0 = \frac{D_0}{\phi.L}[\exp(\phi.C_h) - \exp(\phi.C_l)] \tag{6.4}$$

where L is the membrane thickness, and C_h and C_l are VOC concentrations in the membrane on the feed and permeate sides, respectively. At both sides of the membrane, $C_h = \omega P_h x$ and $C_l = \omega P_l x$, where ω is the equilibrium partition coefficient, which is

assumed to be independent of concentration. This is considered to be adequate because of the generally low permeant concentrations in polymers. For the separation of VOC/N_2 mixtures, $C_l \approx 0$ because of a vacuum applied at the permeate side of the membrane (i.e., $p_l \approx 0$). Then Eqn. (6.4) can be re-written as

$$J^0 = \frac{D_0}{\phi.L}[\exp(\phi.\omega.p_h.x) - 1] \tag{6.5}$$

From the permeation experiments, the three parameters D_0, ϕ and ω cannot be determined individually, but the quantities (D_0/ϕ) and ($\omega\phi$) can be obtained by non-linear regression of the VOC flux at different feed concentrations. Similar treatment has been widely used in pervaporation processes. Table 6.2 shows the lumped parameters so obtained.

Table 6.2 Parameters (D_0/ϕ) and ($\omega\phi$) obtained by non-linear regression

	D_0/ϕ (cm^3/cm.s)	$\omega\phi$ (kPa^{-1})
n-Pentane	1.31×10^{-6}	0.046
n-Hexane	4.28×10^{-7}	0.167
Cyclohexane	4.62×10^{-7}	0.218
n-Heptane	2.89×10^{-7}	0.441
Methanol	6.59×10^{-7}	0.197
Ethanol	2.78×10^{-7}	0.406
n-Propanol	1.11×10^{-7}	0.872
n-Butanol	6.11×10^{-8}	1.531
Acetone	1.08×10^{-6}	0.081
Dimethyl carbonate	1.41×10^{-6}	0.093
Methyl *tert*-butyl ether	1.65×10^{-7}	0.577

Using these parameters, the permeance of VOC can be written as

$$J = \frac{(D_0/\phi)}{L\ p_h\ x}[\exp(\phi\omega\, p_h x) - 1] \tag{6.6}$$

To verify the applicability of the correlation, the calculated permeance using the parameters in Table 6.2 was also plotted in Fig. 6.3 (in solid lines). The agreement with

the experimental data justifies the correlation to represent the VOC permeance in the separation. The lumped parameter ($\omega\phi$) can be used to measure the concentration dependency of the VOC permeance. A large value of ($\omega\phi$) means a strong influence of feed concentration on the VOC permeance. For the groups of paraffins and alcohols evaluated, their ($\omega\phi$) values increase with an increase in their molecular sizes, indicating that the permeation of heavier VOC components was affected by their concentrations more significantly.

As shown in Fig. 6.4, the permeation of nitrogen through the membrane was affected by the presence of VOC components, i.e., the permeance of N_2 in VOC/N_2 separation is much higher than pure N_2 permeance because of membrane swelling caused by VOC sorption in the polymer. Moreover, unlike pure nitrogen permeance, which is almost constant at a given temperature, an increase in the feed VOC concentration tend to increase the permeance of N_2 in the presence of VOC components. The increased permeance of nitrogen by VOC components agrees with physical reasoning that membrane swelling caused by the VOCs will not only enhance the VOC permeation but also make nitrogen permeation easier because of the increased free volume and chain mobility in the polymers. Similar observation can be found for the permeation of toluene/N_2 through polyurethane-based membranes (Park and Lee, 2002). For the two groups of paraffins and alcohols studied, it appears that at a given VOC concentration in the feed, the nitrogen permeance will be enhanced more significantly when the VOC components are more condensable. This is consistent with the results of VOC permeation discussed above.

The membrane selectivity for binary VOC/N_2 separation is shown in Fig. 6.5. Although the permeance of nitrogen increases when the feed VOC concentration increases, the selectivity still increases with an increase in the feed concentration due to the more significant increase in the VOC permeance. The membrane selectivity was shown to be higher for heavier paraffins than light paraffins, whereas for the four alcohol VOCs the membrane selectivity are close. The membrane selectivity for alcohol/N_2 permeation is relatively high compared to other VOC/N_2 gas pairs mainly due to the high permeance of alcohols in the membranes. Fig. 6.6 shows the permeate VOC concentration as a function of VOC concentration in the feed for binary VOC/N_2

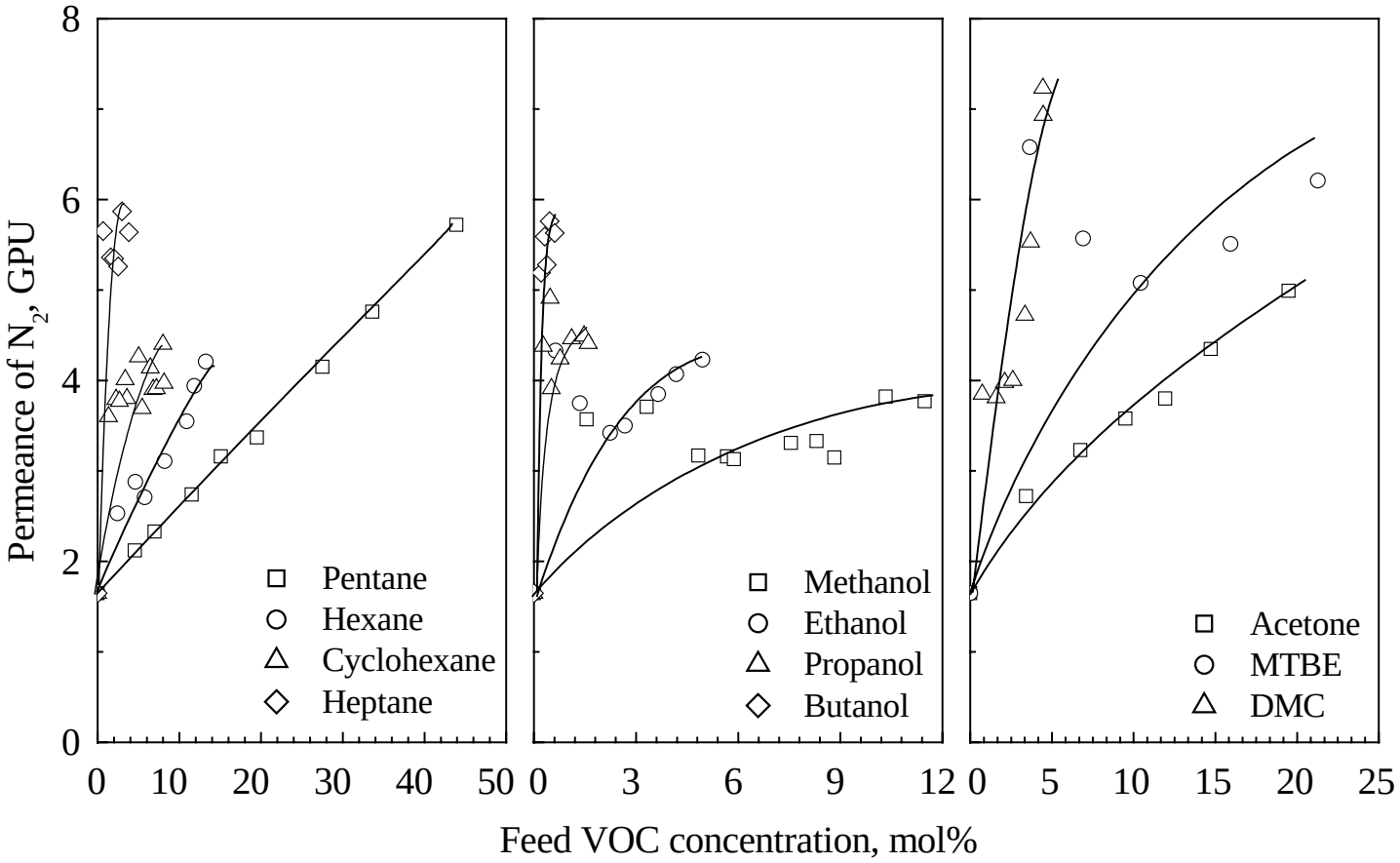

Figure 6.4 Permeance of nitrogen vs. feed VOC concentration.

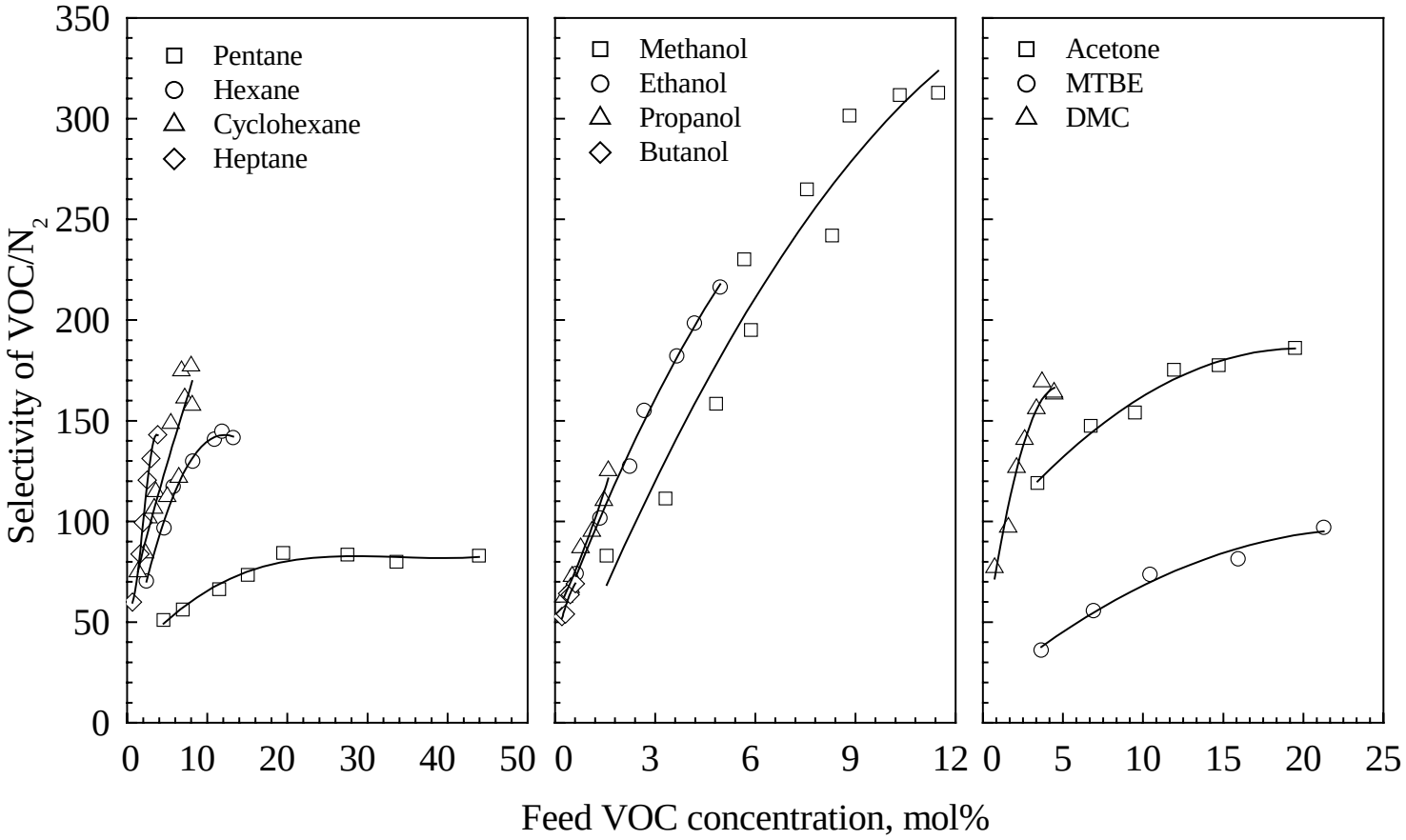

Figure 6.5 Membrane selectivity for VOC/N_2 vs. feed VOC concentration.

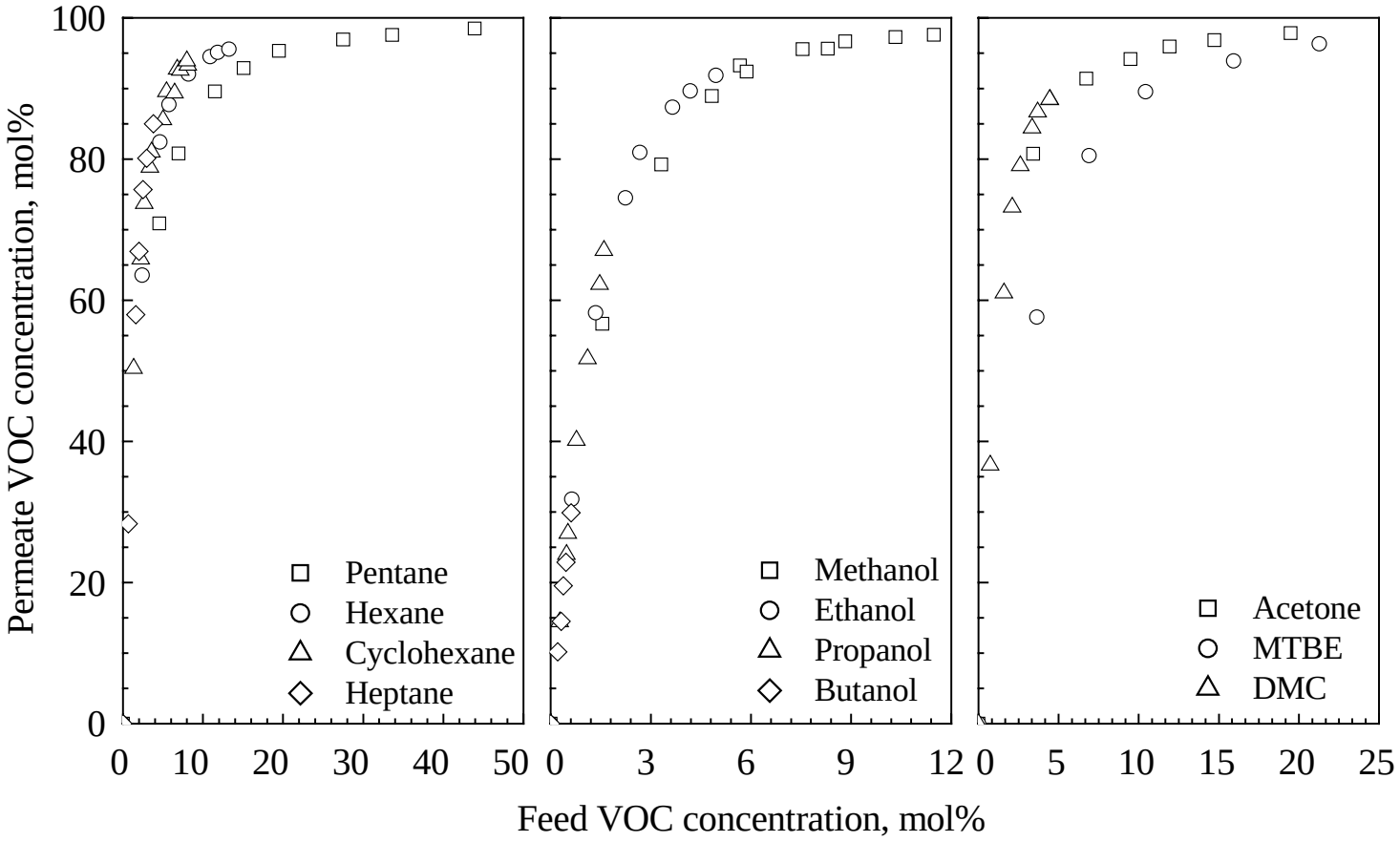

Figure 6.6 Permeate VOC concentration vs. feed VOC concentration.

separation. It is shown that the permeate VOC concentration increases with an increase in the feed VOC concentration, and the effect of feed concentration on the permeate concentration is more significant at relatively low feed VOC concentration. For the group of paraffins studied, at a given feed concentration, the permeate concentration slightly increases with an increase in the carbon number of the paraffin, whereas for the four alcohols the permeate concentrations were essentially the same. For most of the VOCs investigated, when the feed VOC concentration is over 5 mol%, a permeate VOC concentration of over 90 mol% can be achieved readily. These results demonstrate the effectiveness of the membrane for the separation of these VOCs from nitrogen streams.

6.3.2 Effect of temperature

To evaluate the effects of operating temperature on the separation of binary VOC/N_2 mixtures, the permeation of several binary VOC/nitrogen mixtures was carried out as representative feed mixtures at temperatures ranging from 35 to 65ºC with a feed VOC concentration of 44.3 mol% for n-pentane, 13.8 mol% for n-hexane, 8.2 mol% for cyclohexane, 3.8 mol% for n-heptane, 11.7 mol% for methanol, 19.5 mol% for acetone and 4.4 mol% for DMC. Fig. 6.7 shows the permeances of the VOCs and nitrogen for the various VOC/nitrogen mixtures as a function of reciprocal temperature. It is shown that the temperature dependence of permeance for both VOCs and N_2 follows an Arrhenius type of relation. Because of the dominating effect of sorption in permeation and the exothermic sorption process, the VOC permeance decreases with an increase in the temperature. However, the permeance of permanent gas N_2 decreases as the temperature increases, presumably due to a more significant increase in its diffusivity than the decrease in its solubility. Thus, increasing temperature will decrease the VOC/N_2 selectivity significantly, which is also shown in Fig. 6.7. Therefore, a relatively low operating temperature is more favorable for the separation of VOC/N_2 mixtures in terms of membrane selectivity, although the permeation rate will be compromised.

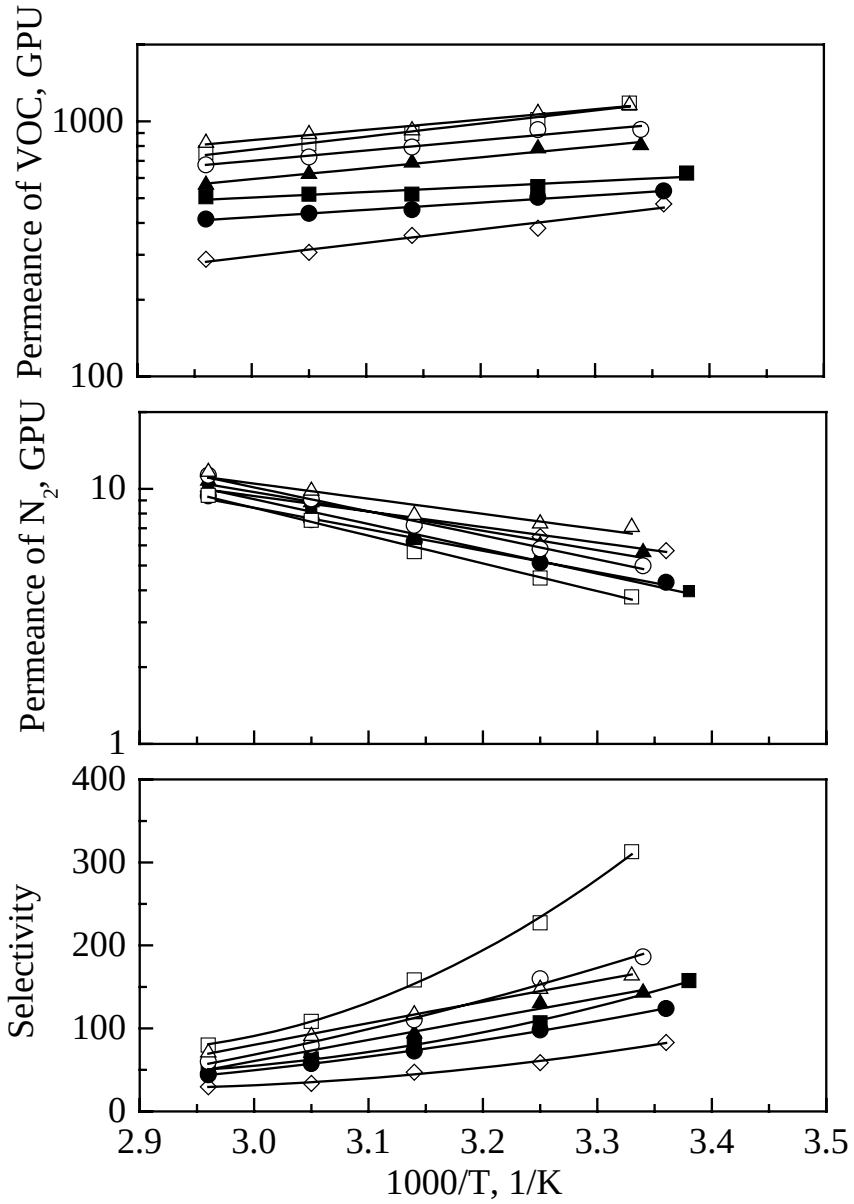

Figure 6.7 Effects of temperature on the separation of binary VOC/N_2 mixtures. Feed VOC concentrations: ◇ n-Pentane 44.3 mol%; ● n-Hexane 13.8 mol%; ■ Cyclohexane 8.2 mol%; ▲ n-Heptane 3.8 mol%; □ Methanol 11.7 mol%; ○ Acetone 19.5 mol%; △ Dimethyl carbonate 4.4 mol%).

6.3.3 Effect of stage cut and process simulation

Stage cut is the ratio of the permeate flow rate to feed flow rate. In the prior work discussed above, the stage cut was kept very low (less than 0.05) so as to retain a relatively constant concentration on the feed side of the membrane. In practical applications, however, a considerably large stage cut should be used in order to achieve a low VOC concentration in the residue and a high VOC recovery in the permeate. Considering that vacuum was applied in the permeate side of the membrane, the VOC/N_2 separation process can be evaluated on the basis of a simple cross flow model. Fig. 6.8 illustrates the VOC/N_2 separation by a membrane with a cross flow configuration, where the pressure variations along both the feed and permeate sides are assumed to be negligible. Based on permeation and mass balance equations for a differential unit of the membrane area, the following equations can be formulated for binary VOC/N_2 separation

$$-ydF = J_{VOC}(p_h x - p_l y).dA \tag{6.7}$$

$$-(1-y)dF = J_{VOC}/\alpha.[(p_h(1-x) - p_l(1-y)].dA \tag{6.8}$$

$$d(F.x) = ydF \tag{6.9}$$

where F is the gas flow rate on the feed side and A is the membrane area. Using the aforementioned correlation [Eqn. (6.6)] for VOC permeance and empirical correlation of membrane selectivity based on the data in Fig. 6.5, for given feed flow rate (F_0) and concentration (x_0), the flow rates and concentrations of the residue and permeate streams can be obtained by solving Eqns. (6.7) - (6.9) with boundary conditions $F = F_0$ and $x = x_0$ at $A = 0$. An atmospheric pressure of the feed (i.e., p_h = 101.3 kPa) was used in all the calculations here. As an illustration, the calculations were performed for feed streams that are 70% saturated with the VOC components. The percentage VOC removal (defined as the fractional amount of VOC in the feed that has been enriched in the permeate stream) and the VOC concentrations in both the residue and permeate streams were evaluated. To test the validity of the cross flow model used in the calculation, experiments for hexane/N_2 separation at a feed concentration of 12.6 mol% at different stage cuts were carried out, and the experimental results are shown in Figs. 6.9 and 6.10, where the model calculated values are also plotted (solid lines). In general, the experimental data agree

with the model calculations, although the permeate VOC concentration was slightly overestimated by the cross flow model at a relatively high stage cut.

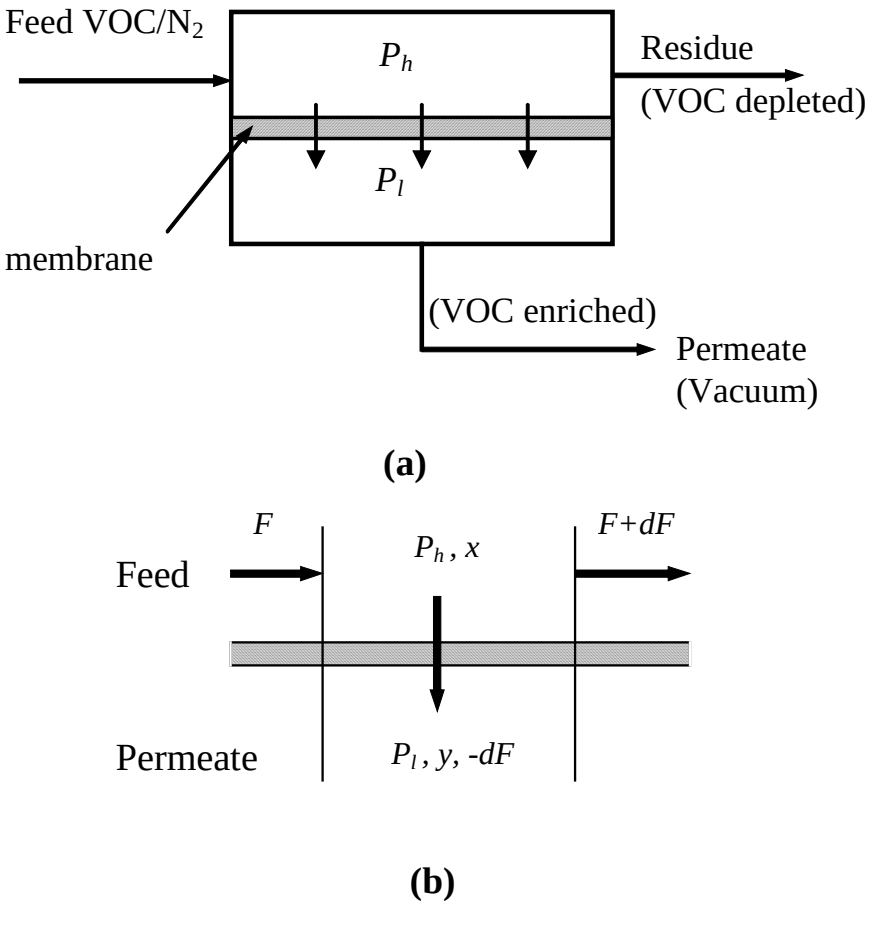

Figure 6.8 a) Schematic diagram of VOC/N_2 separation with cross flow configuration. (b) A differential unit of the membrane for gas separation based on the cross model.

Figs. 6.11 – 6.13 show the calculation results, based on the cross flow model, of residue VOC concentration, percentage VOC removal and permeate VOC concentration, respectively, as a function of stage cut. With an increase in the stage cut, the percentage removal of VOC increases whereas the VOC concentration in residue decreases. This is easy to understand. An increase in stage cut means more VOC in the feed will permeate

through the membrane, resulting in an increase in the VOC removal rate and a decrease in the residue VOC concentration. However, as the VOC in the feed is gradually depleted, the membrane selectivity decreases. As a result, increasing the stage cut will cause a reduction in the permeate VOC concentration.

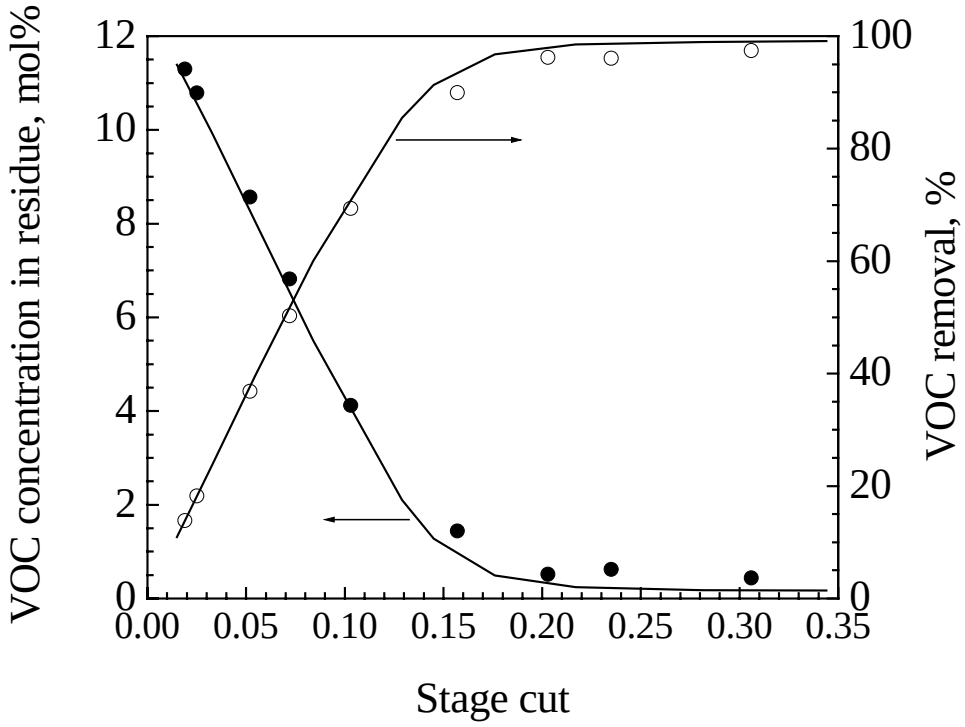

Figure 6.9 Concentration of n-hexane in residue and the percentage hexane removal as a function of stage cut. Feed hexane concentration 12.6 mol%. Symbols represent experimental data and solid lines are calculated data based on the cross flow model.

For the removal of various VOCs studied, over 95% of VOCs was be captured in the permeate when the stage cut was 0.05 - 0.15, and the corresponding residue VOC concentration could be less than 1 mol%. At 95% VOC removal, a permeate VOC concentrations of 10 - 95 mol% can be achieved, which represents a VOC enrichment factor of 3-30. Thus, the VOC concentration in the permeate is much higher than the saturated VOC concentration at ambient conditions. As such, the need for a cold trap to

condense and collect the membrane permeated VOCs could be eliminated in practical application when a positive displacement vacuum pump is used because after exhausting from the vacuum pump, the VOC in the permeate stream can be condensed easily in a chamber when subjected to ambient conditions. The liquid condensate can be removed for reuse, and the VOC-saturated gas phase can be recycled to the membrane unit for further processing. A schematic illustrating this process is shown in Fig. 6.14. It may be mentioned that because of the high permeance of alcohols through the membrane, a very high removed rate (as high as 99%) of alcohol can be reached at a relatively low stage cut. This indicates that the PEBA membrane could be used to recover and capture methanol vapor emitted from pulping and papermaking processes where methanol is emitted as a major air pollutant at many points (Someshwar and Vice, 2005; Burgess and Gibson 2002).

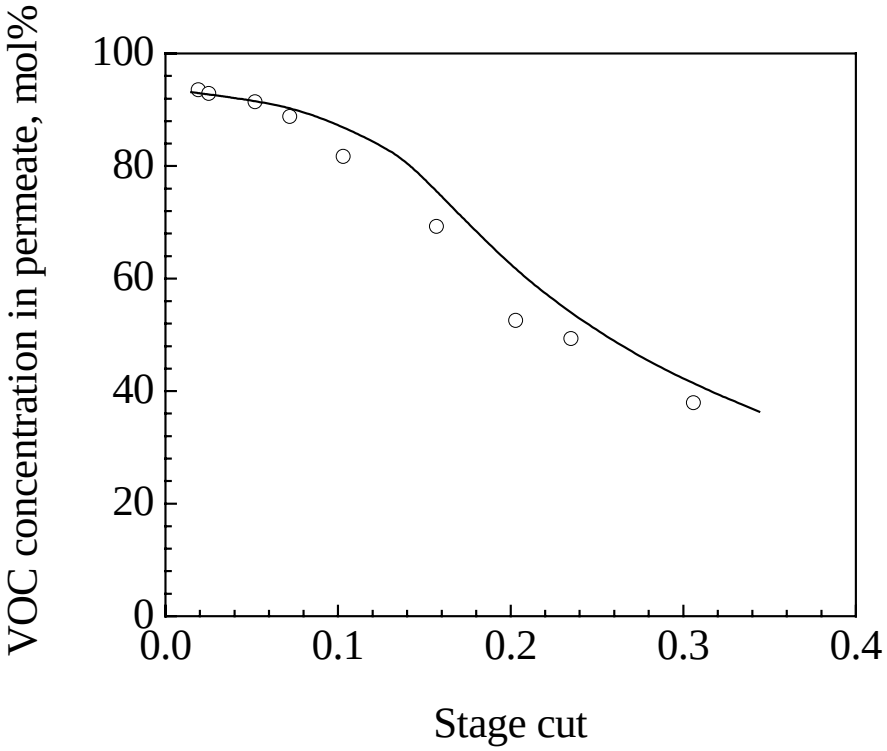

Figure 6.10 Permeate n-hexane concentration as a function of stage cut. Feed hexane concentration 12.6 mol%. Symbols represent experimental data and solid lines are calculated data based on the cross flow model.

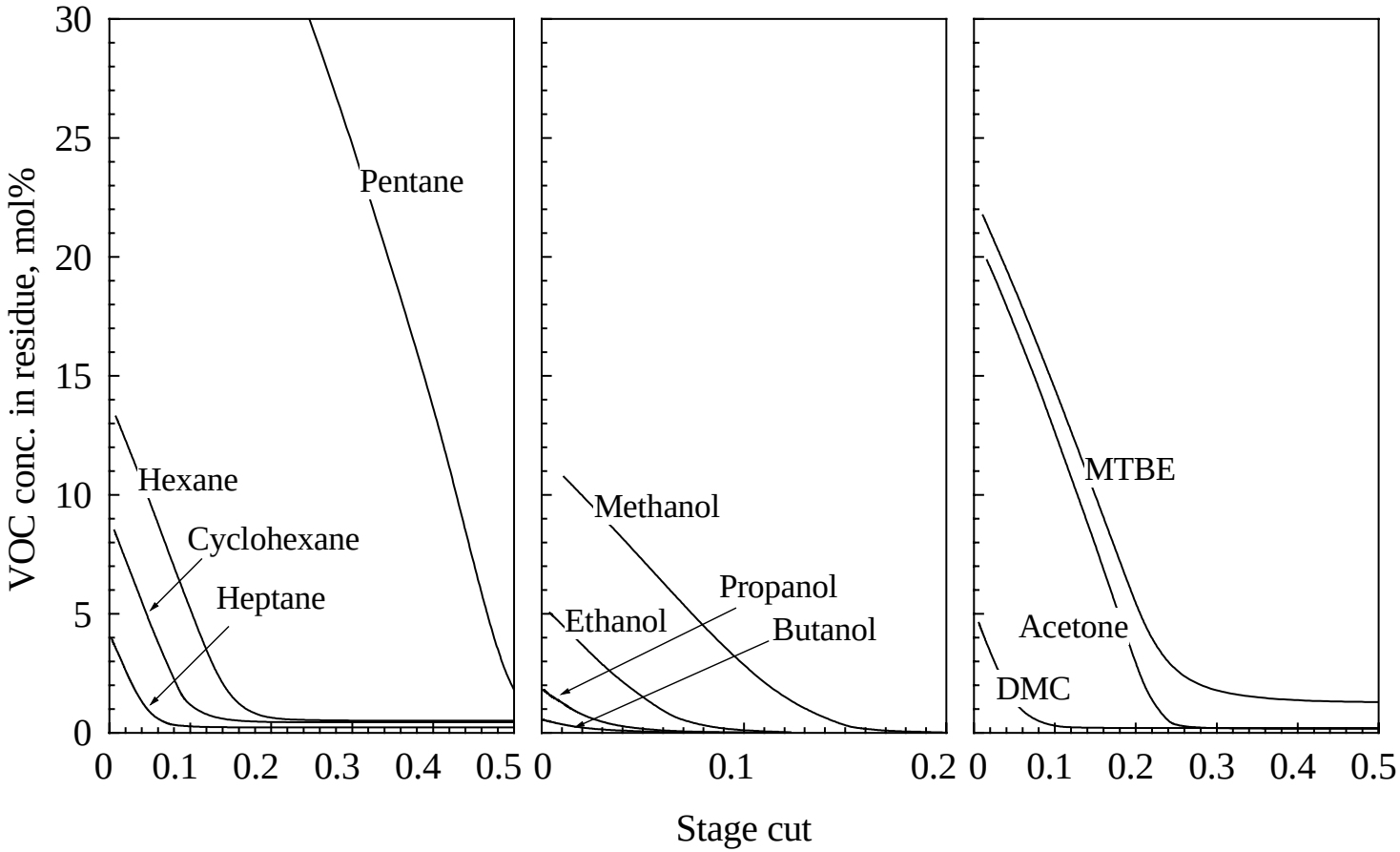

Figure 6.11 VOC concentration in residue as a function of stage cut. Feed mixtures: nitrogen with 70% saturated VOC vapors.

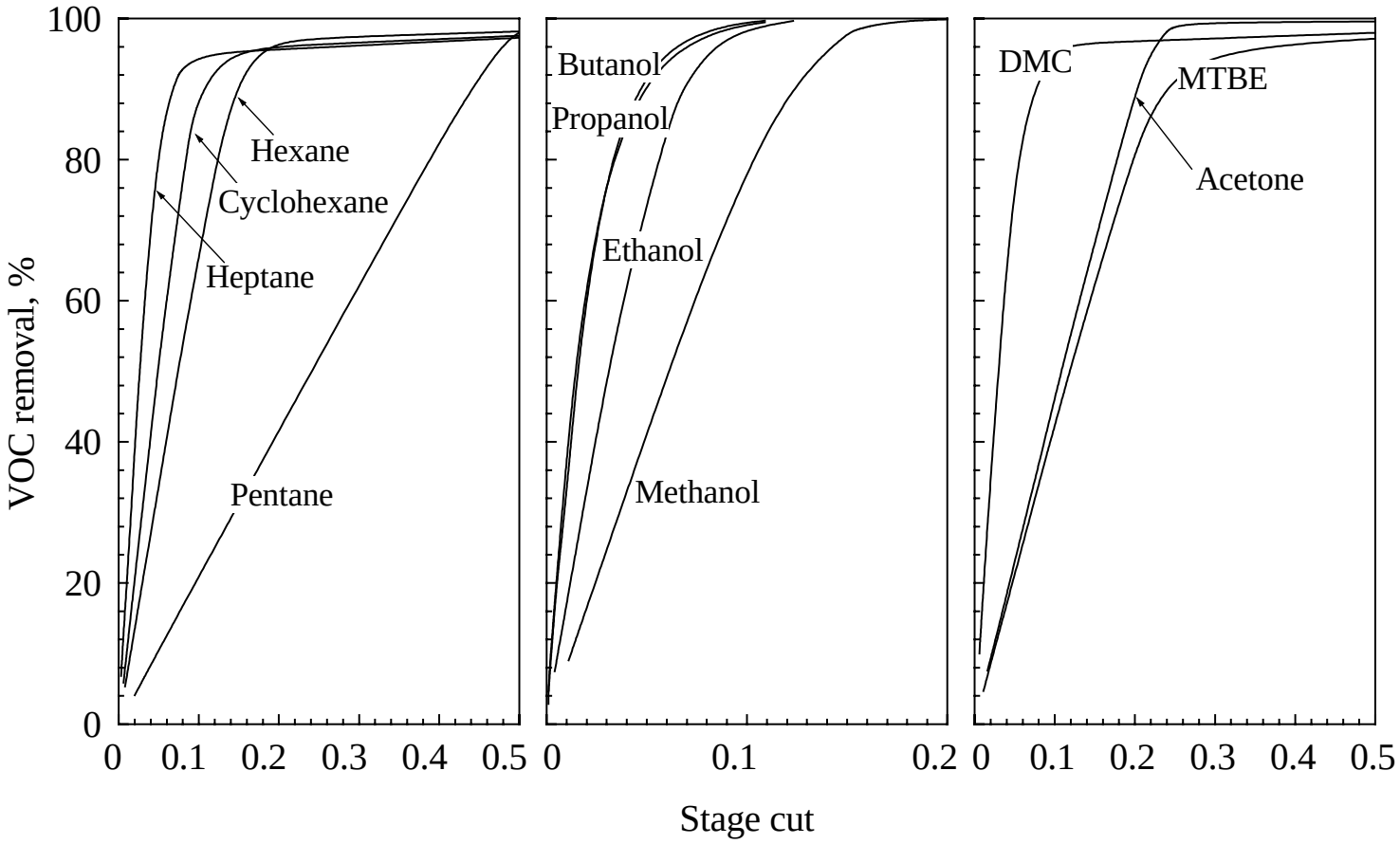

Figure 6.12 Percent VOC removal as a function of stage cut. Feed mixtures: nitrogen with 70% saturated VOC vapors.

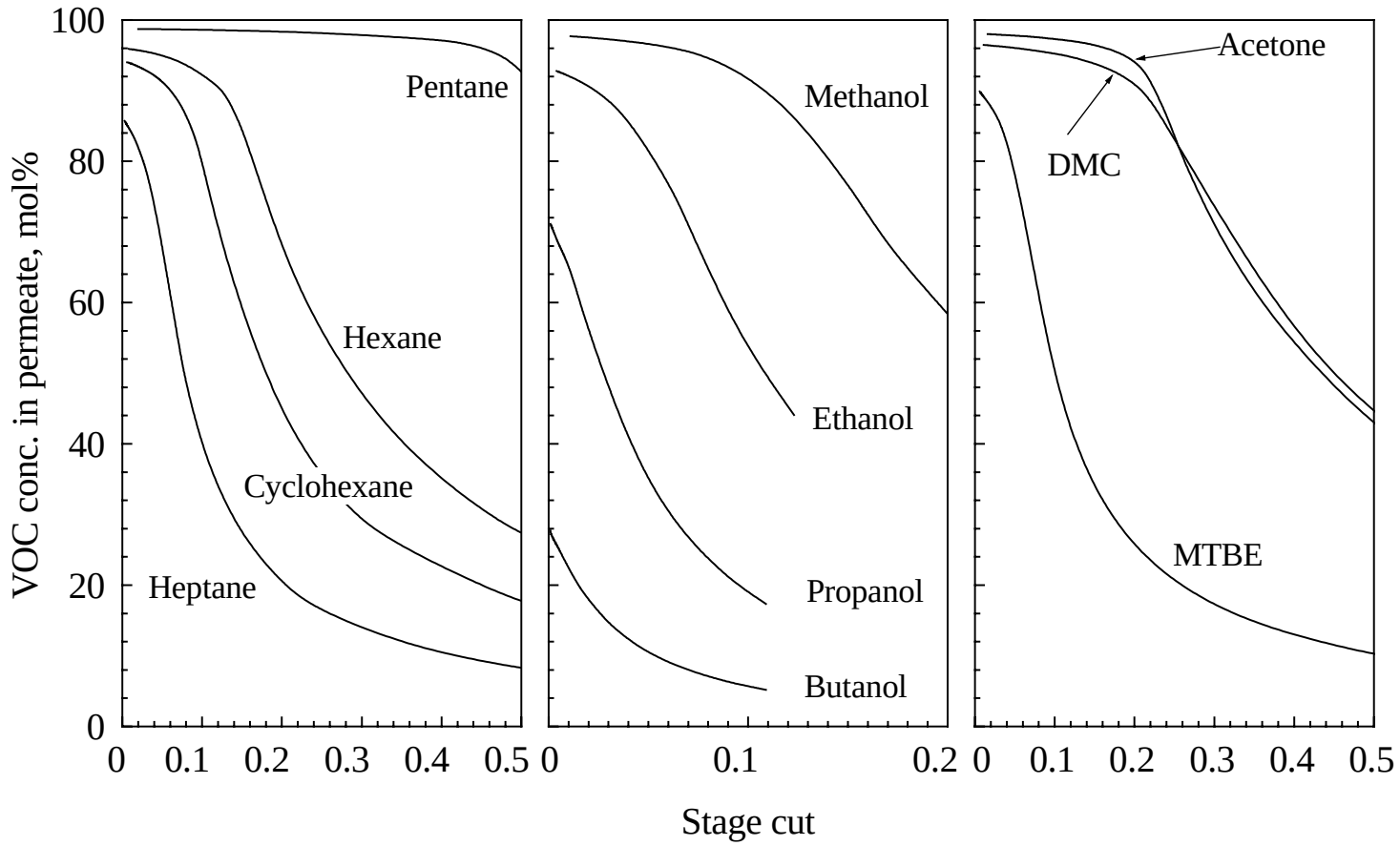

Figure 6.13 Permeate VOC concentration as a function of stage cut. Feed mixtures: nitrogen with 70% saturated VOC vapors.

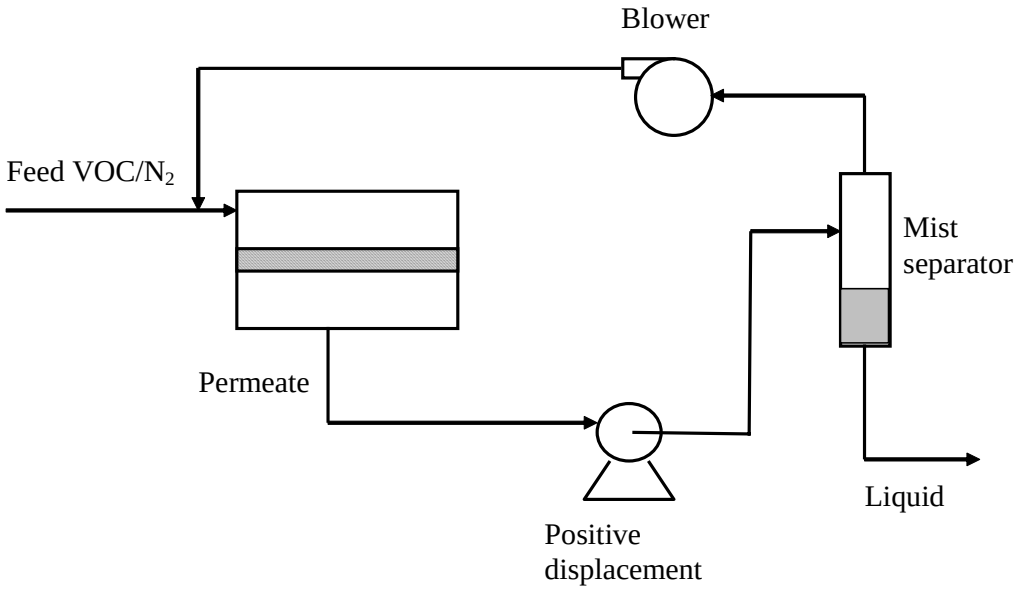

Figure 6.14 A schematic illustrating the VOC separation process without using cold traps.

6.3.4 Effect of permeate pressure

In separating VOC/N_2 mixtures, vacuum was applied on the permeate side to provide the driving force for permeation through the membrane and to remove the VOC enriched permeate. To study the effect of permeate pressure on the VOC/N_2 separation, a binary hexane/nitrogen mixture was used as a representative feed and the separation was carried out at various permeate pressures. Table 6.3 shows the membrane performance. As one may expect, increasing the permeate pressure will lead to a lesser extent of separation. Both the permeation rate and the permeate hexane concentration decrease with an increase in the permeate pressure. Interestingly, the permeance of hexane decreases as the permeate pressure increases, whereas nitrogen permeance increases, resulting in a reduction in the selectivity. Therefore, in actual applications, maintaining a relatively low permeate pressure is important to for effective separation of VOC/N_2 mixtures.

Table 6.3 The effect of the permeate pressure on the separation of hexane/N_2 mixture*

Permeate pressure (kPa)	Permeate hexane concentration (mol%)	Permeation flux (mol/m^2.h)	Permeance (GPU)		Selectivity
			VOC	N_2	
0.3	94.1	12.39	779.0	7.70	101.1
1.8	93.7	11.77	749.6	8.00	93.7
4.4	92.6	10.00	649.7	8.31	78.2
9.8	83.3	4.66	314.5	10.23	30.7
12.8	76.4	3.35	232.6	11.79	19.7

* Feed hexane concentration 14.2 mol%

6.3.5 Separation of multi-component VOCs from nitrogen

The separation of the multi-component VOC compounds from nitrogen was studied. The permeate composition and permeation rate at different feed VOC compositions are shown in Table 6.4; the feed gas mixtures were generated by bubbling nitrogen through quaternary hydrocarbon liquid mixtures containing n-pentane, n-hexane, cyclohexane and n-heptane. The experimental runs may be divided into three groups in terms of feed compositions, and the liquid mixtures contained a relatively high content of n-pentane, n-hexane and n-heptane in producing the gaseous feed streams used in groups I, II and III, respectively. In each group of runs, the overall concentration of the organic vapors was increased by decreasing the bubbling pressure of nitrogen in the liquid tank. The experimental results show that the PEBA membranes remain very effective for separating multi-component VOCs from nitrogen. When the feed stream contains 2.4 - 12.2 mol% of the VOCs, a permeate stream with an overall VOC content of 59.4 - 93.4 mol% can be produced. It may be noticed that in general increasing the concentration of a VOC component in the feed tends to give a higher concentration of this component in the permeate, except for n-pentene when its concentration in the feed is relatively high. This could be due to the complex interactions among the permeating species. Nevertheless, the enrichment factors for all the VOC components in the feed, which is defined as their permeate to feed concentration ratios, are in the order of n-heptane > cyclohexane > n-hexane > n-pentane, as shown in Fig. 6.15. This means the membrane selectivity for mixed VOC separation from nitrogen is consistent with the membrane selectivity for

Table 6.4 Separation of mixed VOC components from nitrogen

Group	Feed Composition (mol%)					Permeate composition (mol%)					Permeation flux
	Nitrogen	n-Pentane	n-Hexane	Cyclohexane	n-Heptane	Nitrogen	n-Pentane	n-Hexane	Cyclohexane	n-Heptane	mol/m^2.h
	94.12	4.01	0.69	0.79	0.39	19.87	45.50	11.27	14.55	8.81	1.68
I	91.04	5.87	1.14	1.31	0.63	12.31	46.66	13.21	17.11	10.71	3.34
	89.16	5.59	1.82	2.22	1.21	8.31	37.33	16.44	22.57	15.35	5.35
	87.78	5.38	2.30	2.90	1.64	6.74	31.24	18.19	25.80	18.03	6.90
	95.47	1.24	2.16	0.72	0.41	25.56	14.67	36.59	13.79	9.40	1.52
II	92.92	1.78	3.47	1.16	0.68	14.87	14.72	42.72	16.06	11.63	2.99
	90.00	2.15	5.09	1.73	1.04	8.45	13.20	46.84	18.00	13.51	5.28
	88.45	1.81	6.18	2.20	1.37	6.49	9.59	48.98	19.64	15.30	7.99
	97.63	0.11	1.02	0.43	0.82	40.55	1.46	23.06	10.50	24.42	1.12
III	96.01	0.37	1.78	0.68	1.16	26.26	4.19	30.25	13.15	26.15	2.07
	94.01	0.40	2.56	1.05	1.98	16.37	3.67	31.49	14.62	33.85	3.85
	92.90	0.50	3.16	1.24	2.20	13.13	3.60	34.47	15.37	33.44	4.98

binary VOC/N_2 separation. Heavier VOC component is enriched in the permeate more significantly than the lighter VOC components in the mixture. However, for the VOCs emitted to nitrogen from the mixed liquid solvent with the same composition, the enrichment factor for all the VOC components becomes lower when the overall feed VOC concentration increases. Presently, it is difficult to quantify how the permeability of a VOC component is affected by other VOC components present in the mixture, but it is expected that the interactions among the permeants will affect both the sorption and diffusion of each VOC in the membrane. The combined swelling effects of the VOCs on the membrane will enhance the diffusivity of individual permeant through the membrane. Nonetheless, the experimental data demonstrate that the membrane can be used to separate the mixed VOC components from nitrogen, which is of practical interest because organic vapor emissions from mixed solvents are often encountered in actual applications, although the degree of separation may be different for different VOC components.

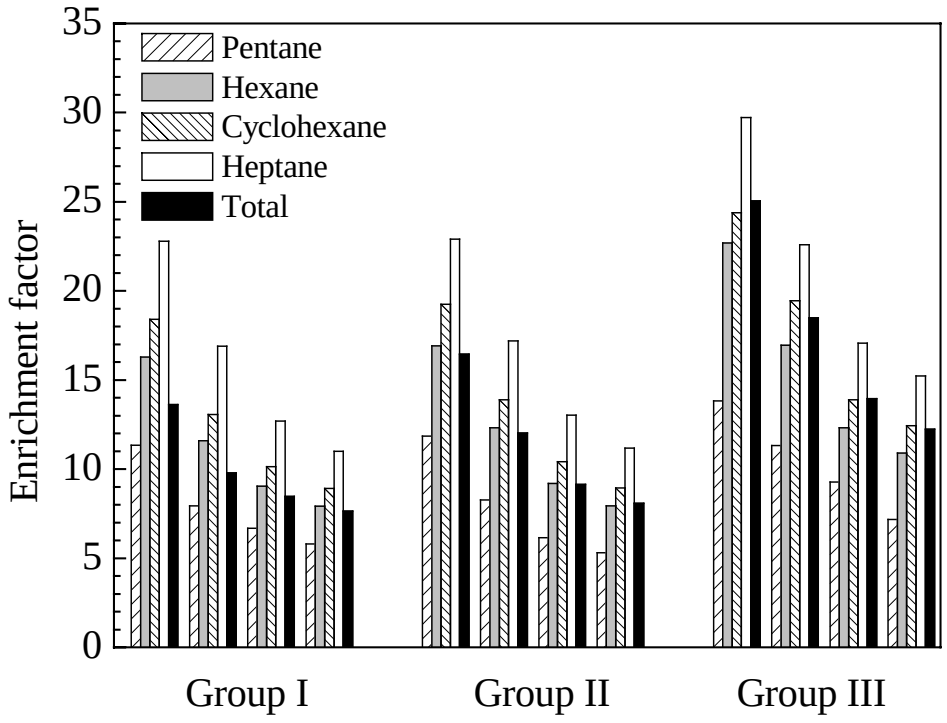

Figure 6.15 Enrichment factors for VOCs in the separation of multi-component VOCs from nitrogen.

6.4 Summary

The permeation and separation performance of a series of VOC/N_2 mixtures through PEBA 2533 membranes were studied. This is relevant to the recovery and capture of organic vapors for emission control. The membrane showed good permselectivity for the various VOCs representing gasoline components and additives (including n-pentane, n-hexane, cyclohexane, n-heptane, methanol, ethanol, dimethyl carbonate and methyl *tert*-butyl ether). In general, the permeance of the VOCs and the VOC/N_2 selectivity increased with an increase in the feed VOC concentration, and the permeance of nitrogen was affected by the presence of the organic compound(s). When the feed VOC concentration is 5 mol%, a permeate stream containing more than 90 mol% of VOC could be achieved in a single stage of permeation. A simple cross flow model was used to evaluate the separation performance, and the validity of model was justified with experimental data. In addition, the membrane demonstrated good permselectivity for separating multi-component VOCs from nitrogen in spite of the strong interactions among the permeating VOC components. Moreover, the effects of the operating temperature, stage cut and the permeate pressure on the separation performance were studied.

CHAPTER 7

Preparation of Hollow Fiber Poly(Ether Block Amide)/ Polysulfone Composite Membranes for CO_2 and N_2 permeation

7.1 Introduction

The capture/separation of carbon dioxide is an important step for green house gas emission control. As presented in Chapter 2, PEBA polymers were found to have high CO_2 permeability and CO_2/N_2 permeability ratio, which is attributed to the strong affinity of the polar ether linkages for CO_2. This suggests that PEBA polymer is a potential candidate material for making membranes to separate CO_2 from flue gas.

Compared with flat membranes, hollow fiber membranes have the advantages of self-supporting and large membrane area per unit module volume, a feature favorable for practical applications, especially for the treatment of flue gas with a large quantity and a low stream pressure. Most industrially important membranes for gas separations are hollow fiber membranes. In spite of the earlier work on the permeability of several gases through dense homogeneous flat PEBA films prepared by melt extrusion or solvent casting, no study has been reported in the literature on the development of hollow fiber composite PEBA membranes.

The present study deals with the development of hollow fiber thin-film composite PEBA membranes for CO_2 separation from nitrogen, which is relevant to CO_2 capture from flue gas. The membranes comprising of a thin PEBA 2533 layer supported on a microporous polysulfone hollow fiber substrate were developed in an attempt to increase the membrane permeance. The effects of parameters involved in the procedure of polysulfone hollow fiber spinning and PEBA coating application on the permselectivity of the resulting composite membranes were investigated. It should be pointed out that the

gas permeability data of PEBA dense membranes reported are quite different (Kim et al., 2001; Bondar et al., 2000; Wilks and Rezac, 2002), presumably due to the different thermal and process histories (e.g. melt extrusion versus solution casting) that the membrane samples underwent, which will be discussed later. Therefore, in order to evaluate how close is the selectivity of the hollow fiber PEBA/polysulfone composite membranes to the intrinsic permselectivity of the PEBA 2533 membranes for CO_2 and N_2 permeation, flat dense PEBA membranes with the similar thermal history (i.e. drying conditions) during membrane formation were also prepared in this study to determine its intrinsic permselectivity.

In principle, the membranes can also be applied to the removal of CO_2 from natural gas or other CO_2-contaning separation process streams. As mentioned in Chapter 2, thin film composite membranes are normally not very suitable for applications with high source pressures (e.g. natural gas) because of the relatively weak mechanical strength of the membranes. Moreover, in rubbery polymers, CH_4 generally has a higher permeability than N_2 (Baker, 2004) and the membrane selectivity for CO_2/CH_4 separation would be lower than for CO_2/N_2 separation. Therefore, considering the membrane property and operating conditions, this work will only focus on the separation of CO_2 from flue gas (CO_2/N_2 separation) where a relatively low operating pressure is preferred.

7.2 Experimental

7.2.1 Materials

Polyethylene glycol (PEG) (average molecular weight 1000) was used as an additive for the preparation of the micropourous hollow fiber substrate. The other materials were the same as used in Chapter 3.

7.2.2 Membrane preparation

The dense PEBA 2533 membranes were prepared by solvent casting technique following the same procedure in Chapter 3. The thickness of the resulting dry membrane was measured to be ~55 μm, and it is used to determine the intrinsic permeation properties of the polymer.

Hollow fiber composite membranes were prepared by dip coating a microporous polysulfone (PSf) hollow fiber substrate with a PEBA solution. The substrate hollow fibers were spun from homogenous solutions of polysulfone dissolved in N-methyl-2-pyrrolidone (NMP), with and without PEG additive, using the phase inversion technique. After degassing under vacuum, the dope solutions were extruded through a tube-in-orifice spinneret with nominal inside and outside diameters of 0.5 and 1.0 mm, respectively. The external coagulation bath was filled with de-ionized water and maintained at room temperature, and de-ionized water was used as the bore fluid. The schematic diagram for hollow fiber spinning is shown in Figure 7.1. The as-spun hollow fibers were kept in water at room temperature for 2 days to ensure complete solvent–nonsolvent exchange followed by thorough rinsing with water. The hollow fibers so prepared had an inside and outside diameters of 350 and 600 μm, respectively.

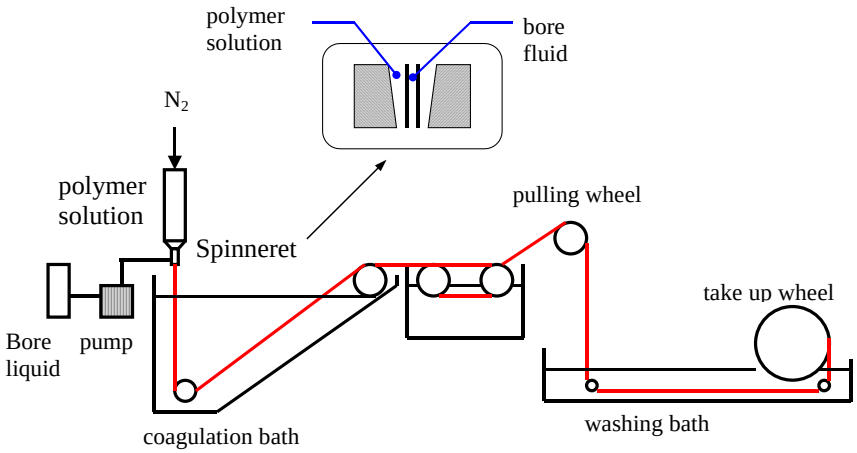

Figure 7.1 Schematic diagram of hollow fiber spinning system.

To prepare the hollow fiber composite membranes, the water–wet polysulfone hollow fiber substrates were dip-coated with a PEBA solution at a given temperature. The PEBA concentration in the coating solution ranged from 0.5 to 5 wt%. After coating, the hollow fiber membranes were dried at the same temperature for 20 min, and the resulting PEBA/PSf hollow fiber composite membranes were further dried at 70 °C in an oven with forced air circulation for 12 h to remove any residual solvent. The composite hollow

fiber membrane formed has a dense PEBA selective layer on the outside wall of the polysulfone substrate, which is schematically shown in Figure 7.2.

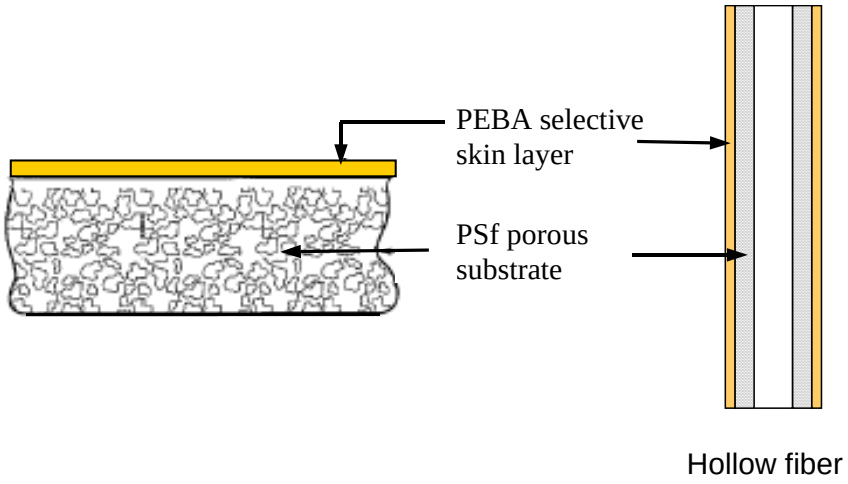

Figure 7.2 PEBA/PSf hollow fiber composite membrane

7.2.3 Gas permeation

The technique and the setup for gas permeation test through flat membrane are the same as that described in Chapter 3. To test the permselectivity of the PEBA/PSf hollow fiber composite membranes, a miniature hollow fiber membrane module (Figure 7.3) was assembled using a bundle of four hollow fibers encased in a 1/4 in. copper tubing. One

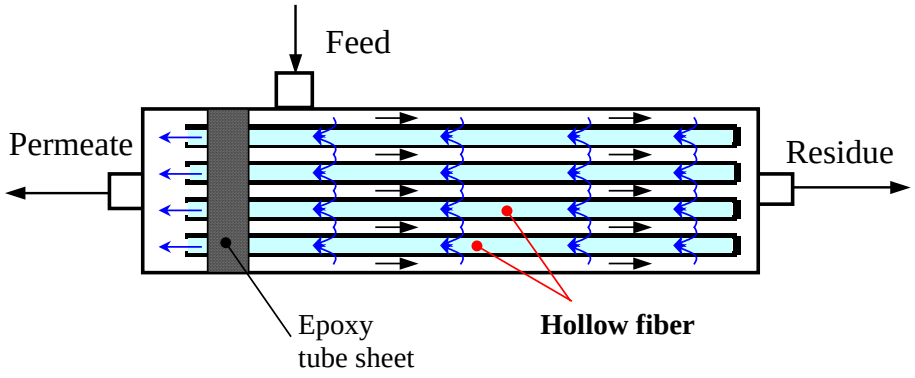

Figure 7.3 Schematic diagram of hollow fiber module

end of the fiber bundle was sealed with an epoxy resin, whereas the other end was potted with epoxy to form a gas-tight tube sheet. The tube sheet was carefully cut to make the fiber bores fully open. The feed gas at a predetermined pressure entered the shell side of the module, and the permeate gas exited at atmospheric pressure from the open end of the fiber bores. The effective length of each hollow fiber was 15 cm, which corresponds to a total permeation area of 11.3 cm^2 in the membrane module. The permeate pressure buildup inside the hollow fibers was found to be negligibly small, and the gas permeance through the hollow fibers was evaluated from the permeation rate measurements using the same method as that used for determining the permeability of flat membrane.

7.3 Results and discussion

7.3.1 Gas permeation through dense flat membranes

The permeation of pure carbon dioxide and nitrogen through a dense PEBA 2533 membrane at different operating pressures and temperatures were investigated to obtain the intrinsic permselectivity of the PEBA membranes. The effect of feed pressure on gas permeability at various operating temperatures is shown in Figure 7.4. The permeability of nitrogen is shown not to be affected significantly by feed pressure. At a high temperature (i.e. 60 °C), nitrogen permeability tends to decrease slightly as the pressure increases, primarily due to compaction of the membrane. When the diffusivity and solubility coefficients of nitrogen in the membrane are constant and if the membrane compaction is insignificant, the membrane permeability will be independent of the gas pressure. This is normally the case for permeation of noncondensable gas molecules in rubbery membranes. However, the permeability of carbon dioxide through the PEBA membrane increases slightly with an increase in the feed pressure, especially when the temperature is relatively low. The latter observation is believed to be the result of membrane plasticization by the permeant. There exists a strong interaction between carbon dioxide and the polymer material, as reflected by the strong sorption of carbon dioxide in the polymer (Bondar et al., 1999). When a sufficiently large amount of CO_2 is sorbed into the membrane, the polymer is swollen and the free volume of the membrane increases, leading to an increase in the gas permeability. The plasticization effect is generally reflected by the dependence of the effective diffusivity coefficient and/or

permeability coefficient on the penetrant concentration in the polymer. It needs to be pointed out that in membrane gas separations applications where a gas mixture is involved, the membrane swelling by a penetrant will affect the permeation of all components in the mixture, and the membrane selectivity is generally lower than that would be obtained on the basis of pure gas permeability.

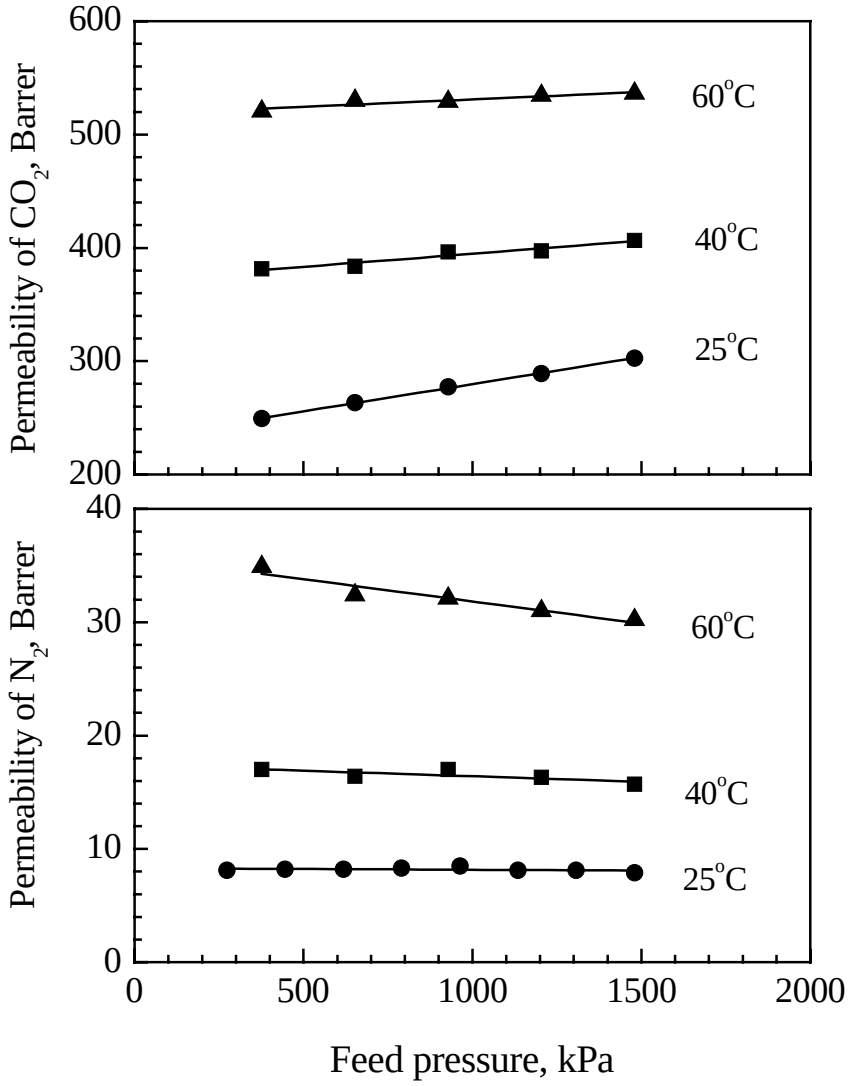

Figure 7.4 Permeability of carbon dioxide and nitrogen through the dense PEBA membrane as a function of feed pressure at different temperatures.

It should be pointed out that the intrinsic CO_2 permeabilities of PEBA 2533 dense membranes reported in the literature are quite different. Kim et al. (2001) measured the CO_2 permeability to be 142 Barrer at 25 °C, while Bondar et al. (2000) and Wilks and Rezac (2002) reported a CO_2 permeability of 222 and 350 Barrer, respectively, at 35 °C. Based on the experimental data of Wilks and Rezac (2002), the CO_2 permeability at 25 °C can be estimated to be 320 Barrer. In this study, the CO_2 permeability at 25 °C was determined to be 260 Barrer, a value that falls within the range of permeabilities reported in the literature. The difference in the permeability, which apparently cannot be attributed only to the different measurement conditions, is due to the fact that PEBA is a block copolymer comprising of soft ether segments and hard amide segments. Hatfield et al. (1993) characterized the structure and morphology of the PEBA polymers using X-ray diffraction, differential scanning calorimetry and solid state nuclear magnetic resonance, and found that the polymer exhibited microphase separated morphology. A recent study on the morphological solid state structure of a series of PEBA polymers verified that the microphase separated morphology existed over a broad temperature range (Sheth et al., 2003), and it was also found that the complex morphology was strongly affected by the sample's thermal and process history. As one expects, the membrane morphology affects the gas permeability. This explains the discrepancy in the permeability coefficients reported. This is why instead of using the literature values, the intrinsic permeability was actually measured here in order to evaluate how well the hollow fiber composite membranes compare with a dense membrane in terms of permselectivity for CO_2/N_2 separation. It may be mentioned that similar observations can also be made on gas permeability through PEBA 3533, a polymer having the same constituent blocks as PEBA 2533 but with a higher content of amide blocks; for example, Kim et al. (2001) determined that at 25 °C and 4 atm the CO_2 and H_2 permeabilities through PEBA 3533 were 132 and 20 Barrer, respectively, which are significantly different from the data reported by Wilks et al. (2002) (230 and 46 Barrer, respectively, at 35 °C and 1 MPa).

Previous studies (Erb and Paul, 1981; Koros and Paul, 1976, 1977; Huvard et al., 1980) have shown that gas sorption in glassy polymers can be characterized by the dual-mode sorption model and as such the permeability tends to decrease with an increase in the feed pressure when the pressure is relatively low due to competitive nature of

Langmuir sorption. However, when the feed pressure is sufficiently high, the permeability tends to increase with a further increase in the feed gas pressure because membrane plasticization is increasingly important (Bos et al., 1999; Wessling, 1995). For rubbery polymer membranes that have no Langmuir "sorption sites", the membrane permeability tends to increase as the feed pressure increases because of membrane swelling. PEBA 2533 is a copolymer comprising of 20 wt% glassy polyamide segments and 80 wt% rubbery polyether segments. Apparently, the above-observed pressure dependence of CO_2 permeability in the PEBA membrane is due to the combined effects of Langmuir sorption on polyamide segments and the swelling of polyether segments.

The experimental data in Figure 7.4 show that at 25 °C an increase in gas pressure from 377 to 1480 kPa increases the permeability of carbon dioxide by about 21%, while at 60 °C the same pressure change results in only 3% increase in the membrane permeability. Clearly this indicates that the plasticization and swelling of the membrane is less significant at higher temperatures. This is in agreement with physical reasoning that the solubility of carbon dioxide in the polymer decreases at higher temperatures, rendering membrane plasticization/swelling by the permeant less significant. Okamoto et al. (1990), who studied CO_2 permeation through glassy polyimide membranes, also found that the plasticization of the membrane became less significant as the operating temperature increased.

Figure 7.5 shows the effect of operating temperature on the membrane permeability for permeation of carbon dioxide and nitrogen through the dense PEBA membrane in a temperature range of 25 – 60 °C. Note that as shown previously, the feed gas pressure has little effect on nitrogen permeability, and the nitrogen permeability data in the figure were obtained at feed pressures of 239 – 1135 kPa. The selectivity of the membrane for CO_2/N_2 expressed in terms of pure gas permeability ratio is also shown in Figure 7.5. It is shown that the temperature dependence of permeability follows the Arrhenius relation for both N_2 and CO_2 permeation. The activation energy for permeation, determined from the slope of the Arrhenius plot, is presented in Table 7.1. Unlike N_2 permeability, which is essentially independent of pressure, the permeability of CO_2 is affected by pressure, and so is the activation energy for CO_2 permeation. The activation energy for permeation can be approximated as the sum of activation energy

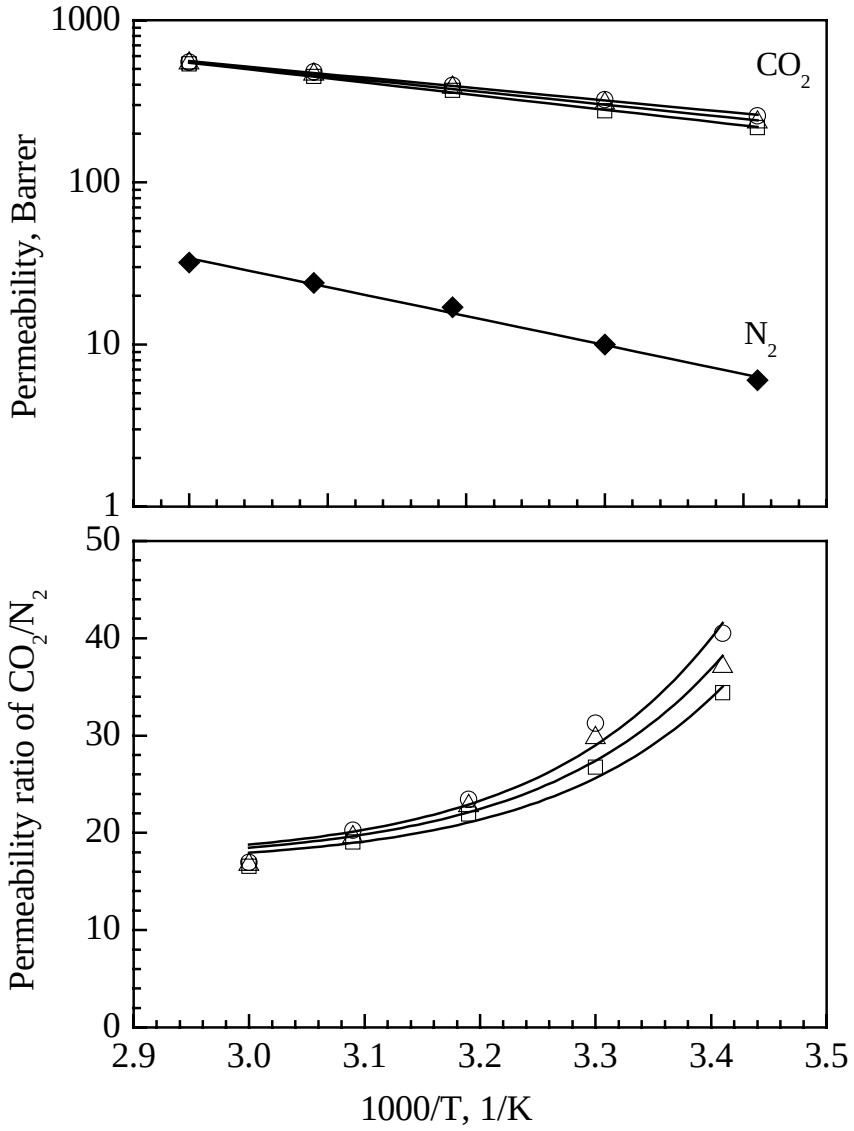

Figure 7.5 Temperature dependence of CO_2/N_2 permselectivity through the dense PEBA membrane. Feed pressure: (□) 446 kPa; (Δ) 791 kPa; (O) 1135 kPa; (◆) 239-1135 kPa.

Table 7.1 Activation energy for permeation

Gas	Pressure (kPa)	E_p (kJ/mol)
Nitrogen	239 – 1135	33.6
Carbon dioxide	446	18.6
	791	17.0
	1135	15.6

for diffusion and the heat of sorption. The activation energy for diffusion may be considered as the minimum energy that molecules must possess to achieve molecular jumps. In general, small molecules tend to have a high diffusivity coefficient and low activation energy for diffusion, whereas condensable gases tend to have a higher solubility and stronger sorption heat effect (which is often exothermic) than noncondensable gases. The activation energy of diffusion for N_2 and CO_2 should be similar considering their similar kinetic diameters (which are 0.36 and 0.33 nm for N_2 and CO_2, respectively (Breck, 1974), and as such the relative magnitude of the activation energy for permeation of CO_2 and N_2 would be mainly determined by their relative sorption heat. Therefore, it is not surprising that the activation energy for N_2 permeation is greater than that for CO_2 permeation considering the fact that CO_2 molecules are more condensable than N_2. As a result, the selectivity of carbon dioxide over nitrogen decreases with an increase in the operating temperature. As the feed pressure increases, the activation energy for carbon dioxide permeation decreases, which may be attributed to the increased swelling of the membrane caused by the increased quantity of CO_2 dissolved in the membrane.At 25 °C and 791 kPa, the dense PEBA membrane exhibited a CO_2 permeability of about 260 Barrer and a CO_2 /N_2 permeability ratio of about 30 – 35, which can be considered to be the intrinsic properties of the membrane in subsequent studies of hollow fiber PEBA/PSf composite membranes.

7.3.2 PEBA/PSf hollow fiber composite membranes

It is well known that the permselectivity of a composite membrane is generally affected by the parameters involved in the formation of both the membrane substrate and the skin layer. The appropriate conditions for preparing PSf hollow fiber substrate and PEBA coating were thus investigated. In preliminary studies, the dope composition for

PSf fiber spinning, the PEBA concentration in coating solution and the coating temperature were found to influence the performance of the resulting composite membranes significantly. These parameters were specifically studied on the basis of the "one variable at a time" method.

7.3.2.1 Effects of dope composition on PSf hollow fiber spinning

Two representative polymer dope solutions containing PSf/NMP/PEG (wt%) 19/78.4/2.6 and 23/77/0, designated as dope I and dope II, respectively, were used to produce microporous PSf hollow fibers for use as a substrate to the composite PEBA membranes. De-ionized water was used as the bore fluid. The air gap between the spinneret and the coagulation bath was 5 cm. The detailed operating conditions for hollow fiber spinning are summarized in Table 7.2. The hollow fibers were coated at 50 °C with PEBA solutions containing 1.5 or 3 wt% PEBA to form composite membranes. It was found to be difficult to achieve a composite membrane with a selectivity reasonably close to the intrinsic selectivity of PEBA 2533 when the PSf hollow fibers prepared from dope I were used as the substrate, even with repeated coating of PEBA layer for several times.

Table 7.2 Hollow fiber spinning conditions

Spinning pressure	30 - 60 kPa gauge
Spinning temperature	23°C
Air gap	5 cm
Bore fluid	Water
Bore fluid flow rate	1.2 - 2.0 ml/min
External coagulant	Water
Coagulation temperature	23 °C
Fiber take-up speed	7 m/min

The typical results of membrane permselectivity achieved under different membrane preparation conditions were presented in Table 7.3. However, when the PSf substrate prepared from dope II was used, only one or two PEBA coatings, depending on PEBA content in the coating solution, were sufficient to obtain PEBA/PSf membranes with a CO_2 /N_2 selectivity of about 30. This is understandable because both the presence

of PEG additive and the relatively small content of PSf in dope I contribute to the formation of large pores in the hollow fiber membrane matrix during the phase inversion process. If the pore size is too large, the PEBA coating solution would penetrate into the pores of the PSf substrate; upon evaporation of the solvent in the PEBA solution, the thin layer of PEBA formed over the pore that is designed to bridge the "gap" may collapse, rendering the membrane surface defective. On the other hand, the penetration of PEBA coating solution in the substrate pores will increase the resistance of the substrate to gas permeation. Consequently, the membrane permeability decreases while the selectivity does not improve significantly. Because of the relatively low polymer content in the PEBA coating solution, even the use of multiple coatings cannot guarantee that the membrane defects will be repaired because of the possible re-dissolution of the prior thin coating layer by the solvent in the coating solution. This explains why increasing the number of coating times does not always reduce the membrane permeability.

Table 7.3 The gas permeation performance of CO_2/N_2 through PEBA/PSf composite membranes

Dope composition for PSf hollow fiber spinning (wt%) (PSf/NMP/PEG)		PEBA wt% in coating solution	Number of coating times	Permeance (GPU)		CO_2/N_2 Selectivity
				CO_2	N_2	
I	19/ 78.4 /2.6	1.5	3	17.0	0.88	19.3
		1.5	4	40.5	1.93	21.0
		3.0	2	27.7	1.14	24.2
		3.0	2	22.1	1.29	17.1
II	23 / 77 / 0	1.5	2	17.0	0.58	30.2
		3.0	1	35.7	1.18	29.1

From a membrane manufacturing point of view, a single coating process is preferred, though this sometimes requires the use of relatively high polymer concentration in the coating solution. The data in Table 7.3 show the two composite membranes prepared using dope II have essentially the same selectivity, but the membrane prepared by single coating of a 3 wt% PEBA solution is about twice as permeable as the membrane prepared by double coatings of a 1.5 wt% PEBA solution. The gas permeance through a composite membrane is determined by the resistance of

both the coating layer and the microporous substrate, while the membrane selectivity to a pair of gases is determined by their relative permeance. When the coating layer dominates the overall resistance to gas permeation, the membrane selectivity will approach to the intrinsic selectivity of the coating material. The above results indicate that by coating the polysulfone substrate with 3 wt% PEBA once or with 1.5 wt% PEBA twice, all the pores on the substrate have essentially been bridged to form a defect-free PEBA layer. Ideally, a thin layer of PEBA layer would form on the surface of the polysulfone substrate, and the PEBA layer is responsible for selective permeation whereas the substrate functions only as a mechanical support. However, because of the relatively low viscosity of the 1.5 wt% PEBA solution, the coating solution is more likely to "leak" into the pores of the substrate, and the pore blocking will decrease the permeance of the composite membrane. Consequently, the selectivity of the membranes will be the same and close to the intrinsic selectivity as long as the PEBA layer dominates the permeation, and the permeance of the composite membrane will be smaller when a low concentration of coating solution is used. An evaluation of the resistance components in the composite membranes on the basis of the resistance model (Feng et al., 2002), which is not pursued here, could be used to provide a quantitative explanation. In subsequent studies, only PSf substrates prepared from dope II were used to prepare composite membranes, and the membrane performance was evaluated at 25 °C and 446 kPa, unless specified otherwise.

7.3.2.2 Effects of coating conditions

The effect of PEBA concentration in coating solution on the permselectivity of the resulting composite membrane is shown in Figure 7.6. A single coating was applied in all cases. Without PEBA coating, the PSf substrate membrane was highly permeable (about 3000 GPU) but of little selectivity. The CO_2 /N_2 permeance ratio was only 0.88, which is just slightly higher than the reciprocal square root of their molecular weight ratio (i.e. 0.80), indicating that Knudsen diffusion dominated the gas permeation through the membrane substrate and there were no large defects that would allow for significant viscous flow. After coating with 0.5 wt% PEBA solution, the membrane permeance for both gases decreased substantially but the permeance ratio was still too low (only 1.2).

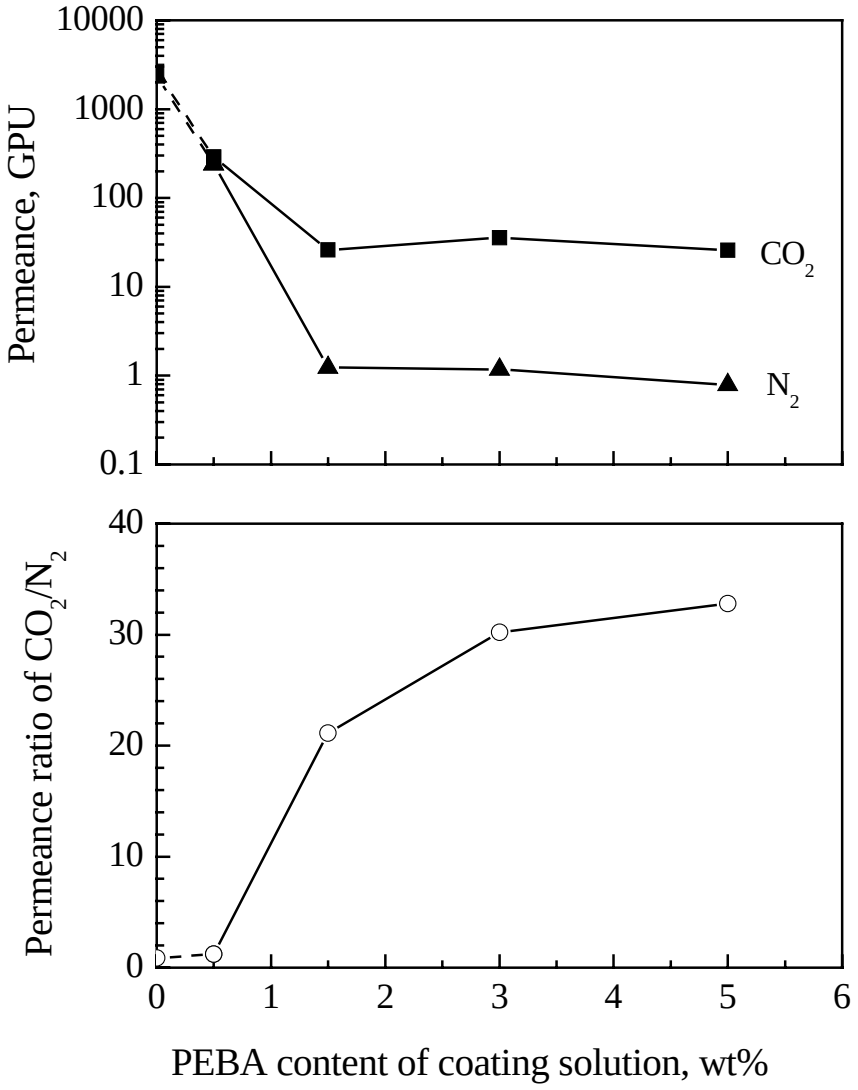

Figure 7.6 Effect of PEBA concentration in coating solution on the performance of PEBA/PSf hollow fiber composite membranes (PEBA coating once, coating temperature 50°C, permeation test at 446 kPa, 25°C).

Apparently, at a low concentration of coating solution, a defect-free PEBA coating layer cannot be formed on the PSf substrate. When the PEBA content in the coating solution was increased to 1.5 wt%, the membrane permeability continued to decrease but the decrease is more discriminative in favor of CO_2 permeation, and as a result the membrane began to exhibit significant selectivity for CO_2/N_2. A further increase in the PEBA coating concentration to 3 or 5 wt% resulted in a CO_2 /N_2 selectivity of 30 – 32, which matches the intrinsic selectivity of PEBA polymer, as shown previously. This suggests that the composite membrane is defect-free and that the PEBA skin layer dominates the permeation.

The effect of coating temperature on the membrane performance is shown in Figure 7.7. The temperature of the coating solution was maintained the same as the coating temperature so that there would be no temperature change during the coating process. The coating temperature influences the viscosity of the coating solution and the rate of solvent evaporation, and both aspects affect the resultant membrane. At a low temperature, the viscosity of the coating solution is high, which help prevent the coating solution from penetrating into the pores of substrate. This, however, is compromised by the slow evaporation of solvent in the coating solution. A reduced solvent evaporation rate means a longer contact time between the coating solution and the substrate membrane, which is undesirable because the prolonged contact favors penetration of the coating solution into the substrate pores. The data in Figure 7.7 show that as the coating temperature increases, both CO_2 and N_2 permeabilities decrease. The selectivity, expressed in terms of CO_2/N_2 permeance ratio, follows a similar trend in spite of the scatter data points. It should be pointed out that the temperature also influences the solubility of PEBA in the solvent, and the temperature of the coating solution should not be too low in order to retain a well-stretched structure of polymer chains in the coating solution. Using 3 wt% PEBA coating solution and at a coating temperature of 50 °C, the PEBA/PSf composite membrane exhibited a CO_2 permeance of 61 GPU and a CO_2/N_2 selectivity of 30.

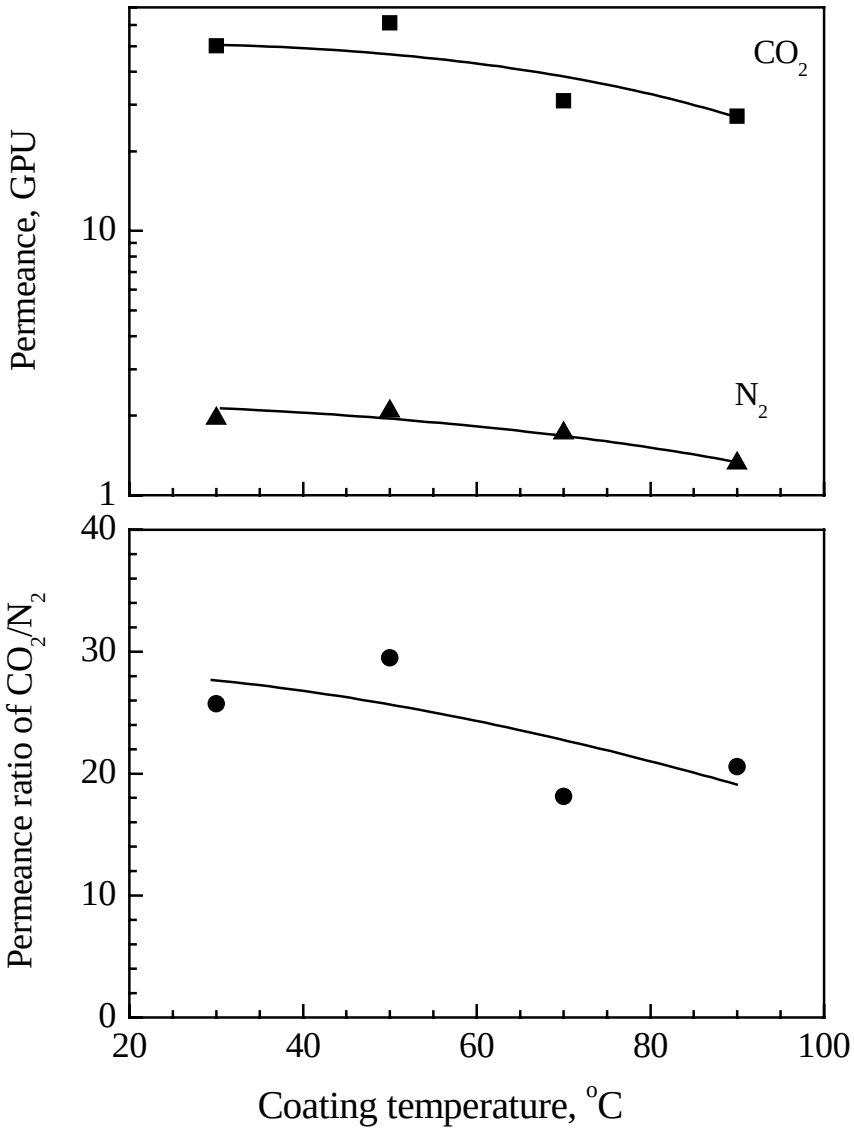

Figure 7.7 Effect of PEBA coating temperature on the performance of PEBA/PSf hollow fiber composite membranes (PEBA concentration in coating solution, 3 wt%, PEBA coating once, permeation test at 446 kPa, 25°C).

7.3.2.3 Effects of operating conditions

Figure 7.8 shows the effects of feed pressure on the permeance of carbon dioxide and nitrogen through PEBA/PSf hollow fiber composite membranes at various temperatures. The permeance of carbon dioxide shows a slight increase with an increase in the gas pressure while that of nitrogen is essentially independent of pressure. This trend is consistent with results obtained with dense PEBA film. The permeance of carbon dioxide increases by about 10% when the feed pressure was increased from 170 to 446 kPa at all three temperatures investigated. This demonstrates that the effect of plasticization of carbon dioxide in the composite membrane is stronger than in the dense PEBA film, in which remarkable plasticization was only observed at relatively low temperatures. Assuming that the PEBA skin layer in the composite membrane dominates the gas permeation, then on the basis of intrinsic permeability the thickness of the PEBA layer in the composite membrane can be estimated to be less than 5 μm, which is much smaller than the thickness of the dense film (about 55 μm). Wessling et al. (2001) also observed that the significance of plasticization of carbon dioxide in glassy polyimide membranes depends on whether the membrane is a dense film or a thin layer in a composite membrane. A thin layer of polyimide (1.5 – 4 μm thick) in a composite membrane was found to be plasticized more significantly than a thick (20 – 50 μm) dense film membrane.

Plasticization of the membrane by a permeant (which is often the fast permeating component) tends to increase the permeability of other components when a gas mixture is involved in actual separations, rendering the membrane less selective. Further studies with permeation of gas mixtures will be needed to determine how the membrane plasticization affects the actual separation performance. However, for the applications of interest (that is, CO_2 capture from flue gas), the desired operating pressure is relatively low because of the costs associated with gas compression and the feed CO_2 concentration is moderate, and thus the membrane plasticization may not be very significant especially for bulk separation of CO_2 from flue gas.

Figure 7.9 shows the effect of temperature on the permselectivity of the composite membrane for carbon dioxide and nitrogen permeation. As one may expect, the temperature dependence of membrane permeance follows the Arrhenius type of

equation, which is consistent with the results observed earlier with the dense PEBA film. The selectivity of CO_2/N_2 is shown to decrease with an increase in the temperature. This result further confirms that the composite membrane is defect-free and gas permeation through the membrane is by solution–diffusion mechanism.

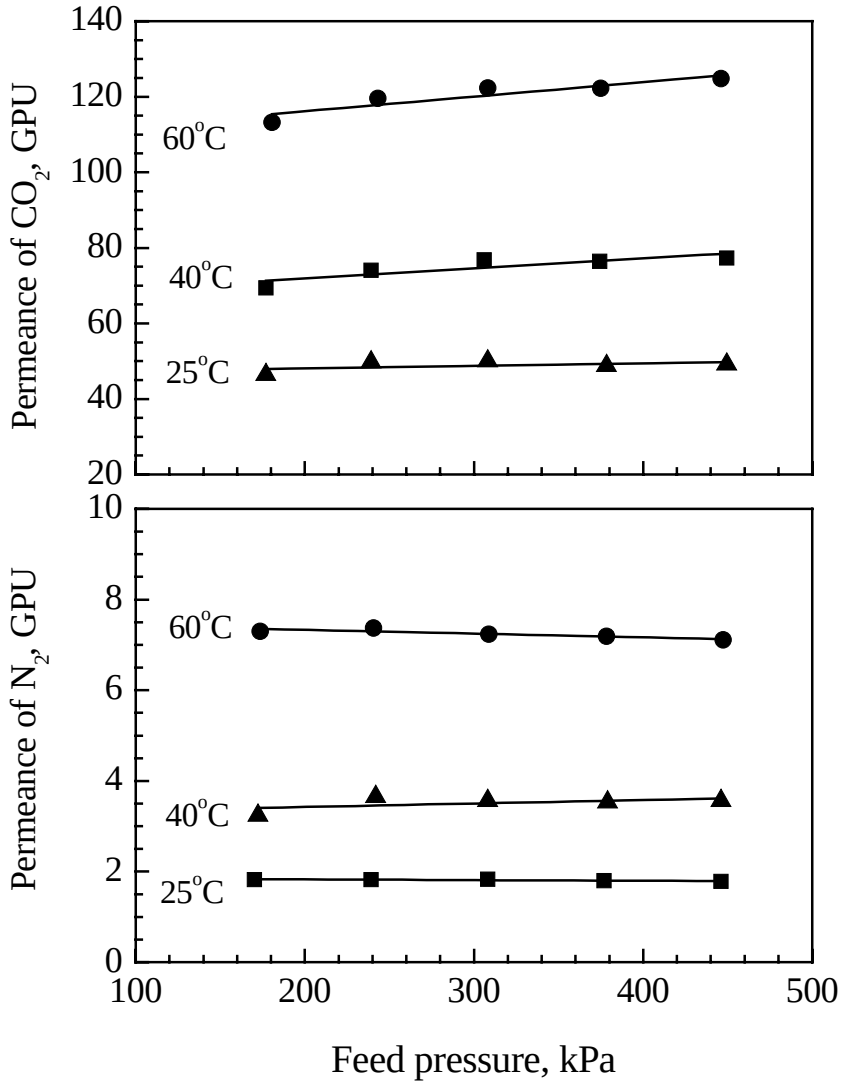

Figure 7.8 Permeance of carbon dioxide and nitrogen through PEBA/PSf hollow fiber composite membrane at various pressures and temperatures.

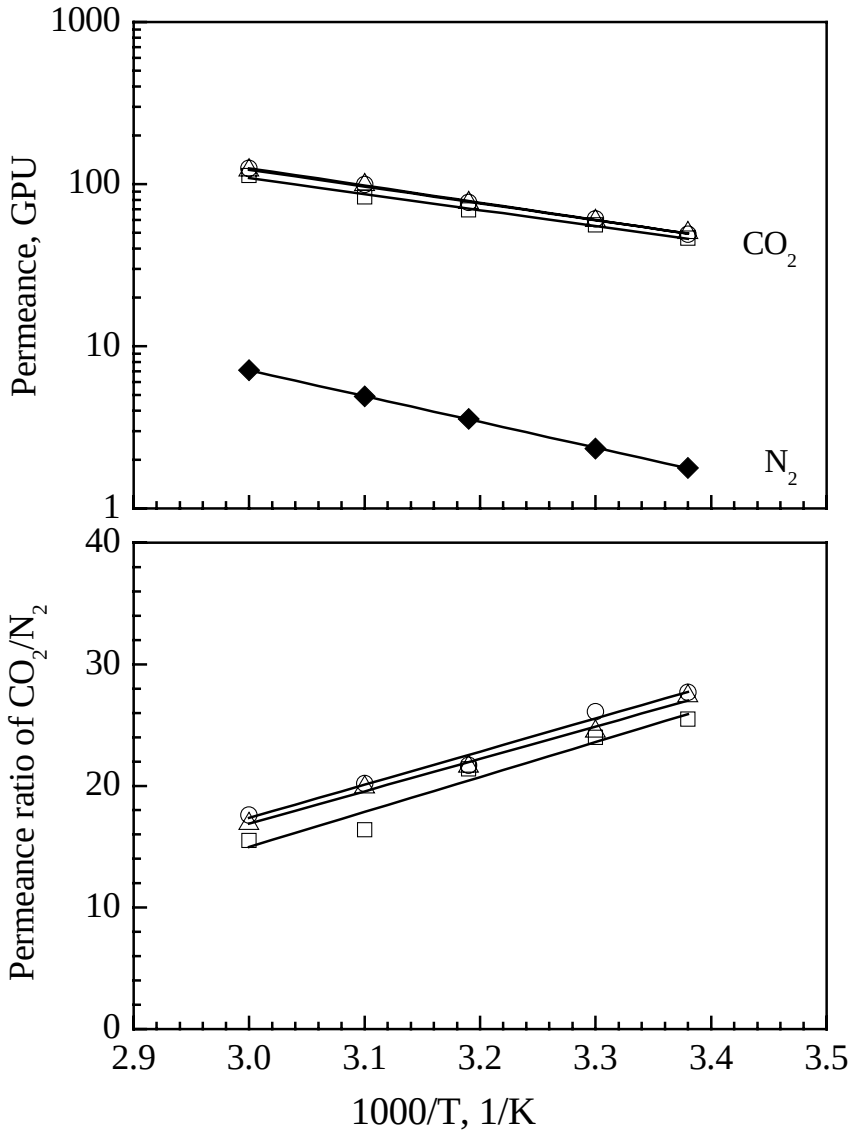

Figure 7.9 Effect of temperature on the permeance and selectivity of carbon dioxide and nitrogen through the PEBA/PSf hollow fiber composite membrane. Feed pressure: (□) 170 kPa; (Δ) 308 kPa; (O) 446 kPa; (♦) 170 - 446 kPa.

7.4 Summary

The permeation of carbon dioxide and nitrogen through poly(ether block amide) (PEBA 2533) dense homogeneous membranes was tested. The polymer showed a good permselectivity for CO_2/N_2 separation; at 25 °C and 791 kPa, a carbon dioxide permeability of about 260 Barrer and a CO_2/N_2 selectivity of 32 were obtained. While the permeability of nitrogen is essentially independent of the gas pressure, the permeability of carbon dioxide tends to increase when the gas pressure increases presumably due to plasticization of the membrane by CO_2. This is typical of rubbery polymer membranes. As temperature increases, the effect of plasticization becomes less significant.

In order to increase the membrane permeance, thin-film composite membranes comprising of a thin PEBA skin layer supported on a microporous polysulfone hollow fiber substrate was prepared. The effects of parameters involved in the procedure of polysulfone hollow fiber spinning and PEBA coating on the permselectivity of the resulting composite membranes were investigated. Composite membranes having a CO_2 permeance of 61 GPU and a CO_2/N_2 selectivity of 30 have been obtained. That the selectivity of the composite membrane is very close to the intrinsic selectivity of PEBA dense membrane implies that the composite membrane is defect-free and the PEBA skin layer dominates the permeation. The membranes formed with good performance will be studied for CO_2/N_2 separation in the next chapter.

CHAPTER 8

Separation of CO_2 from N_2 by Poly(Ether Block Amide) Hollow Fiber Composite membranes

8.1 Introduction

Carbon dioxide, a primary greenhouse gas emitted by human activities, is responsible for over a half of the greenhouse effect. Flue gas from fossil fuel power generation is the largest single contributor to CO_2 emissions. Therefore, the separation and capture of CO_2 from flue gas is one of the most important measures to greenhouse gas emission control. Several technologies may be considered for CO_2 separation and capture, including physical or chemical absorption, low temperature distillation, pressure swing adsorption, and membrane separation. Membrane-based gas separation holds great promise for bulk separation due to its low energy consumption, easy operation and low maintenance. Unlike absorption or adsorption that requires regeneration of sorbent, the membrane process does not involve any material regeneration. In addition, membrane process has the advantages of modular design and light weight, making it particularly suitable for retrofit into existing processes.

Generally, the flue gas from power plants has a large volume and a relatively low concentration in CO_2 (typically 10 - 18 mol%). A membrane system with a high processing capacity and a reasonably high selectivity for CO_2/N_2 is required in order to compete with other separation techniques. The strong affinity of the polyether segments to CO_2 molecules is believed to result in the high permselectivity.

For practical applications, asymmetric and/or composite membranes comprising of a thin skin layer supported on a microporous substrate are often used in order to achieve a high permeation flux. In addition, among the various designs of membrane

modules, hollow fibers are preferred because of their high packing density and self-supporting characteristics. These are especially useful for treating a large volume of gas streams. A few hollow fiber membranes have been studied that involved the separation of CO_2 from a gas stream. Feng et al. (2002) investigated the feasibility of separating CO_2 from N_2 using integral asymmetric cellulose acetate-based hollow fiber membranes for nitrogen generation from combustion exhaust gas, and a full-scale module comprising of several hundreds of thousand hollow fibers was also tested using simulated flue gas (Ivory, 2002). Sada et al. (1992) evaluated the performance of CO_2 separation from air with asymmetric cellulose triacetate hollow fiber membranes that had an ideal separation factor of 21-24 for CO_2/N_2 at 30^oC. The separation of ternary gas mixtures (CO_2, O_2 and N_2) by polysulfone hollow fiber membranes was studied with single and multiple membrane modules (Ettouney, 1999). Li et al. (1990) studied the separation of CO_2 from breathing gas mixtures using silicone rubber capillary membranes, and it was found that the separation efficiency could be improved by purging an impermeable gas on the permeate side. This approach is, however, not suitable for CO_2 separation from flue gas as the CO_2 removed from the feed will end up in the permeate purge stream and additional separation is needed to capture CO_2.

In this work, PEBA/polyetherimide (PEI) thin film composite hollow fiber membranes prepared in Chpater 7 were used. A laboratory scale hollow fiber membrane module was constructed and the membrane performance for CO_2/N_2 separation was evaluated using a simulated flue gas. The present study involves the permeation of both pure gases and gas mixtures. The experiments on the separation of gas mixtures were carried out over a wide range of stage cuts for three different flow configurations (i.e., counter-current, co-current and a combination of both). The effects of operating parameters such as pressure and temperature were also investigated.

8.2 Experimental

8.2.1 Membrane preparation

The hollow fiber membranes were prepared as described in Chapter 7. The PEI hollow fiber substrates were coated by a 5 wt% PEBA solution at 50 ^oC.

A 1/4-in copper tubing was used as the shell casing to assemble the hollow fiber membrane module. Both ends of the copper tubing were connected to Swagelok tees and appropriate port connectors. A bundle of the hollow fibers were encased in the tubing, with both ends of the fiber bundle potted with epoxy resin to form a gas-tight tube sheet. The effective length of each hollow fiber was 22 cm, which corresponds to a total permeation area of 43.5 cm^2 in the membrane module. The tube sheets were carefully cut to make the fiber bores fully open at both ends so that the feed gas can flow at either the shell side or the lumen side. The gas permeation tests for both pure gases and gas mixtures were carried out by the traditional volumetric technique. Figure 8.1 shows the schematic of the experimental setup for shell side feed and counter-current flow. The gas

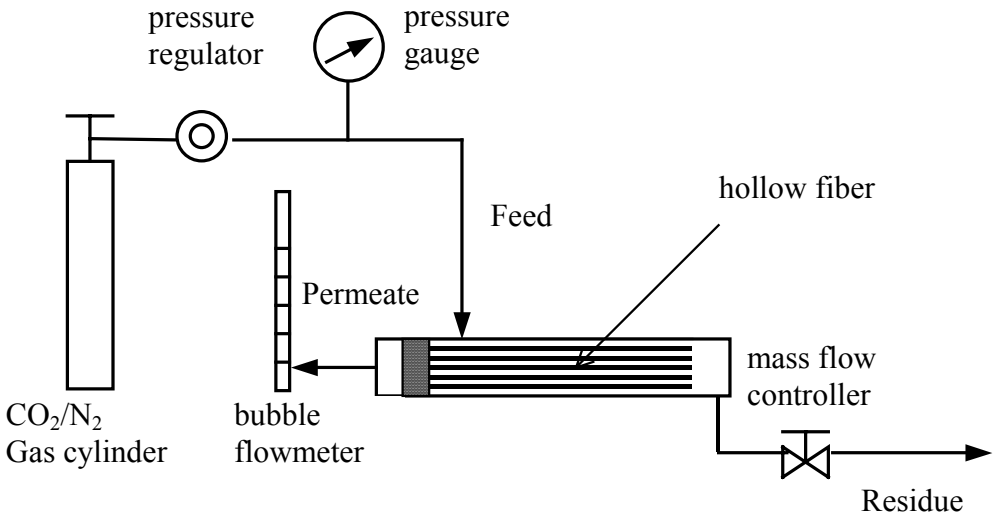

Figure 8.1 Schematic diagram of the experimental set-up for CO_2/N_2 separation by a hollow fiber membrane module.

inlet and outlets were changed appropriately for other feeding and flow configurations. The feed gas at a predetermined pressure was admitted to one side of the membrane, and the permeate gas exited at atmospheric pressure from the downstream side of the membrane. The flow rate of permeate was measured by a bubble flow meter. For the gas mixture permeation, the flow rate of the residue stream was controlled by a Metheson mass flow controller. The compositions of the feed, residue and permeate streams were

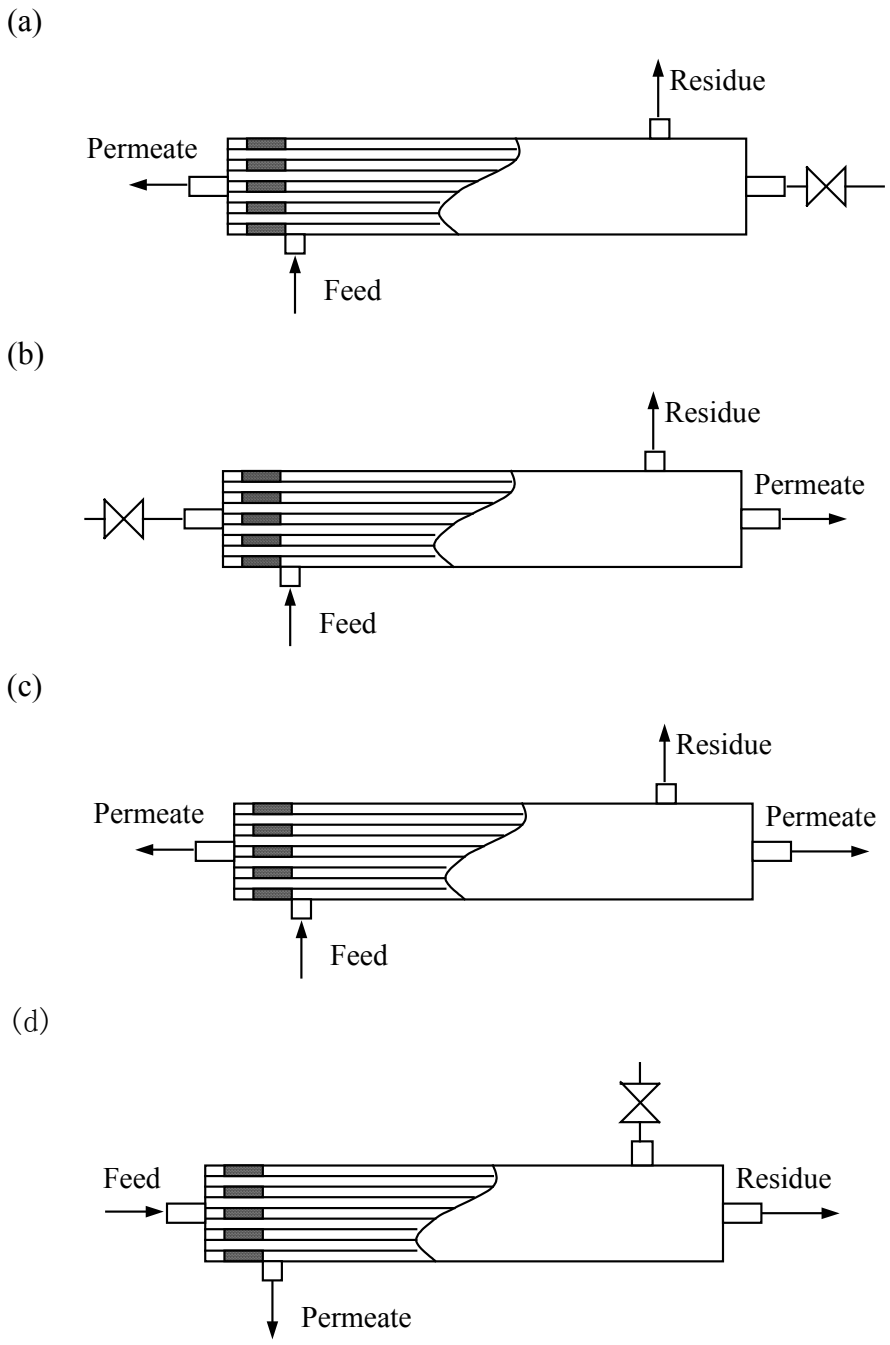

Figure 8.2 Configurations of membrane modules: (a) shell side feed, counter-current flow; (b) shell side feed, co-current flow; (c) shell side feed, counter-/co-current flow (permeate withdrawal from both ends of the fiber bores); (d) bore side feed, counter-current flow.

determined by a gas chromatograph (HP 5898 Series II) equipped with a packed column and a thermal conductivity detector. The membrane module was tested for both shell side feed (feed flowing in the space between the fibers) and bore side feed (feed flowing in the fiber lumens) with different flow patterns (as shown in Figure 8.2) which will be discussed later. A binary gas mixture containing 15.3 mol% CO_2 (balance N_2) was used as the feed in the gas mixture separation experiments.

Unless specified otherwise, the experiments were conducted at the ambient temperature (23^oC). For experiments at other operating temperatures, a thermal bath was used to control the temperature. The test sequence of gases was taken into account during experiments in order to minimize the experimental error that could be caused by membrane plasticization. For pure gas permeation, N_2 was tested first, followed by CO_2,; for gas mixture permeation, the experiments were conducted from a low pressure to a high pressure.

8.3 Results and discussion

8.3.1 Comparison of flow configurations

The thin film composite hollow fiber membranes consist of a PEBA selective skin layer and a microporous PEI substrate. Ideally, the skin layer dominates the mass transfer while the substrate provides mechanical support but offers no resistance to the permeation. The hollow fiber membrane module was first tested for pure gas permeation to see whether the skin layer indeed dominates the permeation. At 23^oC and a feed pressure of 790 kPa, the permeance of the membrane was 48.2 and 1.7 GPU for pure CO_2 and pure N_2, respectively, corresponding to a permeance ratio of 29. Under similar operating conditions, the CO_2/N_2 permeance ratio of dense homogenous PEBA 2533 membranes is shown to be 30-35 from the previous chapters. Clearly, the permeance ratio of the thin film composite membrane approaches the intrinsic permselectivity of PEBA 2533. This indicates that the PEBA/PEI hollow fiber composite membranes are defect-free, and the PEI substrate does not offer significance resistance to permeation. As such, the membrane performance will be mainly determined by the PEBA skin layer.

In the gas mixture permeation, the membranes are preferentially permeable to carbon dioxide, resulting in a permeate stream enriched in carbon dioxide and a residue

stream enriched in nitrogen. The hollow fiber membrane module can assume many configurations. The module design in the shell side feed configuration is relatively simple and most commercial hollow fiber membrane devices adapt the shell side feed configuration (Feng et al., 1999, 2001), especially for operations at relatively low stage cuts. Normally, a permeate flow counter-current to the feed flow is more efficient than the co-current flow. However, considering the pressure build-up of the permeate in the fiber lumen, it is sometimes advantageous to withdraw the permeate from both ends of the hollow fiber bores, which is essentially a combination of the counter-current and co-current flows. As such, the performance of the PEBA/PEI thin film hollow fiber membranes for CO_2/N_2 separation was evaluated for all three flow arrangements, as shown in Figure 8.2 (a)-(c). A feed pressure of 790 kPa was used in the work; it is believed to be uneconomical if the flue gas is to be compressed to a high pressure in practical applications. In addition, after the CO_2 is removed, the nitrogen-enriched residue stream, still at a pressure close to the feed pressure, can also be utilized for various applications such as blanketing, sparging and under-balanced drilling.

Figures 8.3 and 8.4 show respectively the concentrations of CO_2 in the permeate and N_2 in the residue at various stage cuts. As the stage cut increases, the CO_2 concentration in the permeate decreases, while N_2 concentration in the residue increases. Obviously, either a high CO_2 concentration or a high N_2 concentration can be obtained but not both. As the feed gas flows along the hollow fiber, the CO_2 concentration gradually decreases due to its preferential permeation through the fiber wall. At a low stage cut, most of the gas fed to the membrane unit exits the membrane module as the residue stream and only a small portion permeates through membrane as the permeate stream. As a result, the CO_2 concentration on the feed side does not decrease significantly along the hollow fibers at low stage cuts. Because the CO_2 is not significantly depleted, a high concentration of nitrogen in the residue stream is unobtainable. On the other hand, a high driving force for CO_2 permeation is maintained in this case, and therefore a relatively high concentration of CO_2 is obtained in the permeate stream.

The membrane productivity can be measured in terms of the permeate and residue flow rates produced per membrane area. Figure 8.5 and 8.6 show the membrane productivity and the product recovery (CO_2 in the permeate and N_2 in the residue). Here,

the recovery is defined as the fractional quantities of CO_2 (and N_2) in the feed that are ended up in the permeate and the residue streams respectively as the product gases. Obviously, for both CO_2-enriched permeate and nitrogen-enriched residue products, there is a trade-off between the product recovery and the product purity. The permeate flow rate and recovery of CO_2 also existed a trade-off relation. In addition, a high CO_2 concentration in the permeate is accompanied with a high permeate flow rate, while the opposite is true for the nitrogen residue stream. This is understandable because at a high residue flow rate, there is little depletion in CO_2 on the feed side along the flow path through the membrane module, which causes little reduction in the local driving force for CO_2 permeation along the hollow fiber membranes, leading to a high CO_2 permeation rate. In the limit of zero stage cut, both the permeate flow rate and the permeate CO_2 concentration will reach maximum.

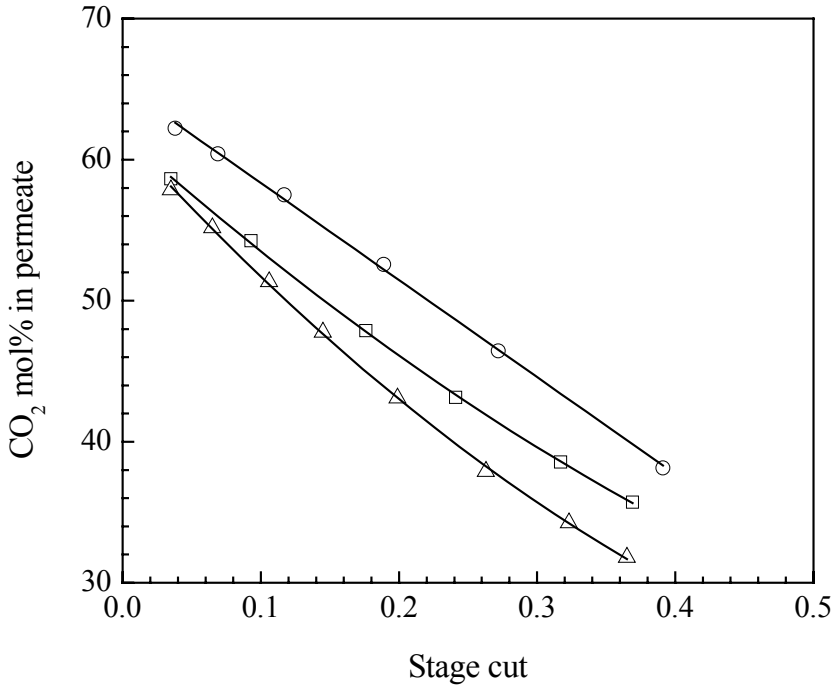

Figure 8.3 Concentration of CO_2 in permeate as a function of stage cut at a feed pressure of 790 kPa and 23°C. Module configurations: (o) counter-current flow; (Δ) co-current flow; (□) combination of counter-current and co-current flows.

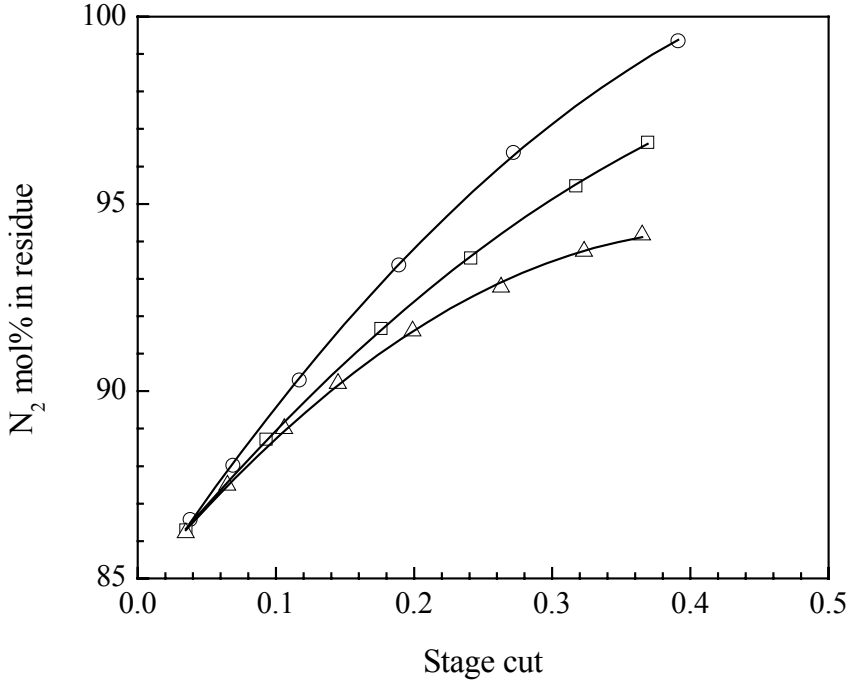

Figure 8.4 Concentration of N_2 in residue as a function of stage cut. Operating conditions and module configurations are the same as those given in Fig. 8.3.

Comparing the above three flow configurations, it can be seen that at a given stage cut, the counter-current flow outperforms the co-current flow in terms of product recovery and purity, and the separation performance lies in between when the permeate is removed from both ends of the hollow fiber bores, for which the flow arrangement is equivalent to a combination of counter- and co-current flows. This is mainly caused by the difference in the driving force for permeation obtainable in the three different flow arrangements. Among the three flow configurations, counter-current flow offers the maximum driving force across the membrane, resulting in the best separation efficiency. Therefore, the counter-current flow is the preferred design in hollow fiber membrane separation processes. The experimental data show that the permeate and residue flow rates are not significantly affected by the flow configurations over the range of stage cuts investigated.

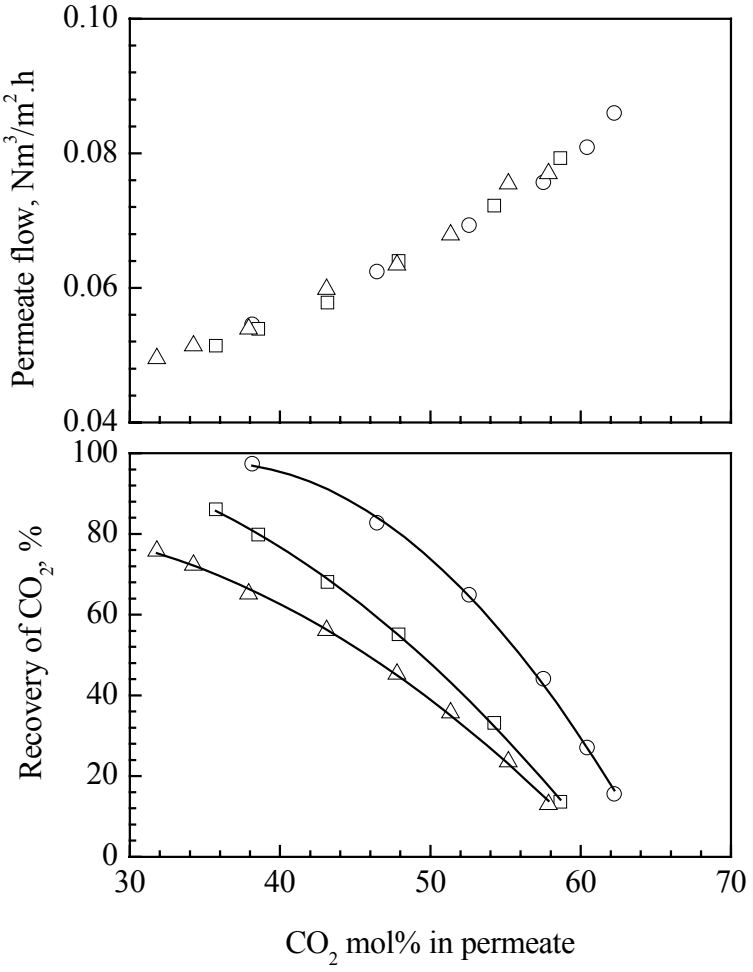

Figure 8.5 Productivity and recovery of CO_2 as a function of CO_2 concentration in permeate. Operating conditions and module configurations are the same as those given in Fig. 8.3.

For the present hollow fiber system, the co-/counter-current flow configuration is shown to be inferior to the counter-current flow. However, in certain cases where the permeate pressure is considerably high, this configuration may be more advantageous. The pressure drop builds up inside the fiber lumen along axial permeate flow for shell side feed operation. For long and narrow fibers with a high permeability, the high permeation rate can result in a significantly high build-up in the permeate pressure, which will decrease the driving force for the permeation through the fiber wall and deteriorate the separation performance. In this case, the withdrawal of the permeate stream from both

ends of the fibers will help reduce the pressure build-up inside the hollow fibers. This advantage is not very obvious in the present work because of the relatively short fibers used. The experimental results show that the separation performance of the co-/counter-current flow is not much better than the co-current flow when the stage cut is sufficiently low, but their difference is more evident at higher stage cuts when the permeate flow rate inside the hollow fiber becomes high.

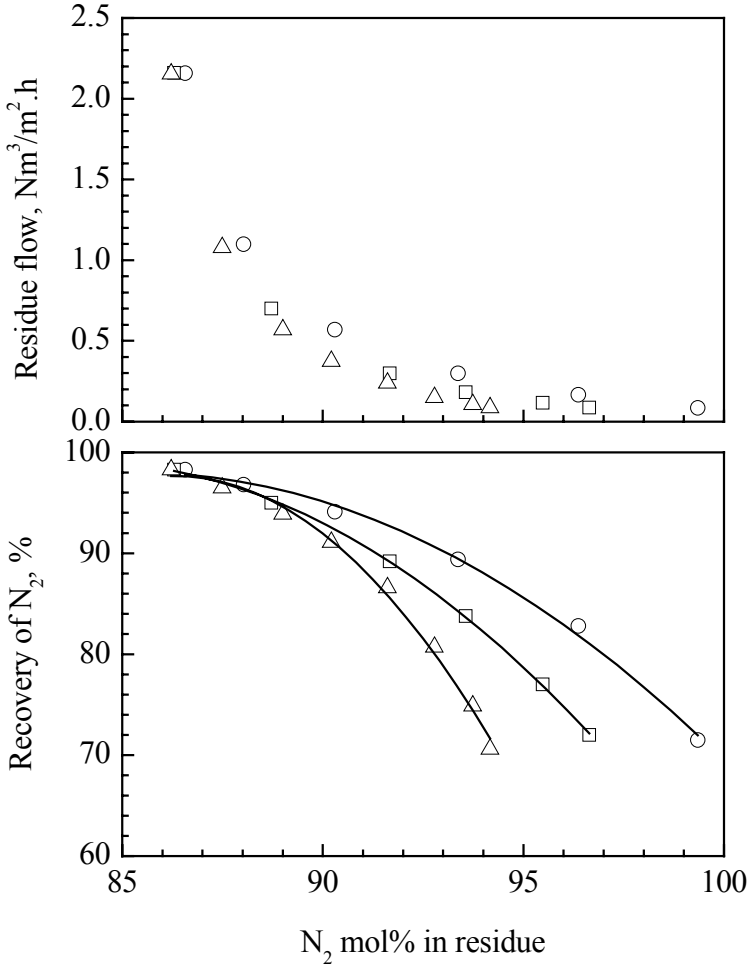

Figure 8.6 Productivity and recovery of N_2 as a function of N_2 concentration in residue. Operating conditions and module configurations are the same as those given in Figure 8.3.

In a single stage separation process, a permeate stream containing 62 mol% CO_2 is obtained using the counter-current flow at a low stage cut of 0.05. This corresponds to

a CO_2 recovery rate of only 20%. Consequently, a multi-stage membrane system will have to be used for effective separation of CO_2 from flue gas in practical application for greenhouse gas emission control. Alternatively, the membrane system can be combined with such conventional processes as amine absorption to form a hybrid process so that the membrane is used only for bulk separation while the amine process is for high purity. On the other hand, a residue stream containing 99.4 mol% can be produced at a stage cut of 0.39, with a nitrogen recovery rate of 72%. The purity of nitrogen stream from the single stage operation is sufficient for numerous applications including blanketing, sparging, and pressure transfer.

8.3.2 Effect of operating pressure

Membrane gas separation is a pressure driven process. For a given product purity and/or recovery, an increase in the operating pressure will increase the processing capacity of the membrane unit. As shown earlier, at a given operating pressure, a change in the stage cut can result in different feed processing rate with different product purity and recovery. In order to evaluate quantitatively the effect of operating pressure on membrane performance, experiments were carried at different feed pressures and feeding rates. Similar to the membrane permeance which is the permeation rate per unit membrane area per unit transmembrane pressure, the membrane processing capacity is expressed by the flow rate (at standard pressure) of feed processed per unit membrane area per unit operating pressure, which is equivalent to the volumetric flow rate of feed (at operating temperature and pressure) per unit membrane area (i.e., feeding rate). Figures 8.7 and 8.8 show the effects of operating pressure on the concentration and recovery of CO_2 and N_2 in the permeate and the residue streams, respectively, at different gas feeding rates.

It is clear that increasing the operating pressure will increase both the concentration and recovery of CO_2 in the permeate, while an increase in the feeding rate tend to increase the permeate CO_2 concentration and decrease the CO_2 recovery. The effect of operating pressure on the permeate CO_2 concentration is more profound at

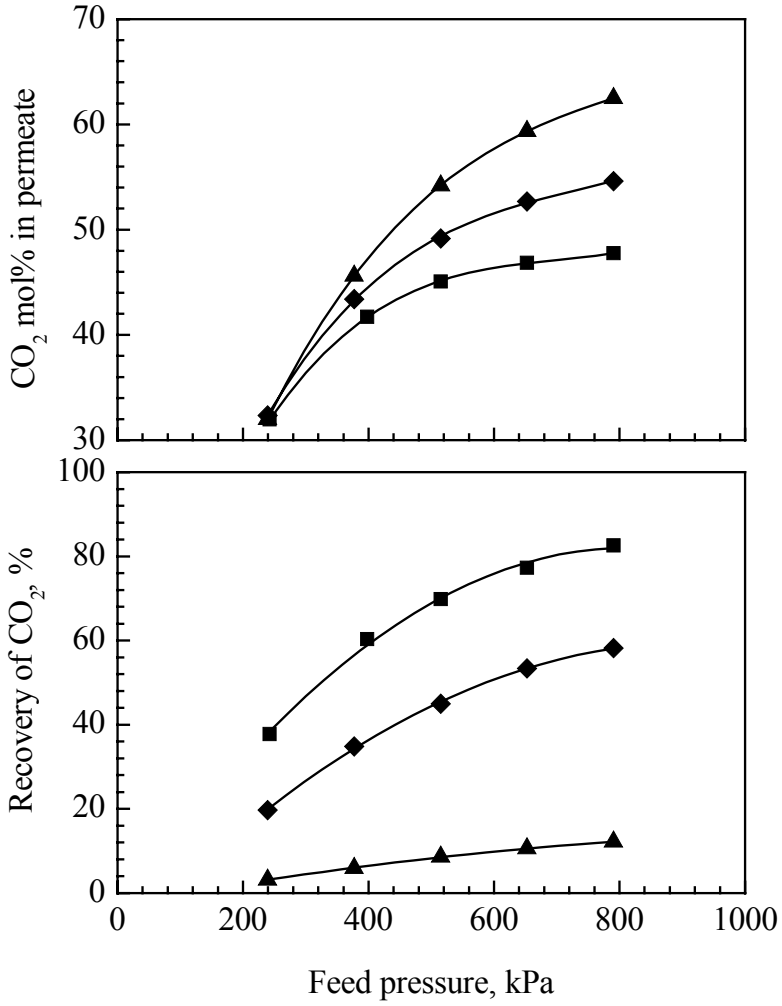

Figure 8.7 Effects of feed pressure on CO_2 concentration and recovery in permeate for counter-current flow at 23°C. Feeding rate ($m^3/m^2.h$): (▲) 0.343; (♦) 0.051; (■) 0.029.

higher feed processing rates. At a feeding rate of 0.029 $m^3/m^2.h$, the permeate CO_2 concentration increased from 32 to 48 mol% when the pressure was increased from 240 to 790 kPa; when the feeding rate is increased to 0.343 $m^3/m^2.h$, the same pressure change resulted in a permeate CO_2 concentration from 32 to 63 mol%. This is understandable considering that the CO_2 concentration decreases along the direction of gas flow on the feed side of the hollow fiber membranes because of the preferential permeation of CO_2 over nitrogen. An increase in the feed pressure and/or a decrease in

the feeding rate will intensify the depletion of CO_2 on the feed side, leading to a higher recovery of CO_2 in the permeate and a higher nitrogen concentration in the residue. On the other hand, as CO_2 is gradually depleted as the feed flows through the hollow fiber module, nitrogen is enriched and the thus the local permeation rate of nitrogen is enhanced, which tends to dilute the CO_2 collected in the permeate side. As a result, lowering the feeding rate will prolong the residence time of the feed in the membrane unit, leading to a decrease in both the permeate CO_2 concentration and the residue nitrogen recovery.

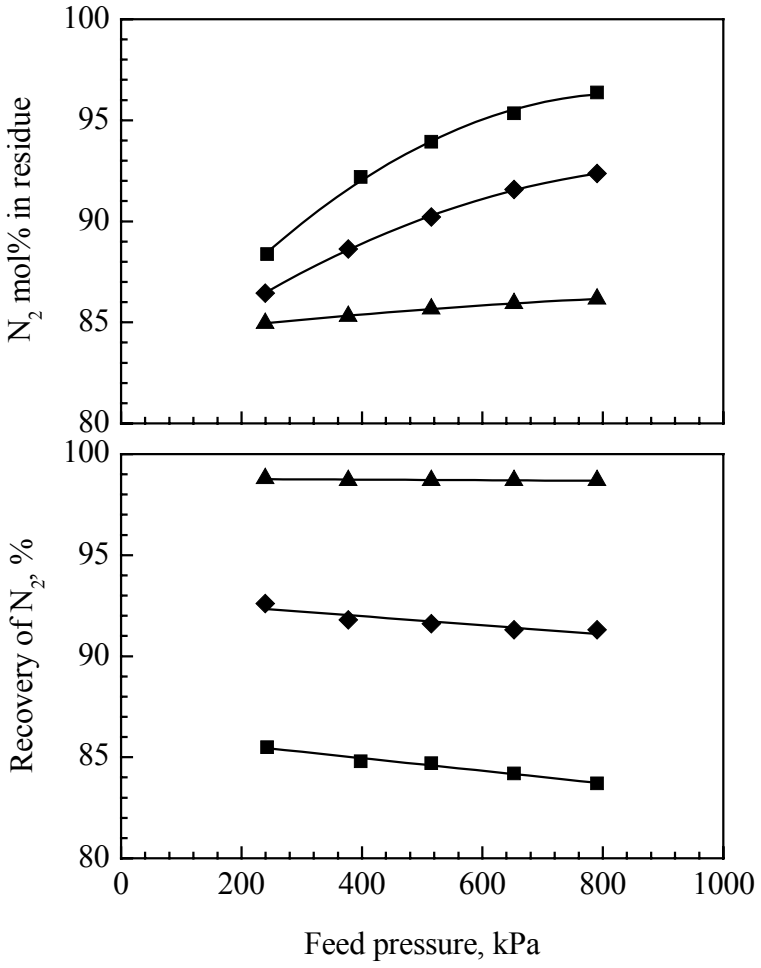

Figure 8.8 Effects of feed pressure on N_2 concentration and recovery in residue for counter-current flow. Operating conditions are the same as those given in Fig.8.7.

It may be mentioned that although a relatively high operating pressure favors the CO_2 separation, the capital and energy costs associated with compression should be taken into account in determining the optimal operating pressure. This is especially the case for flue gas separation because of the low source pressures (generally atmospheric) available.

Compared to most noble gases (e.g., N_2, H_2, O_2), carbon dioxide may plasticize or swell the membrane due to its high sorption capacity in the membrane. As mentioned before, the polyether linkages in PEBA 2533 copolymer have a strong affinity to CO_2 molecules, and the solubility of CO_2 in the membrane is quite high. The membrane plasticization and swelling will increase the membrane permeability. Our previous work in Chapters 3 and 7 showed that the permeability of CO_2 through PEBA 2533 increased with an increase in the feed pressure. It is thus expected that the membrane permselectivity for CO_2/N_2 mixture permeation will be different from that based on pure gas permeation. This is shown in Figure 8.9 where the gas permeance and the CO_2/N_2 permeance ratio for the pure gas and gas mixture permeation are presented; in the gas mixture permeation experiments a very small stage cut (below 0.01) was used so that the variations in the gas composition along the hollow fibers on both sides of the membrane were negligible.

From Figure 8.9 it can be seen that for both pure gas and gas mixture permeation, the permeance of CO_2 increased slightly with an increase in the feed pressure, and the N_2 permeance was relatively constant. At a given feed pressure, the permeance of CO_2 in the gas mixture is about 26% lower than the permeance of pure CO_2. This may be attributed to two factors: i) in the gas mixture permeation, the sorption uptake of CO_2 in the membrane is low because of its low partial pressure, and ii) the presence of nitrogen in the mixture will compete with CO_2 for the sorption sites in the glassy polyamide domain, which also causes a reduction in CO_2 sorption in the membrane. As a result, the membrane will be less plasticized by CO_2 in the gas mixture than pure CO_2 at the same pressure. Similar observations can also be found in CO_2/N_2 mixture permeation through cellulose triacetate membranes (Sada et al.). Generally speaking, when a membrane is plasticized by one component in a mixture, the membrane will be more permeable to other components in the mixture as well. However, the nitrogen permeance data in Figure 8.9 show that nitrogen permeation is not significantly affected by the presence of CO_2,

and the pure nitrogen permeance is almost the same as the permeance of nitrogen in the gas mixture. Consequently, the permeance ratio of CO_2/N_2 for mixture gas permeation is lower than the pure gas permeance ratio. Clearly, the lower selectivity for gas mixture separation is derived from the decreased CO_2 permeance, not the enhanced nitrogen permeation. At a feed pressure of up to 790 kPa, the hollow fiber membranes exhibited a CO_2/N_2 permeance ratio of around 20 for the gas mixture permeation.

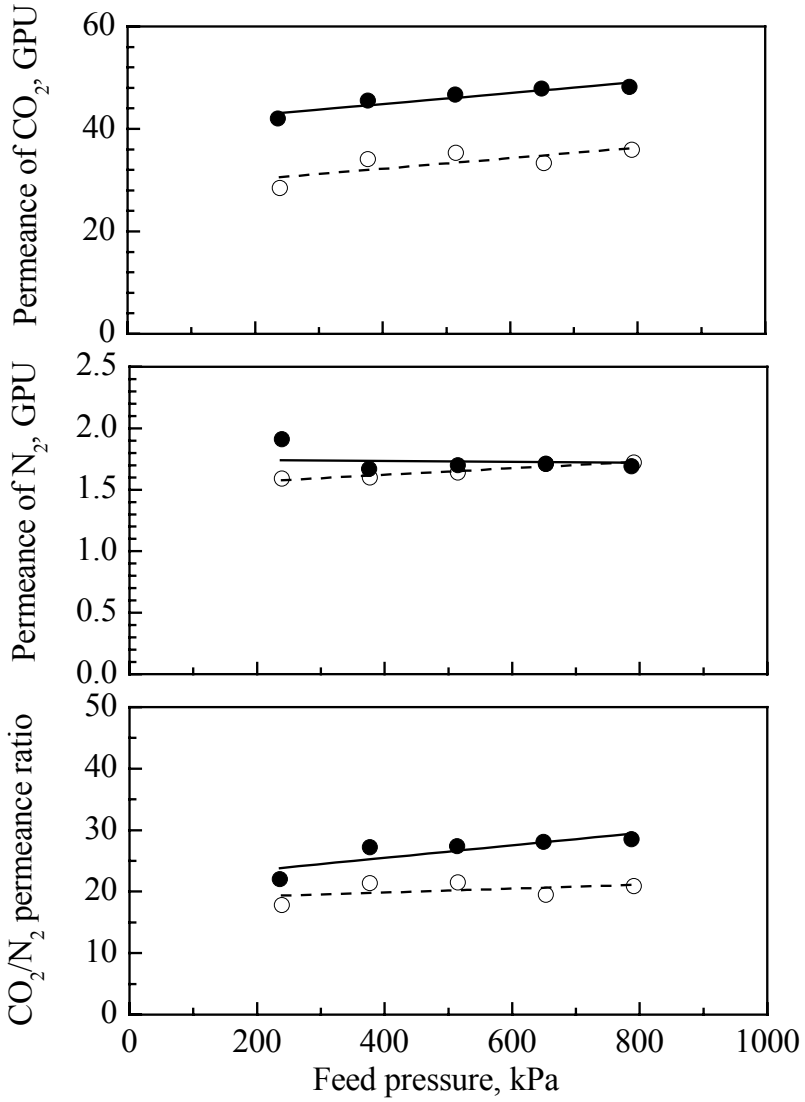

Figure 8.9 Comparison of pure gas and gas mixture permeating through the hollow fiber membranes at 23°C. Solid and dashed lines represent the permeation of pure gas and the gas mixture, respectively.

8.3.3 Effect of operating temperature

Figure 8.10 shows the permeance and the permeance ratio of pure CO_2 and N_2 through the hollow fiber membrane module at different operating temperature. Obviously, the temperature dependence of CO_2 and N_2 permeance follows the Arrhenius type of relation. Like many other gases permeating through non-porous polymeric membranes, as the temperature increased, the permeance of both two gases increased, whereas their permeance ratio decreased. This implies that a high operating temperature may lead to a high productivity, but the product purity will be compromised.

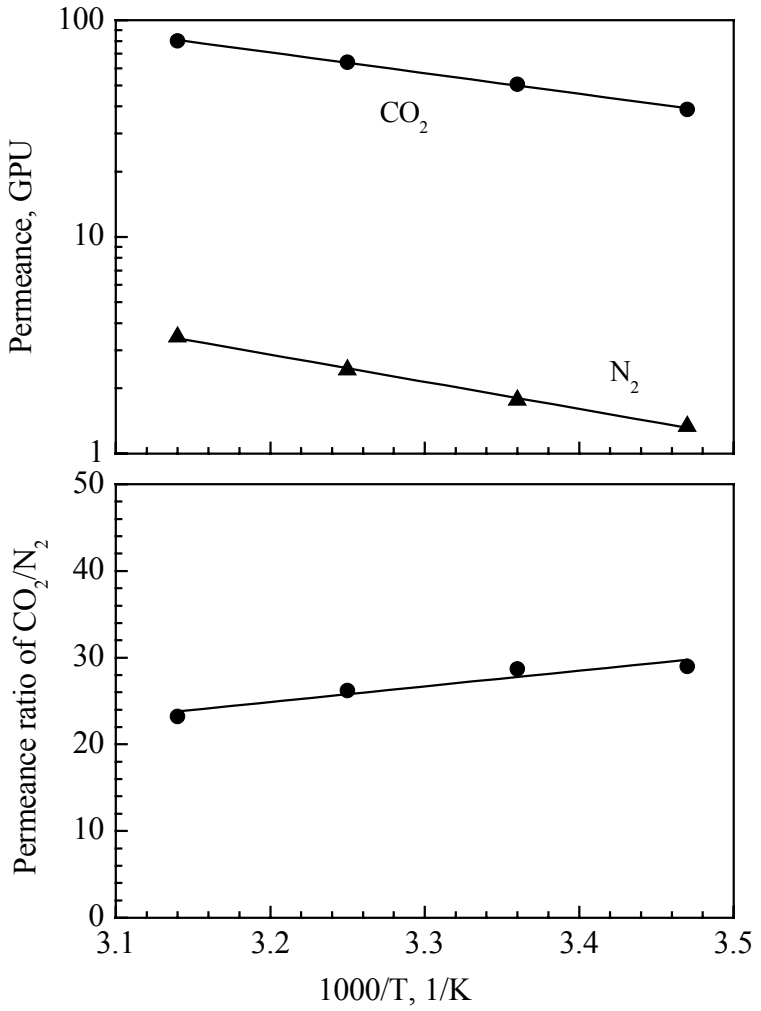

Figure 8.10 Permeance and permeance ratio of pure gases as a function of operating temperature. Feed pressure, 790 kPa.

Figures 8.11-8.13 show the membrane performance for CO_2/N_2 separation at 23 and 45°C. At a given stage cut, both the permeate CO_2 and residue N_2 concentrations obtained at 45°C are lower than what would be obtained at 23°C. At a CO_2 concentration of 50 mol% in the permeate stream, increasing the operating temperature from 23 to 45°C will double the CO_2 productivity. This is, however, accompanied by a loss of up to 28% in the CO_2 recovery rate. In addition, at a lower stage cut, the operating temperature tends to have a more significant effect on the CO_2 concentration and the recovery and production

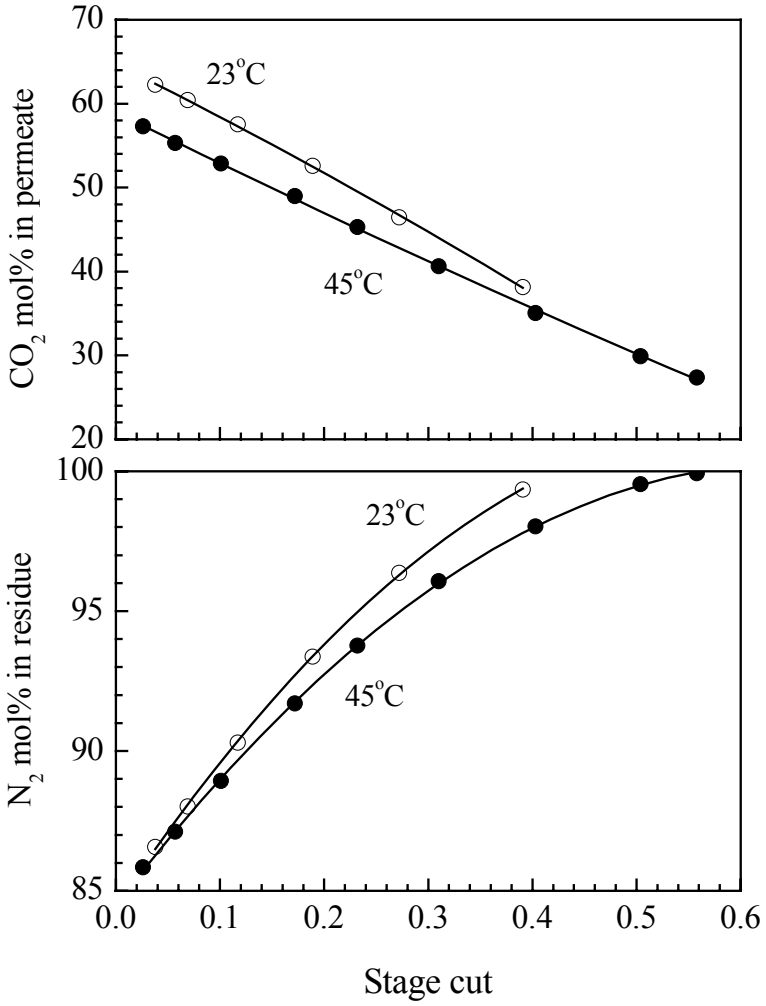

Figure 8.11 CO_2 concentration in permeate and N_2 concentration in residue at different temperatures. Feed pressure 790 kPa.

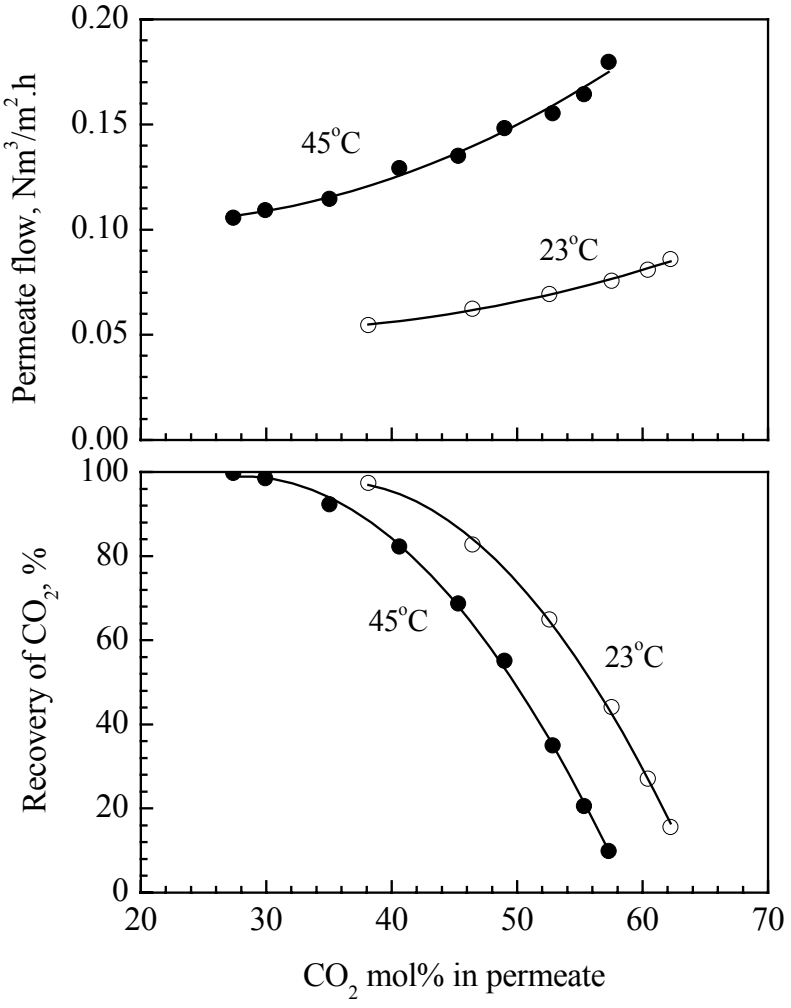

Figure 8.12 Effects of temperature on CO_2 recovery and productivity. Feed pressure 790 kPa.

rates of CO_2 in the permeate stream. On the residue side, when the N_2 product concentration is over 90 mol%, increasing the operating temperature will decrease the N_2 concentration and recovery, and the residue flow rate is only slightly increased. Therefore, in practical application the overall separation performance (i.e. product purity, recovery and production rate) should be considered to determine the most suitable operating temperature.

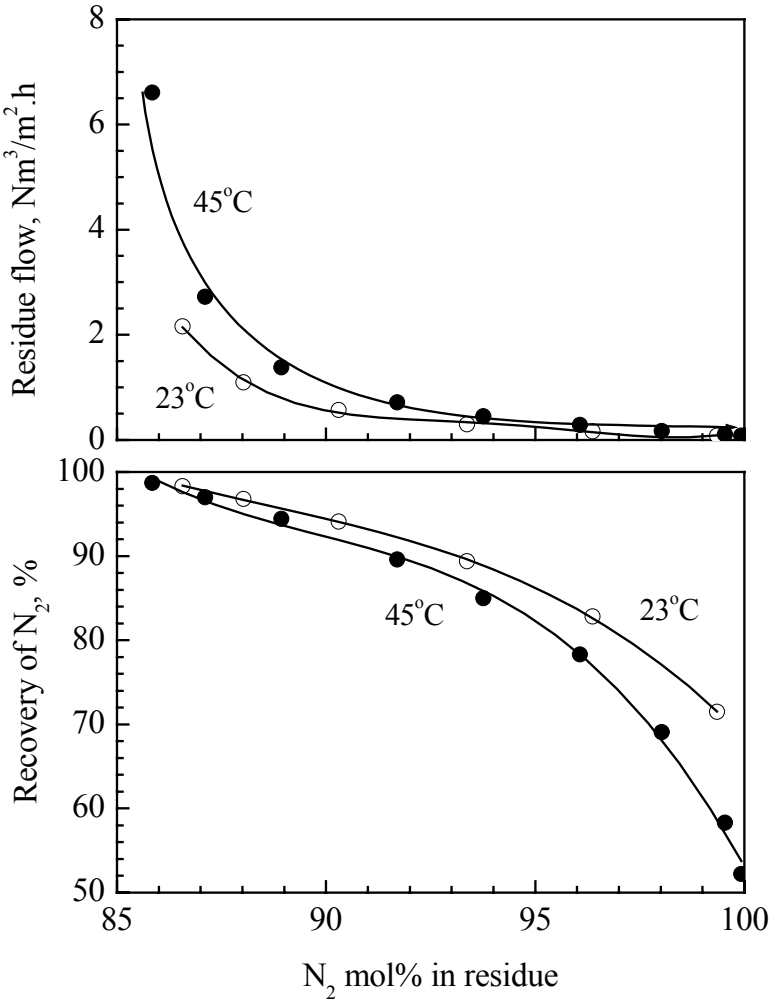

Figure 8.13 Effects of temperature on N_2 recovery and productivity. Feed pressure 790 kPa.

8.3.4 Bore side feed vs shell side feed

The feed gas can be fed to either the shell side or the bore side a hollow fiber membrane module. While the module design is generally simpler for shell side feed than the bore side feed, the bore side feed is more advantageous under certain circumstances. In general, the hollow fiber membranes used in industrial scale applications are relatively long (1 - 3m). For high stage cut applications, the pressure build-up in the fiber lumen can be substantial when a shell side feed configuration is used. An excessive permeate pressure build-up will deteriorate the separation performance of the membrane because of

the decreased driving force, as discussed earlier. This problem can be overcome by using the bore side feed operation since generally there is more space for gas flow in the shell side of the membrane module than in the lumen side. In addition, the potential problems associated with flow channelling and maldistribution of the feed flow are eliminated in the bore side feed operation. Figures 8.14 and 8.15 show the separation performance of counter-current flow with both bore side feed [schematically shown in Fig. 8.2 (d)] and shell sides feed.

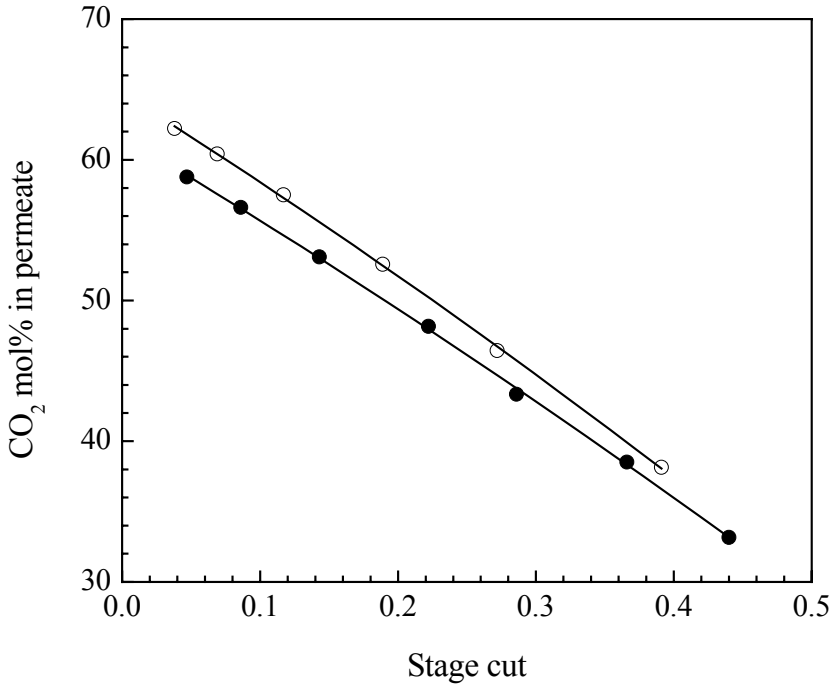

Figure 8.14 CO_2 concentration in permeate as a function of stage cut with bore side feed (●) and shell side feed (o). Temperature 23°C, feed pressure 790 kPa.

It can be seen that unlike the integrally asymmetric cellulose acetate-based hollow fiber membranes reported in the literature (Feng et al., 1999, 2000) the separation performance of bore side feed is not superior to the shell side feed for the PEBA/PEI thin film composite hollow fiber membranes. At a given CO_2 concentration in the permeate, the permeate flow rate with bore side feed is higher than the permeate flow obtained with shell side feed, whereas the opposite is true for the CO_2 recovery rate. These results can

be explained from the standpoints of membrane structure and potential concentration polarization. For bore side feed, the fiber lumen is pressurized, and the selective coating layer, which is on the outer surface of the hollow fiber, is no longer supported mechanically by the PEI substrate. As such, the membrane integrity may be affected by the internal pressure applied in the fiber bores. To verify this, experiments were carried out to test the membrane permselectivity with pure gases and the results are shown in Figure 8.16.

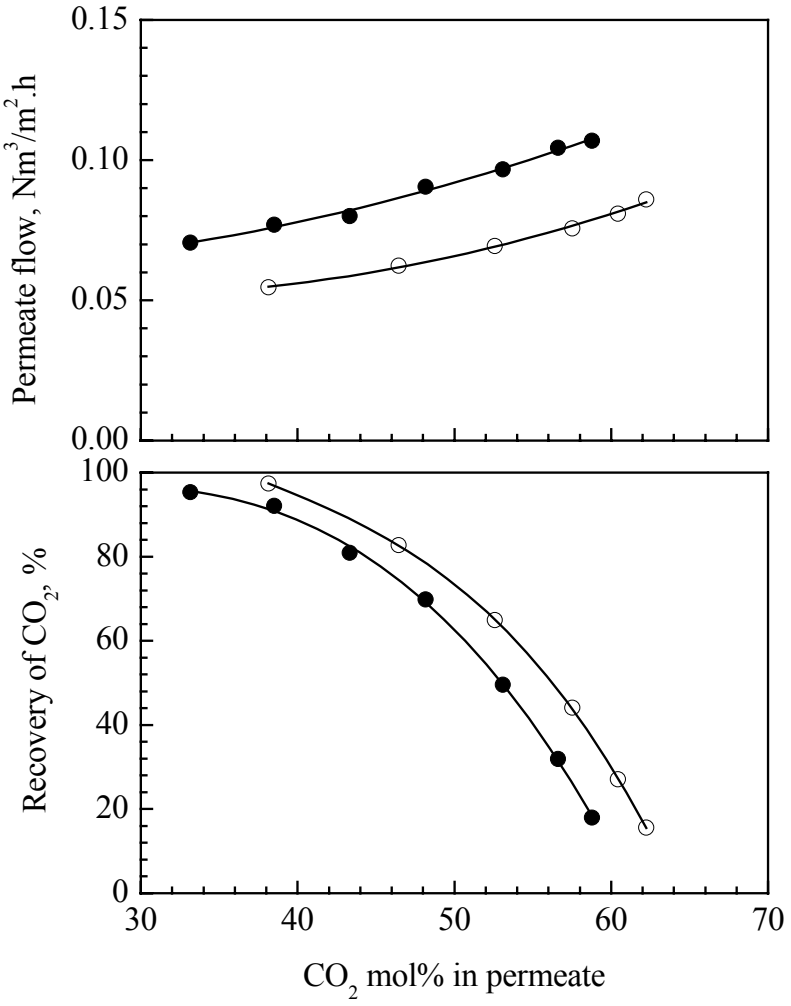

Figure 8.15 Permeate productivity and CO_2 recovery as a function of CO_2 concentration by bore feed (●) and shell side feed (o). Temperature 23°C, feed pressure 790 kPa.

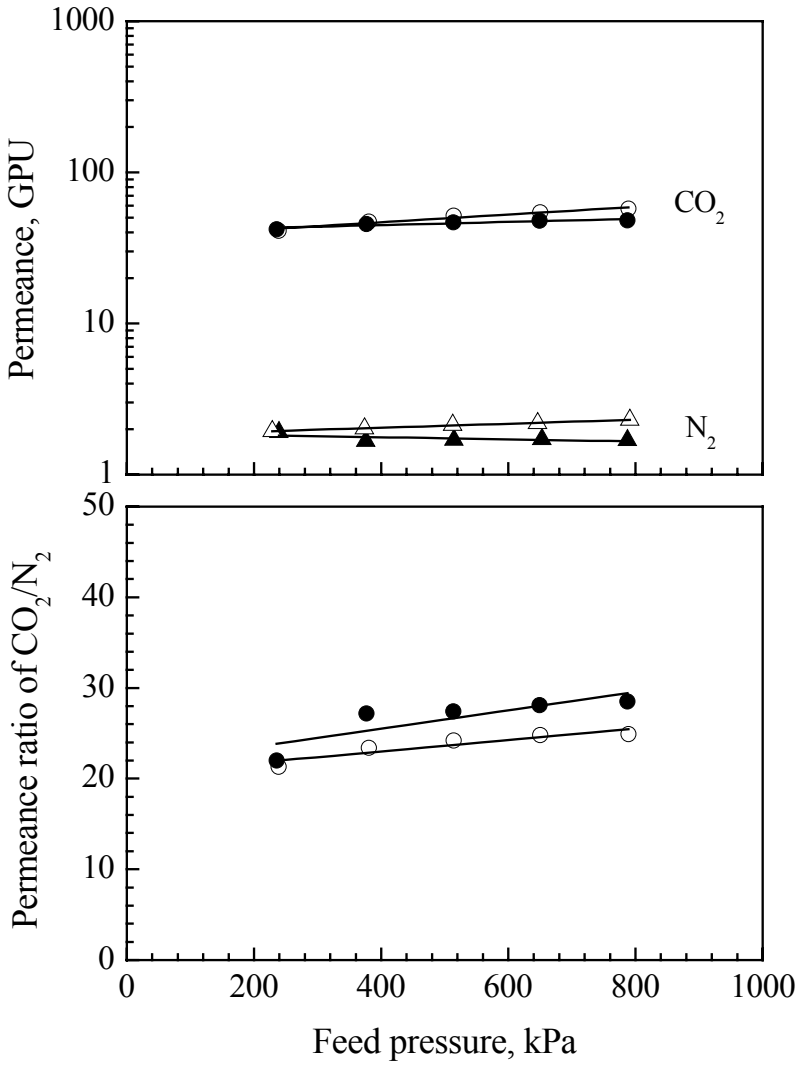

Figure 8.16 Pure gas permeance and permeance ratio for shell side feed (solid symbols) and bore side feed (open symbols). Temperature 23°C.

It is shown that the permeance of both CO_2 and N_2 with bore side feed is higher than the permeance with shell side feed, but the CO_2/N_2 peremance ratio for bore side feed is lower. It should be pointed out that the experiments were performed with shell side feed first, followed by bore side feed. After the bore side feed tests, the membrane permeance was measured again under shell side feed, and the membrane permeance was found to be larger than that obtained in the first round of shell side feed tests. This means the bore side pressurization has caused an irreversible change in the structure of the

composite membrane. On the other hand, during gas mixture permeation with bore side feed, the concentration polarization may occur in the microporous substrate due to the retention of the slow permeating nitrogen component. The concentration polarization has shown to be an issue in bore side feed operation of integrally asymmetric hollow fiber membranes for air separation (Feng at al., 1999). It is clear that the bore side feeding does not seem to be suitable for the thin film composite hollow fiber membranes used in the present study.

8.4 Summary

The separation of carbon dioxide from nitrogen using PEBA 2355/PEI thin film composite hollow fiber membranes was investigated, and the membrane performance was evaluated using a simulated flue gas containing 15.3 mol % CO_2 (balance N_2). The membrane module was tested with various flow configurations, and it was shown that shell side feed with counter-current flow yielded the best separation performance at different stage cuts in terms of product purity, recovery, and productivity. At 23 °C and 790 kPa, a permeate stream containing 62 mol % CO_2 is obtained at a CO_2 recovery of 20% in a single-stage operation, whereas over 99.4 mol % nitrogen can be produced in the residue with a nitrogen recovery of 72%. The effects of operating pressure and temperature on the performance of the hollow fiber membranes for CO_2/N_2 separation were investigated. The permeance of CO_2 in the gas mixture was lower than the permeance of pure CO_2, while there was little difference in nitrogen permeance between pure gas permeation and gas mixture permeation. Increasing the operating temperature increased the feed processing capacity, but both the product purity and the recovery were decreased. The PEBA/PEI thin film hollow fiber composite membrane was not suitable for bore side feed operation because of the potential problems associated with the concentration polarization in the microporous substrate and the structural integrity of the membrane when a high pressure was applied in the fiber lumen.

CHAPTER 9
General Conclusions, Original Contributions and Recommendations

9.1 General conclusions and contributions

Ultra thin flat PEBA membranes and PEBA hollow fiber composite membranes were developed in this work to achieve a high permeation rate, which is crucial for practical applications. Transport mechanism and permeation behavior of gases and vapors (especially condensable gases and vapors, e.g., light olefins and paraffin, CO_2, and VOCs) in the membranes were investigated. The potential applications of the PEBA membranes related to environment and energy, including the recovery of light olefins from N_2, VOCs separation, and CO_2 separation from flue gas, were explored. The following is the conclusion drawn from this research and the contribution to original research:

1. A new method of preparing ultra thin poly(ether block amide) (PEBA) 2533 membranes was developed based on spontaneous spreading of a copolymer solution on a water surface. Solvent exchange with water induces polymer precipitation during the solution spreading, thereby forming a thin membrane floating on the water surface. The spreading process is accompanied by evaporation of the solvent, but the solvent-nonsolvent exchange is primarily responsible for the membrane formation. The formation of a uniform and defect-free membrane was found to be determined by the solvent system (thermodynamic properties of the solvents and the composition in case of mixed solvent), polymer concentration in the casting solution and temperature.

2. Propylene separation from nitrogen using PEBA/polysulfone thin film composite membranes was studied. The propylene permeance was affected by the presence of nitrogen, and vice versa, due to interactions between the permeating components. Semi-empirical correlations were developed to relate membrane permeance to the pressures and compositions of the gas on both sides of the membrane, and the membrane separation performance at different operating conditions was analyzed in terms of product purity, recovery and productivity based on a cross flow model.
3. To further understand the transport of gases in the membranes, sorption, diffusion, and permeation of three olefins (i.e., C_2H_4, C_3H_6 and C_4H_8) in homogenous PEBA membranes at different temperatures and pressures were investigated to elucidate the relative contributions of solubility and diffusivity to the preferential permeation of olefins. It was revealed that the favorable olefin/nitrogen permselectivity was primarily attributed to the solubility selectivity, whereas the diffusivity selectivity could affect the permselectivity negatively or positively, depending on the temperature and pressure. The limiting solubility at infinite dilution could be correlated with the reduced temperature of the penetrant, and the limiting diffusivity at zero pressure was related to temperature by an Arrhenius type of equation.
4. PEBA/PSf composite membranes showed good performance for the separation of a series of VOCs/N_2 binary and multi- gas mixtures in spite of the strong interactions among the permeating VOC components. The VOC concentration in the permeate can exceed 90 mol% when the feed VOC concentration is 5 mol% or higher. The permeance of VOCs and the selectivity of VOCs/N_2 increase with an increase in the VOC feed concentration, and the permeance of N_2 was affected by the existence of VOCs. A simple cross flow model was used to evaluate the separation performance, and the model was verified with experimental data.
5. Hollow fiber composite membranes comprising of a thin PEBA layer supported on a microporous polysulfone substrate was prepared by a dip-coating technique. The effects of parameters involved in the procedure of polysulfone hollow fiber spinning and PEBA coating on the permselectivity of the resulting composite

membranes were investigated. CO_2 permeance of 61 GPU and CO_2/N_2 permeance ratio of 30 were obtained on the composite membranes. The selectivity of the composite membrane is very close to the intrinsic selectivity of PEBA membrane, implying that the composite membrane is defect-free.

6. The separation of CO_2 from N_2 by a lab scale PEBA hollow fiber composite membrane module was investigated using a stimulated flue gas containing 15.3 mol% CO_2. It was shown that shell side feed with counter-current flow yielded the best separation performance at different stage cuts in terms of product purity, recovery and productivity. The effects of operating pressure and temperature on the performance of the hollow fiber membranes were studied. The permeance of CO_2 in a gas mixture was lower than the permeance of pure CO_2 at the same partial pressure, while there was little difference in N_2 permeance between pure gas and gas mixture permeation.

9.2 Recommendations for future work

1. Improvement of composite membrane permeance

- **Reducing thickness of PEBA layer**

Although PEBA composite membranes were developed in this study, the membrane structure was not optimized. Reducing the thickness of the selective PEBA layer can increase the membrane permeance, but it becomes likely to cause defects on the membrane surface. The integrity of the composite membrane is affected by the morphology of the substrate, such as surface roughness, pore size and pore size distribution. Therefore, the improvement of the membrane permeance depends on the optimization of both the thickness of the selective PEBA layer and the structure of the substrate.

- **Decreasing substrate resistance**

PEBA membranes exhibit good permselectivity for VOCs/N_2 separation. However, the substrate of the composite membranes may have a relatively high resistance to the permeation of VOCs due to their high permeation rates, which will compromise the intrinsic permeability and selectivity of the PEBA material. The membrane performance can be improved by optimizing the structure of the substrate to

reduce the resistance of VOCs permeation. Choosing a porous membrane with higher porosity and larger pore size may achieve higher permeance and selectivity. However, the mechanical strength for both the substrate and the PEBA selective layer should be considered as well.

2. Separation in real-life streams

The PEBA composite membranes were used for propylene/N_2, VOCs/N_2 and CO_2/N_2 separations. Most studies were carried out at low stage cuts to keep a relatively constant concentration along the feed side of the membrane. It is recommended that the separations under various stage cuts are investigated to evaluate the product purity, recovery and productivity of the separation process from an engineering standpoint.

3. Fabrication technique of PEBA ultra thin membranes

For practical applications of the PEBA composite membranes, it is recommended to develop techniques for continuous fabrication of ultra thin membranes (i.e., spreading polymer solution on water surface to form ultra thin membranes and laminating them on porous substrates).

APPENDIX: Estimation of Experimental Errors

— Sample calculation

The permeance J of pure propylene through the membrane can be calculated by

$$J = \frac{V}{t.A.\Delta p}$$

where V is the volume of the gas permeation, t the time of permeation, A effective membrane area, and Δp the pressure difference across the membrane. The experimental results are:

$V = 24 \pm 0.1\,\mathrm{cm}^3$

$A = 13.9 \pm 0.1\,\mathrm{cm}^2$

$\Delta p = 414 \pm 2\,\mathrm{kPa}$

t = 23.35s, 23.60s, and 23.90s for three measurements. The average t is 23.62s, so

$t = 23.62 \pm 0.19\,\mathrm{s}$

ΔJ, ΔV, Δt, ΔA, and $\Delta(\Delta p)$ were used to represent the absolute uncertainties of J, V, t, A, and Δp, respectively. The error of J (relative uncertainty) can be derived by

$$\frac{\Delta J}{J} = \frac{\Delta V}{V} + \frac{\Delta t}{t} + \frac{\Delta A}{A} + \frac{\Delta(\Delta p)}{\Delta p} = \frac{0.1cm^3}{24cm^3} + \frac{0.19s}{23.62s} + \frac{0.1cm^2}{13.9cm^2} + \frac{2}{414}$$

$$= 0.42\% + 0.80\% + 0.72\% + 0.48\% = 2.42\%$$

Propagation of Errors

Suppose that we measure two quantities x and y, with estimated absolute uncertainties Δx and Δy. If z is a quantity calculated from x and y, we have the following rules of thumb:

If $z = x + y$, then $\Delta z = \Delta x + \Delta y$ (the absolute errors add)

If $z = x - y$, then $\Delta z = \Delta x + \Delta y$ (the absolute errors still add)

If $z = xy$, then $\Delta z/z = \Delta x/x + \Delta y/y$ (the relative errors add)

If $z = x/y$, then $\Delta z/z = \Delta x/x + \Delta y/y$ (the relative errors still add)

If $z = x^n$, then $\Delta z/z = n\, \Delta x/x$ (the relative error is multiplied by n)

If $z = \sqrt[m]{x}$, then $\Delta z/z = \dfrac{\Delta x / x}{m}$ (the relative error is divided by m)

The first four rules generalize in an obvious way for more than two quantities.

The other experimental errors in the thesis (e.g., permeance in gas mixture separation, permeability, solubility, and diffusivity) can be estimated by the similar method.

Bibliography

Adamson, A.W., and A.P. Gast, *Physical Chemistry of Surfaces*, 6th ed., Wiley, New York (1997).

Baker, R.W., *Membrane Technology and Applications*, 2nd ed., MaGraw-Hill, New York (2004).

Baker, R.W., "Future directions of membrane gas separation technology", *Ind. Eng. Chem. Res.*, **41**, 1393-1411 (2002).

Baker, R.W., and M. Jacobs, "Improved monomer recovery from polyolefin resin degassing", *Hydrocarbon Processing*, **75**, 49-51 (1996).

Baker, R.W., J.G. Wijmans, and J.H. Kaschemekat, "The design of membrane vapor gas separation systems", *J. Membr. Sci.*, **159**, 55-62 (1998).

Barbi, V., S.S. Funari, R. Gehrke, N. Scharnagl, and N. Stribeck, "SAXS and the gas transport in polyether-block-polyamide copolymer membranes", *Macromolecules*, **36**, 749-758 (2003).

Barrer, R.M., "Permeation, diffusion and solution of gases in organic polymer", *Trans. Faraday Soc.*, **35**, 628-643 (1939).

Barrer, R.M., and D.W. Brook, "Molecular diffusion in chabazite, mordenite and levynite", *Trans. Faraday Soc.*, **49**, 1049-1059 (1953).

Baudot, A., I. Souchon, and M. Marin, "Total permeate pressure influence on the selectivity of the pervaporation of aroma compounds", *J. Membr. Sci.*, **158**, 167-185 (1999).

Beuscher, U., and C.H. Gooding, "Characterization of the porous support layer of composite gas permeation memrbanes", *J. Membr. Sci.*, **132**, 213-227 (1997).

Beuscher, U., and C.H. Gooding, "The influence of the porous support layer of composite membranes on the separation of binary gas mixtures", *J. Membr. Sci.*, **152**, 99-116 (1999).

Billmeyer, F.W., *Textbook of Polymer Science*, 2nd ed., Wiley, New York (1971).

Bhanddarkar, M, A.B. Shelehim, A.G. Dixon, and Y.H. Ma, "Adsorption, permeation, and diffusion of gases in microporous membranes. I. Adsorption of gases on microporous glass membranes", *J. Membr. Sci.*, **75**, 221-231 (1992).

Blume, I., and I. Pinnau, "Composite membrane, method of preparation and use", *US Patent* 4,963,165 (1990).

Bo, I.D., H.V. Langenhove, and J.D. Keijser, "Application of vapor phase calibration method for determination of sorption of gases and VOC in polydimethylsiloxane membranes", *J. Membr. Sci.*, **209**, 39–52 (2002).

Boddeker, K.W., H. Pingel, and K. Dede, " Continuous pervaporation of aqueous phenol on a pilot plant scale", *Proceedings of the 6th International conference on Pervaporation Processes in the Chemical Industry*, Ottawa, Canada, 514-519 (1992).

Bondar, V.I, B.D. Freeman, and I. Pinnau, "Gas sorption and characterization of poly(ether-b-amide) segmented block copolymers", *J. Polym. Sci.: Polym. Phys.*, **37**, 2463-2475 (1999a).

Bondar, V.I, B.D. Freeman, and I. Pinnau, "Gas transport properties of poly(ether-b-amide) segmented block copolymers", *J. Polym. Sci.: Polym. Phys.*, **38**, 2051-2062 (2000).

Bondar, V.I., B.D. Freeman, and Y.P. Yampolskii, "Sorption of gases and vapors in an amorphous glassy perfluorodioxole copolymer", *Macromol.*, **32**, 6163-6171 (1999b).

Bos, A., I.G.M. Punt, M. Wessling, and H. Strathmann, "CO_2 -induced plasticization phenomena in glassy polymer", *J. Membr. Sci.*, **155**, 67-78 (1999).

Breck, D.W., *Zeolite Molecular Sieves*, Wiley, New York (1974).

Burgess, T.L., A.G. Gibson, S.J. Furstein, and I.E. Wachs, "Converting waste gases from pulp mills into value-added chemicals", *Environmental Progress*, **21,** 137-141 (2002).

Cabasso, I., and K.A. Lundy, "Method of making membranes for gas separation and the composite membranes", *US Patent* 4,602,922 (1986).

Cen, Y., C. Staudt-Bickel, and R.N. Lichtenthaler, "Sorption properties of organic solvents in PEBA membranes", *J. Membr. Sci.*, **206,** 341-349 (2002).

Chen, J.C., X. Feng, and A. Penlidis, "Gas permeation through poly(ether-b-amide) (PEBAX 2533) block copolymer membranes", *Sep. Sci. Tech.*, **39**, 149-164 (2004).

Chung, T.S., J.J Shieh, W.W.Y. Lan, M.P. Srinivasan, and D.R. Pad, "Fabrication of multi-layer composite hollow fibers for gas separation", *J. Membr. Sci.*, **152**, 211-215 (1999).

Clausi, D.T., S.A. McKelvey, and W. J. Koros, "Charaterization of substructure resistance in asymmetric gas separation membranes", *J. Membr. Sci.*, **160**, 51-64 (1999).

Crank, J., *The Mathematic of Diffusion*, 2nd ed., Oxford, Clarendon (1975).

Crank, J., and G.S. Park, *Diffusion in polymers*, Academic Press, London (1968).

David R. Lide, ed., *CRC Handbook of Chemistry and Physics, Internet Version 2007, (87th Edition), <http:/www.hbcpnetbase.com>,* Taylor and Francis, Boca Raton, FL, (2007).

Dean, J.A. (ed.), *Lange´s Handbook of Chemistry*, 15th ed., McGraw-Hill, New York (1999).

Deng, S., A. Tremblay, and T. Matsuura, "Preparation of hollow fibers for the removal of volatile organic compounds from air", *J. Appl. Polym. Sci.,* **69**, 371-379 (1998).

Deng, S., A. Sourirajan, T. Matsuura, and B. Farnand, "Study of volatile hydrocarbon emission control by an aromatic poly(ether imide) membrane", *Ind. Eng. Chem. Res.*, **34**, 4494-4500 (1995).

Djebbar, M.K., Q.T. Nguyen, R. Clement, and Y. Germain, "Pervaporation of aqueous ester solutions through hydrophobic poly(ether-block-amide) copolymer membranes", *J. Membr. Sci.*, **146**, 125-133 (1998).

Elf Atochem, *PEBAX® — Basis of Performance, Polyether Block Amide*, Elf Atochem Technical Document.

Enneking, L., A. Heintz, and R.N. Lichtenthaler, "Sorption equilibria of the tenary mixture benzene/cyclohexane/cycloheaxane in polyurethane- and PEBA-membrane polymers", *J. Membr. Sci.*, **115,** 161-170 (1996).

Erb, A.J., and D.R. Paul, "Gas sorption and transport in polysulfone", *J. Membr. Sci.*, **8**, 11-22 (1981).

Ettouney, H.M., H.T. El-Dessouky, and W.A. Waar, "Separation characteristics of ternary gas mixtures in serial cells of polysulfone hollow fiber membranes", *Chem. Eng. Res. Des.*, **77**, 395-404 (1999).

Favre, E, "Temperature polarization in pervaporation", *Desalination*, **154**, 129-138 (2003).

Feng, X., *Study on pervaporation membranes and pervaporation processes*, PhD thesis, University of Waterloo, Waterloo, Ontario (1994).

Feng, X., and R.Y.M. Huang, "Liquid separation by pervaporation: a review", *Ind. Eng. Chem. Res.*, **36**, 1048-1066 (1997).

Feng, X., and J. Ivory, "Hollow fiber membrane device including a split disk tube sheet support", *US Patent* 6,224,763 (2001).

Feng, X., and J. Ivory, "Development of hollow fiber membrane systems for nitrogen generation from combustion exhaust gas. Part I. Effect of module configurations", *J. Membr. Sci.*, **176**, 197-207 (2000).

Feng, X., J. Ivory, and V.S.V. Rajan, "Air separation by integrally asymmetric hollow-fiber membranes", *AIChE J.*, **45**, 2142-2152 (1999).

Feng, X., G. Jiang, and B. Zhu, "Effects of structure parameter and coating layer permeability of asymmetric composite membrane on the gas permeability", *Membr. Sci. Tech.*, **9**, 7-13 (1989).

Feng, X., P. Shao, R.Y.M. Huang, G. Jiang, and R. Xu, "A study of silicone rubber/polysulfone composite membranes: correlating H_2/N_2 and O_2/N_2 permselectivites", *Sep. Puri. Tech.*, **27**, 211-223 (2002).

Feng, X., S. Sourirajan, H. Tezel, and T. Matsuura, "Separation of organic vapor from air by aromatic polyimide membranes", *J. Appl. Poly. Sci.,* **43**, 1071-1079 (1991).

Feng, X., S. Sourirajan, F.H. Tezel, T. Matsuura, and B.A. Farnand, "Separation of volatile organic compound/nitrogen mixtures by polymeric membranes", *Ind. Eng. Chem. Res.*, **32**, 533-539 (1993).

Fleming, G.K., and W.J. Koros, "Dilation of polymers by sorption of carbon dioxide at elevated pressure: I. Silicone rubber and unconditioned polycarbonate", *Macromol*, **19**, 2285-2291 (1986).

Flory, P.J., "Statistical mechanics of swelling of network structures", *J. Chem. Phys.*, **18**, 108-111 (1950).

Flory, P.J., *Principles of Polymer Chemistry*, Ithaca, Cornell University, NY (1969).

Fouda, A., Y. Chen, J. Bai, and T. Matsuura, "Wheatstone bridge model for the laminated poly-dimethylsiloxane/polyethersulfone membrane for gas separation, *J. Membr. Sci.*, **64**, 263-271 (1991).

Fiess, K., M. Sipek, V. Hynek, P. Sysel, K. Bohata, and P. Izak, "Comparison of permeability coefficients of organic vapors through non-porous polymer membranes by two different experimental techniques", *J. Membr. Sci.*, **240**, 179-185 (2004).

Figoli, A., W.F.C. Sager, and M.H.V. Mulder, " Facilitated oxygen transport in liquid membranes: Review and new concepts", *J. Membr. Sci.*, **181**, 97-110 (2001).

Freeman, B., and I. Pinnau, "Separation of gases using solubility-selective polymers", *Trends in Polymer Science*, **5**, 167-173 (1997).

Gaines, G.L.J., "Monolayers of dimethylsiloxane-containing block copolymers", in: R.F. Gould (ed.), *Monolayers*, American Chemical Society, Washington, DC, 338–346, (1975).

Gales, L., A. Mendes, and C. Costa, "Removal of acetone, ethyl acetate and ethanol vapors from air using a hollow fiber PDMS membrane module", *J. Membr. Sci.*, **197**, 211-222 (2002).

Groβ, A., and A. Heintz, "Sorption isotherms of aromatic compounds in organophilic polymer membranes used in pervaporation", *J. Solution Chem.*, **28**, 1159-1174 (1999).

Groβ, A., and A. Heintz, "Diffusion coefficients of aromatic in nonporous PEBA membranes", *J. Membr. Sci.*, **168**, 233-242 (2000).

Gilliland, E.R., R.F. Baddour, and J.L. Russel, "Rates of flow through microporous solids", *AIChE J*., 4, 90-96 (1958).

Greenlaw, F.W., R.A. Shelden, and E.V. Thompson, "Dependence of diffusive permeation rates on upstream and downstream pressures. II. Two component permeant", *J. Membr. Sci.*, **2**, 333-348 (1977).

Hatfield, G.R., Y. Guo, W.E. Killinger, R.A. Andrejak, and P.M. Roubicek, "Characterization of structure and morphology in two poly(ether-block-amide) copolymers", *Macromolecules*, **26**, 6350-6353 (1993).

Henis, J.M.S., and M.K. Tripodi, "A novel approach to gas separation using composite hollow fiber membranes", *Sep. Sci.* Tech., **12**, 1059- 1068 (1980).

Henis, J.M.S., and M.K. Tripodi, "Composite hollow fiber membranes for gas separation: the resistance model", *J. Membr. Sci.*, **8**, 233-246 (1981).

Ho, W.S.W, and K.K. Sirkar, *Membrane Handbook*, Van Nostrand Reinhold, New York (1992).

Huang. R.Y.M, *Pervaporation membrane separation processes*, Elsevier, Amsterdam, (1991).

Huang, R.Y.M., and X. Feng, "Pervaporation of water/ethanol mixtures by aromatic polyetherimide membrane", *Sep. Sci. Tech.*, **27**, 1583-1597 (1992).

Huang, R.Y.M, and X. Feng, "Resistance model approach to asymmetric polyetherimide membranes for pervaporation of isopropanol/water mixtures", *J. Membr. Sci.*, **84**, 15-27 (1993).

Huang, R.Y.M., and X. Feng, "Studies on solvent evaporation and polymer precipitation pertinent to the formation of asymmetric polyetherimide membranes", *J. Appl. Polym. Sci.*, **57**, 613-621 (1995).

Huvard, G.S., V.T. Stannett, W.J. Koros, and H.B. Hopfenberg, "The pressure dependence of CO_2 sorption and permeation in poly(acrylonitrile)", *J. Membr. Sci.*, **6**, 185-201 (1980).

Ivory, J., X. Feng, and G. Kovacik, "Development of hollow fiber membrane systems for nitrogen generation from combustion exhaust gas. Part II. Full scale module test and membrane stability", *J. Membr. Sci.*, **202**, 195-204 (2002).

Ji, W., S.K. Sirdar, and S.T. Hwang, "Modeling of multicomponent pervaporation for removal of volatile organic compounds from water", *J. Membr. Sci.*, **93**, 1-19 (1994a).

Ji, W., A. Hilaly, S.K. Sirdar, and S.T. Hwang, "optimization of multicomponent pervaporation for removal of volatile, organic-compounds from water", *J. Membr. Sci.*, **97**, 109-125 (1994b).

Jiraratananon. R, P. Sampranpiboon, D. Uttapap, and R.Y.M. Huang, "Pervaporation separation and mass transport of ethylbutanoate solution by polyether block amide (PEBA) membranes", *J. Membr. Sci.*, **210**, 389-409 (2002).

Joseph, R., and J.R. Flesher, "PEBA® polyether block amide — a new family of engineering thermoplastic elastomers", in: R.B. Seymour, G.S. Kirshenbaum (eds.), *High Performance Polymer: Their Origins and Development*, Elsevier, New York, (1986).

Kamiya, Y., Y. Naito, K. Mizoguchi, K. Terada, and J. Moreau, "Themodynamic interactions in rubbery polymer/gas systems", *J. Polym. Sci:, Polym. Phys.*, **35**, 1049-1053 (1997).

Kesting, R.E., *Synthetic Polymeric Membranes*, 2nd ed., Wiley, New York (1985).

Kesting, R.E., A.K. Frizsche, C.A. Cruse, M.K. Murphy, A.C. Handermann, C.A. Cruse, and R.F. Malon, "Process for forming asymmetric gas separation membranes having graded density skins", *US Patent* 4,871,494 (1989).

Kesting, R.E., A.K. Frizsche, C.A. Cruse, M.K. Murphy, A.C. Handermann, R.F. Malon, and M.D. Moore, "The second-generation polysulfone gas separation membranes. I. The use of Lewis acid: base complexes as transient templates to increase free volume", *Appl. Polym. Sci.*, **40**, 1557-1574 (1990).

Kim, J.H., S.Y. Ha, and Y.M. Lee, "Gas permeation of poly(amide-6-b-ethylene oxide) copolymer", *J. Membr. Sci.*, **190**, 179-193 (2001).

Kim, J.H., and Y.M. Lee, "Gas permeation properties of poly(amide-6-b-ethylene oxide)-silica hybrid membranes", *J. Membr. Sci.*, **193**, 209-225 (2001).

Kimura,S.G., R.G. Lavigne, and W.R. Browall, "Method for casting ultrathin methylpentene polymer membranes", *US Patent* 4,132,824 (1979).

Kondo, M and H. Sato, "Treatment of waste-water from phenolic resin process by pervaporation", *Desalination*, **98**, 147-154 (1994).

Koros W.J., "Model for sorption of mixed gases in glassy polymers", *J. Polym. Sci.: Polym. Phys. Ed.*, **18**, 981-992 (1980).

Koros W.J., "Evolving beyond the thermal age of separation processes: Membrane can lead the way", *AIChE J.*, **50**, 2326-2334 (2004).

Koros, W.J., A.H. Chan, and D.R. Paul, "Sorption and transport of various gases in polycarbonate", *J. Membr.. Sci.*, **2**, 165-190 (1977).

Koros, W.J., and R.T. Chern, "Separation of gaseous mixtures using polymer membranes", in: R.W. Rousseau (ed.), *Handbook of Separation Process Technology*, Wiley, New York, 862-953 (1987).

Koros, W.J., and G.K. Fleming, "Membrane-based gas separation", *J. Memb. Sci.*, **83**, 1-80 (1993).

Koros, W.J. and R. Mahajan, "Pushing the limits on possibilities for large scale gas separation: which strategies?", *J. Membr. Sci.*, **175**, 181-196 (2000).

Koros, W.J., and D.R. Paul, "Carbon dioxide sorption and transport in polycarbonate", *J. Polym. Sci., Polym. Phys. Ed.*, **14**, 687-702 (1976).

Koros, W.J., and D.R. Paul, "Sorption and transport of various gases in polycarbonate", *J. Membr. Sci.*, **2**, 165-190 (1977).

Krol, J.F., M. Boerrigter, and G.H. Koops, "Polyimide hollow fiber gas separation membranes: Preparation and the suppression of plasticization in propane/propylene environments", *J. Membr. Sci.*, **184**, 275-286 (2001).

Kroschwitz, J., M. Howe-Grant (Eds.), *Encyclopedia of Chemical Technology*, Wiley, New York (1998).

Kujawski W, and B. Ostrowska-Gumkowska, "Preparation and properties of organiphilic membranes for pervaporation of water-organics mixtures", *Sep. Sci. Tech*., **38**, 3669-3687 (2003).

Kujawski, W, A. Warszawski, W.Ratajczak, T. Porebski, W. Capala, and I. Ostrowska,, "Removal of phenol from wastewater by different separation techniques"**,** *Desalination*, **163,** 287-296 (2004).

Kamiya, Y., Y, Naito, K. Mizoguchi, K. Terada, and J. Moreau,, "Thermodynamic interactions in rubbery polymer/gas system", *Poly. Phys.*, **35**, 1049-1053 (1997).

Lee, K., and S. T. Hwang, "The transport of condensable vapor through a microporous Vycor glass membrane", *J. Coll. Inter. Sci.*, **110**, 544-555 (1986).

Li, K., D.R. Acharya, and R. Hughes, "removal of carbon dioxide from breathing gas mixtures using a hollow fiber membrane permeator", *Gas Sep. Purif.*, *4*, 197-2-2 (1990).

Lide, D.R. (ed.), *CRC Handbook of Chemistry and Physics*, 85rd ed., CRC Press, Cleveland, OH (2004).

Lin, H., and B.D. Freeman, "Materials selection guidelines for membranes that remove CO_2 from gas mixtures ", *J. Mole. Struct.*, 7**39**, 57-74 (2005).

Lin, H., and B.D. Freeman, "Gas solubility, diffusivity and permeability in poly(ethylene oxide)", *J. Membr. Sci.*, **239**, 105-117 (2004).

Lin, H., E. Van Wagner, B.D. Freeman, L.G. Toy, and R.P. Gupta, "Plasticization-enhanced hydrogen purification using polymeric membranes", S*cience,* **311**, 639-642 (2006a).

Lin, H., E. Van Wagner, R. Raharjo, B.D. Freeman, and I. Roman, "High-performance polymer membranes for natural gas sweetening", *Adv. Mater*., **18**, 39-44 (2006b).

Liu, L., Y. Chen, S. Li, and M. Deng, "The effect of support layer on the permeability of water vapor in asymmetric composite membranes", *Sep. Sci. Tech.*, **36**, 3701-3720 (2001).

Liu, L., X. Feng, and A. Chakma, "Unusual behavior of poly(etherlene oxide)/$AgBF_4$ polymer electrolyte membranes for olefin-paraffin separation", *Sep. Puri. Tech.*, **38**, 255-263 (2004).

Liu, Y., X. Feng, and D. Lawless, "Separation of gasoline vapor from nitrogen by hollow fiber composite membranes for VOC emission control", *J. Membr. Sci.*, **271**, 114-124 (2006).

Loeb, S., and S. Sourirajan, "Sea water demineralization by means of an osmotic membrane", in S*aline Water Coversion-II*, Advances in Chemistry Series Number 28, American Chemical Society, Washington DC (1963).

Marchese, J., E. Garis, M. Anson, N.A. Ochoa, and C. Pagliero, "Gas sorption, permeation and separation of ABS copolymer membranes", *J. Membr. Sci.*, **221**, 185-197 (2003).

Matsumoto, Y., M. Kondo, and T. Fujita, "Transport mechanism in PEBA membrane", *Proceedings of the 6th International Conference on Pervaporation Processes in the Chemical Industry*, Ottawa, Canada, 55-65 (1992).

Matsuura, T., *Synthetic Membranes and Membrane Separation Processes*, CRC Press, Florida (1994).

Merkel T.C., V.I. Bondar, K. Nagai, B.D. Freeman, and I. Pinnau, "Gas sorption, diffusion, and permeation in poly(dimethylsiloxane), *J. Polym. Sci.: Polym. Phys.*, **38**, 415-434 (2000).

Michaels, A.S., and H. J. Bixler, "Solubility of gases in polyethylene", *J. Polym. Sci.*, **1**, 393-412 (1961).

Mulder, M, *Basic Principles of Membrane Technology*, Kluwer Academic, the Netherlands (1996).

Muller., J., K.V. Peinemann, and J. Muller, "Development of facilitated transport membranes for the separation of olefins from gas streams", *Desalination*, **145**, 339-345 (2002).

Okamoto, K., K. Tanaka, T. Shigematsu, H. Kita, A. Nakamura, and Y. Kusuki, "Sorption and transport of carbon dioxide in a polyimide from 3,3′,4,4′-biphenyltetracarboxylic dianhydride and dimethyl-3,7-diaminodibenzothiophene-5,5′-dioxide", *Polymer*, **31**, 673-678 (1990).

Park, H.B., and Lee Y.M., "Separation of toluene/nitrogen through segmented polyurethane and polyurethane urea membranes with different soft segments", *J. Membr Sci.*, **197** 283-296 (2002).

Park, H.H., J. Won, S.G. Oh, and Y.S. Kang, "Effect of nonionic *n*-octyl β-D-glucopyranoside surfactant on the stability improvement of silver polymer electrolyte membranes for olefin/paraffin separation", *J. Membr. Sci.*, **217**, 285-293 (2003).

Paul, D.R., and W.J. Koros, "Effect of partially immobilizing sorption on permeability and diffusion time lag", *J. Polym. Sci:, Polym. Phys. Ed.*, **14**, 675 (1976).

Paul, D.R., and Y. Yampol'skii, *Polymeric Gas Separation Membranes*, CRC Press, Boca Raton, Florida (1994).

Petropoulos, J.H., "Mechanisms and theories for sorption and diffusion of gases in polymers", in: D.R. Paul, Y.P. Yampol´skii (eds.), *Polymeric Gas Separation Membranes*, CRC Press, Boca Raton, FL, 17–81 (1994).

Prasad, R., R.L. Shaner, and K.J. Doshi, "Comparison of membranes with other gas separation technologies", in: D.R. Paul and Y. Yampol'skii (eds.), *Polymeric Gas Separation Membranes*, CRC Press, Boca Raton, Florida, 531-614 (1994).

Pinnau, I., and L.G. Toy, "Transport of organic vapors through poly(1-trimethylsilyl-1-propyne), *J. Membr. Sci.*, **116**, 199-209 (1996).

Pinnau, I., and L.G. Toy, "Solid polymer electrolyte composite membranes for olefin/paraffin separation", *J. Membr. Sci.*, **184**, 39-48 (2001).

Pinnau, I., L.G. Toy, and C. Casillas, "Olefin separation membrane and process", *US Patent* 5,670,051 (1997).

Qiu, M.M, and S. T. Hwang, "Continous vapor-gas separation with a porous membrane permeation system", *J. Membr. Sci.*, **59**, 53-72 (1991).

Raucher, D., and M.D. Sefcik, "Sorption and transport in glassy polymers", in: T.E. Whyte, C.M. Yon, and E.H. Wagener (eds.), *ACS Symp. Ser. No. 233*, *Industrial Gas Separations*, American Chemical Society, Washington DC, 111-124 (1983).

Reid, R.C., JM. Prausniz, and B.E. Poling, *The properties of gases and liquids*, McGraw-Hill, New York, 1987.

Rezac, M.E., T. John, and P.H. Pfromm, "Effect of copolymer composition on the solubility and diffusivity of water and methanol on a series of polyether amides", *J. Appl. Polym. Sci.*, **65**, 1983-1993 (1997).

Rezac, M.E., and T. John "Correlation of penetrant transport with polymer free volume: additional evidence from block copolymers", *Polym.*, **39**, 599-603 (1998).

Robeson, L.M., "Correlation of separation factor versus permeability for polymeric membranes", *J. Membr. Sci.*, **62**, 165-185 (1991).

Sada, E., H. Kumazawa, J. Wang, and M. Kopzumi, "Separation of carbon dioxide by asymmetric hollow fiber membrane of cellulose triacetate", *J. Appl. Polym. Sci.*, 45, 2181-2186 (1992).

Sampranpiboon, P., R. Jiraratananon, D. Uttapap, X. Feng, and R.Y.M. Huang, "Pervaporation separation of ethyl butyrate and isopropanol with polyester block amide (PEBA) membranes", *J. Membr. Sci.*, **173**, 53-39 (2000).

Semenova, S., "Polymer membranes for hydrocarbon separation and removal", *J, Membr. Sci.*, **231**, 189-207 (2004).

Shah, V.M., B.J. Hardy, and S.A. Stern, "solubility of carbon dioxide, methane and propane in silicone polymers: effect of polymer side chains", *J. Polym. Sci.: polym. Phys.*, **24**, 2033-2047 (1986).

Sheth, J.P., and J. Xu, G.L. Wilkes, "Solid state structure–property behavior of semicrystalline poly(ether-block-amide) PEBAX thermoplastic elastomers", *Polymer*, **44**, 743-756 (2003).

Shieh, J.-J., and T.S. Chung, "Cellulose nitrate-based multilayer composite membranes for gas separation", *J. Membr. Sci.*, **166**, 259–269 (2000).

Shieh, J.-J., T.S. Chung, and D.R. Paul, "Study of multi-layer composite hollow fiber membranes for gas separation", *Chem. Eng. Sci.*, **54**, 675-684 (1999).

Singh, A., B.D. Freeman, and I. Pinnau, "Pure and mixed gas acetone/nitrogen permeation properties of polydimethylsiloxane [PDMS]", *J. Polym. Sci.: Polym. Phys.*, **36**, 289-301 (1998).

Someshwar, A.V., and K. Vice, "A comprehensive comparison of Canadian and U.S. pulp and paper mill air emission data", *NCASI Special Report No. 05-03*, The National Council for Air and Stream Improvement (NCASI), November, pp.85 (2005).

Spillman, R.W., "Economics of gas separation by Membranes", *Chem. Eng. Prog.*, **85**, 41-62 (1989).

Stannett, V.T., W.J. Koros, D.R. Paul, H.K. Lonsdale, and R.W. Baker, "Recent advances in membrane science and technology", *Adv. Polym. Sci.*, **32**, 69-121 (1979).

Stannett, V.T., G.R.Ranade and K.J. Koros, "Characterization of water vapor transport in glassy polyacrylonitrile by combined permeation and sorption techniques", *J. Membr. Sci.*, **10**, 219-233 (1982).

Staudt-Bickel, C., and W.J. Koros, "Olefin/paraffin gas separations with 6FDA-based polyimide membranes", *J. Membr. Sci.*, **170**, 205-214 (2000).

Stern, S.A., "Polymers for gas separation: the next decade", *J. Membr. Sci.*, **94**, 1-65 (1994).

Stern, S.A., J.T. Mullhaupt and P.J. Gareis, "The effect of pressure on the permeation of gases and vapors through polyethylene. Usefulness of the corresponding states, *AIChE J.*, **14**, 64-73 (1969).

Stern, S.A., V.M. Shah, and B.J. Hardy, "Structure-permeability relationships in silicone polymers", *J. Polym. Sci.: Polym. Phys.*, **25**, 1263-1298 (1987).

Suwandi, M.S., and S.A. Stern, "Transport of heavy organic vapors through silicone rubber", *J. Polym. Sci.: Polym. Phys. Ed.*, **11**, 663-381 (1973).

Uhlhorn, R.J.R., K. Keizer, and A.J. Burggraaf, "Gas transport and separation with ceramic membranes. Part I. Multilayer diffusion and capillary condensation", *J. Membr. Sci.*, **66**, 259-269 (1992).

Urkiaga, A., N. Bolano, and L.D.L. Fuentes, "Removal of micropolutants in aqueous streams by organophilic pervaporation", *Desalination*, **129**, 55-60 (2002).

Ward III, W.J., "Method for the casting of ultrathin polymer membranes", *US Patent* 4,279,855 (1981).

Ward III, W.J., "Ultrathin polymer membranes", *US Patent 4,374,891* (1983).

Ward III, W.J., W.R. Browall and R.M. Salemme, "Ultrathin silicone/polycarbonate membranes for gas separation processes", *J. Membr. Sci.*, **1**, 99-108 (1976).

Waston, J.M., and M.G. Baron, "Precise static and dynamic permeation measurements using a continuous-flow vacuum cell", *J. Membr. Sci.*, **106**, 259-268 (1995).

Wessling, M., I. Huisman, T. Boomgaard, and C.A. Smolders, "Time-dependent permeation of carbon dioxide through a polyimide membrane above the plasticization pressure", *J. Appl. Polym. Sci.*, **58**, 1959--1966 (1995).

Wessling M., M.L. Lopez, and H. Strathmann, "Accelerated plasticization of thin-film composite membranes used in gas separation", *Sep. Purif. Tech.*, **24**, 223-233 (2001).

Wilks, B., and M.E. Rezac, "Properties of rubbery polymers for the recovery of hydrogen sulfide from gasification gases", *J. Appl. Polym. Sci.*, **85**, 2436-2444 (2002).

Wijmans, J.G., and R.W. Baker, "The solution-diffusion model: a review", *J. Membr. Sci.*, **107**, 1-21 (1995).

Yeom, C.K., J.M. Lee, Y.T. Hong, K.Y. Choi, and S.C. Kim, "Analysis of permeation transients of pure gases through dense polymeric membranes measured by a new permeation apparatus", *J. Membr. Sci*., **166**, 71–83 (2000).

Yeom, C.K., S.H., Lee, J.M. Lee, and H.Y. Song, "Modeling and evaluation of boundary layer resistance at feed in the permeationof VOCs/N_2 mixtures through PDMS membranes", *J. Membr. Sci*., **204,** 303-322 (2002a).

Yeom, C.K., S.H. Lee, H.Y. Song, and J.M. Lee, "Vapor permeations of a serious of VOC_2/N_2 mixtures through PDMS memrbane", *J. Membr. Sci*., **198**, 129-143 (2002b).

Yeom, C.K., S.H. Lee, H.Y. Song, and J.M. Lee, "A characterization of concentration polarization in a boundary layer in the permeation of VOCs/N_2 mixtures through PDMS membrane", *J. Membr. Sci*., **205**, 155-174 (2002c).

Publications Resulting from the Thesis Research

1. **L. Liu**, A. Chakma, X. Feng, Separation of VOCs from N_2 using poly(ether block amide) membranes, *Cana. J. Chem. Eng.*, Accepted.

2. **L. Liu**, A. Chakma, X. Feng, Sorption, diffusion, and permeation of light olefins in poly(ether block amide) membranes, *Chem. Eng. Sci.*, 61 (2006) 6142-6253.

3. **L. Liu**, A. Chakma, X. Feng, Propylene separation from nitrogen by poly(ether block amide) membranes, *J. Membr. Sci.*, 279 (2006) 645-654.

4. **L. Liu**, A. Chakma, X. Feng, CO_2/N_2 separation by poly(ether block amide) thin film hollow fiber composite membranes, *Ind. Eng. Chem. Res.*, 44 (2005) 6874-6882.

5. **L. Liu**, A. Chakma, X. Feng, Preparation of hollow fiber poly(ether block amide)/polysulfone composite membranes for the separation of carbon dioxide from nitrogen, *Chem. Eng. J.*, 105 (2004) 43-51.

6. **L. Liu**, A. Chakma, X. Feng,, A novel method of preparing ultrathin poly(ether block amide) membranes, *J. Membr. Sci.*, 235 (2004) 43-52.